Cancer Metastasis – Biology and Treatment 17

Wen G. Jiang *Editor*

Electric Cell-Substrate Impedance Sensing and Cancer Metastasis

Springer

Electric Cell-Substrate Impedance Sensing and Cancer Metastasis

Cancer Metastasis – Biology and Treatment

VOLUME 17

Recent Volumes in this Series

Volume 8: Cell Motility in Cancer Invasion and Metastasis
Editor: Alan Wells
ISBN 978-1-4020-4008-3

Volume 9: Cell Adhesion and Cytoskeletal Molecules in Metastasis
Editors: Anne E. Cress and Raymond B. Nagle
ISBN 978-1-4020-5128-X

Volume 10: Metastasis of Prostate Cancer
Editors: Richard J. Ablin and Malcolm D. Mason
ISBN 978-1-4020-5846-2

Volume 11: Metastasis of Breast Cancer
Editors: Robert E. Mansel, Oystein Fodstad and Wen G. Jiang
ISBN 978-1-4020-5866-7

Volume 12: Bone Metastases: A Translational and Clinical Approach
Editors: Dimitrios Kardamakis, Vassilios Vassiliou and Edward Chow
ISBN 978-1-4020-9818-5

Volume 13: Lymphangiogenesis in Cancer Metastasis
Editors: Steven A. Stacker and Marc G. Achen
ISBN 978-90-481-2246-2

Volume 14: Metastasis of Colorectal Cancer
Editors: Nicole Beauchemin and Jacques Huot
ISBN 978-90-481-8832-1

Volume 15: Signal Transduction in Cancer Metastasis
Editors: Wen-Sheng Wu and Chi-Tan Hu
ISBN 978-90-481-9521-3

Volume 16: Liver Metastasis: Biology and Clinical Management
Editor: Pnina Brodt
ISBN 978-94-007-0291-2

Wen G. Jiang
Editor

Electric Cell-Substrate Impedance Sensing and Cancer Metastasis

Springer

Editor
Wen G. Jiang
Metastasis and Angiogenesis Research Group
Institute of Cancer and Genetics
Cardiff University School of Medicine
Cardiff, U.K.

ISSN 1568-2102
ISBN 978-94-007-4926-9 ISBN 978-94-007-4927-6 (eBook)
DOI 10.1007/978-94-007-4927-6
Springer Dordrecht Heidelberg New York London

Library of Congress Control Number: 2012948594

Printed on acid-free paper

Springer is part of Springer Science+Business Media (www.springer.com)

Preface

Automation, throughput and new methods for routine tasks have been some of the challenges in cell-based function analyses. Recent progress and availability in impedance-based cell analysis technologies have been one of the shining examples that a technology platform may help to deal with some of these challenges. Impedance-based cell analyses have been developed for the last three decades and are now a relatively mature platform for research applications in cell biology and life science–based laboratories. Of the limited choice, some are able to offer broad range of cell analytic methods, namely, automated tracking of cell growth, migration, invasion, cell-matrix and cell-cell interactions and beyond. These applications have made automation of analyses on living cells possible and frequently with good capability of high throughput. While this technology platform is actively under development, this volume aims to provide some basic mechanisms of impedance-based cell analysis, useful applications and some examples of the studies using this technology.

I am very grateful to Dr Ivar Giaever, the Nobel Laureate for physics and Dr Charles Keese who jointly lay down the context of this technology. This excellent chapter has described the concept, development and history of impedance sensing technologies and also provided future prospective of this exciting field. The remaining sections of the book cover the ideas, methods, applications and example of investigation in cancer cell signalling, cell functions commonly associated with cancer metastasis, namely cell migration, invasion, cell-cell and cell-matrix adhesions and tight junction. The potential applications of impedance sensing in some specific cellular events including epithelial to mesenchymal transition and wound healing are also discussed. ECIS may find its use in screening the effect and identifying mechanisms of actions of traditional medicines. Two chapters have demonstrated the early development of using ECIS in evaluating TCM in cell models.

The potential applications of impedance sensing are clearly beyond the scope of a single volume. I hope this volume will provide a useful reference for this evolving technology in years to come.

I wish to thank all the contributors for their contribution and Springer for their editorial assistance.

Wen G. Jiang

Contents

Electric Cell-Substrate Impedance Sensing Concept to Commercialization

Ivar Giaever and Charles R. Keese

Abstract A personal account of the invention, growth and commercialization of Electric Cell-substrate Impedance Sensing (ECIS) by the inventors of the technology. From the first experiments at the General Electric Research and Development Center in the early 1980s to the outgrowth of applications and finally the incorporation of Applied BioPhysics, Inc., the chapter provides an historical and often amusing account of the evolution of ECIS.

1 The Birth of ECIS

The birth of ECIS took place over 25 years ago when Ivar Giaever was a staff member at General Electric Research Laboratory in Niskayuna NY, and Charles R. Keese joined him on an NSF grant. Originally we worked in immunology, specifically on various ways to detect antibodies, but research soon shifted into work with mammalian cells. Charlie had an extensive background in tissue culture from his PhD thesis at Rensselear Polytechnic Institute, and Ivar had briefly worked with cells in a short sabbatical stint at the Salk Institute in California following his Nobel Prize. Working together in 1981, one of the first problems we tackled was growing cells on fluorocarbon oil to investigate the forces that cells apply to their substrate. This work also resulted in a new liquid micro-carrier system (Keese and Giaever 1983).

Not surprisingly, like most people with a background in physics, we soon drifted into studies of the effects of electromagnetic fields upon cells. The simplest experiment we tried first was to put cells on two electrodes and apply a DC voltage. What happened is that, at not a too high voltage, the cells died on one of the electrodes.

I. Giaever (✉) • C.R. Keese
Applied BioPhysics, Inc., 185 Jordan Road, Troy, NY 12180, USA
e-mail: Giaever@biophysics.com; Keese @biophyscs.com

W.G. Jiang (ed.), *Electric Cell-Substrate Impedance Sensing and Cancer Metastasis*, Cancer Metastasis - Biology and Treatment 17, DOI 10.1007/978-94-007-4927-6_1,

This was not because of the electrical field but rather because of electrochemistry and the resulting ions stemming from the current. This problem was rather quickly resolved by moving to AC current, where the frequency was sufficiently high to prevent serious buildup of electrochemical products and polarization of the electrodes. One early observation during this work was that we noticed using large electrodes that the resistance of the system did not change whether we had cells on the electrodes or not. This was a puzzling fact and had to mean that the resistance of the solution was much higher than the resistance caused by the tight cell layer on the two electrodes.

At this same time another GE staff scientist, Dr. Charles Bean, was electrically measuring virus particles as they passed through small pores in a plastic sheet, similar to the well known Coulter counter used for cell counting. When a virus or a cell passes through the pore, the resistance of the pore increases as the conductive salt solution is replaced with an insulating particle. In making these measurements, however, one has to account for the total resistance of the pore including the end effect of the pore known as the constriction resistance. This resistance at each end of the pore can be shown to equal:

$$R(\text{constriction}) = \rho/4r$$

where ρ is the resistivity of the solution and r, the radius of the pore.

In addition, at this time Ivar had a visitor from Norway, Dr. Jens Feder, who wanted to learn some biophysics. He placed a plastic sheet with a single pore onto a gold electrode and next managed to attach a single fibroblastic cell over the top of the hole. Again the resistance change due to the cells was rather insignificant because of the resistance of the long pore in series with that of the cell over the pore.

With this background information we now rather quickly realized how to detect the cells electrically. We did not need the plastic sheet and the pore; instead, why not just use a small gold electrode as the cell's substrate. Although the small electrode would have a fairly large constriction resistance, by making the electrode sufficiently small to become a bottleneck in the system, the cells should show up, and they did. Electrical Cell-substrate Impedance Sensing (ECIS) was born.

2 Description of ECIS

The original ECIS arrays were very different than what we have today. The early ECIS arrays were made by first evaporating gold through a mask to yield four relatively narrow gold strips (130 μm wide) and a larger gold film electrode on the surface of a petri dish. Then we soldered a copper wire to each of the four strips using pure indium and a wire also to the larger gold pad that would serve as a counter electrode. Since indium has a low melting point, it is possible to do this soldering without damaging the plastic – a neat technique. Next we covered the four narrow strips with a glass microscope cover slip such that only about 100 μm of the tips

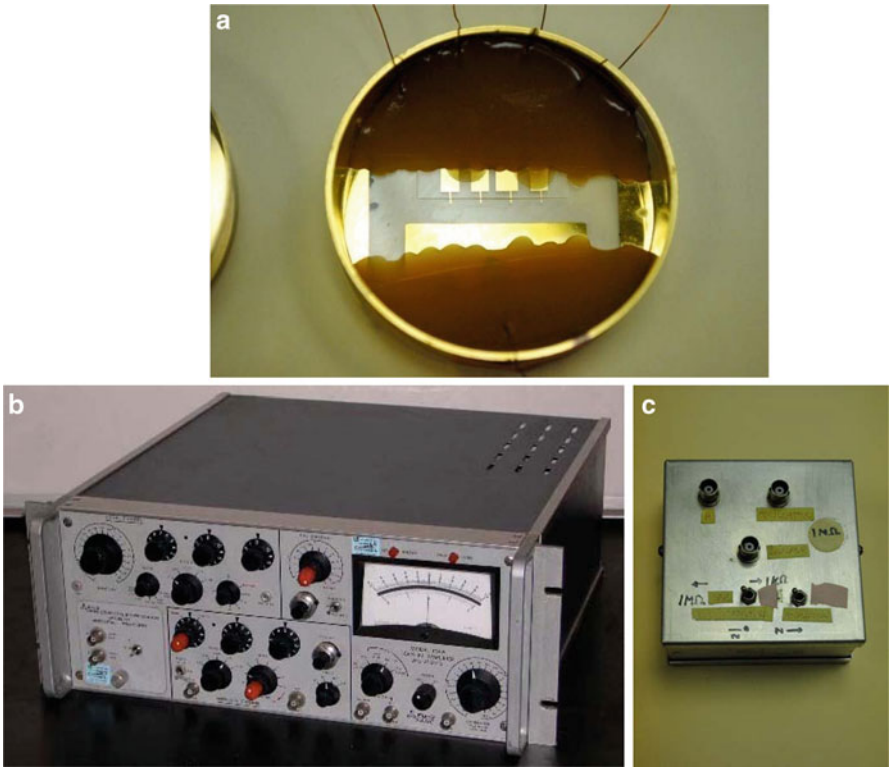

Fig. 1 The early ECIS system (**a**) An example of the early ECIS electrodes at the base of a petri-style dish. Here the active electrodes were four small tips of gold delineated with insulating wax beneath a glass coverslip. The same wax covered the wire-indium-gold solder junctions. The large gold rectangle served as a counter electrode. The electrodes were connected to an analogue lock-in amplifier (**b**) The AC output of the lock-in was in series with the ECIS electrodes and a load box (**c**) with a 1MΩ resistor to provide an approximate constant current to the electrodes. The voltage across the ECIS electrodes was followed using a chart recorder and later a personal computer

extended beyond the glass. Placing the dish on a hotplate, we let molten wax be drawn by capillary action between the glass slide and the gold electrodes to define the four small electrode tips. This same nontoxic wax was then used to cover the indium solder junctions, and the dish was ready to receive the cells.

Using standard culture medium as the electrolyte, the first ECIS instrumentation applied an AC signal of 1 V at 4,000 Hz through a 1 MΩ resistor in series with the two gold electrodes. Since the resistance of the electrode system was much smaller than 1 MΩ, we had an approximate constant current source of slightly less than 1 μA. As the counter electrode was much larger than the small electrode, the measured voltage across the petri dish was almost entirely due to the small electrode.

Let's return to the issue of electrode size that was alluded to above. The surface resistance of a small circular electrode, including the contributions of any attached cells, changes inversely with the area:

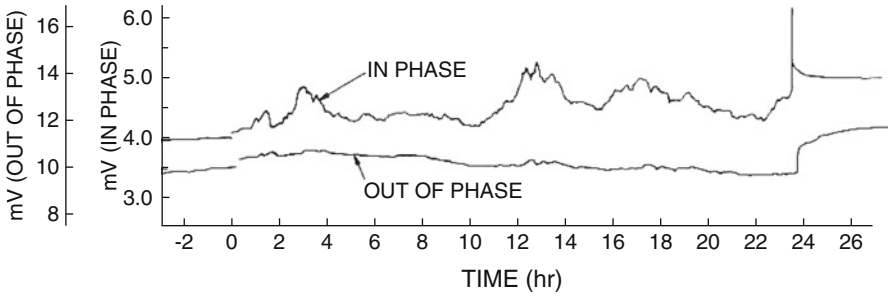

Fig. 2 Earliest Published Data. The first ECIS data, published in 1984, demonstrating the detection of WI-38 fibroblastic cells using ECIS and the effect of formalin (added at ~24 h) resulting in changes in the impedance and the loss of impedance fluctuations (Giaever and Keese 1984)

$$R(\text{surface}) \sim 1/\text{area} \sim 1/r^2$$

While the constriction resistance (solution resistance) changes inversely with the radius:

$$R(\text{solution}) \sim 1/r$$

Thus, by making the radius of the electrode sufficiently small, the electrode resistance can be made to dominate the solution resistance. Most of the modern ECIS electrode arrays feature circular electrodes that have a diameter of 250 μm – large enough to accommodate many cells but small enough to have a relatively small constriction resistance.

In the early commercial version of the ECIS instrumentation, as in many of our instruments today, voltage and phase data from the electrode systems were measured with a lock-in amplifier, and data were stored and processed with a PC. The same computer controlled the applied AC signal and switched the measurement to different electrodes in the course of an experiment. As cells anchored and spread on the active small electrodes, their insulating plasma membranes constrained the electrical current and forced it to flow beneath and between the cells. This convoluted current path resulted in large changes in the measured impedance. In addition, small fluctuations in the impedance were observed because the live cells continuously altered their morphology. These impedance variations were numerically analyzed to report levels of cell motility and, indirectly, cell metabolism.

It is important to note that the small current (~1 μA) and the resulting voltage drops (a few millivolts) across the cells had no detectable effects upon them; the measurement was non-invasive. The size of the electrode restricted the maximum cell populations that could be observed – using a single electrode to about 100 cells – but by using more electrodes in parallel more cells could be monitored. Note that we could not simply increase the size of the electrode to accommodate additional cells, because then the solution resistance would dominate. It should also be noted that although populations of cells were commonly studied, the activities of even a single cell could easily be measured.

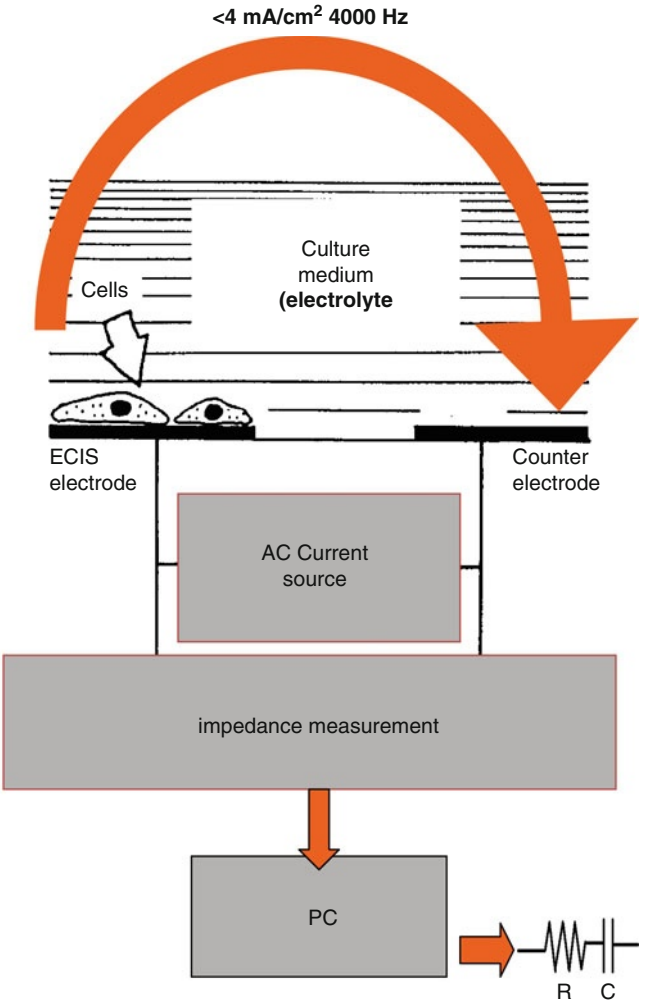

Fig. 3 Basic Setup of ECIS Instrumentation. Using standard tissue culture medium as the electrolyte, the ECIS electronics deliver a constant current to the electrodes while measuring the voltage and phase as a function of time. To assure that the ECIS measurement is non-invasive, the current is maintained very low. This AC current results in very slight hyper- and hypo-polarization of the plasma membranes that has no measurable effect upon cell behavior. From the earliest measurements with ECIS, we have interpreted the impedance as a pure resistor and capacitor coupled in series

From the earliest work with ECIS, we have interpreted the measured impedance as a resistor and capacitor coupled in series; this was just for convenience, we could equally well have interpreted the result as a resistor and a capacitor in parallel. It should be recognized that whatever you do, both the capacitance and the resistance will depend on frequency.

Today the ECIS system has been refined considerably, but the principle remains the same. The standard electrodes are circular with a diameter of 250 μm, and the constant current source is 2 μA.

3 Biological Assays

3.1 The Early Years

The early experiments with ECIS were done with fibroblastic WI-38 cells and the transformed cancer-like WI-38 VA13 cells, and the results were first published in June 1984 (Giaever and Keese 1984). The point of the paper was to show that the cells could be detected by measuring the impedance of the system and, using cytochalasin, to draw attention to the cytoskeleton's role in bringing about impedance changes. We followed up with a second paper in 1986, where we showed that these same two cell types attached and spread differently depending upon the protein layers adsorbed on the electrodes. We also analyzed the impedance fluctuations from the cells showing that the VA13 cells were much "noisier" than the WI38 cells (Giaever and Keese 1986). In this early work we questioned whether there were regular oscillations in the impedance fluctuations from these cells, but time series analysis found no specific frequency in this signal and in fact the data from fibroblastic cells were shown to be fractal.

Interestingly, in later work one of our student at Rensselaer discovered that MDCK cells did sometimes break into regular oscillations with a period of ~2.5 h, but to this day we have not understood why this happens (Lo et al. 2001). In addition, and not as unexpectedly, one ECIS user in Japan working with murine cardiomyocytes, also showed regular oscillations in the impedance signal, but this was related to the regular beating of these heart cells in culture.

During this early period we also tried to understand why and how the cells affected the measured impedance. It is important to note that what we basically measure is the change in the impedance of the electrode when it gets populated with cells. To gain more understanding, the system was modeled using disk-shaped cells hovering a small distance over the electrode (the focal contacts were ignored) and this resulted in a simple second order linear equation. The solution was straight forward resulting in a complex formula that accounts for the impedance measured using three cellular parameters, namely the barrier function of the cell layer (Rb), the combined apical and basal membrane capacitance and a parameter related to the passages beneath the cells that we termed alpha (Giaever and Keese 1991).

3.2 Response of Cells to External Agents

With this basic understanding of the measurement we began to explore its usefulness in dealing with relevant biological problems. Mammalian cells when challenged by different substances and conditions such as ligands, DNA, drugs, temperature, pH, etc., will respond by changing their morphology. When the cell's morphology changes, the measured impedance will change, and therefore the ECIS system

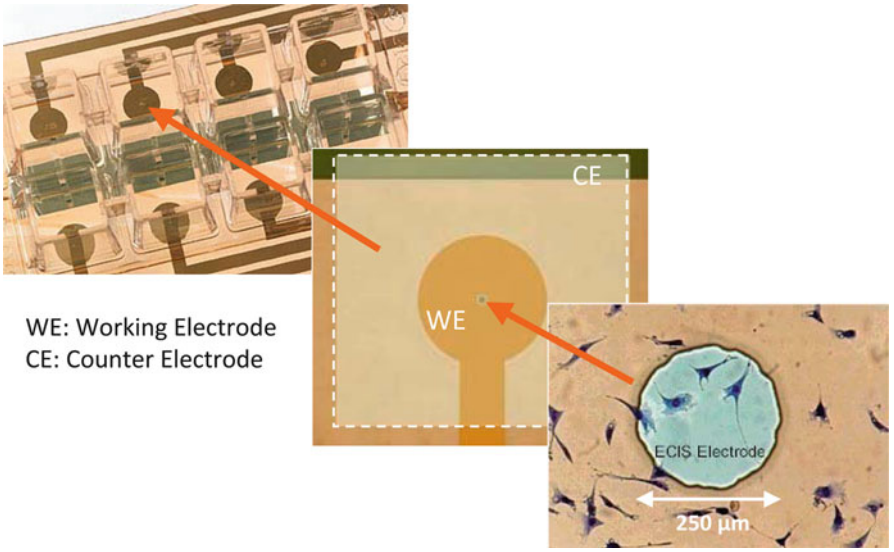

Fig. 4 Commercial ECIS 8W1E array. The layout of a commercial eight well array is shown, where each well has an active circular electrode that is 250 µm in diameter (WE) and a much larger counter electrode (CE) to complete the circuit when medium (electrolyte) is present in the well. In the figure with the highest magnification, fibroblastic cells near and upon the small electrode have been fixed and stained to provide an easy visual reference of the relative size of the electrode

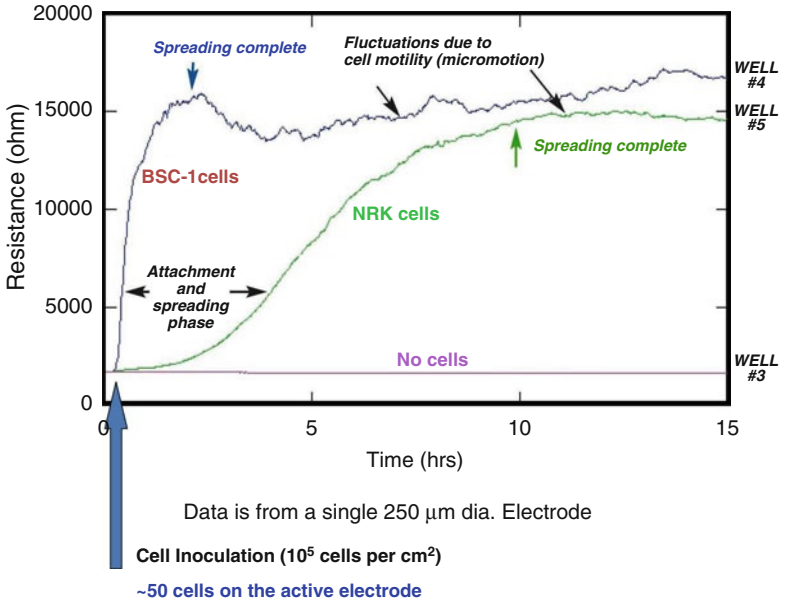

Fig. 5 Typical ECIS data following cell attachment and spreading. Shortly after time zero, ECIS arrays with a single active 250 µm diameter electrode were inoculated with BSC-1 or NRK epithelial kidney cells; one well with medium only serves as a control. The attachment and spreading of the cells result in dramatic increases in the resistive portion of the impedance measured at 4,000 Hz. Following spreading, fluctuations can be seen in the data due to movement of cells in the confluent monolayers. This activity, termed micromotion, is completely absent in the data with medium only

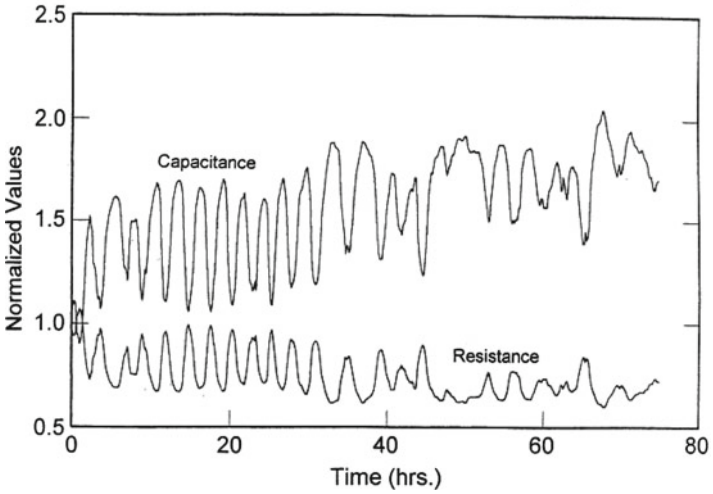

Fig. 6 Regular oscillation in impedance signal from MDCK cells. Confluent Madin-Darby canine kidney cells (strain II) were measured at 4,000 Hz. After confluence was achieved, these cells broke into regular oscillations that, in this case, continued for many hours (Lo et al. 2001)

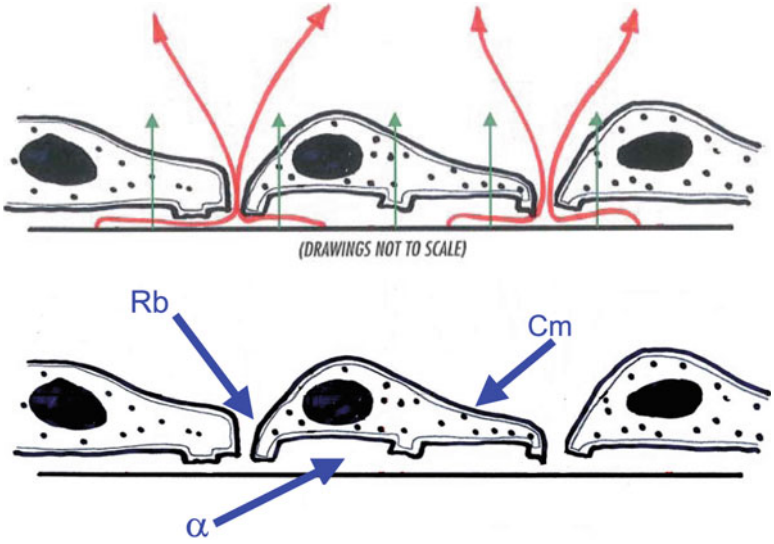

Fig. 7 The ECIS Model. The upper cartoon shows cells upon an ECIS electrode with current flowing either in the narrow spaces beneath and between the cells (*red arrows*) or capacitively coupling through the cell plasma membranes (*green arrows*). The relative amount of current through these two routes is dependent upon the AC frequency. By measuring the complex impedance of cell-covered electrodes at different AC frequencies, it is possible to model the impedance data in terms of three different parameters – namely Rb, the barrier function of the cell monolayer, alpha, related to the size and extent of the passages beneath the cells, and Cm, the combined series apical and basal plasma membrane capacitance (Giaever and Keese 1991)

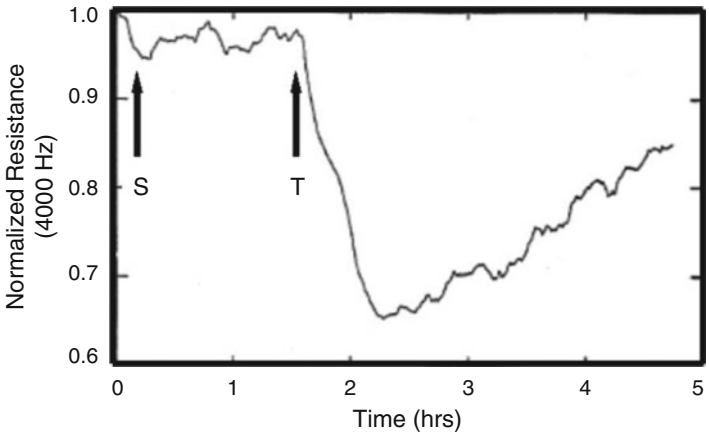

Fig. 8 Measurements of barrier function with endothelial cells. Response of bovine pulmonary microvascular endothelial cells to thrombin. Cells were first grown to confluence and then the ECIS measurements were begun. At S, a sham of simply medium was added resulting in essentially no response; at T, the same volume of medium containing alpha-thrombin was added to give a final concentration of 100 nM. This resulted in a major drop in the resistance due to the loss of barrier function of the cell monolayer. The resistive portion of the impedance divided by its starting value (normalized) is presented as a function of time (Tiruppathi et al. 1992)

becomes a powerful biosensor. In addition, because of the quantitative nature of an electrical measurement, we can quantify the morphological changes rather than just describing them. Let's begin by considering three very different experiments where we see ECIS measuring the response of cells to different compounds as well as a viral infection.

Endothelial cells line the entire vascular system and are the cells that make up the capillaries. Cell physiologists are much interested in the barrier function of these endothelial cells, as the increased permeability of these cells results in loss of fluid from the blood (edema) and health issues such as pneumonia. One of the first ECIS studies we carried out was to challenge endothelial cells in culture with various chemicals known to change the permeability of these cell monolayers. When these cells were exposed to a sham such as a small volume of normal medium there was little if any response. However, if this medium contained small amounts of thrombin, an agent known to increase the permeability of the cells layer, there was a rapid and substantial drop in the measured impedance. We could also follow the recovery of the cell layer as it reestablished it normal tight contact between the cells. With the ECIS system, we not only saw this response, but we could measure the cells' condition every second or so (Tiruppathi et al. 1992). The use of ECIS to monitor the barrier function of endothelial cells in culture is now widespread, as it has proven to be a reliable measurement without the need of radioactive tracers or other chemical labels to access how readily material moves through endothelial cell monolayers.

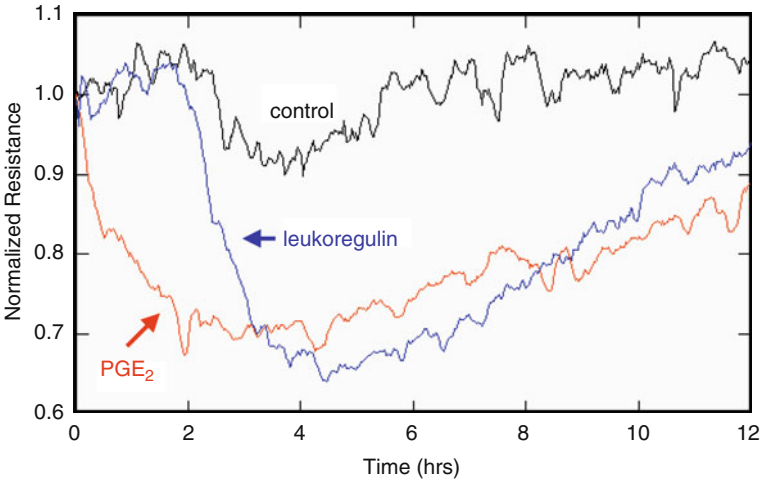

Fig. 9 Comparison of the effect of prostaglandin E_2 and leukoregulin upon confluent monolayers of orbital fibroblastic cells from patients with Graves' disease. Confluent cell monolayers were exposed to PGE_2 (1 μM) or leukoregulin (1U/ml) in fresh medium or fresh medium alone (control) at time zero, and the normalized resistive portion of the impedance at 4,000 Hz was followed as a function of time. The morphological changes detected by ECIS showed that, although the response was essentially the same for both agents, the response to leukoregulin was delayed, as protein synthesis was required to generate the response (Reddy et al. 1998)

Another more dramatic example of the use of ECIS was published in 1998. In this work we used ECIS to monitor human orbital fibroblastic cells after exposure to two different kinds of drugs – prostaglandin and leukoregulin – that were known to have similar effects upon the cells. Upon addition of prostaglandin, the cells quickly responded with a drop in resistance, but with leucoregulin, nothing immediately happened. It took 2 h before the cells finally responded with a drop in resistance to the addition of this macromolecule. The reason for this was that the cells had to synthesize proteins before they could respond and that synthesis required about 2 h. Here was a great example of the power of ECIS as a real time, label-free assay. In a single experimental run, one could see the effect of a compound in real time and also distinguish between an immediate response and one that required processing of the information by the cells (Reddy et al. 1998).

This delayed response of cells was also readily seen when ECIS was used to detect the cytopathic effects of viral infection of fish cells in culture. When carp EPC cells were infected with different titers of HNV virus and monitored with ECIS, nothing happened during the latent period, and then when virion production began, the infection started altering and killing the cells. This showed up as a drop in resistance whose timing depended upon the titer used. By 180 h post infection all of the cells, regardless of titer, were dead as revealed by a drastic drop in the resistance down to levels associated with cell-free electrodes (Campbell et al. 2007).

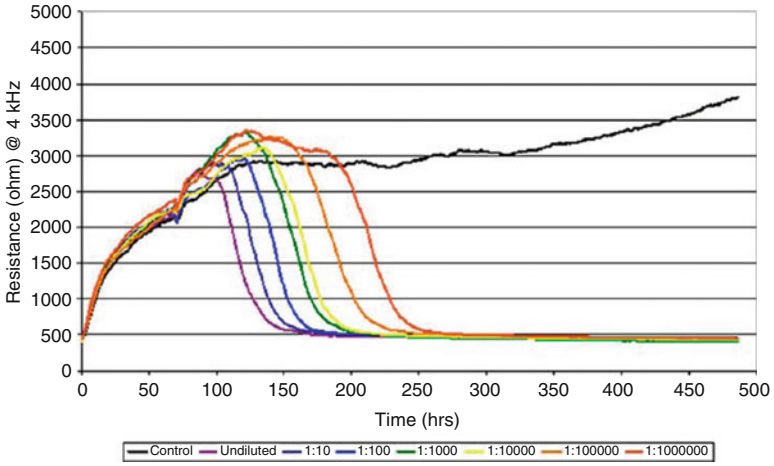

Fig. 10 Cytopathic Effects of Viral Infections Measured Using ECIS. Epithelioma cells from carp were inoculated into ECIS wells at time zero and allowed to grow. At ~70 post inoculation, cells were infected with serial dilutions of infectious hematopoeitic necrosis virus. Following a latent period of ~40 h for the *highest* titer, the resistive portion of the impedance began to drop and ultimately reached open electrode values as the cells were killed. *Lower* titers showed similar effects but with higher latent periods (Campbell et al. 2007)

3.3 Cancer Research

Of course, research requires funding and early on we got support from a private cancer organization, The National Foundation for Cancer Research, to apply biophysical approaches, such as ECIS, to the problem of cancer. We focused on prostatic cancer, and obtained a series of cell sublines from John Hopkins University. These cells were all derived from the same rat prostatic tumor but through mutagenesis and testing, eventually several different sublines were obtained that had varying metastatic abilities. If you took these cells and injected them into a rat, the G cell line essentially did not spread; they were at best weakly metastatic. If on the other hand you used a line referred to as AT2 then the cancer spread, but not very aggressively. Finally, the AT3 cell lines and the MML lines were very metastatic and would quickly spread throughout the rat. We wondered, could ECIS measurements be used to grade the metastatic ability of these cells? The reason this question it is important in real life is that if one gets prostate cancer, the cancer is normally very slow-growing, but occasionally it can be very virulent and life threatening. If you are diagnosed with prostate cancer, you do not know *a priori* what you have. So, if you have the one that grows very slowly, you do not have to do anything. If, however, you have the one that grows very rapidly, you have to do something fast, otherwise the cancer will spread probably to the bone marrow. So the interesting problem is, can you find out what kind of metastatic potential your cancer cells have without just waiting to find out?

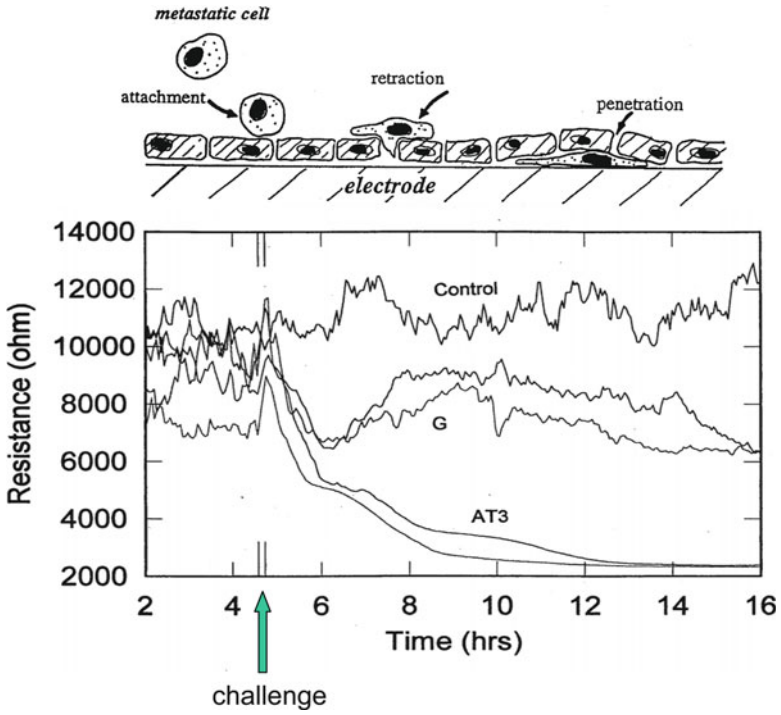

Fig. 11 The ECIS metastatic assay. To evaluate the metastatic potential of cells we attempted to see the extravasation process suggested in the cartoon. Here a layer of normal endothelial cells in tissue culture is challenged with a suspension of metastatic cancer cells. Previous workers had shown the activities depicted in the figure, where the metastatic cells attached to the normal cells and ultimately caused them to retract allowing penetration of the cell layer – a mimic of the in vivo metastatic process seen in vitro. In the ECIS experiment, impedance measurements began with a layer of confluent normal human endothelial cells (the first 2 h of the run are not shown). At the arrow, this layer was challenged by adding a suspension of either the weakly metastatic G or the highly metastatic AT3 rat prostate cancer cell subline obtained from researchers at Johns Hopkins. One well served as a control receiving the same treatment but without the cancer cells. In the two ECIS wells that received the highly metastatic AT3 subline, there was a striking drop in the resistive portion of the impedance as the normal cell layer was breached by the cancer cells, whereas the two wells that received the weakly metastatic G subline showed considerably less response (Keese et al. 2002)

The idea for the ECIS metastatic assay was based upon previous microscopic observations by others. First, we inoculated an ECIS array with HUVEC (human umbilical vein endothelial cells) using ECIS impedance signals to verify when we had established a complete monolayer of cells. When this was accomplished, suspensions of the rat prostatic cancer cells were added over the HUVEC layer where we expected the highly metastatic sublines would work through the layer just as *in vivo* to enter into the blood stream. In the control well where no cells were added over the endothelial layer, nothing happen. In the well where we used the G subline over the HUVEC cells, you could see a small change taking place. However, when

a highly metastatic subline, such as AT3, was added, there was an intense, easily detectable drop in impedance as the cancer cells disrupted the normal endothelial monolayer (Keese et al. 2002).

We found it very exciting that we could actually tell the difference between these different cell lines in an assay, ECIS and its relevance to cancer research was established. We have since tried many other prostate cancer cell lines that come from humans, and they all work very well in the assay. So we are now hoping that ECIS, which we have primarily sold to research scientists, can graduate from the academic laboratory to become a clinical instrument. Of course, at the moment, this is far away from being realized, but if it does happen, we may become rich. If not, it was fun anyway.

3.4 Invasive Electric Fields

Since we were looking at the cells using electrical fields, one question continually came up – Do the ECIS electrical fields cause changes to the cells? To answer this important question, we began to explore the use of higher currents and the resulting higher voltage drops across the cells. The normal noninvasive ECIS measurement was made using current in the microampere range. If we increased this ten times and applied this higher current for 1 s, there was no visible effect upon the cells both microscopically and in the ECIS measurement. But we did not stop there, and when the current was increased 50 times its normal level, the cells showed a small response and a quick recovery. Interestingly, the only way we could detect this effect was using ECIS itself in its low current mode; there were no detectable microscopic changes. The cells in some manner sensed the electrical fields (Lo et al. 2001).

Now at this point, we have to say very specifically, these ECIS fields were very high, so don't be afraid of talking on your cellular phone or of buying a house under a power line. These weak electrical field will not make you sick, but be aware, if you buy a house under a power line you may have difficulty selling the house, but other than that, you got a cheap house to begin with, so that should be okay.

Returning again to the cells, we did not stop with 50 times the current but continued on up to the milliampere range – 1,000 times that used in the normal measurement! When we reached this level, the high electrical field punched holes in the cell membrane, and the current passed directly through the cell membrane, and if you timed it just right, say a few hundred milliseconds, the holes sealed up. This is the well-known technique called electroporation. The reason such experiments are done is that the cell membrane is very selective, and therefore lots of molecules cannot enter into the cells. To get these molecules into the cells, you electroporate the cells. When these pores are open, the molecules diffuse into the cell, and when the pores seal, the cells are just as good as they were before the treatment but now with the membrane impermeable molecules within them.

The basic principle of the technique can be easily demonstrated using membrane impermeable fluorescence dye molecules in solution and a microscope. After mixing

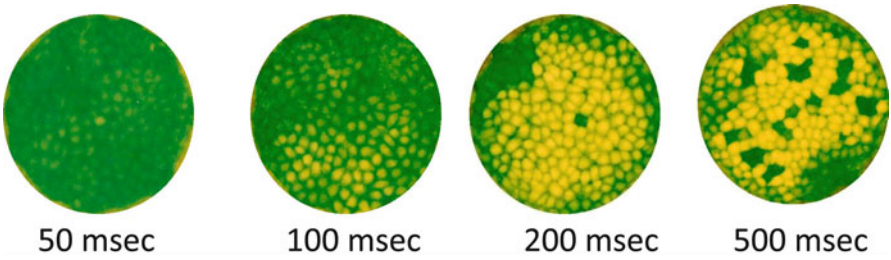

Fig. 12 Uptake of dye by electroporation. The figures show 4 of the 250 μm diameter electrodes that are being viewed in a fluorescence microscope. A confluent MDCK Type II cell layer was first grown upon the electrodes. The wells were next filled with of solution of the membrane impermeable dye, *Lucifer Yellow* and then a high current pulse was applied for the times indicated. The electroporation that ensued resulted in uptake of the dye into the cells, and the amount of dye increased as the length of the high current pulse increased. At 500 ms the pores in some cells have not resealed, and the dye has been lost from these presumably dead cells accounting for the dark areas that are evident

the dye molecules into the medium, one applies an electroporation shock to the cells. Later, looking at the cells in a microscope, one can see the fluorescent molecules inside the cells located on the electrode but not inside the surrounding cells.

When people do electroporation the ordinary way, they put the cells in a large chamber and apply very high voltage, since to punch hole in a cell membrane you will need about 1 V across the membrane. This requires a very large electric field of say 100,000 V/cm. By experimenting with our system we found that electroporation worked best at 40 kHz with about 3–4 V applied across the electrode. The reason we could get away with such a low voltage is that the cells are directly upon the small electrodes. By using these conditions we were able to put large molecules into the cells and then observe their effect on the still viable cells using the low ECIS monitoring current. This combined technique of using both invasive and non-invasive electric fields to study effects of membrane impermeable molecules is unique to the ECIS technology (Wegener et al. 2000; Stolwijk et al. 2011).

Later, we applied this ability to electrically break down the cell membranes to modify a procedure traditionally known as a "wound healing" assay. If you cut your finger, various cells will crawl (migrate) in to heal the wound. So early on, people tried "wound healing" in tissue culture. The idea was simple. First cells were grown in culture to form a confluent monolayer, and then one would scrape the cell sheet with a pipette tip or other sharp object to create the "wound" – an open swath of cells maybe 1 or 2 mm wide. One could then microscopically watch the healthy cells as they crawled back in to "heal" or repopulate the open area. This took several hours or even days as cells typically crawl at only a few micrometers per hour. This has become a traditional way of doing cell migration measurements in tissue culture, but it is fraught with problems of reproducibility and quantification.

To carry out wound-healing assays with ECIS, we used the same conditions established for electroporation, except now we applied the high field for maybe 15 s. When we did this, the cells were instantly killed and detached from the electrode's surface. This event was easily seen in the time course changes in the

impedance. Upon application of the high field for 15 s, the resistance of the cell-covered electrode plummeted to levels associated with the bare electrode, the "wound" had been established. Now the cells came crawling in from all sides to repopulate the open area. As they did, the impedance began to gradually increase until the "wound" was completely "healed" and a new healthy monolayer of cells was reestablished upon the electrode. In the time from the high current application until the impedance returned back to control levels, the cells had moved the 125 μm radius of the small circular electrode. The migration rate was simply the ratio of these numbers. To obtain this migration rate traditionally would have required a great deal of technical labor; with ECIS it was done without even opening the door of the cell incubator (Keese et al. 2004).

4 Applied BioPhysics

4.1 The Beginning Years

We are in business today because there was a change of directors at the GE Research Laboratory towards the end of 1980s, and the new director's motto was: "All research at GE R&D center should be directly connected to *present* GE products and processes". Well, our work was not, and before long we were both at Rensselaer Polytechnic Institute (RPI) where we could continue our research. We were fortunate to have a small grant from The National Foundation for Cancer Research (NFCR), but we found it difficult to obtain funding for interdisciplinary research from the traditional government agencies. We tried for an R01 grant from NIH and were promptly rejected. Then Charlie learned about the Small Business Innovation Research (SBIR) program and suggested that we start a business to take advantage of this opportunity. Ivar was not enthusiastic about this change in our program, but recognized that it was necessary to be able to continue to work together.

Briefly speaking, all government agencies that give grants for university research have to spend 2–2.5% of their budget on SBIR research grants to small businesses. The research must be shown to ultimately have the potential for commercialization. To qualify, at least one person involved has to work for the business more than 51% of their time, and the business must be a domestic US company with fewer than 500 employees. The grants are given out in three phases: Phase I currently funds up to $150,000 to be used in a 6 month feasibility study to try out your idea. If you are successful in Phase I, you can apply for a $1,000,000 Phase II grant with 2 years to take the idea to the edge of commercialization. In the last phase, Phase III, you get no more money but are expected to commercialize your idea.

Our second attempt to get a SBIR Phase I grant (which by the way was based on the rejected R01 proposal to NIH) was successful, and in principle we were on our way. But wait a minute; we did not really have a business. So we went to a lawyer who incorporated us for $562.86. That was easy, except for deciding on a name for the business. Imitating Hewlett-Packard, Ivar thought we should call it Giaever & Keese but Charlie preferred Keese and Giaever. Since one name was difficult to

spell let alone pronounce, we finally compromised with Applied BioPhysics, Inc. One thing you have to do in business is to have an accountant, because in our opinion, there is very little difference between startup companies and GE or IBM as far as the Internal Revenue Service is concerned. We also had a choice of becoming a C-corporation or an S-corporation and were advised to chose the latter. In an S-corporation the owners have to take the profit every year on their own income tax, and we believe the accounting is a little simpler. The main thing is that you must have limited liability protection.

We also needed a location. Fortunately, in an old brick building at the edge of the campus, RPI had a business incubator where fledgling small high tech business startups could share Xerox machines, secretaries, meeting rooms, internet connections, etc. For RPI, the incubator was just a break even proposition, but for us it was home and a place hopefully to grow. On a bitterly cold New Year's Eve day in 1993 we rented a Ryder truck, hauled used furniture and equipment and moved in – Applied BioPhysics was on its way.

We were fortunate, our Phase I grant qualified us for the more lucrative Phase II grant, and we had some financial breathing room. We also sold our first unit to a medical school in the Midwest. The sale was entirely by word of mouth, because at that time we only advertised our efforts with publications and talks and posters at scientific conferences. We were certainly not properly prepared for this sale, as we did not have a user-friendly computer program at hand. We both went to install our first commercial machine, and Ivar can remember programming maybe 12 h in one stretch at the medical school to get the system up and running. When we left we were very proud of the instrument, and we had sold something and were really in business and making a small, but very real, profit.

Then as today, when you buy the ECIS system you must also buy the consumable electrode arrays, and this provides a steady flow of extra income. Making the arrays from raw materials was very labor intensive and to free up our time to continue research and grow the company, we hired a technician – our first technical employee. To this date, most of the electrode arrays are made in-house using photolithographic methods, and we have this process well in hand.

We sold a few more systems back in the 1990s but still only to people that we knew or had interacted with in the past. For example a lucky sale came about because Ivar was invited to give a lecture at a conference in Japan. A physiologist translated his talk, and he ended up buying a unit.

All along we continued to improve the system, and we got some free advertising here and there. For example **Nature** called us out of the blue and asked us to write a product review that created some inquiries. Then **Business Week** ran a little story about how ECIS could result in using fewer animals for toxicity testing, and as a result, several people, including an investment firm, wanted to invest in us, but we did not think we were ready for that. We were on radio show "Pulse of the Planet", because for fun we interpreted the impedance fluctuations of the cells as music, and "The song of the cancer cells" sounded sexy to many people.

In spite of all of these fortunate happenings, sales continued relatively slowly and were more or less random happenings. Our only presence in the media was our website – biophysics.com – and that domain name remains probably one of our

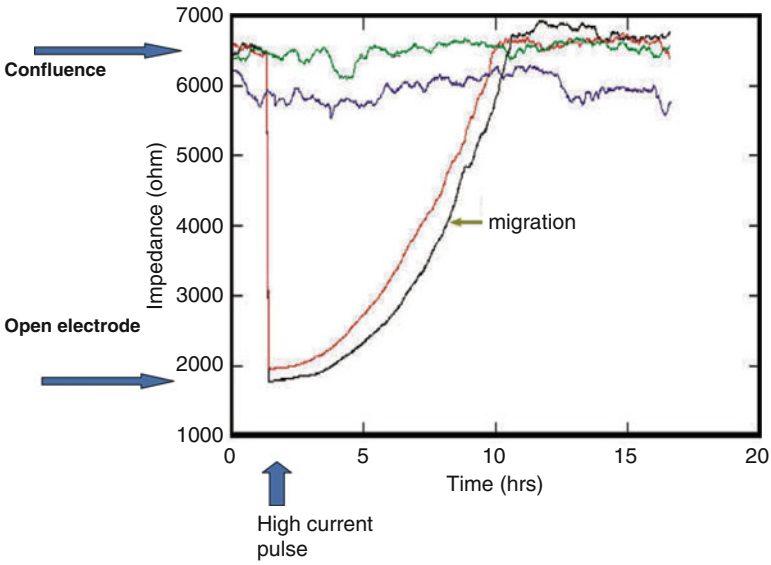

Fig. 13 The ECIS cell migration assay. BSC-1 cells were grown to confluence in four wells containing the 250 μm diameter ECIS electrodes and their impedance was followed at 4,000 Hz. Approximately 2 h into the run, two of the electrodes received high milliampere current pulses (40,000 Hz) for several seconds killing the cells upon the electrodes and dropping their impedance to that of open, cell-free electrodes. Over the next several hours, the impedance of these electrodes returns to control levels, as cells migrate inward to repopulate the electrodes. Assuming the cells move at a fixed radial speed, they migrate the 125 μm radius in approximately 7 h for a migration rate of ~17 μm/h

strong assets. Even though we were early in that game, a web site is not very effective by itself. We had maybe ten visitors to the site every day, but many of those were searching for cell phones and not mammalian cells. We then tried to participate in a few tradeshows. First we entered conference for SBIR companies, but that was not very successful for us, because we did not come in contact with any biologists. Later we tried the American Society for Cell Biology, and in spite of actually bringing live cells and a complete incubator and ECIS system to the show, we were mainly a curiosity and didn't get serious leads.

4.2 The Importance of Marketing

It was becoming increasing clear to us that we needed help, and it was one of life's wonderful coincidences that at the turn of the twenty-first century, Chris Dehnert, an electrical engineer with a MBA, came walking through the door. After some negotiations we accepted him as a partner if his work with us could significantly increase sales. It is clear to us now that our new partner has had a very significant impact, not only on our business, but also upon our thinking.

There is a myth that technical people do not have the foggiest notion of how to market their inventions, and we can testify that the myth is in fact reality. We had, for example, talked about making a brochure for several years; Chris had completed one after only 1 month. In April of 2001 we participated in a third trade show at Experimental Biology in, Orlando, Florida. Unlike our previous experiences, this time we mailed out several thousand cards beforehand to those going to the show. We also paid an extra amount to get a booth in a choice location and had graphic artists help give us an informative and professional appearance. The show was a real success, and we received many serious inquiries that we followed up and that eventually became sales. This strong response was heartening and reassured us of the real need for our instrument. A relatively recent proof that we had a good and useful idea is that we have acquired competitors, who essentially have copied what we did – the truest form of flattery. The market place is an unbiased judge, and perhaps we should have taken on investor's money earlier when we had a chance. One never knows these things for sure.

4.3 Looking Towards the Future

As we look to the future, we have learned that one of our biggest current obstacles is overcoming the limited understanding of electrical circuits and impedance by many biologists. Thus we need to develop better methods to explain and demonstrate our technology. We have also learned that fundamentally new approaches to solve a problem are accepted slowly by the marketplace and that a lot of work on our part is needed to prove that the system works as promised. We hope this will get easier as more key researchers in each of our markets adopt the ECIS approach. Our next big challenge is to penetrate the pharmaceutical industry and in particular to appeal to their need for new high throughput assays. This market is not nearly as sensitive to price as our academic customers. Industrial concerns are primarily looking to increase efficiency, and, in addition, to obtain more effective measurements. To this point, we initially introduced a 96 well ECIS machine that measured only simple impedance; we now have introduced another 96 well machine that can measure complex impedance to provide more relevant information to the pharmaceutical researcher. Again, this is where the old fashioned approach of asking the customer what he needs and listening closely works best. This is how we intend to grow Applied BioPhysics and to define products that will be successful in the marketplace providing researchers with new approaches to their research.

Reference

Campbell CE, Motzfeldt-Laane M, Haugarvoll E, Giaever I (2007) Monitoring viral induced cell death using electric cell-substrate impedance sensing. Biosens Bioelectron 23(4):536–542

Giaever I, Keese CR (1984) Monitoring fibroblast behavior in tissue culture with an applied electric field. Proc Natl Acad Sci USA 81:3761–3764

Giaever I, Keese CR (1986) Use of electric fields to monitor the dynamical aspect of cell behavior in tissue culture. IEEE Trans Biomed Eng BME-33:242–247

Giaever I, Keese CR (1991) Micromotion of mammalian cells measured electrically. Proc Natl Acad Sci USA 88:7896–7900

Keese CR, Giaever I (1983) Cell growth on liquid microcarriers. Science 219:1448–1449

Keese CR, Bhawe K, Wegener J, Giaever I (2002) Real-time impedance assay to follow the invasive activities of metastatic cells in culture. Biotechniques 33:842–850

Keese CR, Wegener J, Walker S, Giaever I (2004) Electrical wound-healing assay for cells in vitro. Proc Natl Acad Sci USA 101:1554–1559

Lo CM, Linton M, Keese CR, Giaever I (2001) Correlated motion and oscillation of neighboring cells in vitro. Cell Commun Adhes 8(3):139–145

Reddy L, Wang H, Keese CR, Giaever I, Smith T (1998) Assessment of rapid morphological changes associated with elevated cAMP levels in human orbital fibroblasts. Exp Cell Res 245:360–367

Stolwijk J, Hartmann C, Balani P, Albermann S, Keese CR, Giaever I, Wegener J (2011) Impedance analysis of adherent cells after in situ electroporation: non-invasive monitoring during intracellular manipulations. Biosens Bioelectron 26:4720–4727

Tiruppathi C, Malik A, Del Vecchio PJ, Keese CR, Giaever I (1992) Electrical method for detection of endothelial cell shape change in real time: assessment of endothelial barrier function. Proc Natl Acad Sci USA 88:7919–7923

Wegener J, Keese CR, Giaever I (2000) Electroporation of adherent cells on a conductive substrate and electrical in situ monitoring of the cell response. Biotechniques 33:348–357

Protein Kinase C Isoforms in the Formation of Focal Adhesion Complexes: Investigated by Cell Impedance

Havovi Chichger, Katie L. Grinnell, and Elizabeth O. Harrington

Abstract Protein kinase C (PKC) is a ubiquitous family of ten serine-threonine kinases involved in transmitting signals throughout the cell and a key regulator in numerous cellular functions, including cellular proliferation, apoptosis, adhesion, migration, and monolayer integrity. PKC isoforms are thought to modulate cellular function through enzymatic phosphorylation of substrates, however few have been identified. We will review the evidence demonstrating crosstalk between the PKC family of enzymes and the focal adhesion complex structure and how modulation of these cell-extracellular matrix interactions affects cell function. We will further review how investigations measuring changes in cell impedance have provided insight in the role of PKC in regulation cell function through the focal adhesion complexes.

Keywords Protein kinase C • Focal adhesion • Cell impedance • Cell-extracellular matrix • Focal adhesion kinase

Abbreviations

PKC	Protein kinase C
ECM	Extracellular matrix
MAPK	Mitogen activated protein kinase
DAG	Diacylglycerol
MLC	Myosin light chain
FAK	Focal adhesion kinase
HSP90	Heat shock protein 90

H. Chichger • K.L. Grinnell • E.O. Harrington, Ph.D. (✉)
Vascular Research Laboratory, Providence VA Medical School, Department of Medicine, Warren Alpert Medical School of Brown University, Providence, RI, 02908, USA
e-mail: Elizabeth_Harrington@brown.edu

W.G. Jiang (ed.), *Electric Cell-Substrate Impedance Sensing and Cancer Metastasis*, Cancer Metastasis - Biology and Treatment 17, DOI 10.1007/978-94-007-4927-6_2,

PLC	Phospholipase C
PIP_2	Phosphatidylinositol 4,5-bisphosphate
PDK-1	Phosphoinositide dependent kinase-1
mTOR2	Mammalian target of rapamycin complex-2
RACK	Receptors for activated C kinase
AKAP12	A-kinase anchoring protein-12
INAD	Inactivation no after potential D
MEK	MAP kinase kinase
PAK	p21-Activated kinase
ECIS	Electrical cell-substrate impedance sensing
TEER	Trans-epithelial electrical resistance
HSP70	Heat shock protein 70
LIMK	LIM kinase
PLD2	Phospholipase D2
S1P	Sphingosine 1-phosphate
LPA	Lysophosphatidic acid
VASP	Vasodilator-stimulated protein
MLCK	myosin light chain kinase

1 Introduction

1.1 Protein Kinase C (PKC)

1.1.1 Family and Structure

Protein kinases are fundamental signaling molecules involved in regulating cell growth, differentiation, proliferation and death, specifically in embryogenesis and angiogenesis. The protein kinase C (PKC) family of serine/threonine kinases is comprised of ten established isoforms, divided into three subgroups depending on their structure and the cofactor(s) required for activation (Fig. 1). The conventional PKC subfamily consists of PKCα, the alternatively spliced variants, β_I and β_{II}, and γ. All conventional PKC isoforms are activated by diacylglycerol (DAG), phorbol esters or calcium; whereas, the novel PKC isoforms, δ, ε, η, and θ, are activated in a calcium-independent manner by DAG and phorbol esters and the atypical PKC isoforms, ζ and λ/ι, are activated independently of DAG, phorbol esters and calcium. The latter subgroup of PKC isoforms are stimulated by protein-protein interactions mediated by their Phox and Bem1 (PB1) domain and carboxyl terminal PDZ ligand (Lamark et al. 2003) and potentially in response to growth factor signaling (Neri et al. 1999). PKC isoforms are expressed as cytosolic proteins until recruited to the plasma membrane upon activation by effectors. PKC proteins are ubiquitously expressed, with PKCα the most widely expressed, found in most peripheral tissue including the spleen, liver, brain, kidney, muscle, heart and lung (Kosaka et al. 1988).

PKC family members share a conserved carboxyl-terminal kinase domain linked by a flexible hinge segment to an amino-terminal regulatory domain. The

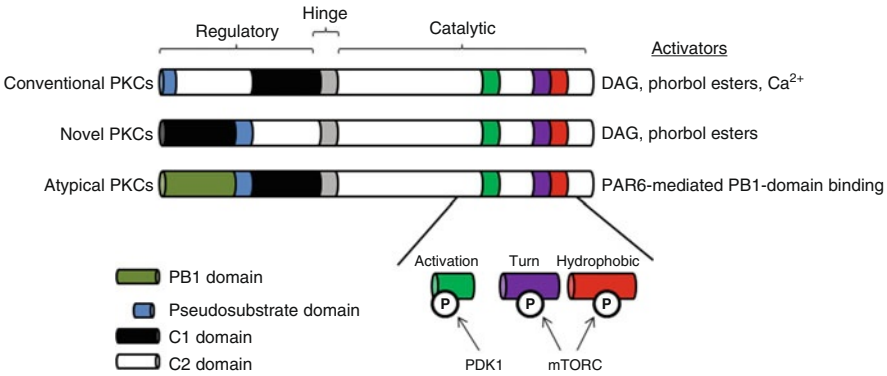

Fig. 1 ***Protein Kinase C isoforms: Schematic diagram of the domain structure of the mammalian PKC family.*** The PKC family is divided into three subgroups with differing regulatory domains and activators to relieve auto-inhibition via the pseudosubstrate domain. Conventional PKCs (α, β_I, β_{II} and γ), novel PKCs (δ, ε, η and θ) and atypical PKCs (ζ and λ) share a catalytic domain containing an activation, turn and hydrophobic motif. The activation loop is phosphorylated at serine and/or threonine by PDK1 to activate the PKC whilst the turn and hydrophobic regions are phosphorylated at serine residues by mTORC to stabilize the active PKC conformation (Figure adapted from Rosse et al. 2010)

carboxyl tail of PKC acts as a phosphorylation-dependent docking site for regulatory molecules, whilst the amino terminal contains an auto-inhibitory pseudosubstrate sequence responsible for maintaining the inactive PKC state by occupying the substrate binding cavity within the kinase domain. Additionally, the regulatory domains C1 and C2 are located within the amino-terminus and mediate ligand binding and enzymatic activation. The C1 regulatory domain consists of 1–2 tandem repeats of cysteine-rich zinc fingers, which are responsible for interactions with membrane-bound DAG and phorbol esters. The C1 domain of different isoforms exhibits varying affinities for secondary lipid messengers, enabling specific targeting and activation of the relevant isoform, depending on the signal released. The amino-terminal region of conventional PKC isoforms contains a C1 domain to bind DAG and a C2 domain for calcium-dependent phospholipid-binding. This PKC subgroup is primarily found in the cytosol awaiting calcium binding in the C2 domain, after which the PKC is translocated to the plasma membrane and the C1 domain binds membrane-bound DAG resulting in enzymatic maturation. The conformational changes associated with lipid-binding of conventional PKC isoforms generate the release of the pseudosubstrate domain from the substrate-binding cavity, freeing the isoform for catalytic activation and subsequent substrate phosphorylation (Orr and Newton 1994). The C2 domain, of conventional PKC isoforms binds calcium to induce conformational changes, whereas novel PKC isoforms contain a variant of the C2 domain, specific to this subgroup, which is insensitive to calcium (Sossin and Schwartz 1993). This C2 region is regulated by phosphorylation to enhance the ability of novel PKCs to bind to membranes. Atypical PKC isoforms are comprised of a variant of the C1 domain with an impaired ligand-binding pocket.

1.1.2 Regulation of PKC

Phosphorylation

PKC phosphorylation is directed to three conserved regions in the C-terminus: the activation loop, the turn motif and the hydrophobic motif. All three conserved regions within the C-terminus are important in controlling the catalytic activity, protein stability, and intracellular localization of PKC (Orr and Newton 1994). PKC phosphorylation is affected by the conformation of the isoform. Immediately following translation, when the PKC protein is in an open conformation, the N-terminal pseudosubstrate domain does not block the substrate binding site within the kinase domain. Instead, the heat shock protein-90 (HSP90) binds to the conserved amino acid motif, PXXP, found within the carboxy-terminus end of the kinase domain (Gould et al. 2009). PKC is then phosphorylated by phosphoinositide dependent kinase-1 (PDK-1) in the activation loop at the plasma membrane (Dutil and Newton 2000; Orr and Newton 1994). Upon dissociation of PDK-1, mammalian target of rapamycin complex-2 (mTORC2)-mediated phosphorylation occurs in the turn and hydrophobic motifs of PKC. This series of phosphorylation events enables the PKC enzyme to adopt a closed conformation in the cytosol, with the pseudosubstrate domain occupying the substrate-binding site, while awaiting activation by secondary messenger molecules (Marín-Vicente et al. 2008; Newton 2010; Pearce et al. 2010; Stensman and Larsson 2007). PKC activation is mediated by receptor-dependent activation of phospholipase C (PLC), triggering the hydrolysis of phosphatidylinositol 4, 5-bisphosphate (PIP_2), resulting in the production of DAG and a rise in intracellular calcium; cofactors key for the activation of multiple PKC isoforms. Once activated, PKC translocate to the plasma membrane where binding with phospholipids occurs.

Phosphorlyation of PKC occurs posttranslationally to prime the isoform for catalytic activation in response to lipid second messengers, such as DAG. However, recent studies have found that PKC isoforms may be stimulated solely by phosphorylation, and potentially independently of interactions with secondary lipid messenger molecules, in regions of the PKC which are non-conserved, variable regions within specific isoforms (Freeley et al. 2011). Novel phosphorylation sites in PKC are continuously being identified; some of which can be constitutively phosphorylated, while others are more dynamically regulated.

As stated above, the phosphorylation of the three conserved regions of PKC serves to regulate its activity, stability, and subcellular localization. Within the activation loop of PKC, phosphorylation by PDK-1 is vital for enzymatic catalysis and stabilization of the active conformation by ionically crosslinking the activation loop to the kinase domain via a series of hydrogen bonds (Huse and Kuriyan 2002). Mutational studies within the activation loop of most PKC isoforms cause the abolition of kinase activity (Orr and Newton 1994) with the exception of PKCδ. The PKCδ isoform is stabilized via a series of amino acids, located NH_2-terminal relative to the kinase domain, which are predicted to form a number of hydrophobic chains stabilizing the folded molecule (Liu et al. 2006). Similar to the activation loop, phosphorylation of the turn motif influences PKC stability; however, phosphorylation

of this region is not essential for catalytic activity. Phosphorylation of the PKC turn-motif at a conserved leucine residue regulates PKC stability by promoting the interaction with the chaperone protein, heat shock protein-70 (HSP70); these protein-protein interactions protect PKC from degradation hence preserving enzymatic function (Gao and Newton 2006). The hydrophobic motif site for phosphorylation is also responsible for PKC protein stability, with intramolecular hydrogen bonds forming between the phosphate group and an invariant glycine residue within this motif. However, this site is absent in atypical PKC isoforms, which possess a glutamic acid residue in the hydrophobic motif site and plays the same role in protein stabilization (Parekh et al. 2000). Additionally, the hydrophobic motif can act as a docking site for the activation loop kinase, PDK1 (Balendran et al. 2000). This tightly regulated and constitutive phosphorylation of PKC isoforms, via binding of cofactors and a myriad of effector proteins, including PDK-1, HSP90, and the mTORC2 heteromeric protein complex, matures the isoforms to ensure stability and catalytic ability (Ikenoue et al. 2008; Le Good et al. 1998). Indeed cells lacking the mTORC2 complex are unable to phosphorylate PKC and thus PKC enzymatic and protein levels remain low as the majority of PKC remains unphosphorylated and highly susceptible to degradation (Ikenoue et al. 2008).

Protein Scaffolding

In addition to the regulation of PKC function via phosphorylation, scaffold proteins have also been identified as an essential part of PKC regulation. The binding of the receptors for activated C kinase (RACK) family of scaffold proteins to PKC relieves autoinhibition (Ron and Mochly-Rosen 1995), as well as enables the locking of PKC in its activated conformation, resulting in sustained PKC signaling in the absence of ligand-binding via secondary messengers (Mochly-Rosen and Gordon 1998). This family of scaffold proteins has also been shown to bind to select PKC isoforms causing the subcellular compartmentalization of the isoforms in the proximity of its targeted substrates, bestowing signaling specificity and cell function of the isoforms (Mackay and Mochly-Rosen 2001). Since the discovery of the RACK proteins, PKC has also been shown to interact with other scaffold proteins, including the A-kinase anchoring protein-12 (AKAP12), also called *src*-suppressed C kinase substrate (SSeCKs) or Gravin (Guo et al. 2011), as well as a protein termed Inactivation No After potential D (INAD) identified in *Drosophila melanogastser* (Venkatachalam et al. 2010). As such, peptide motifs within these scaffold proteins might be used as tools to regulate select PKC isoforms by promoting or preventing subcellular targeting of select PKC isoforms, as described by some investigators (Mackay and Mochly-Rosen 2001).

Downregulation via Dephosphorylation and Proteolysis

Downregulation of the PKC enzymes also occurs. Leontieva and Black have described two pathways by which PKC is downregulated via degradation. One mechanism

involves the ubiquitination and subsequent proteosomal degradation of the mature, phosphorylated form of PKC, whereas the other pathway involves the translocation of caveolae-associated PKC to the perinuclear region, where it is dephosphorylated and proteolyzed (Leontieva and Black 2004). The dephosphorylation events are thought to occur when PKC is maintained in the open conformation during prolonged periods of activation. This allows for protein phosphatases to target residues important in PKC activation. The PH domain leucine-rich repeat protein phosphatase (PHLPP) was recently identified as a phosphatase responsible for PKC downregulation via dephosphorylation of the hydrophobic motif, but not of the turn motif or the activation loop (Gao et al. 2008). In addition, okadaic acid sensitive protein phosphatases are also thought to downregulate PKC via dephosphorylation (Gao et al. 2008), however the precise phosphate involved has not yet been identified.

1.1.3 PKC Signal Transduction

PKC isoforms transduce signals in response to numerous growth factors, including vascular endothelial growth factor (VEGF) and platelet derived growth factor (PDGF). PKC is particularly critical in signaling by the latter. PDGF binds to its receptor to stimulate the turnover of phosphoinositol via the activation of PLC, resulting in elevated DAG and calcium and subsequent activation of PKC (Moriya et al. 1996). Subsequent PKC phosphorylation and activation of cRaf-1, the serine/threonine kinase responsible for the signaling cascade of MAP kinase (MAPK) and MAP kinase kinase (MEK), results in direct phosphorylation of transcription factors, such as c-Jun. In a similar ligand-receptor binding scenario, PKC-mediated substrate phosphorylation is responsible for the stimulation of membrane proteins, such as transporters and receptors, cytoskeletal proteins involved in cellular structure, as well as the transcription of structural proteins (Soh 2011). Through these effects of PKC activation, the kinase is able to induce cell proliferation and adhesion to the extracellular matrix (ECM). Prolonged treatment with phorbol esters has been shown to cause sustained activation of PKC and amplify these effects of receptor-ligand binding on the kinase. However, this increased PKC activity can exert contradictory functions on cell migration and proliferation depending on the PKC isoform studied (Ács et al. 1997; Harrington et al. 1997), leading to pathologic changes (Gomez et al. 1999). For example, PKCα activation results in increased cancer cell invasiveness, with overexpression noted in prostate and bladder cancer, whilst down-regulation of the isoform has been reported in colon cancer cells (Aziz et al. 2007). Despite the variation in PKC expression associated with different tumours, agents able to modulate PKC are currently under clinical trials, such as the PKC activator, bryostatin-1 and the phospholipid analogues edelfosine and ilmofosine.

In addition to the regulation of tumor cells, the activation of PKC by phorbol esters promotes endothelial monolayer permeability, whereas PKC inhibition reduces thrombin, cytokine and growth-factor mediated disruption of the endothelial monolayer. Endothelial cells express many PKC isoforms, including α, β, δ, ε, η, λ, μ and ζ (Klinger et al. 2007), involved in the contraction of microvessel endothelial cells and intercellular gap formation. For example, PKCα overexpression promoted an augmented response of

microvascular endothelial cells to thrombin-induced barrier disruption (Harrington et al. 2003). These alterations in endothelial permeability correlate with the enhanced agonist-induction of stress fibers and signaling via the small G-protein, RhoA (Holinstat et al. 2003). Conversely, PKCδ has been shown to be an important regulator of endothelial barrier function in the absence of agonists; with inhibition of PKCδ promoting barrier dysfunction and overexpression of the isoform causing a tighter monolayer (Harrington et al. 2003; Klinger et al. 2007). PKC is one of many families of protein kinases which have been shown to phosphorylate components in focal adhesions, indeed PKC isoforms α, δ, and ε have been identified as a major component of immature focal adhesions, suggesting a role for PKC in maturation of focal adhesions (Barry and Critchley 1994; Haller et al. 1998; Lim et al. 2003).

1.2 Cell-Extracellular Matrix (ECM) Structures

1.2.1 Structural Definition and Mechanical Role

Adhesion of various cell types, including endothelial cells, to the ECM surface regulates many functions, such as migration, proliferation, apoptosis, monolayer permeability, differentiation, and morphology (Cheresh and Stupack 2008; Romer et al. 2006). Adhesive interactions with the ECM are established by multiple structures such as integrins, heparin sulfate proteoglycans, and glycosaminoglycans. These cell-ECM interactions in turn mechanically link the cells to its environment by monitoring changes in biochemical and physical stresses (Zaidel-Bar et al. 2004; Zaidel-Bar and Geiger 2010). The integrin-mediated adhesive structures are termed focal adhesions, fibrillar adhesions, and focal complexes; each defined as multimeric protein complexes incorporating distinct subsets of proteins (Table 1) (Critchley 2000; Ridley et al. 2003; Turner 2000). Focal complexes are early cell-ECM adhesions that are small in size and typically found at the edge of migrating cell protrusions, such as lamellipodia and filopodia. Newly formed focal complexes consist of protein aggregates of αβ integrin pairs, paxillin, and talin. Mature focal complexes have recruited additional proteins including focal adhesion kinase (FAK), vinculin, VASP, and α-actinin. Focal complex formation is mediated by Rac1 activation of p21-activated kinases (PAK). PAK in turn regulates actin stress fiber formation through activation of LIMK and inhibition of myosin light chain kinase (MLCK). Focal complexes transform into the larger focal adhesions upon clustering of integrins and recruitment of additional proteins, including zyxin and tensin, and polymerized actin via a RhoA–mediated pathway. Focal adhesions are larger adhesive structures associated with the ends of bundles of actin stress fibers. Finally, fibrillar adhesions form from focal adhesions upon $\alpha_5\beta_1$ integrin medated interactions with fibronectin fibrils. Focal complexes formed in the periphery of migrating cells exert stronger tractional force on the ECM than do focal adhesions (Beningo et al. 2001). Yet, in stationary cells, focal adhesions generate greater adhesive forces than do focal complexes (Geiger and Bershadsky 2001).

Table 1 Integrin-mediated ECM adhesive structures

Adhesive structure	Proteins associated with structure
Focal complex	$\alpha_v\beta_3$, talin, paxillin, α-actinin, Arp2/3, VASP, FAK, vinculin, phosphotyrosine
Focal adhesion	$\alpha_v\beta_3$, talin, paxillin, α-actinin, Arp2/3, VASP, FAK, vinculin, phosphotyrosine, tensin, zyxin
Fibrillar adhesion	$\alpha_v\beta_3$, talin, paxillin, α-actinin, Arp2/3, VASP, FAK, vinculin, phosphotyrosine, tensin, zyxin, $\alpha_5\beta_1$

Adapted from Zaidel-Bar et al. 2004

Integrins are heterodimeric transmembraneous glycoprotein receptors which anchor the ECM to the actin cytoskeleton via scaffold proteins. Integrin receptors are comprised of α and β subunits, which are non-covalently associated. The cytoplasmic tails of β integrins are responsible for the localization of the integrin within the focal contacts. There are currently 18 α subunits and 8 β subunits, resulting in 24 potential integrin subunit pairings; with the heterodimeric αβ pairing determining the ligand binding affinity. Integrins participate in transmitting signals into and out of cells, often referred to 'inside out' signaling (Ginsberg et al. 1992). Modification of the cytoplasmic domain of the integrin pair by intracellular signaling proteins, such as phosphorylation, lipid binding, or protein-protein interactions, can lead to altered integrin affinity with the extracellular ligand resulting in modulated cellular functions, including adhesion, migration, proliferation, aggregation, apoptosis, and cell cycle progression. As described above, the integrin-mediated cell-ECM interactions are established via the aggregation of a number of proteins. Recently, Zaidel-Bar and colleagues reported over 150 different proteins components establish cell-ECM structures with greater than 690 interactions occurring amongst these components to regulate these dynamic structures (Zaidel-Bar et al. 2007). This review will hone in on a few key components, however, an extensive listing may be found at the ADHESOMEFAnetwork (www.adhesome.org) and in Zaidel-Bar et al. (2007).

Another component critical to establishing cell-ECM interactions is FAK. FAK is a ubiquitously expressed cytoplasmic, non-receptor tyrosine kinase responsible for relaying signals from soluble growth factors, cytokines, mechanical stimuli, and integrin arrangement. FAK was initially shown to be recruited to focal adhesions upon integrin receptor clustering and ligation with ECM protein, resulting in FAK activation. FAK activation, in turn, promotes the formation of a signaling complex with c-src and adaptor proteins, including $p130^{CAS}$ and paxillin, and leading to regulation of cellular functions, such as cell motility (Mitra and Schlaepfer 2006). Other recent data has shown that FAK regulates the integrin-mediated cell adhesive and contractility forces at the focal adhesion complex in a vinculin-dependent manner, suggesting modulation of cell-ECM response by FAK (Dumbauld et al. 2010; Michael et al. 2009). Furthermore, in settings of FAK inhibition or ablation, cell spreading and stress fiber formation is inhibited and cells can undergo apoptosis (Almeida et al. 2000; Ilic et al. 1995, 1998; Richardson et al. 1997; Sieg et al. 2000), however data suggests disparate functional role of FAK depending on the cell type examined. For example, conditional suppression of FAK protein in mouse endothelial cells caused an embryonic lethal phenotype through dysregulated angiogenesis and

increased endothelial cell apoptosis (Shen et al. 2005). Conversely, a conditional deficiency in FAK activity protected epidermal cells from chemically induced tumorigenesis via apoptosis, and caused disrupted cell-ECM interactions in neuronal cells without significantly affect apoptosis (Beggs et al. 2003; Essayem et al. 2005).

1.2.2 Regulation of Cell-ECM Dynamic Flux

The cell-ECM interactions are in a constant state of flux with focal adhesion structures assembled and disassembled, growing and shrinking in size, and relocalizing within the cell depending upon signals which are transmitted from external and internal sources. Monomeric small GTPases, RhoA and Rac1, are intimately involved in the dynamic flux of focal adhesion formation and disruption. RhoA is stimulated through increased tension and is associated with the recruitment of multiple effector proteins, clustering of integrin molecules, and actomyosin filament contraction to form focal adhesions (Chrzanowska-Wodnicka and Burridge 1996); whereas, Rac1 activation of PAK promotes focal complex maturation into focal adhesions through action on LIMK and MLCK (Brown et al. 2002). PAK activation has also been implicated in focal adhesion disassembly or turnover (Zhao et al. 2000).

RhoA regulates cell function by modulating the formation of stress fibers and focal adhesions through signaling pathways both dependent upon and independent of Rho kinase (Adamson et al. 2002; Garcia et al. 1999; Hirase et al. 2001; van Nieuw Amerongen et al. 1998). The RhoA-Rho kinase dependent pathway enhances the level of myosin light chain (MLC) phosphorylation by inhibiting its dephosphorylation by MLC phosphatase or by direct phosphorylation. Other investigators have demonstrated a role for paxillin in regulating focal adhesion turnover. Paxillin phosphorylated on residues Y^{31} and Y^{118} can compete with the p190RhoGAP/p120RasGAP complex for p120RasGAP, resulting in the release of p190RhoGAP to act on and inhibit RhoA (Tsubouchi et al. 2002). Also, paxillin binding with Crk results in Rac1 activation (Lamorte et al. 2003; Valles et al. 2004). Furthermore, phorbol ester activation of PKC has been shown to block paxillin Y^{31} and Y^{118} phosphorylation (Schmidt and Hall 2002). Our studies have demonstrated the PKCδ isoform to regulate focal adhesion stabilization and actin polymerization through a RhoA and FAK dependent process, but independent of p190RhoGAP (Fordjour and Harrington 2009; Harrington et al. 2003; Klinger et al. 2007).

1.3 Assessment of PKC Regulation of Focal Adhesion Complexes via Measuring Cell Impedance

1.3.1 Principles of Cell Impedance Technology

Electrical Cell-substrate Impedance Sensing (ECIS) is a tool useful in assessing the adhesive properties of cells in real time. Created by Giaever and Keese (Giaever and Keese 1993), this biosensor involves the use of specialized slides containing a series

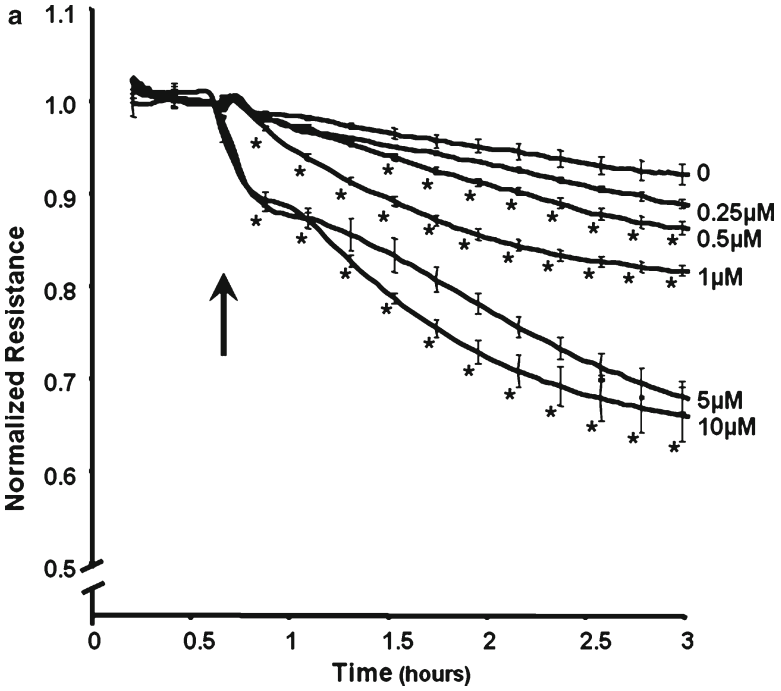

Fig. 2 Interogation of the role of PKCδ in endothelial cell function *in vitro* and *in vivo.* *Panel a:* Changes in endothelial monolayer permeability were assessed in rat lung microvascular endothelial cells by assaying changes in resistance of endothelial monolayers grown on collagen coated gold electrodes (8W10E) using the ECIS. Vehicle (DMSO) or indicated concentration of rottlerin was added to the monolayers, with *arrows* indicating time of addition. The mean±SE of the normalized electrical resistance are presented. n = 6–12; $*p < 0.05$ vs. vehicle. *Panel b:* Monolayers containing equivalent numbers of rat fat pad epididymal endothelial cells were infected with indicated adenovirus. Protein overexpression was confirmed by immunoblot analyses (*inset*) and the effect of the overexpressed protein on monolayer permeability was determined by measuring the electrical resistance across the monolayers 24 h post-infection. The mean±SE are presented in all panels. n = 16; $*p < 0.05$ vs. Ad GFP or uninfected. *Panels c–f:* rat fat pad epididymal endothelial cells were infected with Ad GFP (*panels c* and *e*) or Ad PKCδ dn (*panels d* and *f*) for 24 h. The adenovirus infected cells were immunofluorescently stained for vinculin using *Texas-red* conjugated secondary antibodies directed against the vinculin antibody (*panels c, d*) or filamentous actin using *Texas Red* conjugated (*panel e*) or Alexa-488 conjugated (*panel f*) phalloidin. In all views, the cell nuclei were visualized using DAPI stain. Representative images are shown. n = 3. *Panel g*, rat fat pad epididymal monolayers containing equivalent numbers of endothelial cells were either not infected or infected with indicated adenovirus. At 24 h post-infection, cells were harvested and FAK activity was determined by measuring the level of phosphorylation at FAK Y^{397} by immunoblot analysis. The immunoblotted membranes were subsequently stripped and reprobed for FAK (*lower panel* of *inset*). Transient overexpression of PKCδ wild type or dominant active protein was also confirmed by immunoblot analysis. Immunoblot signals were quantitated by densitometry and the level of FAK activity is presented as the ratio of FAK Y^{397} phosphorylation to total FAK relative to uninfected cells. Representative immunoblots are shown. n = 5, $*p < 0.01$ Ad PKCδ dn vs. uninfected, Ad GFP, or Ad PKCδ wt. *Panel h:* Anesthetized rats were injected with a bolus of vehicle (DMSO) or 5 μM rottlerinin 1 ml 0.9% NaCl and the animals were sacrificed at 50 min after injection. The wet and dry weights of the harvested lungs were determined. n = 7–8 for each treatment. $*p < 0.05$ vs. vehicle

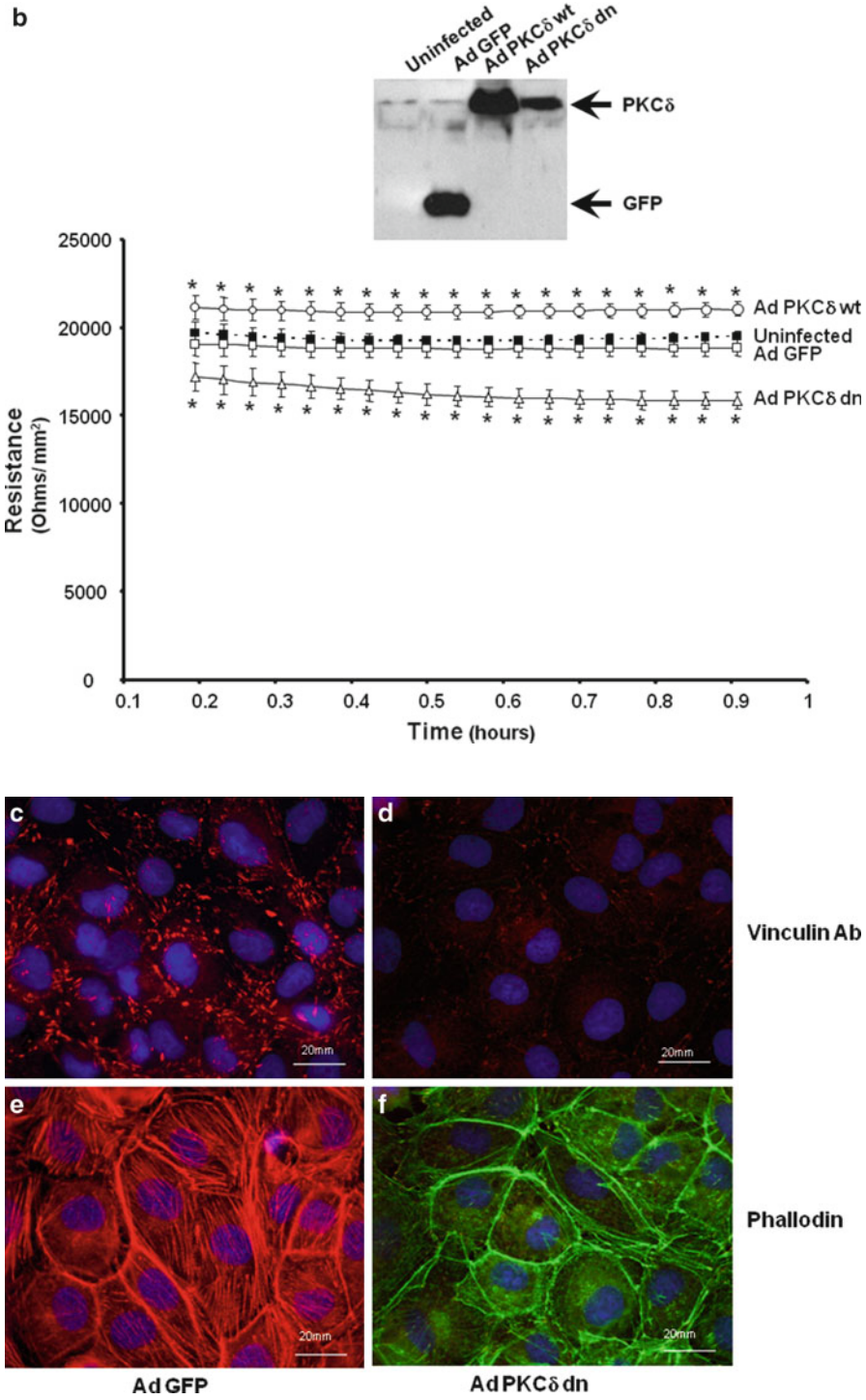

Fig. 2 (continued)

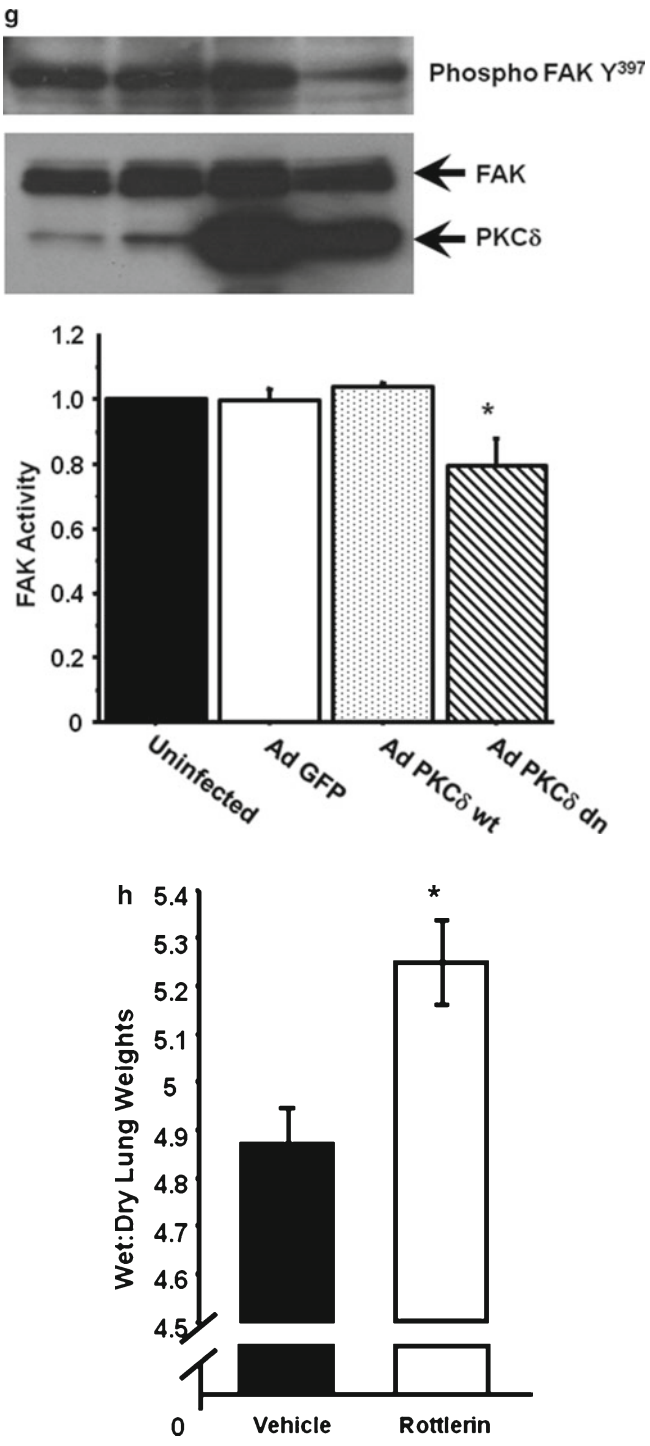

Fig. 2 (continued)

of gold-coated electrodes, which allows for conduction of electrical current from a computer-based control system through cultured cells. Most systems which measure cell impedance use an alternating current, which, as opposed to a direct current, prevents electrolytes present within the culture medium from being deposited on the electrodes. Cellular resistance to electrical current, which involves both cell-cell and cell-matrix components, can then be measured based upon Ohm's law. According to Ohm's law, the impedance to electrical flow is equal to the voltage divided by the alternating current applied to the electrode.

Since the initial description of measuring changes in cell impedance as a biosensor of cells *in vitro* and the creation of the ECIS system by Applied Biophysics, Inc., several other systems have been developed whereby changes in impedance is measured across cell monolayers, including the xCELLingence System and the RTCA Instrument, E-Plate, and C-Plate from Roche Applied Science and ACEA Biosciences, respectively. The xCELLingence System is used to monitor many cell functions including cell toxicity, proliferation, adhesion, spreading, migration, invasion, and barrier function. Using the xCELLingence System platform, the RTCA Instrument has been tailored to perform high-throughput screening of compounds, while the E-Plate has been designed to measure changes in single cells, and the C-Plate modified to measure cell invasion and migration. In addition, World Precision Instruments developed similar technologies in which the Trans Epithelial Electrical Resistance (TEER) is measured and changes in the output have been shown to correlate with cell proliferation, spreading, and disruption in intercellular junctions.

Traditionally, a constant current of 1 microampere is applied through the electrode. This current is non-invasive and does not cause any damage to the cells. The impedance to electrical flow is then sampled at varying intervals. By varying the frequency of the applied current, the cell impedance system has the ability to dissect cellular resistance recordings into independent assessments of intercellular resistance, cell-substrate resistance, and cell membrane capacitance. Impedance measurements made at lower frequency currents (~40 kHz) provide data regarding cell-matrix interactions, whereas higher frequency currents (~400 kHz) allow for analysis of cell-cell contacts. Thus, to measure changes between the cell and the substrate, as in studies of cell spreading, low frequency fixed current would be optimal; whereas, to measure changes at intercellular junctions, a high frequency fixed current would be employed. However, to assess the dynamic changes in cell morphology during multiple phases, data would be acquired using a scanning frequency mode to allow for simultaneous analysis of both cell-cell and cell-ECM interactions; such analyses would be used to monitor changes in focal adhesion complex formation.

1.3.2 Assets and Limitations of Measuring Cell Impedance

In addition to a variety of data analysis options, there are a number of cell culture array configurations used to measure changes in cell impedance or resistance across

electrodes. The original cell impedance array from Applied Biophysics, consists of eight culture wells, each containing a single circular electrode with a diameter of 250 μm. The 250 μm electrode can accommodate between 50 and 100 cells, depending upon cell size. For measurements across numerous regions of a cell monolayer, arrays which contain ten 250 μm electrodes, have been widely used to study the effects on monolayer integrity and changes in overall cell morphology. In addition, a variety of other arrays are available, including the larger arrays containing 96 wells with either one or ten electrodes per well. These large arrays are commonly used for high-throughput, wound healing, and migration assays and permit the examination of cell responses under a wide variety of experimental conditions. Another array is designed such that each well contains two 250 μm diameter electrodes which are on independent circuits enabling the analysis of two regions of the well. For analysis of cell proliferation, an array which contains wells underlain with two interlocked sets of four rectangular electrodes providing a large surface area for cell sampling has been used. In addition, an array developed by Hadjout and colleagues with a linear electrode perpendicular to the direction of movement of cell monolayer permits the measurement of cell migration in response to chemotactic agents (Hadjout et al. 2001). Arrays have also been developed which are equipped with electrodes that reside at the base of a flow channel and allow for the measurement of changes in resistance across cells in settings of shear stress. To perform cell invasion or migration assays, arrays have been generated based on the Boyden chamber model (Boyden 1962). For these arrays, cell monolayers are plated on the surface of the upper chamber which has an 8 μm porous membrane and a chemoattractant agent may be placed in the lower chamber. Cell migration through the porous membrane is detected as cells cross the gold plated electrodes coating the bottom surface of this chamber.

The current cell impedance technology also provides the ability to transfect mammalian cells via electroporation. While the standard voltage of 1 μA will not cause any notable effects on cell morphology or cell viability, the time and intensity of the voltage can be carefully increased to induce electroporation. In addition, the design permits the monitoring of cell impedance during electroporation and to correlate this data with changes in cell morphology and adhesion.

Of the few limitations to the cell impedance technology, the effect of artificial ECM on cell morphology and adhesion is one possible limitation. Due to the fact that most cells will not adhere to gold-coated tissue culture plastic, the culture wells are often coated with fibronectin, collagen, or gelatin. While this is standard practice in cell culture, these ECM materials can alter the inherent biophysical properties of a cell and do not recreate the extracellular environment an endothelial cell is exposed to in an intact blood vessel.

1.3.3 Investigation of the Crosstalk Between PKC and Focal Adhesion Complexes

The cell impedance technology has been widely used to study the effects of the PKC isoforms on cell functions, including adhesion, migration, monolayer barrier function,

and cell proliferation. For example, Gorshkova and colleagues used this system to assess the combined effects of the various PKC isoforms and the sphingolipid, sphingosine 1-phosphate (S1P), on lung endothelial cell migration (Gorshkova et al. 2008), using the cell impedance system to induce a wound across the cell monolayer. By measuring the resistance across the electrodes over time, the authors demonstrated S1P enhanced endothelial migration via pathways involving phospholipase D activation of PKCε, as well as PLD2-mediated activation of Rac1 via PKC-ζ. While this study did not measure focal adhesions directly using cell impedance technology, the results correlated well with previous work which has shown S1P promotes an enhancement in endothelial monolayer function through the generation of cortical actin rings and recruitment of focal adhesion protein components to both cell-ECM and cell-cell junctions (Belvitch and Dudek 2012; Shikata et al. 2003). Nyguen and colleagues did note a direct correlation in focal adhesion disruption in fibroblasts with diminution in cell impedance upon incubation with the PKC general inhibitor, H-7 (Nguyen et al. 2004). Interestingly, upon removal of the PKC inhibitor, the electrical impedance of the monolayer was partly restored to the initial levels. We have demonstrated that PKCδ modulates the barrier function of lung endothelial cells, effects which correlated with lung edema formation *in vivo* and decreased FAK activation and a reduction in the number of focal adhesion contacts *in vitro* (Fig. 2) (Fordjour and Harrington 2009; Harrington et al. 2005; Klinger et al. 2007).

Crosstalk between focal adhesion associated proteins and other cell structures has also been elucidated by assaying changes in cellular impedance. For example, lysophosphatidic acid (LPA) promoted an increase transelectrical resistance across bronchial epithelial cell monolayers correlating with increased cell-cell junctions and recruitment of E-cadherin, as well as FAK tyrosine phosphorylation and activation; events which were dependent upon PKCδ or PKCζ activity and protective against lipopolysaccharide-induced acute lung injury (He et al. 2009). Also, the actin filament associated protein (110 kDa), AFAP-110, a PKCα regulated protein important in scaffolding proteins to actin stress fibers, was shown to be required for cell spreading and adhesion on cell impedance arrays and focal adhesion formation (Dorfleutner et al. 2007; Gatesman et al. 2004). PKCε has also been implicated as a positive regulator of focal adhesion formation in settings of cardiomyocyte hypertrophic response to endothelin-1, through Rho kinase and cofilin to cause enhanced FAK activation (Heidkamp et al. 2003). Inhibition of PKCα or MLC kinase, an enzyme crucial for stress fiber formation, attenuated increased permeability and monocyte transmigration of human brain microvascular endothelial cell by the HIV-1 glycoprotein gp120, as measured by changes in TEER over time (Kanmogne et al. 2006).

2 Conclusion

Using cell impedance as an output measurement of changes in cell function and cell response to cytotoxic agents or metastatic capacity has lead to a great deal of insight into real time response of the cells to their surrounding environment. Indeed

this approach has begun to elucidate the role of select PKC isoforms in regulating cell-ECM interactions; evidence which has lead to the correlation of signaling events important in pathogenesis of a variety of disease states such as fibrosis, acute lung injury, tumorigenesis, and metastasis. The examination of modulators of cell impedance *in vitro* may lead to the identification of signaling events critical in the pathological progression of disease states and therapeutic targets for future interventions.

References

Ács P et al (1997) The catalytic domain of protein kinase C chimeras modulates the affinity and targeting of phorbol ester-induced translocation. J Biol Chem 272:22148–22153

Adamson RH et al (2002) Rho and rho kinase modulation of barrier properties: cultured endothelial cells and intact microvessels of rats and mice. J Physiol (Lond) 539:295–308

Almeida EA et al (2000) Matrix survival signaling: from fibronectin via focal adhesion kinase to c-Jun NH(2)-terminal kinase. J Cell Biol 149:741–754

Aziz MH et al (2007) Protein kinase Cε interacts with signal transducers and activators of transcription 3 (Stat3), phosphorylates Stat3Ser727, and regulates its constitutive activation in prostate cancer. Cancer Res 67:8828–8838

Balendran A, Biondi RM, Cheung PCF, Casamayor A, Deak M, Alessi DR (2000) A 3-phosphoinositide-dependent protein kinase-1 (PDK1) docking site is required for the phosphorylation of protein kinase Cζ (PKCζ) and PKC-related kinase 2 by PDK1. J Biol Chem 275:20806–20813

Barry ST, Critchley DR (1994) The RhoA-dependent assembly of focal adhesions in Swiss 3T3 cells is associated with increased tyrosine phosphorylation and the recruitment of both pp 125FAK and protein kinase Cδ to focal adhesions. J Cell Sci 107:2033–2045

Beggs HE et al (2003) FAK deficiency in cells contributing to the basal lamina results in cortical abnormalities resembling congenital muscular dystrophies. Neuron 40:501–514

Belvitch P, Dudek SM (2012) Role of FAK in S1P-regulated endothelial permeability. Microvasc Res 83:22–30

Beningo KA, Dembo M, Kaverina I, Small JV, Wang Y (2001) Nascent focal adhesions are responsible for the generation of strong propulsive forces in migrating fibroblasts. J Cell Biol 153:881–888

Boyden S (1962) The chemotactic effect of mixtures of antibody and antigen on polymorphonuclear leucocytes. J Exp Med 115:453–466

Brown MC, West KA, Turner CE (2002) Paxillin-dependent paxillin kinase linker and p21-activated kinase localization to focal adhesions involves a multistep activation pathway. Mol Biol Cell 13:1550–1565

Cheresh DA, Stupack DG (2008) Regulation of angiogenesis: apoptotic cues from the ECM. Oncogene 27:6285–6298

Chrzanowska-Wodnicka M, Burridge K (1996) Rho-stimulated contractility drives the formation of stress fibers and focal adhesions. J Cell Biol 133:1403–1415

Critchley DR (2000) Focal adhesions: the cytoskeletal connection. Curr Opin Cell Biol 12:133–139

Dorfleutner A, Stehlik C, Zhang J, Gallick GE, Flynn DC (2007) AFAP-110 is required for actin stress fiber formation and cell adhesion in MDA-MB-231 breast cancer cells. J Cell Physiol 213:740–749

Dumbauld DW, Shin H, Gallant ND, Michael KE, Radhakrishna H, García AJ (2010) Contractility modulates cell adhesion strengthening through focal adhesion kinase and assembly of vinculin-containing focal adhesions. J Cell Physiol 223:746–756

Dutil EM, Newton AC (2000) Dual role of pseudosubstrate in the coordinated regulation of protein kinase C by phosphorylation and diacylglycerol. J Biol Chem 275:10697–10701

Essayem S et al (2005) Hair cycle and wound healing in mice with a keratinocyte-restricted deletion of FAK. Oncogene 25:1081–1089

Fordjour AK, Harrington EO (2009) PKCδ influences p190 phosphorylation and activity: events independent of PKCδ-mediated regulation of endothelial cell stress fiber and focal adhesion formation and barrier function. Biochim Biophys Acta (BBA) General Subjects 1790:1179–1190

Freeley M, Kelleher D, Long A (2011) Regulation of protein kinase C function by phosphorylation on conserved and non-conserved sites. Cell Signal 23:753–762

Gao T, Newton AC (2006) Invariant Leu preceding turn motif phosphorylation site controls the interaction of protein kinase C with Hsp70. J Biol Chem 281:32461–32468

Gao T, Brognard J, Newton AC (2008) The phosphatase PHLPP controls the cellular levels of protein kinase C. J Biol Chem 283:6300–6311

Garcia JGN et al (1999) Regulation of endothelial cell myosin light chain kinase by Rho, cortactin, and p60src. Am J Physiol 276:L989–L998

Gatesman A, Walker VG, Baisden JM, Weed SA, Flynn DC (2004) Protein kinase Cα activates c-Src and induces podosome formation via AFAP-110. Mol Cell Biol 24:7578–7597

Geiger B, Bershadsky A (2001) Assembly and mechanosensory function of focal contacts. Curr Opin Cell Biol 13:584–592

Giaever I, Keese CR (1993) A morphological biosensor for mammalian cells. Nature 366:591–592

Ginsberg MH, Du X, Plow EF (1992) Inside-out integrin signalling. Curr Opin Cell Biol 4:766–771

Gomez DE, Skilton G, Alonso DF, Kazanietz MG (1999) The role of protein kinase C and novel phorbol ester receptors in tumor cell invasion and metastasis. Oncol Rep 6:1363–1433

Gorshkova I et al (2008) Protein kinase C- regulates sphingosine 1-phosphate-mediated migration of human lung endothelial cells through activation of phospholipase D2, protein kinase C-ζ, and Rac1. J Biol Chem 283:11794–11806

Gould CM, Kannan N, Taylor SS, Newton AC (2009) The chaperones Hsp90 and Cdc37 mediate the maturation and stabilization of protein kinase C through a conserved PXXP motif in the C-terminal tail. J Biol Chem 284:4921–4935

Guo LW, Gao L, Rothschild J, Su B, Gelman IH (2011) Control of protein kinase C activity, phorbol ester-induced cytoskeletal remodeling, and cell survival signals by the scaffolding protein SSeCKS/GRAVIN/AKAP12. J Biol Chem 286:38356–38366

Hadjout N, Laevsky G, Knecht DA, Lynes MA (2001) Automated real-time measurement of chemotactic cell motility. Biotechniques 31:1130–1138

Haller H, Lindschau C, Maasch C, Olthoff H, Kurscheid D, Luft FC (1998) Integrin-induced protein kinase Cα and Cε translocation to focal adhesions mediates vascular smooth muscle cell spreading. Circ Res 82:157–165

Harrington EO, Löffler J, Nelson PR, Kent KC, Simons M, Ware JA (1997) Enhancement of migration by protein kinase Cα and inhibition of proliferation and cell cycle progression by protein kinase Cδ in capillary endothelial cells. J Biol Chem 272:7390–7397

Harrington EO, Brunelle JL, Shannon CJ, Kim ES, Mennella K, Rounds S (2003) Role of protein kinase C isoforms in rat epididymal microvascular endothelial barrier function. Am J Respir Cell Mol Biol 28:626–636

Harrington EO, Shannon CJ, Morin N, Rowlett H, Murphy C, Lu Q (2005) PKCδ regulates endothelial basal barrier function through modulation of RhoA GTPase activity. Exp Cell Res 308:407–421

He D et al (2009) Lysophosphatidic acid enhances pulmonary epithelial barrier integrity and protects endotoxin-induced epithelial barrier disruption and lung injury. J Biol Chem 284:24123–24132

Heidkamp MC, Bayer AL, Scully BT, Eble DM, Samarel AM (2003) Activation of focal adhesion kinase by protein kinase C epsilon in neonatal rat ventricular myocytes. Am J Physiol Heart Circ Physiol 285:H1684–H1696

Hirase T et al (2001) Regulation of tight junction permeability and occludin phosphorylation by RhoA-p160ROCK-dependent and -independent mechanisms. J Biol Chem 276:10423–10431

Holinstat M, Mehta D, Kozasa T, Minshall RD, Malik AB (2003) Protein kinase Cα-induced p115RhoGEF phosphorylation signals endothelial cytoskeletal rearrangement. J Biol Chem 278:28793–28798

Huse M, Kuriyan J (2002) The conformational plasticity of protein kinases. Cell 109:275–282
Ikenoue T, Inoki K, Yang Q, Zhou X, Guan KL (2008) Essential function of TORC2 in PKC and Akt turn motif phosphorylation, maturation and signalling. EMBO J 27:1919–1931
Ilic D et al (1995) Reduced cell motility and enhanced focal adhesion contact formation in cells from FAK-deficient mice. Nature 377:539–544
Ilic D, Almeida EA, Schlaepfer DD, Dazin P, Aizawa S, Damsky CH (1998) Extracellular matrix survival signals transduced by focal adhesion kinase suppress p53-mediated apoptosis. J Cell Biol 143:547–560
Kanmogne GD, Schall K, Leibhart J, Knipe B, Gendelman HE, Persidsky Y (2006) HIV-1 gp120 compromises blood–brain barrier integrity and enhance monocyte migration across blood–brain barrier: implication for viral neuropathogenesis. J Cereb Blood Flow Metab 27:123–134
Klinger JR et al (2007) Rottlerin causes pulmonary edema in vivo: a possible role for PKCδ. J Appl Physiol 103:2084–2094
Kosaka Y, Ogita K, Ase K, Nomura H, Kikkawa U, Nishizuka Y (1988) The heterogeneity of protein kinase C in various rat tissues. Biochem Biophys Res Commun 151:973–981
Lamark T et al (2003) Interaction codes within the family of mammalian phox and Bem1p domain-containing proteins. J Biol Chem 278:34568–34581
Lamorte L, Rodrigues S, Sangwan V, Turner CE, Park M (2003) Crk associates with a multimolecular paxillin/GIT2/β-PIX complex and promotes Rac-dependent relocalization of paxillin to focal contacts. Mol Biol Cell 14:2818–2831
Le Good JA, Ziegler WH, Parekh DB, Alessi DR, Cohen P, Parker PJ (1998) Protein kinase C isotypes controlled by phosphoinositide 3-kinase through the protein kinase PDK1. Science 281:2042–2045
Leontieva OV, Black JD (2004) Identification of two distinct pathways of protein kinase Cα down-regulation in intestinal epithelial cells. J Biol Chem 279:5788–5801
Lim ST, Longley RL, Couchman JR, Woods A (2003) Direct binding of syndecan-4 cytoplasmic domain to the catalytic domain of protein kinase Cα (PKCα) increases focal adhesion localization of PKCα. J Biol Chem 278:13795–13802
Liu Y, Belkina NV, Graham C, Shaw S (2006) Independence of protein kinase C-δ activity from activation loop phosphorylation. J Biol Chem 281:12102–12111
Mackay K, Mochly-Rosen D (2001) Localization, anchoring, and functions of protein kinase C isozymes in the heart. J Mol Cell Cardiol 33:1301–1307
Marín-Vicente C, Nicolás FE, Gómez-Fernández JC, Corbalán-García S (2008) The PtdIns(4,5)P2 ligand itself influences the localization of PKCα in the plasma membrane of intact living cells. J Mol Biol 377:1038–1052
Michael KE, Dumbauld DW, Burns KL, Hanks SK, Garcia AJ (2009) Focal adhesion kinase modulates cell adhesion strengthening via integrin activation. Mol Biol Cell 20:2508–2519
Mitra SK, Schlaepfer DD (2006) Integrin-regulated FAK-Src signaling in normal and cancer cells. Curr Opin Cell Biol 18:516–523
Mochly-Rosen D, Gordon AS (1998) Anchoring proteins for protein kinase C: a means for isozyme selectivity. FASEB J 12:35–42
Moriya S et al (1996) Platelet-derived growth factor activates protein kinase C epsilon through redundant and independent signaling pathways involving phospholipase C gamma or phosphatidylinositol 3-kinase. Proc Natl Acad Sci 93:151–155
Neri L, Martelli AM, Borgatti P, Colamussi ML, Marchisio M, Capitani S (1999) Increase in nuclear phosphatidylinositol 3-kinase activity and phosphatidylinositol (3,4,5) trisphosphate synthesis precede PKC-ζ translocation to the nucleus of NGF-treated PC12 cells. FASEB J 13:2299–2310
Newton AC (2010) Protein kinase C: poised to signal. Am J Physiol Endocrinol Metab 298:E395–E402
Nguyen DD, Huang XQ, Greve DW, Domach MM (2004) Fibroblast growth and H-7 protein kinase inhibitor response monitored in microimpedance sensor arrays. Biotechnol Bioeng 87:138–144
Orr JW, Newton AC (1994) Requirement for negative charge on "activation loop" of protein kinase C. J Biol Chem 269:27715–27718

Parekh DB, Ziegler W, Parker PJ (2000) Multiple pathways control protein kinase C phosphorylation. EMBO J 19:496–503
Pearce LR, Komander D, Alessi DR (2010) The nuts and bolts of AGC protein kinases. Nat Rev Mol Cell Biol 11:9–22
Richardson A, Malik RK, Hildebrand JD, Parsons JT (1997) Inhibition of cell spreading by expression of the C-terminal domain of focal adhesion kinase (FAK) is rescued by coexpression of Src or catalytically inactive FAK: a role for paxillin tyrosine phosphorylation. Mol Cell Biol 17:6906–6914
Ridley AJ et al (2003) Cell migration: integrating signals from front to back. Science 302:1704–1709
Romer LH, Birukov KG, Garcia JGN (2006) Focal adhesions. Circ Res 98:606–616
Ron D, Mochly-Rosen D (1995) An autoregulatory region in protein kinase C: the pseudoanchoring site. Proc Natl Acad Sci 92:492–496
Rosse C, Linch M, Kermorgant S, Cameron AJM, Boeckeler K, Parker PJ (2010) PKC and the control of localized signal dynamics. Nat Rev Mol Cell Biol 11:103–112
Schmidt A, Hall A (2002) Guanine nucleotide exchange factors for Rho GTPases: turning on the switch. Genes Dev 16:1587–1609
Shen TL et al (2005) Conditional knockout of focal adhesion kinase in endothelial cells reveals its role in angiogenesis and vascular development in late embryogenesis. J Cell Biol 169:941–952
Shikata Y, Birukov KG, Garcia JGN (2003) S1P induces FA remodeling in human pulmonary endothelial cells: role of Rac, GIT1, FAK, and paxillin. J Appl Physiol 94:1193–1203
Sieg DJ et al (2000) FAK integrates growth-factor and integrin signals to promote cell migration. Nat Cell Biol 2:249–256
Soh JW (2011) PKC Lab http://www.pkclab.org/index.htm (Type of Medium)
Sossin WS, Schwartz J (1993) Ca(2+)-independent protein kinase Cs contain an amino-terminal domain similar to the C2 consensus sequence. Trends Biochem Sci 18:207–208
Stensman H, Larsson C (2007) Identification of acidic amino acid residues in the protein kinase Cα V5 domain that contribute to its insensitivity to diacylglycerol. J Biol Chem 282:28627–28638
Tsubouchi A et al (2002) Localized suppression of RhoA activity by Tyr31/118-phosphorylated paxillin in cell adhesion and migration. J Cell Biol 159:673–683
Turner CE (2000) Paxillin and focal adhesion signaling. Nat Cell Biol 2:E231–E236
Valles AM, Beuvin M, Boyer B (2004) Activation of Rac1 by paxillin-Crk-DOCK180 signaling complex is antagonized by Rap1 in migrating NBT-II cells. J Biol Chem 279:44490–44496
van Nieuw Amerongen GP, Draijer R, Vermeer MA, van Hinsbergh VWM (1998) Transient and prolonged increase in endothelial permeability induced by histamine and thrombin: role of protein kinases, calcium, and RhoA. Circ Res 83:1115–1123
Venkatachalam K et al (2010) Dependence on a retinophilin/myosin complex for stability of PKC and INAD and termination of phototransduction. J Neurosci 30:11337–11345
Zaidel-Bar R, Geiger B (2010) The switchable integrin adhesome. J Cell Sci 123:1385–1388
Zaidel-Bar R, Cohen M, Addadi L, Geiger B (2004) Hierarchical assembly of cell-matrix adhesion complexes. Biochem Soc Trans 32:416–420
Zaidel-Bar R, Itzkovitz S, Ma'ayan A, Iyengar R, Geiger B (2007) Functional atlas of the integrin adhesome. Nat Cell Biol 9:858–868
Zhao Z, Manser E, Loo TH, Lim L (2000) Coupling of PAK-interacting exchange factor PIX to GIT1 promotes focal complex disassembly. Mol Cell Biol 20:6354–6363

ECIS as a Tool in the Study of Metastasis Suppressor Genes: Epithelial Protein Lost In Neoplasm (EPLIN)

Andrew J. Sanders, Vladimir M. Saravolac, Malcolm D. Mason, and Wen G. Jiang

Abstract Metastasis is a major determining factor in the clinical outcome of cancer patients and accounts for the vast majority of cancer mortality. The process through which cancer cells metastasise is complex, requiring the cells to overcome a number of restraints and barriers to enable them to successfully disseminate and survive away from the primary tumour. Alterations to so-called metastasis genes can grant cells a greater potential to undertake this process and these genes represent interesting targets for study and therapeutic intervention. The current chapter reviews EPLIN as a gene that is gaining interest as a potential metastasis suppressor and describes the ECIS system as a valuable tool for use in characterising a number of metastatic cells traits.

Abbreviations

EPLIN	Epithelial Protein Lost In Neoplasm
HGF	Hepatocyte Growth Factor
ECIS	Electrical Cell-substrate Impedance Sensing
NPI	Nottingham Prognostic Indicator

A.J. Sanders (✉) • W.G. Jiang
Metastasis and Angiogenesis Research Group, Department of Surgery, Cardiff University School of Medicine, University Hospital of Wales, Heath Park, Cardiff CF14 4XN, UK
email: sandersaj1@cf.ac.uk

V.M. Saravolac
Metastasis and Angiogenesis Research Group, Department of Wound Healing, Cardiff University School of Medicine University Hospital of Wales Heath Park Cardiff CF14 4XN UK

M.D. Mason
Metastasis and Angiogenesis Research Group, Department of Clinical Oncology, Cardiff University School of Medicine University Hospital of Wales Heath Park Cardiff CF14 4XN UK

W.G. Jiang (ed.), *Electric Cell-Substrate Impedance Sensing and Cancer Metastasis*, Cancer Metastasis - Biology and Treatment 17, DOI 10.1007/978-94-007-4927-6_3,

TNM	Tumour, Node, Metastasis
ERK	Extracellular Signal-Regulated Kinase
VEGF	Vascular Endothelial-cell Growth Factor
TRAMP	Transgenic Adenocarcinoma Mouse Prostate

1 Introduction

Despite the many years of research and advancement in the management and treatment of cancer patients cancer continues to be a leading cause of mortality and morbidity worldwide, presenting substantial problems to health services. According to data compiled by the National Statistics Office, there were approximately 306,100 newly diagnosed cases of cancer per year in the UK during the 2006–2008 period, with deaths from cancer accounting for 155,600 patients per year over this period (Office for National Statistics 2011). A key factor in the high mortality rates of cancer patients is associated with the metastatic spread of tumour cells away from the primary tumour and establishment of secondary tumours at distant sites. Without this ability to spread, the majority of cancers would be manageable, through surgical removal of the tumour, only becoming problematic when location of the tumour around vital tissues made removal impossible.

2 Cancer Metastasis

2.1 The Metastatic Cascade

Metastatic spread of cancer cells from a primary tumour to distant secondary sites is a major determining factor in patient outcome, yet this process remains poorly understood. The metastatic cascade is a complex process consisting of a number of key steps or stages that cancer cells must undergo in order to escape the tumour and disseminate through circulatory (used as an example here) or lymphatic systems (Fig. 1). Within the tissue an initial mutation or trigger occurs bringing about the formation of a local tumour. Initially tumour growth will be relatively slow, as with no established vascular system the tumour can only access resources through simple diffusion. As the tumour grows, through direct expansion, it will come into contact with a tissue barrier, such as the basement membrane, and will begin to invade through it. Invasion of local barriers is believed to involve both the secretion of proteolytic enzymes to break down the basement membrane, such as members of the matrix metalloprotease (MMP) family, and also the mechanical force exerted on the peripheral cells by the bulk of the rapidly growing tumour. The increasing size and requirements of the tumour will facilitate the need for its own vasculature, which is achieved through the secretion of various angiogenic factors, such as Vascular Endothelial-cell Growth Factor (VEGF) and the formation of new blood vessel growth to the tumour. This tumour vasculatures facilitate rapid growth and

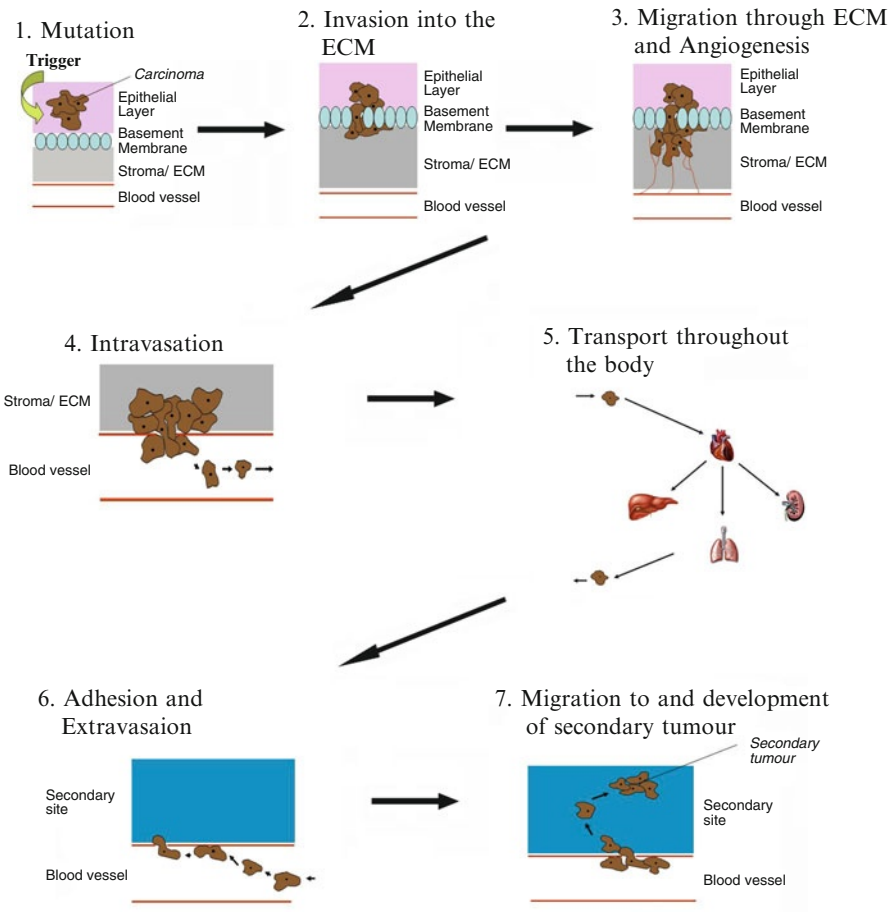

Fig. 1 The metastatic cascade. Outline of key steps and events involved in the metastatic spread of cancer cells from the primary tumour to distant secondary sites

development of the tumour and also supplies a means of escape for tumour cells, which can invade into the blood vessel (intravasation) and are shed from the main tumour body into the circulatory system. Once access has been gained to the circulatory system the tumour cells are transported around the body to a secondary site, where the cells will arrest, invade through the blood vessel wall (extravasation) and migrate into the secondary tissue to form distant metastasis (Chaffer and Weinberg 2011; Nguyen and Massague 2007; Ruddon 1987).

Whilst the above description gives a basic account of key events in metastasis, the process remains highly complex. For tumour cells to successfully disseminate from the primary tumour they need to acquire numerous traits to survive and successfully establish themselves at distant sites. Early studies have indicated the difficulty of this process, indicating that only a very small proportion of tumour cells will survive long enough to establish distant metastasise (Fidler 1970). Additionally, there appears to be

a degree of "tissue tropism", whereby different cancer cells will preferentially metastasise to different sites (e.g. prostate cancer cells to bones), a trend recognised more than 100 years ago in Paget's "seed and soil" hypothesis outlining that certain cancer cells (seeds) will only readily grow in specific tissues (soil) (Paget 1889). Currently, considerable scientific attention and studies have focused on cancer initiation events and changes within the tumour, the area of cancer metastasis and the biology behind events determining how, when and why cancer cells spread away from the primary tumour is one of the more poorly understood areas of this field and perhaps the key determining factor in patient outcome. Studies have emerged to challenge the current canonical theory outlining that accumulation of stepwise mutations, in a genetically unstable population of cells, gives rise to cells adapted to escape, survive and develop away from the primary tumour. These new concepts suggest metastasis may be an early event and aim to address issues such as how certain metastasis can remain dormant for prolonged periods before establishing aggressive secondary tumours. Advances in this field have been reviewed in depth in a number of recent publications (Coghlin and Murray 2010; Nguyen and Massague 2007).

2.2 Metastasis Genes

As previously outlined, the process of metastasis in complex, consisting of a number of barriers a cancer cell must overcome in order to escape and disseminate from the main tumour body. In normal physiology, in the vast majority of tissues there are regulations in place to prevent the shedding and movement around the body of individual cells. In order to progress through the metastatic cascade cancer cells must acquire certain traits enabling them to overcome tissue regulations and enabling them to survive and establish secondary tumours.

In their review Nguyen and Massague distinguish three classes of metastasis genes namely; metastasis initiation genes (genes conferring advantage at the primary tumour and facilitating entry to the circulatory system, including traits such as invasiveness, motility and angiogenesis); metastasis progression genes (genes which fulfil rate-limiting functions in the primary tumour and functions in metastatic colonisation, potentially giving rise to target organ specificity) and metastasis virulence genes (genes conferring an advantage in secondary but not primary tumour sites, such as traits facilitating adaptation to the new environment) (Nguyen and Massague 2007). Alterations or mutations in these metastasis genes, either gain in function of metastasis promoter genes of loss in function of metastasis suppressor genes can enhance the potential of cancer cells to successfully spread and establish secondary tumours. The study of metastasis genes are thus of wide scientific interest for their potential therapeutic intervention to prevent cancer spread and improve patient outcomes.

One example of a metastasis suppressor gene showing promise for therapeutic intervention is KAI1. KAI1/CD82 is a member of the tetraspanin family, identified as playing a role in cellular invasiveness and metastasis and the expression of which has been found to be reduced in a number of cancers and in cancer progression

(Malik et al. 2009). The potential for KAI1 to interfere with the metastasis process has been established in prostate and pancreatic models. One study has demonstrated that the phytoestrogen genistein (at 5 and 10 μM doses) could induce KAI1 expression and reduce invasiveness in the TRAMP-C2 cell line, a trend which could be negated when TRAMP-C2 cells were transfected with siRNA to KAI1 were similarly dosed with genistein. This study also demonstrated that the age-dependant downregulation of KAI1 expression in the Transgenic Adenocarcinoma Mouse Prostate (TRAMP) model could be reversed by a genistein enriched diet (El Touny and Banerjee 2007). Similarly, in pancreatic cancer MiaPaca II cells, transfection with KAI1 cDNA reduced cell invasion *in vitro* and *in vivo* administration of KAI1 gene therapy, through direct injection into the body of the adenocarcinoma could inhibit tumour growth and metastasis in this model but was correlated with the time of gene therapy administration post-tumour inoculation with later administrations having minimal effect (Xu et al. 2008).

Work within our laboratories has recently focused on Epithelial Protein Lost in Neoplasm (EPLIN), a molecule which is gaining scientific potential as a metastasis suppressor gene, in breast and prostate cancer and angiogenesis.

3 Epithelial Protein Lost In Neoplasm (EPLIN)

3.1 Discovery/Characterisation

EPLIN was initially discovered in 1998 by Chang et al. in a study that searched for transformation related genes in oral cancer. The authors used cDNA representational difference analysis to identify genes that were differentially expressed between normal oral epithelial and HPV-immortalised oral epithelial cell lines and identified EPLIN as one such gene (Chang et al. 1998). Subsequent study by Maul & Chang identified the ORF of EPLINα to comprise 600 amino acids and also identified an isoform, termed EPLINβ, which extended an additional 160 amino acids at the amino terminus. Analysis of the predicted amino acid structure identified a central LIM domain (Maul and Chang 1999). The human EPLIN gene contains 11 exons and spans more than 100 kb, with transcription arising from different starting points accounting for the two EPLIN isoforms (Chen et al. 2000).

Early studies highlighted the localisation of both EPLINα and β as being observed in the cytoplasm with a fibrillar pattern similar to that of actin fibers and over-expression of EPLINα and β have been associated with reduced growth potentials (Maul and Chang 1999). EPLIN has been characterised as a cytoskeletal protein and studies have implicated its involvement in a variety of processes. Maul et al., demonstrated the ability of EPLIN to regulate actin structures, finding that expression of EPLINα can increase actin stress fiber numbers and can inhibit membrane ruffling mediated by Rac1. EPLINα is also able to bind actin monomers at both NH_2 and COOH ends but not at the LIM domain, with reduced binding efficiency being seen in truncated rather than full length EPLINα, suggesting at least two independent

binding sites situated either side of the LIM domain. Similarly, EPLINα is able to bind F-actin in a ratio of at least two actin molecules per EPLIN and can cause actin filament bundling. Further evidence supporting EPLINs role in actin stabilisation is demonstrated through the ability of EPLINα to delay actin filament depolymerisation whilst having little effect on actin polymerisation and that binding of EPLINα to actin filaments can prevent secondary activation of nucleation mediated by Arp2/3 complex (Maul et al. 2003).

In 2007 EPLIN was identified as an Extracellular Signal-Regulated Kinase (ERK) substrate by Han et al., undergoing ERK phosphorylation at Ser360, Ser602 and Ser692 *in vitro* and in living cells. This phosphorylation was found to decrease the C-terminal region affinity for actin filaments and it was discovered that a non ERK – phosphorylatable EPLIN mutant inhibited PDGF actin stress fiber disassembly, cell migration and membrane ruffling suggesting phosphorylation of EPLIN by ERK plays a role in EPLINs regulation of actin dynamics and motility (Han et al. 2007). An additional study by Abe et al., found that EPLIN could complex with the cadherin-catenin complex through its interaction with α-catenin (Abe and Takeichi 2008). This interaction appears to be through both the N- and C- terminal EPLIN domains, involved in actin binding, and the VH3-C region of α-catenin as deletion of any of these regions removed the interaction. EPLIN can then function to combine the cadherin-catenin complex to F-actin, through its binding with α-catenin and thus, link cadherin to F-actin. Whilst EPLIN is required to link cadherin to F-actin to form the adhesion belt it doesn't seem to be required for the interaction between cadherin and radial actin fibers, with EPLIN depletion resulting in adhesion belt conversion into zig-zag forms. The study demonstrates the importance of EPLIN in both linking the actin bundles to the cadherin-catenin complex and also in the stabilisation of these actin bundles and suggests that in cancerous cells, where EPLIN is frequently lost, cadherin-mediated cell adhesion may also be disrupted and could thus contribute to enhanced invasive cell potential (Abe and Takeichi 2008).

3.2 Implications in Cancer

EPLIN was initially discovered as a protein whose expression was reduced in transformed compared to normal oral cells (Chang et al. 1998). Since its discovery EPLIN, particularly EPLINα, levels have been shown to be frequently reduced or absent in a wide variety of cancer cells and tissues. Early studies identified EPLINα as being significantly reduced in aggressive PC-3 and DU-145 cell lines compared to prostate epithelial cells, similar to this EPLINα levels are non-detectable in LNCaP and LAPC4 cells, whilst expression of EPLINβ was comparable to prostate epithelial cells. The same study identified similar trends in the MCF-7, T-47D and MDA-MB-231 breast cancer cell lines, where again EPLINα levels were either absent or reduced in the breast cancer cell lines and EPLINβ levels were unchanged or increased compared to the mammary epithelial cells (Maul and Chang 1999).

In keeping with these early results, work conducted within our laboratories has similarly reported differential expression of EPLIN in clinical breast (Fig. 2) and

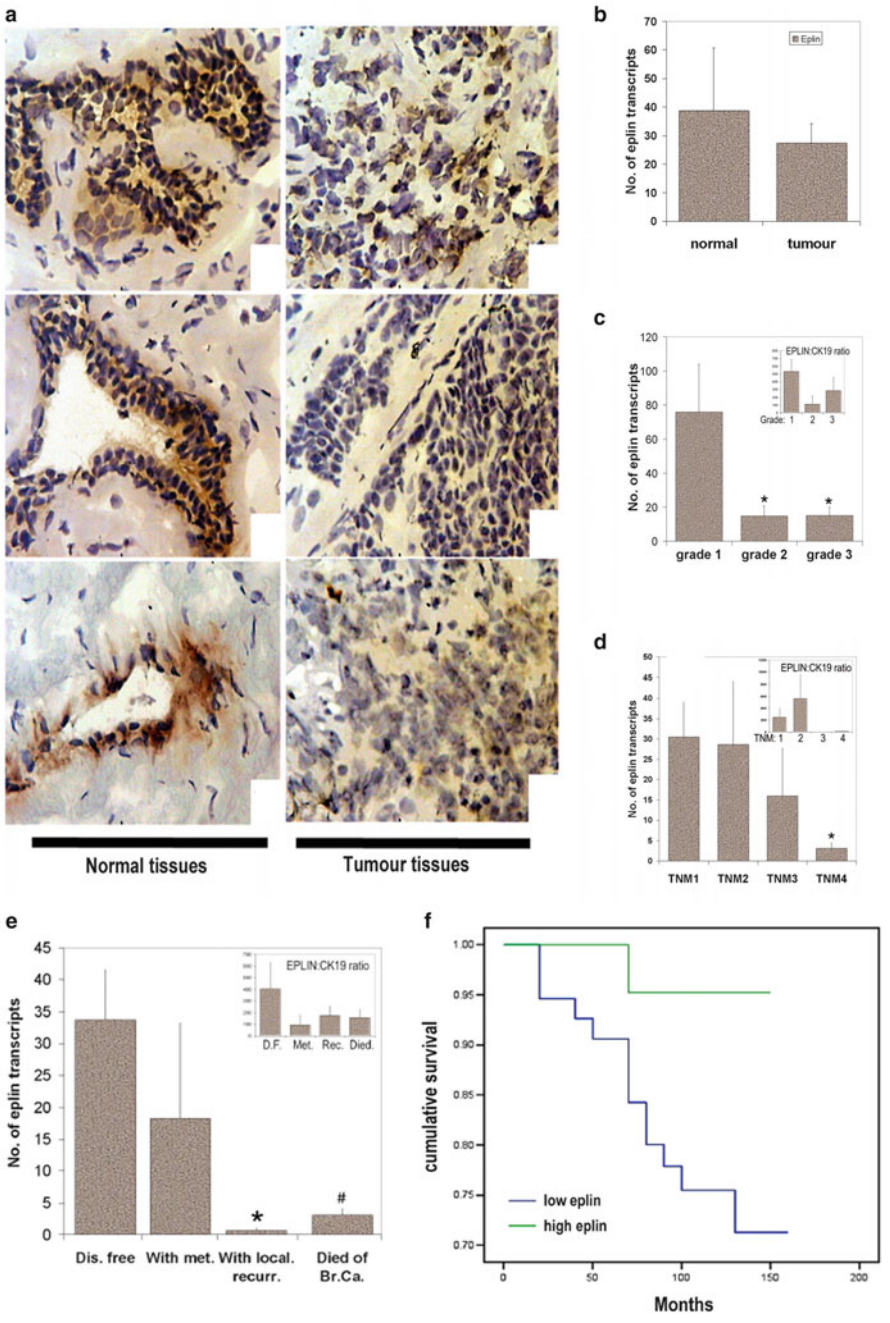

Fig. 2 EPLIN expression in clinical breast cancer. (**a**) Representative immunohistochemical analysis of EPLIN expression in a cohort of breast cancer patients. (**b**–**d**) Quantitative PCR analysis of EPLIN transcript levels in the cohort of breast cancer patients and its associated expression level in different grade and stage tumours. (**e**–**f**) Association of EPLIN transcript expression levels with patient prognosis data (Figure modified from Jiang et al. 2008)

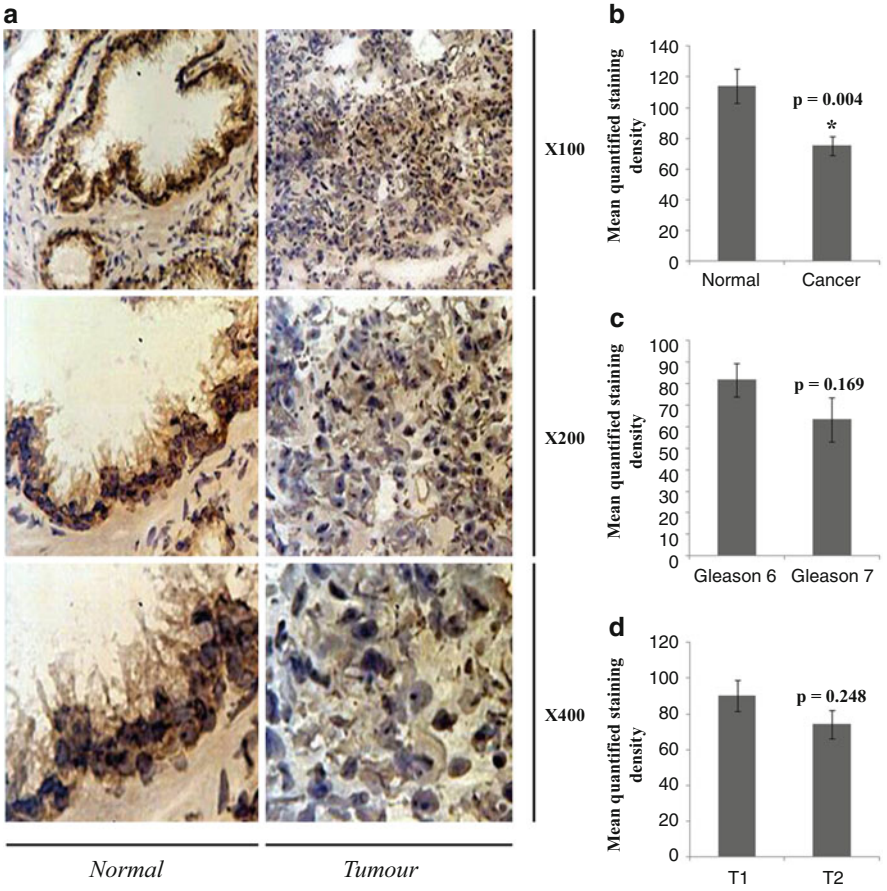

Fig. 3 EPLIN expression in clinical prostate cancer. (**a**) Representative immunohistochemical analysis of EPLIN expression in a cohort of prostate cancer patients. (**b**–**d**) Quantification of immunohistochemical staining intensities throughout the prostate cohort and association of EPLIN staining levels with clinical patient data (Figure reproduced from Sanders et al. 2011)

prostate (Fig. 3) cancer (Jiang et al. 2008; Sanders et al. 2011). Examination of EPLINα expression throughout a cohort consisting of 120 tumour and 32 normal breast samples revealed a reduction in EPLINα expression in breast tumour sections compared to normal breast sections following immunohistochemical analysis. Additionally, analysis of EPLINα transcript levels, using quantitative polymerase chain reaction, in these samples also demonstrated a reduction in tumour versus normal breast samples. Interestingly, further correlation of EPLINα together with clinical patient data indicated that, within the breast cancer specimens, EPLINα expression reduced as cancer predictive factors, such as Nottingham Prognostic Index (NPI), grade and TNM stage increased and lower levels of EPLINα transcript could be associated with poorer patient prognosis and shorter overall and disease free survival rates (Jiang et al. 2008). A similar analysis of EPLIN expression was

conducted in a prostate sample cohort consisting of 20 tumour and 11 normal prostate samples. Immunohistochemical analysis of these sections once again revealed a reduction in EPLIN expression in tumour sections compared to normal sections which, through quantification of staining intensity was found to be significant. However, due to the limited size of the prostate cohort, analysis of patient data did not demonstrate significant reductions between grade 6 and grade 7 samples and T1 compared to T2 stage samples, though it was noted that EPLIN levels were generally reduced in the higher stage and grade samples (Sanders et al. 2011).

A study by Chircop et al., has linked EPLIN to cytokinesis, where EPLINs role in this process seems to be through its ability to associate with cytoskeletal systems needed for membrane ingression and formation of the cleavage furrow and depletion of EPLIN in HeLa cells resulted in a large number of multinucleated cells, characteristic of cytokinesis failure (Chircop et al. 2009). This study provides additional implications for EPLIN in cancer as the failure of cells to undergo cytokinesis results in aneuploidy and genomic instability, a trend frequently seen in cancer cells.

3.3 EPLIN as a Potential Tumour/Metastasis Suppressor

To further examine the role of EPLINα in cancer progression our laboratory generated a mammalian plasmid (pEF6/V5-His-TOPO, Invitrogen, Paisley, UK) containing the full coding sequence of EPLINα (Jiang et al. 2008). This EPLINα expression plasmid was subsequently used in a number of studies to assess the impact of enhancing EPLINα expression in a range of breast, prostate and endothelial cell lines (Jiang et al. 2008; Sanders et al. 2010, 2011).

Over-expression of EPLINα in MDA-MB-231 breast cancer cells brought about a number of changes to this aggressive cell line. MDA-MB-231 cells over-expressing EPLINα became less invasive and were no longer responsive to the pro-invasive effect of Hepatocyte Growth Factor (HGF), which could substantially increase *in vitro* invasiveness in MDA-MB-231 wild type and plasmid control cells but had minimal effect of MDA-MB-231 cells transfected with the EPLINα expression plasmid. Additionally, over-expression of EPLINα reduced *in vitro* growth over three day incubation. This trend was also observed *in vivo* where MDA-MB-231 cells over-expressing EPLINα inoculated into CD-1 athymic nude mice produced significantly smaller tumours than those arising from inoculation of control MDA-MB-231 cells. Over-expression of EPLINα was also seen to have a profound effect on MDA-MB-231 motility, substantially decreasing migrational rates compared to control cells (Jiang et al. 2008). Similar to the trends seen in the breast cancer study, a decrease in aggressive traits was seen in PC-3 prostate cancer cells following enhancement of EPLINα expression. Over-expression of EPLINα in PC-3 cells similarly reduced cellular invasiveness and could negate the pro-invasive effect induced by HGF. Similar to the breast cancer cells, EPLINα over-expressing PC-3 cells displayed slower growth rates *in vitro* and produced significantly smaller tumours *in vivo* following inoculation into nude mice. EPLINα also seemed to impact on cell-matrix adhesion where over-expression of this protein reduced the ability of PC-3 cells to adhere to an artificial basement membrane (Sanders et al. 2011).

In the breast and prostate cancer studies carried out by our labs the over-expression of EPLINα reduced cell growth rates and *in vivo* development. This ability has similarly been observed in other studies (Maul and Chang 1999) and suggests that this protein may have some role in regulating cell growth in the tumour. This could have implication in tumorigenesis and the local growth and development of the tumour, suggesting a potential tumour suppressive role for EPLINα. In addition to this, the ability of EPLINα to interfere with the processes of cellular invasion, migration and cell-matrix adhesion have implications on the metastatic escape of tumour cells from the primary tumour, indicating a potential metastasis suppressor role for EPLINα. In support of this, the ability of EPLINα to reduce the sensitivity of breast and prostate cancer cells to the HGF molecule is interesting. HGF is widely recognised in the literature as enhancing the processes of tumorigenesis and enhancing aggressive traits required for cells to undergo metastasis (Cecchi et al. 2010; Jiang et al. 2005; Martin and Jiang 2010; Nakamura et al. 2010, 2011). Thus, the observations reported in these two studies could indicate one potential mechanism through which EPLINα can act to slow cancer progression.

The ability of EPLIN to reduce aggressive traits in both breast cancer and prostate cancer cell lines implies that the loss of EPLIN may be a contributing factor in cancer development and progression and indeed other studies have proposed that the loss of EPLIN and the associated cytoskeletal changes associated with this may aid to enhance the invasive migration seen in cancerous cells (Maul et al. 2003). Further evidence in support of a metastasis suppressive role for EPLIN has been recently provided by Zhang et al., in a study examining the potential of EPLIN to contribute to the Epithelial-Mesenchymal Transition (EMT) process utilising a previously established Androgen Refractory Cancer of the Prostate (ARCaP) cell lineage model that resembles characteristics of EMT and mimics the pathophysiology of prostate cancer metastasis (Zhang et al. 2011). The EMT process, whereby epithelial cells gain a more mesenchymal like morphology, is essential to normal development and physiological processes such as wound healing. However, EMT also appears to play a role in pathological conditions and cancer progression where this process has been observed in cells of the invasive front of tumours and EMT has been suggested to correlate with poor clinical outcomes (reviewed fully in Thiery et al. 2009). Zhang et al., discovered that EPLIN expression was abundant in the epithelial like $ARCaP_E$ cells but was significantly reduced in the mesochymal like $ARCaP_M$ cells. Similarly, immunohistochemical staining of tumours formed from subcutaneous inoculation of $ARCaP_E$ cells showed abundant EPLIN expression whereas those formed from inoculation of $ARCaP_M$ showed significantly reduced EPLIN levels (Zhang et al. 2011). Additionally, the depletion of EPLIN levels through siRNA or shRNAs in $ARCaP_E$ cells resulted in a loss of cell-cell contacts and the formation of spindle shape mesenchymal like morphology characteristic of EMT, induced Actin remodelling, enhanced migratory properties and the capability to infiltrate Matrigel. Depletion of EPLIN in $ARCaP_E$ cells resulted in a decreased expression of E-cadherin, increased expression of vimentin, brought about the translocation of β-catenin to the nucleus and activation of T-cell reporter presenting further evidence for a role for EPLIN in the regulation of EMT. Reduced expression

of EPLIN was also apparent in lymph node metastatic tumours of prostate, breast, colorectal and squamous cell carcinoma of the head and neck in comparison to the respective matched primary tumour, implicating the downregulation of EPLIN as a potential indicator of clinical metastasis in a number of epithelial cancers (Zhang et al. 2011).

4 Use of ECIS as a Model System in the Implication of EPLIN as a Metastasis Suppressor

Currently, the ECIS system is being utilised within our laboratories to detect and examine a number of cellular functions such as cellular attachment and migration. The ECIS system presents a number of advantages over the older conventional methodologies previously used to detect cell migration, such as the scratch wounding assay. Older methodologies such as the scratch wound assay previously used by our department (Jiang et al. 1999) were time consuming; requiring the tracking of wound fronts over several hours and subsequently the quantification and calculation of wound closure over time. The ECIS system of detection is fully automated and with the development of 8 and, more recently, 96 well array formats allows rapid generation of data simultaneously across large numbers of test samples. This is illustrated in Fig. 4 detailing results from two individual studies (Jiang et al. 2008; Sanders et al. 2010), one study using conventional scratch wounding and the other ECIS to analyse cell migration. Both studies highlight the importance of EPLINα in the process of cell migration, however, the high throughput ECIS method of data acquisition and analysis facilitates easy applications of multiple treatments or inhibitors to cell cultures, allowing for enhanced scrutiny of cell attachment or migratory responses (Fig. 4c). ECIS detection of migration also has a number of other advantages over conventional scratch wound methodologies, allowing the establishment of consistent "wound" sizes as only cells directly situated on the 250 μm diameter electrode are killed and having no effect on protein coating. As cell migration and matrix adhesion are key cellular traits influencing metastatic spread and cancer progression, the use of EICS to identify cellular factors which can influence these traits represent a vital resource for research into prevention of cellular metastasis. This system is currently being widely used within our laboratories to examine a number of cancer cell lines stably over-expressing or targeted for a variety of candidate genes (Ablin et al. 2011; Davies and Jiang 2010; Jiang et al. 2008).

5 Conclusions and Future Implications

The ECIS system is proving to be a suitable methodology for the high throughput screening of cellular migration and attachment with both 8 well and 96 well arrays currently commercially available. The data obtained can be used to aid in the analysis

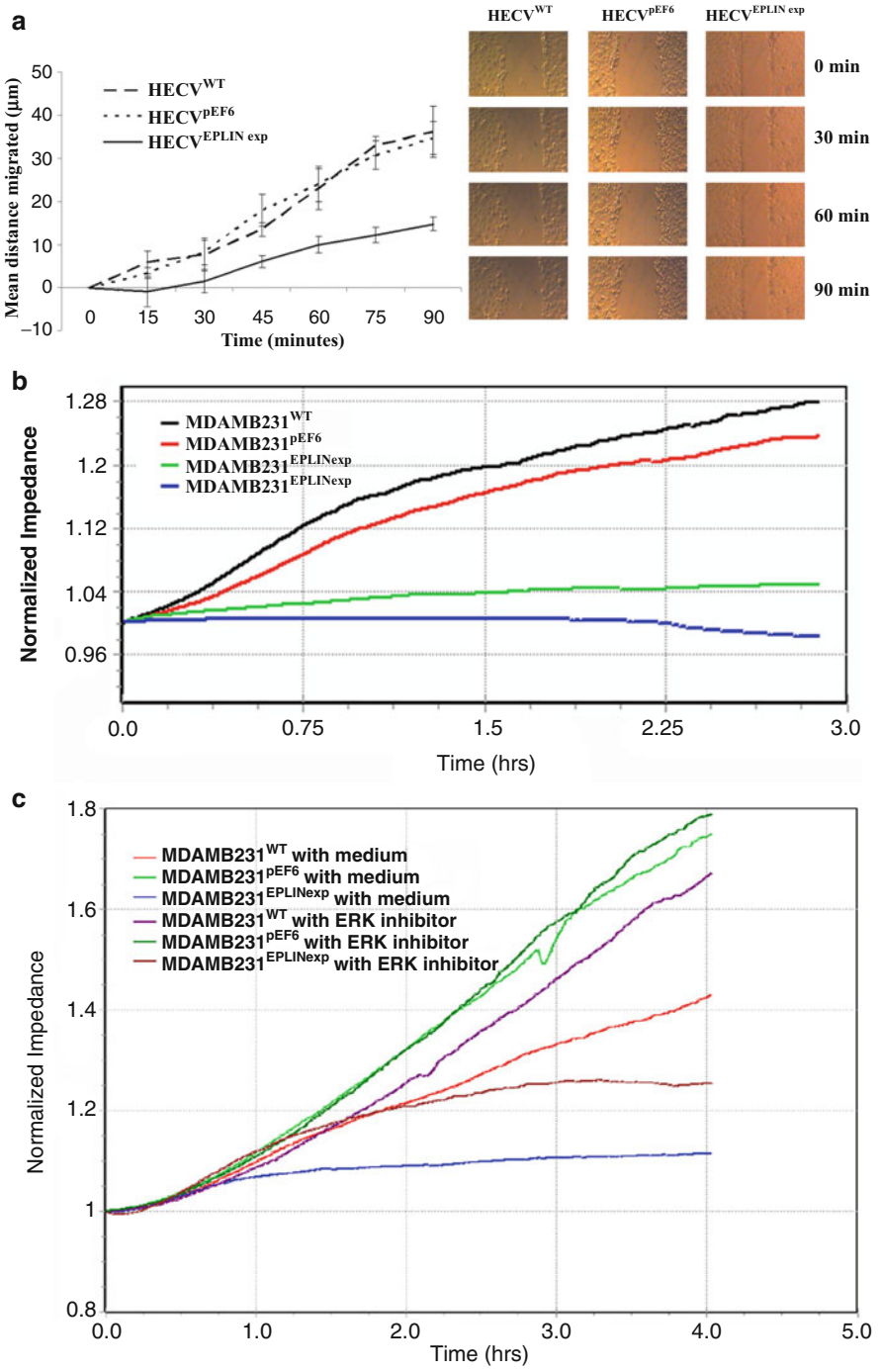

Fig. 4 Comparison between ECIS system of migration detection to conventional scratch wounding assay. (**a**) Conventional scratch wounding assay with representative pictures of scratches for analysis. (**b**) ECIS timecourse data tracking migration of cells onto electrically generated wound. Use of automated data recording and multiple welled arrays allows high throughput analysis using simultaneous detection over multiple samples (**c**) (Source Jiang et al. 2008; Sanders et al. 2010)

of the function of various proteins and their roles in these processes in cancer or other cell types. This data, when combined with additional information can be useful in providing insight into whether certain proteins of interest could have metastasis suppressive properties or may promote the likelihood of cellular metastasis.

Within the short life of the ECIS system we have already seen advancements in the technology and software with production of 96 well arrays enhancing the potential of this system for screening purposes. Further advances or fine tuning of methodologies and software in the future may enhance the efficacy of this system further and may extend the potential of this system to detect other metastatic traits on a large scale basis.

Acknowledgements The authors wish to thank Cancer Research Wales and Breast Cancer Hope Foundation for supporting their work.

References

Abe K, Takeichi M (2008) EPLIN mediates linkage of the cadherin catenin complex to F-actin and stabilizes the circumferential actin belt. Proc Natl Acad Sci U S A 105(1):13–19

Ablin RJ, Kynaston HG, Mason MD, Jiang WG (2011) Prostate transglutaminase (TGase-4) antagonizes the anti-tumour action of MDA-7/IL-24 in prostate cancer. J Transl Med 9:49

Cecchi F, Rabe DC, Bottaro DP (2010) Targeting the HGF/Met signalling pathway in cancer. Eur J Cancer 46(7):1260–1270

Chaffer CL, Weinberg RA (2011) A perspective on cancer cell metastasis. Science 331(6024):1559–1564

Chang DD, Park NH, Denny CT, Nelson SF, Pe M (1998) Characterization of transformation related genes in oral cancer cells. Oncogene 16(15):1921–1930

Chen S, Maul RS, Kim HR, Chang DD (2000) Characterization of the human EPLIN (Epithelial Protein Lost in Neoplasm) gene reveals distinct promoters for the two EPLIN isoforms. Gene 248(1–2):69–76

Chircop M, Oakes V, Graham ME, Ma MP, Smith CM, Robinson PJ, Khanna KK (2009) The actin-binding and bundling protein, EPLIN, is required for cytokinesis. Cell Cycle 8(5):757–764

Coghlin C, Murray GI (2010) Current and emerging concepts in tumour metastasis. J Pathol 222(1):1–15

Davies S, Jiang WG (2010) ALCAM, activated leukocyte cell adhesion molecule, influences the aggressive nature of breast cancer cells, a potential connection to bone metastasis. Anticancer Res 30(4):1163–1168

El Touny LH, Banerjee PP (2007) Genistein induces the metastasis suppressor kangai-1 which mediates its anti-invasive effects in TRAMP cancer cells. Biochem Biophys Res Commun 361(1):169–175

Fidler IJ (1970) Metastasis: quantitative analysis of distribution and fate of tumour emboli labelled with 125I-5-iodo-2′-deoxyuridine. J Natl Cancer Inst 45:773–782

Han MY, Kosako H, Watanabe T, Hattori S (2007) Extracellular signal-regulated kinase/mitogen-activated protein kinase regulates actin organization and cell motility by phosphorylating the actin cross-linking protein EPLIN. Mol Cell Biol 27(23):8190–8204

Jiang WG, Hiscox SE, Parr C, Martin TA, Matsumoto K, Nakamura T, Mansel RE (1999) Antagonistic effect of NK4, a novel hepatocyte growth factor variant, on in vitro angiogenesis of human vascular endothelial cells. Clin Cancer Res 5(11):3695–3703

Jiang WG, Martin TA, Parr C, Davies G, Matsumoto K, Nakamura T (2005) Hepatocyte growth factor, its receptor, and their potential value in cancer therapies. Crit Rev Oncol Hematol 53(1):35–69

Jiang WG, Martin TA, Lewis-Russell JM, Douglas-Jones A, Ye L, Mansel RE (2008) Eplin-alpha expression in human breast cancer, the impact on cellular migration and clinical outcome. Mol Cancer 7:71

Malik FA, Sanders AJ, Jiang WG (2009) KAI-1/CD82, the molecule and clinical implication in cancer and cancer metastasis. Histol Histopathol 24(4):519–530

Martin TA, Jiang WG (2010) Hepatocyte growth factor and its receptor signalling complex as targets in cancer therapy. Anticancer Agents Med Chem 10(1):2–6

Maul RS, Chang DD (1999) EPLIN, epithelial protein lost in neoplasm. Oncogene 18(54):7838–7841

Maul RS, Song Y, Amann KJ, Gerbin SC, Pollard TD, Chang DD (2003) EPLIN regulates actin dynamics by cross-linking and stabilizing filaments. J Cell Biol 160(3):399–407

Nakamura T, Sakai K, Matsumoto K (2010) Anti-cancer approach with NK4: bivalent action and mechanisms. Anticancer Agents Med Chem 10(1):36–46

Nakamura T, Sakai K, Matsumoto K (2011) Hepatocyte growth factor twenty years on: much more than a growth factor. J Gastroenterol Hepatol 26(Suppl 1):188–202

Nguyen DX, Massague J (2007) Genetic determinants of cancer metastasis. Nat Rev Genet 8(5):341–352

Office for National Statistics (2011) Cancer incidence and mortality in the UK, 2006–2008. Statistical bulletin

Paget S (1889) The distribution of secondary growth in cancer of the breast. Lancet 133:571–573

Ruddon RW (1987) Biology of tumour metastasis. In: Cancer biology, 2nd edn. Oxford University Press Inc, New York, pp 443–467

Sanders AJ, Ye L, Mason MD, Jiang WG (2010) The impact of EPLINα (epithelial protein lost in neoplasm) on endothelial cells, angiogenesis and tumorigenesis. Angiogenesis 13:317–326

Sanders AJ, Martin TA, Ye L, Mason MD, Jiang WG (2011) EPLIN is a negative regulator of prostate cancer growth and invasion. J Urol 186(1):295–301

Thiery JP, Acloque H, Huang RY, Nieto MA (2009) Epithelial-mesenchymal transitions in development and disease. Cell 139(5):871–890

Xu JH, Guo XZ, Ren LN, Shao LC, Liu MP (2008) KAI1 is a potential target for anti-metastasis in pancreatic cancer cells. World J Gastroenterol 14(7):1126–1132

Zhang S, Wang X, Osunkoya AO, Iqbal S, Wang Y, Chen Z, Muller S, Josson S, Coleman IM, Nelson PS, Wang YA, Wang R, Shin DM, Marshall FF, Kucuk O, Chung LW, Zhau HE, Wu D (2011) EPLIN downregulation promotes epithelial-mesenchymal transition in prostate cancer cells and correlates with clinical lymph node metastasis. Oncogene 30:4941–4952

Electrical Cell-Substrate Impedance Sensing for Measuring Cellular Transformation, Migration, Invasion, and Anticancer Compound Screening

Bryan Plunger, Chang Kyoung Choi, and Tim E. Sparer

Abstract The first step in cancer development is the transformation of a primary cell into an immortalized state. Characteristics of a transformed cell include increased proliferation, loss of contact inhibition and attachment, and the ability to form tumors in mice. Electrical cell substrate impedance sensing (ECIS) is the measurement of resistance and reactance across an electrode containing the growing cells. As they grow, the characteristics of transformed cells can be evaluated including migration and invasion. This chapter will review the current uses of ECIS and speculate on its future uses in cancer biology. ECIS has allowed the experimental evaluation of compounds that induce cellular transformation (i.e. potential carcinogens) and individual pathways involved in aspects of cellular transformation. Also explored is the possibility of using ECIS as a high throughput screen of anti-cancer compounds. In the future, ECIS could be used to evaluate "personalized" anticancer treatments where anticancer compounds are tested on an individual's cancer cells in order to design personalized anti-proliferation or anti-metastasis treatments.

1 Introduction

Electrical cell-substrate impedance sensing (ECIS), also called impedance measurements, is a method for monitoring many aspects of cellular behavior, including proliferation, adhesion, motility, and morphologic changes (Giaever and Keese

B. Plunger • C.K. Choi
Mechanical Engineering-Engineering Mechanics, Michigan Technological University, Houghton, MI 49931, USA

T.E. Sparer (✉)
Department of Microbiology, The University of Tennessee, Knoxville, TN 37996, USA
e-mail: tsparer@utk.edu

W.G. Jiang (ed.), *Electric Cell-Substrate Impedance Sensing and Cancer Metastasis*, Cancer Metastasis - Biology and Treatment 17, DOI 10.1007/978-94-007-4927-6_4,

1984, 1986, 1991, 1993).One of the most difficult cellular activities to detect with traditional assays, like chemical staining or optical examination, is cellular transformation. Cellular transformation refers to the process of "transformation" from a non-cancerous state into a cancerous one. In the early stages of transformation, microscopic evaluation of transformation is difficult, and chemical assays such as staining and DNA based genotyping are time consuming and provide only a static endpoint resulting in the destruction of the cell (Combes et al. 1999; Sakai 2007; Poth et al. 2008). ECIS is a useful continuous and non-invasive tool for early detection of cellular transformation.

ECIS is a useful predictor of cellular transformation because it sensitively measures many of the cellular characteristics that change during transformation. ECIS measurements are highly dependent on the cell-cell and cell-substrate adhesions, cellular membrane properties, motility, and thickness of the cellular layer (Choi et al. 2007a, b; Park et al. 2009). Impedance sensing can detect minute changes in these factors that are indistinguishable with microscopy alone and allows monitoring a large sample size (i.e. the entire well) with a single reading. Impedance also allows for continuous sampling, compared with manually measuring chemical and optical differences at select time points.

ECIS is more efficient for examining potential carcinogens compared to current assays. Typically for studies investigating the effects of carcinogens that potentially could transform cells, the sample must be grown for 4–6 weeks (Combes et al. 1999). After this period the sample is fixed, stained, imaged, and foci are counted either by hand or with computer imaging software. More recently developed methods use a two-stage assay, wherein non-foci forming amounts of carcinogen are added in the first stage followed by a foci-inducing condition in the second. This approach requires weeks to complete and yields only an end-point measurement (Sakai 2007).

Over the years the ECIS system has been commercialized. Drs. Giaever and Keese, the initial developers of this method, founded Applied Biophysics, which brought this device to market. ACEA Biosciences Inc produces a modified ECIS system, which is now marketed as the xCELLigence System (Roche). This commercialization has made this technique more widely available to researchers without an engineering background. The standardization of this technique with different sized wells and the ability to monitor migrations with a modified migration chamber, allows the measurement of cell viability, proliferation, morphology, migration, invasion, and adhesion. This chapter will review the uses of impedance measurements for different aspects of cancer biology and speculate on its futures uses.

1.1 Characteristics of Cellular Transformation and Its Effect on Impedance

ECIS has been used to study cellular transformation in different cell types. The phenotypic changes of a normal fibroblast into an immortalized one include

unlimited cellular growth, increased growth rates, loss of contact inhibition, and foci formation (Park et al. 2009; Yang et al. 2011). These changes are easily detectable with impedance measurements. As cells die, they have lower impedance than living cells. Their membranes disintegrate and no longer act as barriers to the current traveling from the electrode to the counter electrode. Dead cells also decrease focal contacts with the substrate freeing electrode space and once again reducing impedance. Immortalization (i.e. cellular growth and proliferation) of cells increases impedance due to a decrease in dead cells and cells undergoing apoptosis. The resistance between electrodes increases as the cells increase in size and number, akin to installing a larger resistor in a circuit. Loss of contact inhibition allows cells to form "colonies" of piled-up cells termed foci. These foci increase impedance as layers of dividing cells are added (Park et al. 2009; Yang et al. 2011). Tumor formation in an animal often correlates with the cell's ability to form foci and proliferate unchecked. This is one way that impedance can be predictive of tumor formation.

1.1.1 Chemical/Membrane Structure

The chemical makeup and subsequent electrical properties of the cell are another contributing factor to impedance and may be utilized as a transient readout of transformation. Cell types can have vastly different inherent electrical qualities (i.e. resistance, capacitance, and conductivity). The lipid membrane is inherently electrically insulating, but the embedded proteins and the overall distribution of these non-lipid structures lead to differences in conductivity in different cell types. Capacitance is another unique identifying feature of a cell that can be indicative of differentiation (Bagnaninchi and Drummond 2011). The internal chemistry of the cell (i.e. the components within the cytoplasm) is also a determinant of a cell's electrical signature. Some cell types, such as neurons, inherently conduct an electrical signal (Park et al. 2011). The impedance measurements composed of the resistance and reactance is a reflection of the summation of all these cellular properties.

During cellular transformation, the cell membrane and chemical properties of the cell change. This transition is indistinguishable optically and often difficult to detect even with chemical assays. However, ECIS allows for accurate and real-time tracking of these changes (Bagnaninchi and Drummond 2011). It is important to keep in mind that some of these changes can be subtle and could be overshadowed in the ECIS reading by more dominant factors such as morphology and motility (Yang et al. 2011). With a properly controlled study, ECIS can be used to assess these changes when compared to untransformed cells.

1.1.2 Morphological Factors

ECIS measurements are very sensitive to morphological changes in the cell. Cellular transformation often leads to changes in both cell size and proliferation. Changes in shape and size affect the cell-electrode interaction. For instance, given a cell with a

fixed volume, if one were to stretch that cell thinly over the electrode surface, a higher impedance (primarily due to a greater resistance) would be measured than if that cell were spherical (Poth et al. 2008; Park et al. 2009). Any signal that is transmitted only through the medium, i.e. the uncovered or "naked" electrode, has a lower resistance value than a signal that must travel through or around a cell. This is why ECIS readings should be referenced to the electrode with cell coverage. By normalizing the readings to the area with cell coverage, along with comparisons to naked scans, impedance readings become more sensitive and interpretable. Otherwise differences in impedance readings are difficult to interpret (Park et al. 2009; Yang et al. 2011). When a confluent cellular layer fully covers the electrode, this concern is mitigated.

Besides coverage of the electrode, the thickness of the cellular layer, cell-cell and cell-electrode adhesions also factor into ECIS measurements. A layer of cells that is only one cell thick (i.e. 1–10 μm depending on the cell line) has a much different impedance reading than a layer that is three to four cells thick (i.e. 4–40 μm). Different cell types also vary in the strength of their cell-cell adhesion. A very tightly packed monolayer with strong focal adhesions between the cells results in significantly higher impedance than those that form a loosely packed layer, that is, as long as all other parameters are constant (Choi et al. 2007a, b, 2010). Increased cellular adhesion and packing densities are indicative of cellular transformation. Some transformed cells form colonies of closely packed cells known as foci. These foci greatly increase the local cellular impedance. Even when a sample is confluent, ECIS can detect the formation of these foci and can assess the number and rate of foci formation (Park et al. 2009). Overall impedance measurements can be used to fully monitor real-time cellular transformation events including changes in cell size, shape, cell-cell and cell substrate adhesions.

2 Cellular Transformation

2.1 ECIS for Measuring Cellular Transformation

ECIS measurement has been used in cell biology for decades (Giaever and Keese 1984). Although the system is now commercially available, the basic tenants of impedance measurements have not changed. It consists primarily of a large counter electrode, a series of smaller sampling electrodes with cell culture medium between them, a signal generator, and lock-in amplifier to record the impedance measurements. This experimental setup is similar whether it is measuring migration, proliferation, adhesion, or transformation.

Two examples of ECIS usage for detecting cellular transformation are reviewed here. ECIS changes were compared between transformed and untransformed cells in an artificially transformed mouse fibroblast cell line (Park et al. 2009), and a cancerous / non-cancerous oral epithelial cell line (Yang et al. 2011). Park et al. used an industry standard gold (Au) electrode with a 250 μm diameter on the active electrodes. Stable NIH3T3 mouse fibroblast transfectants were generated that express either a wild-type chemokine receptor (WT_CXCR2) or a mutant chemokine

receptor (D143V_CXCR2). The mutation of the aspartic acid (D) to a valine (V) leads to a constitutively active chemokine receptor that can transform normal fibroblasts (Burger et al. 1999). This transformation is characterized by increased proliferation and foci formation. These transfectants, as well as the untransfected control NIH3T3 cells, were then used to corroborate impedance measurements as a measure of cellular transformation.

Yang et al. compared ECIS on an oral squamous carcinomas cell line, CAL27, and the non-cancerous oral epithelial cell line, Het-1A (Yang et al. 2011). They used both classical methods and ECIS to measure cell adhesion, spreading, and proliferation differences between these two cell lines. They were able to show that ECIS was a much more rapid method for distinguishing between the cancerous and non-cancerous lines.

2.2 Stable CXCR2 Transfectants

2.2.1 Proliferation

Park et al. found that transfectants overexpressing the constitutively active CXCR2 (D143V_CXCR2) had increased proliferation compared to uninfected controls (Fig. 1). The impedance measurements also showed that both resistance and reactance increased over time. Interestingly, WT_CXCR2, which is not associated with transformation had increasing resistance that eventually leveled off at around 3,000 min while D143V_CXCR2 continued to rise. In this case, reactance mimicked proliferation more closely than resistance. Traditional hemacytometer cell counts were used to show the accuracy of the ECIS.

2.2.2 Foci Formation

Foci formation is the process of cells overcoming contact inhibition and "piling" on top of one another to form cellular colonies. After 2 weeks the plates can be stained and the numbers of colonies enumerated. Transfectants were seeded onto untransfected feeder cells and monitored with ECIS for 61 h. Data was acquired in 2-s intervals with a frequency of 32 Hz. Readings were made with a 30 ms time constant and 12 dB per decade roll-off. The results of the 64 readings made over the interval were then averaged and the standard deviation calculated. Figure 2a shows the visualization of foci from two transfectants. Foci were counted and the averages and the standard deviations calculated (Fig. 2b). As expected, these data show that greater foci formation in transfectants expressing the constitutively active receptor (D143V_CXCR2). The resistance portion of the data was recorded at 5.62 kHz and the reactance data at 56.2 kHz, as these were found to be the most sensitive for these parameters. Foci formation was not the only factor directing the impedance changes. Significant alterations in cellular attachment and proliferation were also contributors. This study showed that the pattern of foci formation corresponded directly to the ECIS-measured resistance and reactance data (Park et al. 2009).

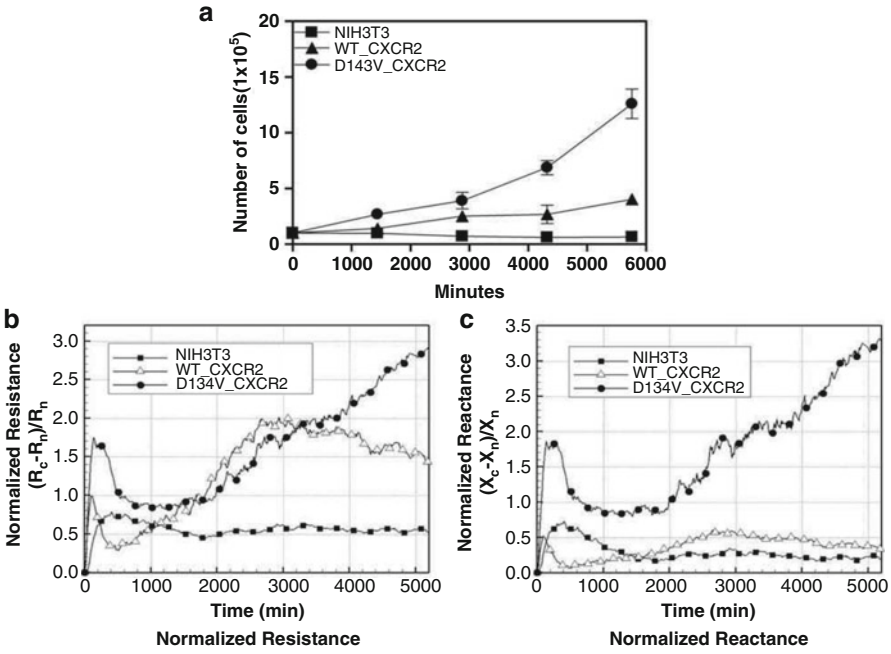

Fig. 1 ECIS measurements correlate with increased cellular growth. (**a**) Cellular growth over time. Each point represents the average of three wells with standard deviation shown. Cells were grown in a six well dish and harvested and counted with a hemacytometer. Growth curves of transfectants expressing constitutively active CXCR2 (D143V_CXCR2), wild type CXCR2 (WT_CXCR2), or the untransfected controls (NIH3T3) are shown. (**b**) The normalized resistance data collected from the impedance where R_n indicates the "naked" scan and R_c the "covered" readings. Symbols were added for clarity even though data were acquired at a rate of 32 Hz for 2 s. Both the WT_CXCR2 and D143V_CXCR2 have increased resistance compared to untransfected cells. The fully transformed D143V_CXCR2 transfectants continues to have increasing resistance while WT_CXCR2 begins to plateau at around 3,000 min. (**c**) The reactance portion of the impedance measurements with the reactance (X) normalization equation shown where subscripts "c" and "n" are the covered and naked reactance readings. Both the WT_CXCR2 and the untransfected control (NIH3T3) remained low while the D143V_CXCR2 transfectants increased comparably to the cell counts (Park et al. 2009) (Reproduced from Park et al. 2009 with permission from Elsevier)

2.3 Oral Epithelial Cells

Yang et al. found similar results in a relatively short time period (72 h) using oral squamous carcinomas cells, CAL27, and the non-cancerous oral epithelial cells, Het- 1A,cell lines (Yang et al. 2011). The cell index (CI), which was based on the greatest impedance recorded across the three test frequencies, was computed. This calculation divides the cell-covered resistance R_c by the naked resistance R_0 then subtracts one. This produces a CI of zero when the cell-covered resistance is the same as naked resistance and a progressively higher number as the cell-covered resistance of the electrode increases. 10 mV was applied across the cell lines grown on gold electrodes and data was recorded at frequencies of 10, 25, and 50 kHz.

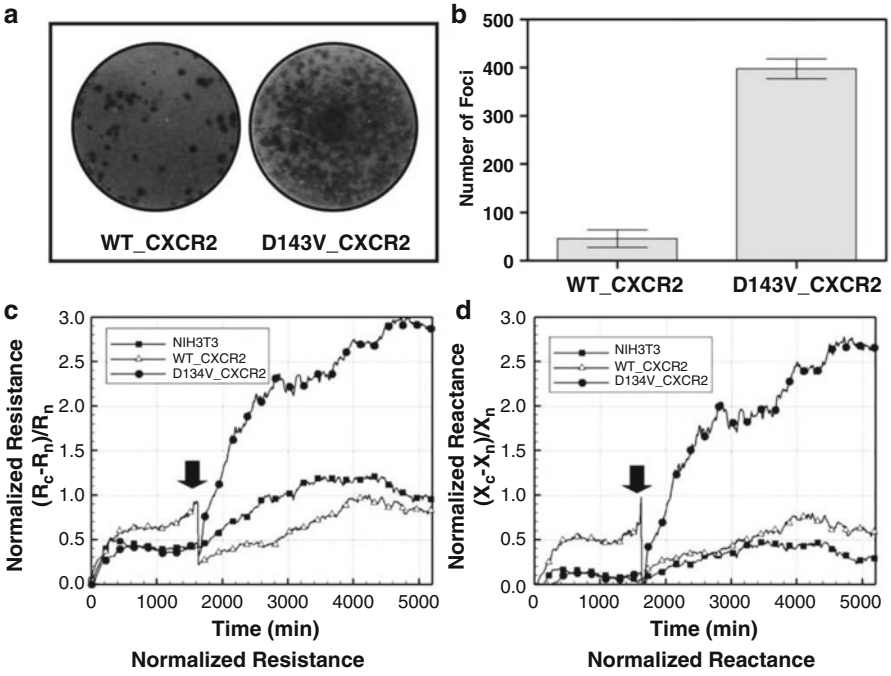

Fig. 2 Impedance measurements correlate with foci formation. (**a**) Staining allows for manual counting of foci in each of the three independent trials. 14 days after plating, the wells were stained. (**b**) The average counts of foci, along with error bars indicating standard deviation, from three experiments. The untransfected controls (NIH3T3) were zero in all experiments. (**c**, **d**) Resistance and reactance data where each symbol represents every 30 data points and arrows indicate time of addition of transfectants to the untransfected monolayer. The data clearly illustrate an increase in both parameters in the D143V transfectants that produce the most foci (Park et al. 2009) (Reproduced from Park et al. 2009 with permission from Elsevier)

Impedance data was recorded at intervals of 5–30 min depending on the trial. Their results (Fig. 3) are similar to those of Park et al. even though their ECIS setup differed. The resistance of the cancerous cell lines rose rapidly within the three day period, clearly distinguishing the cancerous and non-cancerous lines.

3 Migration/Metastasis

The ability of cancer cells to migrate from the site of primary tumor growth to a distant location in the body is called metastasis. Often times the metastatic tumor is more lethal than the initial primary cancer. The more metastatic the cancer, the more lethal it is. This is true of the most common cancers: breast, prostate, lung etc. The ability to predict the metastatic potential of a cancer is useful in deciding the aggressiveness of the treatment regime. The next two sections will address the use of ECIS in assessing two important characteristics of a cancer's metastatic ability: migration

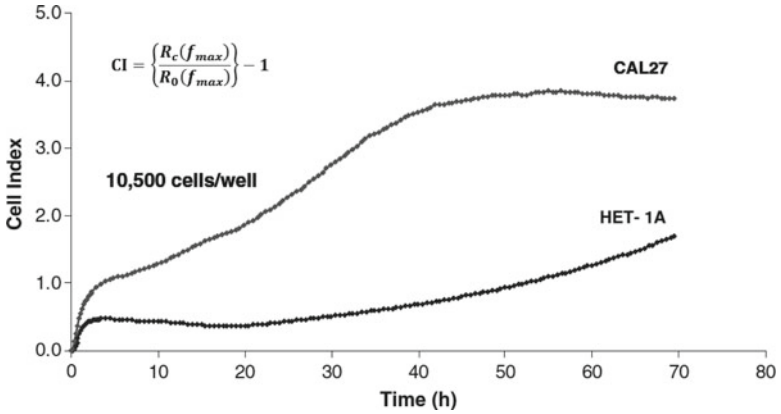

Fig. 3 Impedance measurements can distinguish cancerous from non-cancerous cells. The calculated cell index (equation given) as a function of time is shown for the cancerous oral squamous cell line, CAL27, and the non-cancerous oral epithelial cell line, HET-1A. The parameter f_{max} refers to the frequency on which maximum impedance occurred (10, 25, or 50 kHz). The cancerous cells had a distinctly greater rate of impedance increase and a higher overall level during the test (72 h)[11] (Reproduced with permission from Yang et al. 2011, Fig. 2a)

and invasion. Migration out of the primary tumor is the first step in metastasis. Next the cancer travels via the lymphatics or blood stream to distant sites within the body. Following attachment using a combination of integrins and other adhesion molecules, the cells then actively invade through the extracellular matrix and endothelium into the distant site. Provided the site is favorable for growth, the metastatic tumor will grow. ECIS has been used to measure both the metastatic ability and invasive properties of different cancers.

3.1 ECIS Measurement of Attachment and Migration

Migration of cells involves cytoskeletal rearrangements in order for the cell to extend and contract the leading and trailing edges of the cell. When a cell is migrating through a monolayer, such as the endothelium surrounding the blood vessels or lymphatics, the cell must again rearrange its internal cytoskeleton in order to squeeze through the cell-cell junctions and into the tissues. Inhibitors of actin polymerization, a key cytoskeletal component involved in migration, were used to show the accuracy of ECIS measurements coupled with microscopy of cellular movements (Choi et al. 2007a, b).

Others have used ECIS for demonstrating the efficacy of migration specific inhibitors. Daouti et al. used ECIS for assessing the role of thienopyridone, an inhibitor of an oncolytic phosphatase (PRL-3), to show that migration was inhibited but not cel-

lular proliferation (Daouti et al. 2008). The over expression of PRL is found in a variety of different tumors and its overexpression can lead to cellular transformation and metastasis (Stephens et al. 2005). What made this discovery more interesting was the drug's affect on migration without altering proliferation, making the small molecule inhibitor potentially an anti-metastatic drug. Another study used secreted frizzled-related proteins (sFRPs) to inhibit breast cancer cell attachment and migration that was detected with ECIS (Martin-Manso et al. 2011). sFRPs are proposed to be Wnts inhibitors. Wnts cell signaling proteins that are important for neoplasia development (Dihlmann and von Knebel Doeberitz 2005, Matsuda et al. 2009). The effect of the BK channel inhibitor, paxilline, was shown to decrease migration of glioblastomas via ECIS measurements. Glioblastomas switch from migration to a more invasive/metastatic phenotype upon exposure to sub-lethal irradiation, which can be minimized using paxilline (Wild-Bode et al. 2001; Park et al. 2006).

ECIS was also utilized to demonstrate the differences between normal human melanocytes and melanoma attachment and migration (Bosserhoff et al. 2011). Melanoblasts were dedifferentiated into melanomas and compared with the attachment and migration of normal human melanocytes. These experiments showed that even if proliferation is relatively similar, ECIS could distinguish between attachment and migration of normal versus cancerous cells.

4 Invasion

4.1 Classic Invasion Assays

Invasion differs from migration in that it involves more complex reactions. Invasion is often indicative of a more metastatic phenotype because this assay requires the cells to "invade" into a matrix or through an endothelial cell monolayer. This entails not just movement but upregulation of attachment proteins and matrixmetalloproteases (MMPs). These proteins are utilized in order to get into or out of tissues. Traditional invasion assays consist of adding cells to a matrigel coated insert and then counting the number of cells that enter the gel. Other assays include adding cancer cells on top of monolayer of endothelial cells and inducing migration across it. The greater the number of cells that migrate through the monolayer, the more metastatic (albeit *in vitro*) and/or more invasive a sample is considered (Methods Mol Biol. (2005);294:97–105).

4.2 Invasion Assays with ECIS

Keese et al. established an artificial cell culture system for studying migration through a monolayer (Keese et al. 2002). Using prostate cell lines placed over the top of human umbilical vein endothelial cells (HUVECs), they recorded a

reduction in impedance as the cells migrated through the endothelial monolayer. They compared impedance measurements between a more metastatic versus a less metastatic cell line to show that impedance correlated with metastatic ability. The authors suggest that ECIS could be used to determine the metastatic ability of a biopsy, which in turn could be used as a factor in recommending a treatment course.

As with inhibitors of migration, inhibitors of invasion can be assessed with ECIS. A small interfering RNA (siRNA) was used to knock down mammalian Sec62 expression and classical invasion assays were compared with ECIS measurements (Greiner et al. 2011). Sec62 has been shown to be important in ER trafficking, translation, and the unfolded protein response. Over expression of this protein is associated with the progression of prostate cancers and could be a potential target for anti-cancer therapies. Greiner et al. used ECIS of prostate cancers and other cancer cell lines treated with the siRNA to Sec62. When Sec62 was knocked down there was a reduction in migration/invasion without affecting proliferation.

Rahim et al. discovered an inhibitor of ETS that is capable of inhibiting androgen-induced invasion of endothelial monolayers using ECIS (Rahim et al. 2011). The ETS family of transcription factors is involved in 40–70 % of all prostate cancers (Soller et al. 2006; Demichelis et al. 2007; Nam et al. 2007; Rajput et al. 2007). Researchers screened molecules that inhibit androgen responsive prostate cancer cells (VCaP and LNCaP) but not androgen sensitive prostate line (PC3) invasion. The development of an androgen specific, anti-metastatic drug is a potential alternative to the current non-specific treatment for this type of prostate cancer (i.e. castration or androgen inhibitors). Once again ECIS contributed to the discovery of a molecule that could alter the treatment possibilities for different cancers.

5 Anticancer Compound Screening

The sections have described the discovery of multiple drugs that could be considered anti-cancer compounds because they prevent migration or invasion, In addition, ECIS can be used to screen for anti-proliferative compounds. ECIS and optical imaging was used to test the ability of green tea cachectins to prevent colorectal cancer cell proliferation and adhesion (Sukhthankar et al. 2010; Choi et al. 2011). ECIS was also used to dissect the different pathways involved in apoptosis of colorectal cancer cells using siRNAs to knockdown portions of an anti-apoptotic pathway. In another study, tolfenamic acid was monitored with impedance measurements as well as more traditional methods (Lee et al. 2008). Using ECIS and microscopy Arias et al. showed that inhibition of oral cancer cell (CAL27) growth could be temporally monitored after treatment with a variety of apoptosis inducing compounds and concentrations (Arias et al. 2010). In each of these cases, anti cancer compounds were shown to be effective *in vitro* but whether this efficacy can be translated into actual *in vivo* cancer treatments remains to be tested.

6 Future of ECIS

6.1 New Applications of ECIS

It is clear from these examples that ECIS is a powerful and practical tool for the examination and early detection of cellular transformation. No other tool for such measurements has the versatility and the sampling rate that ECIS is capable of providing. With ever increasing interest and knowledge in the fields of cell and tissue therapy, as well as ongoing cancer research, the demand and applications of ECIS will continue to grow. One drawback of ECIS is that the cells must be adherent to the electrode. This limits its application to adherent cancers, eliminating most of leukemias. Being able to screen anti-cancer compounds in a 96 well format, perhaps even scaling further to 386 wells, with ECIS would allow the assessment of potential inhibitors of cancer migration, attachment, invasion, as well as the more common proliferation inhibitors on an individuals cancers.

6.2 Microscopy in Tandem with ECIS

One innovation that will address some of the current shortfalls of the current system is the use of a transparent electrode. Indium Tin Oxide (ITO) is an optically transparent but electrically conductive material that is a suitable electrode material for ECIS. With a transparency comparable to glass, Choi et al. showed that ITO electrodes produce readings equal to that of the industry standard gold electrodes (Choi et al. 2007b). Gold electrodes, while having excellent biocompatibility and electrical properties, are not conducive to most microscopy techniques. Microscopy allows visual confirmation of cell-cell and cell-substrate adhesions that complement impedance readings. Interference reflection contrast microscopy (IRCM) and differential interference contrast microscopy (DICM) are both compatible with ITO electrodes but not with the opaque gold electrode (Choi et al. 2007a; Chang et al. 2008). ITO electrodes have equivalent biocompatibility, comparable electrical sensing capabilities, and excellent optical properties for most methods of cellular imaging. These electrodes could be used when extensive microscopic analysis is needed in tandem with ECIS.

6.3 ECIS and Stem Cell Differentiation

Because ECIS sensitively measures changes in the cellular state, impedance sensing is being used in stem cell research (e.g. the differentiation of human mesenchymal stem cells (hMSC) into adipocytes or osteoblasts). Stem cell research holds much potential for providing reparative tissue cells that originate from the donor's

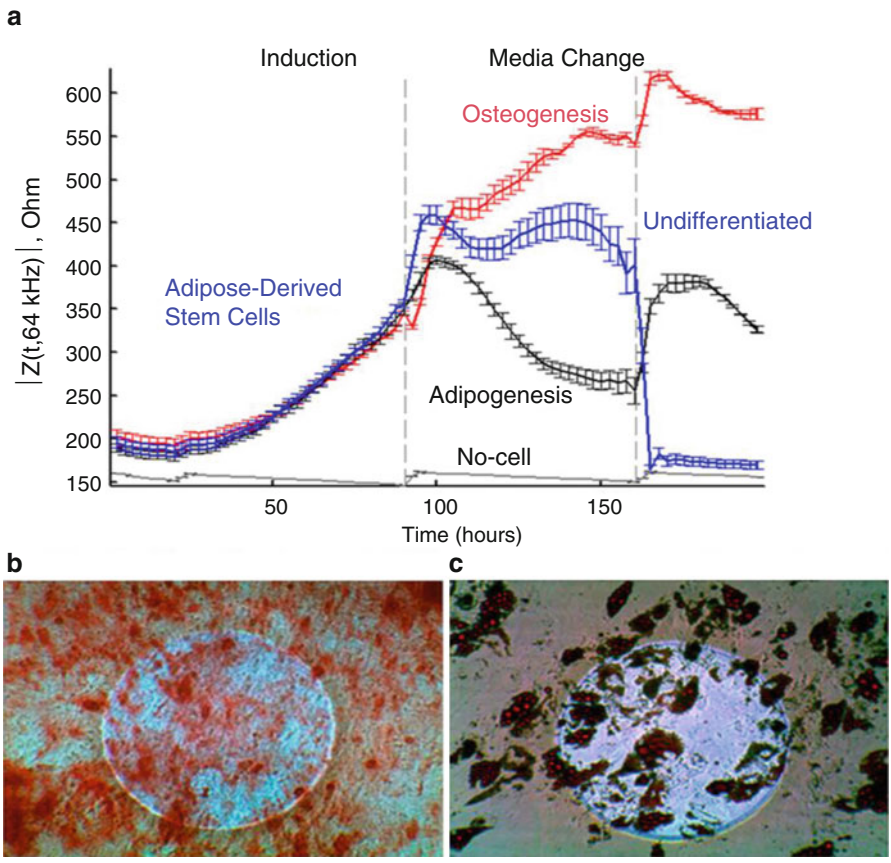

Fig. 4 Impedance measurements to analyze stem cell differentiation. Impedance data of hMSC differentiation (**a**) along with optical confirmation (**b**, **c**). (**a**) The mean impedance with error bars of the impedance of the adipogenic, osteogenic, and non-differentiated cell lines recorded at 64 kHz. Each differentiation produced its own unique impedance signature. Fluctuations occurred when the medium was changed, as indicated with *dotted lines*. (**b**) *Alizarin Red* stain to confirm osteogenesis and (**c**) *Oil Red* O staining to confirm adipogenesis. 250 μm electrodes appear as the *bright circles* in both images (Bagnaninchi and Drummond 2011)

stem cells. The classical method used to confirm this differentiation is either optical evaluation or chemical assays that require waiting days to weeks after initiation of differentiation. Microarray/qPCR analysis, which produces a transcriptional profile of the cell, is costly and results in only a single time point of data (Kelley et al. 2009). Staining assays identify features of differentiated stem cells, but only after the differentiation has advanced to the point of structural formations, such as lipid deposits in adipocytes or calcified matrix in osteoblasts (Bagnaninchi and Drummond 2011) (Fig. 4).

Recently, Bagnaninchi and Drummond used ECIS to identify the differentiation of an hMSC cell line into two distinct types of differentiated cells. Impedance

measurements identified osteogenic and adipogenic differentiation of hMSCs before the morphological differences could be visualized. Differentiation could be identified as early as 12 h post induction and was definitive by 22 h. This is in contrast to the staining technique that required 14 days in order to identify differences between osteoblasts and adipocytes. The researchers attribute this early change in dielectric properties of altered membrane capacitance due to differentiation induction (Bagnaninchi and Drummond 2011). Their research compliments that of others investigating using ECIS for identifying stem cell differentiation (Park et al. 2011; Hildebrandt et al. 2010).

One potential drawback of using ECIS to monitor stem cell differentiation: it is unknown as to whether the minute electrical pulses needed to make ECIS measurements have any effect on differentiation. This is a common obstacle to ECIS measurement but this drawback is largely case specific. It is likely that ECIS has yet to make its full impact on the field of cellular biology.

References

Arias LR, Perry CA, Yang L (2010) Real-time electrical impedance detection of cellular activities of oral cancer cells. Biosens Bioelectron 25:2225–2231

Bagnaninchi PO, Drummond N (2011) Real-time label-free monitoring of adipose-derived stem cell differentiation with electric cell-substrate impedance sensing. Proc Natl Acad Sci 108:6462–6467

Bosserhoff AK, Ellmann L, Kuphal S (2011) Melanoblasts in culture as an in vitro system to determine molecular changes in melanoma. Exp Dermatol 20:435–440. doi:10.1111/j.1600-0625.2011.01271.x

Burger M et al (1999) Point mutation causing constitutive signaling of CXCR2 leads to transforming activity similar to Kaposi's sarcoma herpesvirus-G protein-coupled receptor. J Immunol 163:2017–2022

Choi CK, English AE, Kihm KD, Margraves CH (2007a) Simultaneous dynamic optical and electrical properties of endothelial cell attachment on indium tin oxide bioelectrodes. J Biomed Opt 12(6):064028

Choi CK, English AE, Jun S-I, Kihm KD, Rack PD (2007b) An endothelial cell compatible biosensor fabricated using optically thin indium tin oxide nitride electrodes. Biosens Bioelectron 22:2585–2590

Choi CK, Sukhthankar M, Kim C-H, Lee S-H, English A, Kihm KD, Baek SJ (2010) Cell adhesion property affected by cyclooxygenase and lipoxygenase: opto-electric approach. Biochem Biophys Res Commun 391:1385–1389

Choi CK, Park G, Sparer TE (2012) Choi CK, Park G, Sparer TE (2012) Micro-impedance measurements for cellular transformation and cancer treatments. Herold KE, Rasooly A (eds) Biosensors and molecular technologies for cancer diagnostics. CRC Press/Taylor & Francis, Boca Raton. Print ISBN: 978-1-4398-4165-5. eBook ISBN: 978-1-4398-4166-2

Combes R, Balls M, Curren R, Fischbach M, Fusenig N, Kirkland D, Lasne C, Landolph J, LeBoeuf R, Marquardt H, McCormick J, Müller L, Rivedal E, Sabbioni E, Tanaka N, Vasseur P, Yamasaki H (1999) Cell transformation assays as predictors of human carcinogenicity. The European Centre for the Validation of Alternative Methods, Ispara, Italy, pp 745–767

Daouti S et al (2008) A selective phosphatase of regenerating liver phosphatase inhibitor suppresses tumor cell anchorage-independent growth by a novel mechanism involving p130Cas cleavage. Cancer Res 68:1162–1169. doi:10.1158/0008-5472.can-07-2349

Demichelis F et al (2007) TMPRSS2:ERG gene fusion associated with lethal prostate cancer in a watchful waiting cohort. Oncogene 26:4596–4599
Dihlmann S, von Knebel Doeberitz M (2005) Wnt/β-catenin-pathway as a molecular target for future anti-cancer therapeutics. Int J Cancer 113:515–524. doi:10.1002/ijc.20609
Giaever I, Keese CR (1984) Monitoring fibroblasts behavior in tissue culture with an applied electric field. Proc Natl Acad Sci 81:3761–3764
Giaever I, Keese CR (1986) Use of electric fields to monitor the dynamical aspect of cell behavior in tissue culture. IEEE Trans Biomed Eng BME-33:242–247
Giaever I, Keese CR (1991) Micromotion of mammalian cells measured electrically. Proc Natl Acad Sci 88:7896–7900
Giaever I, Keese CR (1993) A morphological biosensor for mammalian cells. Nature 366:591–592
Greiner M et al (2011) Silencing of the SEC62 gene inhibits migratory and invasive potential of various tumor cells. Int J Cancer 128:2284–2295. doi:10.1002/ijc.25580
Hildebrandt C, Büth H, Cho S, Impidjati, Thielecke H (2010) Detection of the osteogenic differentiation of mesenchymal stem cells in 2D and 3D cultures by electrochemical impedance spectroscopy. J Biotechnol 148:83–90
Keese CR, Bhawe K, Wegener J, Giaever I (2002) Real-time impedance assay to follow the invasive activities of metastatic cells in culture. Biotechniques 33:842–850
Kelley ML, Strezoska Z, Fedorov Y (2009) hMSC differentiation marker detection using Thermo Scientific Solaris™ qPCR Gene Expression Assays. Nat Methods 6:783–856
Lee S-H et al (2008) ESE-1/EGR-1 pathway plays a role in tolfenamic acid-induced apoptosis in colorectal cancer cells. Mol Cancer Ther 7:3739–3750. doi:10.1158/1535-7163.mct-08-0548
Martin-Manso G et al (2011) sFRP-1 binds via its netrin-related motif to the N-module of thrombospondin-1 and blocks thrombospondin-1 stimulation of MDA-MB-231 breast carcinoma cell adhesion and migration. Arch Biochem Biophys 509:147–156. doi:10.1016/j.abb.2011.03.004
Matsuda Y, Schlange T, Oakeley E, Boulay A, Hynes N (2009) WNT signaling enhances breast cancer cell motility and blockade of the WNT pathway by sFRP1 suppresses MDA-MB-231 xenograft growth. Breast Cancer Res 11:R32
Nam RK et al (2007) Expression of TMPRSS2:ERG gene fusion in prostate cancer cells is an important prognostic factor for cancer progression. Cancer Biol Ther 6:40–45
Park C-M et al (2006) Ionizing radiation enhances matrix metalloproteinase-2 secretion and invasion of glioma cells through Src/epidermal growth factor receptor–mediated p38/Akt and phosphatidylinositol 3-kinase/Akt signaling pathways. Cancer Res 66:8511–8519. doi:10.1158/0008-5472.can-05-4340
Park G, Choi CK, English AE, Sparer TE (2009) Electrical impedance measurements predict cellular transformation. Cell Biol Int 33:429–433
Park HE, Kim D, Koh HS, Cho S, Sung J-S, Kim JY (2011) Real-time monitoring of neural differentiation of human mesenchymal stem cells by electric cell-substrate impedance sensing. J Biomed Biotechnol 2011:485173. doi:10.1155/2011/485173
Poth A, Heppenheimer A, Bohnenberger S (2008) Bhas42 cell transformation assay as a predictor of carcinogenicity. AATEX 14:519–521
Rahim S et al (2011) YK-4-279 inhibits ERG and ETV1 mediated prostate cancer cell invasion. PLoS One 6:e19343
Rajput AB et al (2007) Frequency of the TMPRSS2:ERG gene fusion is increased in moderate to poorly differentiated prostate cancers. J Clin Pathol 60:1238–1243. doi:10.1136/jcp.2006.043810
Sakai A (2007) BALB/c 3T3 cell transformation assays for the assessment of chemical carcinogenicity. AATEX 14:367–373
Soller MJ et al (2006) Confirmation of the high frequency of the TMPRSS2/ERG fusion gene in prostate cancer. Genes Chromosomes Cancer 45:717–719. doi:10.1002/gcc.20329
Stephens BJ, Han H, Gokhale V, Von Hoff DD (2005) PRL phosphatases as potential molecular targets in cancer. Mol Cancer Ther 4:1653–1661. doi:10.1158/1535-7163.mct-05-0248

Sukhthankar M, Choi CK, English A, Kim J-S, Baek SJ (2010) A potential proliferative gene, NUDT6, is down-regulated by green tea catechins at the posttranscriptional level. J Nutr Biochem 21:98–106. doi:10.1016/j.jnutbio.2008.11.002

Wild-Bode C, Weller M, Rimner A, Dichgans J, Wick W (2001) Sublethal irradiation promotes migration and invasiveness of glioma cells. Cancer Res 61:2744–2750

Yang L, Arias LR, Lane TS, Yancey MD, Mamouni J (2011) Real-time electrical impedance-based measurement to distinguish oral cancer cells and non-cancer oral epithelial cells. Anal Bioanal Chem 399(5):1823–1833

Epithelial-Mesenchymal Transition and the Use of ECIS

Jane Lane and Wen G. Jiang

Abstract The development of tumour cell invasion and metastasis is a prime factor influencing prognosis of cancer patients. Understanding the mechanisms involved in tumour cell invasion may aid in limiting tumour progression and lead to a reduction in patient mortality. In order to become invasive, tumour cells must overcome the physical barriers imposed by cell–cell adhesions and the basement membrane and attain a motile phenotype. Evidence is emerging which indicates a role for epithelial–mesenchymal transition (EMT) in tumour cell invasion whereby tumour cells would lose E-cadherin-dependent intercellular adhesion and acquire the ability to migrate, enabling these cells to invade adjacent tissues. This current chapter reviews the role of EMT in cancer metastasis and looks at the Electrical Cell-substrate Impedance Sensing system (ECIS) as an important tool for analysing changes in cell motility.

Abbreviations

EMT	Epithelial-mesenchymal transition
ECIS	Electrical cell-substrate impedance sensing
BMP7	Bone morphogenetic protein 7
MMP	Matrix metalloproteinase
EPLIN	Epithelial protein lost in neoplasm

J. Lane (✉) • W.G. Jiang
Metastasis and Angiogenesis Research Group, Institute of Cancer and Genetics,
Department of Surgery, Cardiff University School of Medicine, University Hospital of Wales,
Heath Park, Cardiff CF14 4XN, UK
e-mail: lanej1@cf.ac.uk

W.G. Jiang (ed.), *Electric Cell-Substrate Impedance Sensing and Cancer Metastasis*,
Cancer Metastasis - Biology and Treatment 17, DOI 10.1007/978-94-007-4927-6_5,

ECM	Extracellular matrix
ZO1	Zona occludens 1
HGF	Hepatocyte growth factor
EGF	Epidermal growth factor
TGFβ	Transforming growth factor β
CAM	Cell adhesion molecule
ROCK1	Rho associated serine threonine protein kinase 1
GDF9	Growth and differentiation factor 9
ALK-5	Activin-like kinase 5
PlGF	Placental growth factor
TGase-4	Transglutaminase 4

1 Introduction

1.1 Cancer Metastasis

The single most important factor affecting the prognosis of breast cancer patients is the progression to and the development of tumour cell invasion and metastasis. The process of tumour metastasis involves a series of steps that lead to the formation of secondary tumours in distant organs and accounts for most of the mortality and morbidity of cancer.

Invasion occurs when tumour cells acquire the ability to penetrate the surrounding tissues, passing through the basement membrane and extracellular matrix, leading to intravasation as they enter the lymphatic or vascular circulation. The metastatic cells then travel through the circulatory system and invade the vascular basement membrane and the extracellular matrix in the process of extravasation. Finally these cells will attach at a new site and proliferate to produce the secondary tumour. Focusing research efforts on understanding the mechanisms involved in tumour cell invasion may aid in limiting tumour progression and consequently lead to a reduction in the mortality of breast cancer patients.

1.2 Cell Motility

One of the factors determining the metastatic nature of cancer cells is their motility. Cell motility and migration is essential to normal development and is a major component of organogenesis, inflammation and wound healing. However, alterations in the signalling pathways controlling its regulation can lead to the pathological processes of tumour cell invasion and metastasis.

Cell motility, or locomotion, is governed by a series of distinct biophysical, interdependent processes involving changes in the cytoskeleton, cell-substrate adhesion and alterations in the extracellular matrix. In response to a stimulus, a cell will initiate polarisation and extend protrusions in the direction of migration (Ridley et al. 2003). These processes begin with extension of the leading edge by protrusion of lamellipodia and/or filopodia, driven by actin polymerisation and filament elongation, and are often accompanied by membrane ruffling (Ridley et al. 1992), which extends the cell body to then create new, distal adhesion sites. This protrusion is followed by adhesion between the cell and substratum at the leading edge which is accomplished mainly by integrin and non-integrin receptors binding to specific extracellular matrix protein domains (Faassen et al. 1992; Ridley et al. 2003). The next step in the motility process is actomyosin-mediated contraction of the cell resulting in forward motion of the cell body which is initiated by contractile forces being generated at or near the leading edge, associated with detachment of the trailing edge from the substratum. The migrating cell also secretes proteases necessary to digest the extracellular matrix proteins thus opening a pathway for the advancing cell.

Many different molecules have been implicated in the signalling process leading to cell motility/migration, with the associated loss of epithelial characteristics and the gain of a migratory and mesenchymal phenotype. Acquisition of a mesenchymal-like cell phenotype is one of the hallmarks of metastatic progression of most carcinomas.

2 Epithelial-Mesenchymal Transition

2.1 Mechanisms of EMT

There is a mounting recognition that the detachment and escape of cells from the primary tumour mimics the developmental process known as epithelial–mesenchymal transition (EMT) a dynamic process allowing polarised epithelial cells to undergo multiple biochemical and morphological changes enabling them to assume a mesenchymal phenotype with enhanced migratory and invasive capabilities (Huber et al. 2005; Thierry and Sleeman 2006; Buijs et al. 2007; Guarino 2007).

The mechanics of EMT initiation necessitate the loss of cell-cell adhesions; activation of transcription factors; changes in expression of specific cell-surface proteins; reorganisation and expression of cytoskeletal proteins; and production of ECM degrading enzymes. Therefore the process of EMT entails a shift in the characteristic morphology and gene expression pattern of epithelial cells resulting in the acquisition of a characteristic mesenchymal, migratory phenotype (Thierry 2002, 2003).

2.2 EMT Progression

Epithelial cells are highly polarised cells, closely connected by cell-cell junctions. Loss of these intercellular connections in the form of Tight Junctions, Adherens Junctions, Desmosomes and Gap Junctions, is a critical step during EMT that allows for physical detachment of cancer cells from the primary tumour. EMT is characterised by the combined loss of epithelial cell junction proteins, including E-cadherin, α-catenin, claudins, occludin and ZO1 and an increased expression of mesenchymal markers, such as N-cadherin, vimentin and fibronectin.

In many cancer types, the loss of the cell adhesion molecule E-cadherin coincides with a gain of expression of the mesenchymal cadherin, N-cadherin. This 'cadherin switch' is thought to be required for tumour cells to gain invasive properties and is also a characteristic of EMT (Cavallaro and Christofori 2004).

It is evident from recent studies that EMT-inducing signals are, in part, initiated by growth factors, including hepatocyte growth factor (HGF), epidermal growth factor (EGF) and transforming growth factor β (TGFβ). These induce downstream activation of a number of EMT-inducing transcription factors including Snail, Slug, Twist and zinc finger E-box binding homeobox 1 (ZEB1), (Cano et al. 2000; Thierry 2002; Medici et al. 2008; Peinado et al. 2007).

2.2.1 E-Cadherin

Weakening of cell-cell adhesion must occur before cells can become motile and metastasise and a change in the adhesive properties of cells is an essential part of the metastatic process. Cell adhesion molecules (CAMs) regulate cell-cell and cell-matrix adhesion and are involved in almost all stages of metastasis, therefore disruption in normal levels of CAMs such as E-cadherin will be important in tumour progression. E-cadherin is a member of a family of Ca^{2+} dependent CAMs made up of intracellular, extracellular and transmembrane domains. These domains play vital roles in cellular recognition during morphogenesis and development and are responsible for cell-cell adhesion (Takeichi 1991) playing an important role in maintaining tissue integrity. E-cadherin and its adhesion complex play an essential role in the adhesion of breast cancer cells. This adhesion complex is involved in the control of tumour progression and metastasis with members of the complex, such as β-catenin, acting as regulators of cell adhesion, and also in cell signalling and transcription regulation (Jiang and Mansel 2000). Studies examining the expression of E-cadherin and α-catenin in tumour tissues have shown that loss of both molecules is linked to an increased invasiveness of tumour cells (Zschiesche et al. 1997). While *in vitro* and *in vivo* studies have shown that E-cadherin expression is inversely correlated with the motile and invasive behaviour of tumour cells and also with metastasis in cancer patients (Jiang 1996), further studies have shown that the relocalisation of β-catenin to the nucleus correlates with the acquisition of the mesenchymal phenotype

(Stockinger et al. 2001; Gottardi et al. 2001), and is associated with the loss of E-cadherin. This loss of cell surface E-cadherin causes the cells to be receptive to initiation of EMT (Kim et al. 2002).

2.3 Transcription Factors in EMT

Transcription factors which have been shown to be important in EMT, as they are involved in the regulation of the expression of E-cadherin, are Slug and Snail (SNAI1) (Martin et al. 2005), Zeb-1(Peinado et al. 2004) and Twist (Yang et al. 2004; Rosivatz et al. 2002). Importantly, Snail has been identified as playing a role in the differentiation of epithelial cells into mesenchymal cells during embryonic development (Leptin and Grunewald 1990; Smith et al. 1992) with Slug and Snail effecting the down regulation of E-cadherin expression by binding directly to two proximal E2-boxes of the E-cadherin promoter (Cano et al. 2000; Batlle et al. 2000). It has been shown that Snail and E-cadherin expression are inversely correlated in squamous cell carcinoma (Yokoyama et al. 2001) and cancer of the breast (Blanco et al. 2002).

The basic helix-loop-helix protein Twist is also an important transcription factor in EMT and is known to trigger EMT mechanisms possibly by the regulation of the E-cadherin to N-cadherin switch. It is not known if E-cadherin expression can be repressed directly by Twist however, forced N-cadherin expression exerts a dominant effect over E-cadherin in breast cancer cells (Nieman et al. 1999; Islam et al. 1996). Similarly, expression of N-cadherin in normal epithelial cells results in down-regulation of E-cadherin expression (Islam et al. 1996).

2.4 EMT-Related Factors

2.4.1 Bone Morphogenetic Protein (BMP7)

Numerous signalling pathways have been implicated in the initiation of EMT; in particular, TGF-β1 has been identified as a potent initiator of EMT in renal tubular epithelial cells (Strutz et al. 2002), and also in cancer cells, stimulating cell invasion and metastasis (Akhurst and Derynck 2001). However, it has been reported that a member of the TGF-β superfamily, bone morphogenetic protein 7 (BMP7) reverses TGF-β induced EMT by induction of E-cadherin (Zeisberg et al. 2003). Indeed, BMP7 has been shown to regulate epithelial homeostasis in the human mammary gland by preserving the epithelial phenotype (Buijs et al. 2007). Decreased BMP7 expression leads to the acquisition of a bone metastatic phenotype in human breast cancer (Buijs et al. 2007), with loss of BMP-7 being associated with a more invasive and motile mesenchymal phenotype, in PC3 cells (Ye et al. 2007). Furthermore,

systemic administration of recombinant BMP7 to mice with severe renal fibrosis resulted in EMT reversal and repair of damaged epithelial structures (Zeisberg et al. 2003) with BMP-7 acting to reverse TGF-β1 induced EMT by up-regulating E-cadherin in renal cells. Linked with this, BMP member growth and differentiation factor 9 (GDF-9) has been shown to promote the invasiveness of PC-3 cells together with an induction in the expression of genes including SNAI1, RhoC, ROCK-1 and N-cadherin, while reducing levels of E-cadherin. Thus in PC-3 cells, GDF-9 signalling via ALK-5, promotes cell invasiveness via a complex signalling network working collectively to trigger EMT, thus aiding in the aggressiveness and progression of prostate cancer cells (Bokobza et al. 2011).

2.4.2 Matrix Metalloproteinases (MMPs)

The matrix metalloproteinases (MMPs) are an important component of cell invasion capable of degrading a range of extracellular matrix proteins allowing cancer cells to migrate and invade. In epithelial ovarian cancer TGFβ and EGF act as inducers of MMP2 production and enhance cell motility (Xu et al. 2010), while in breast cancer there is an upregulation of MMP9 (Wang et al. 2011).

In oral squamous cell carcinoma SNAI1 and Slug act as regulators of TGFβ triggered EMT, with Snail upregulating MMP2 and MMP9 initiating EMT; while Slug and Snail maintain longer term EMT by stimulating MMP9 expression (Qiao et al. 2010).

The MMPs not only function in membrane/matrix degradation but are also involved in cell adhesion. Treatment of MCF-7 cells with MMP7 results in E-cadherin cleavage producing an 80 kDa fraction which is detectable in the serum and urine of cancer patients and has been proposed as a biomarker (Lynch et al. 2010). Similarly, MMP9 appears to cleave the tight junction molecule Occludin (personal communication).

2.4.3 Epithelial Protein Lost In Neoplasm (EPLIN)

EPLIN is a cytoskeletal protein which has been identified as a key molecule linking the cadherin-catenin complex to F-actin and stabilising the Zona Adherens in MDCK and DLD-1 cells (Abe and Takeichi 2008). It is an actin cross linking protein that bundles actin in the cells and stabilises the cytoskeletal filaments. By doing so, EPLIN protein inhibits cell motility, and has been found to be down regulated in a number of oral, breast and prostate cancer cell lines. Forced expression of EPLIN in the EPLIN-α negative breast cancer cell line, MDA MB-231 has been shown to reduce migration and invasion in these cells so reducing their aggressiveness (Jiang et al. 2008). Similarly, over-expression of EPLIN in the PC-3 cell line results in a reduction in both *in vivo* and *in vitro* growth potential together with a reduction in cell invasiveness and ability to adhere to extracellular matrix (Sanders et al. 2011).

Thus EPLIN could be seen to be acting as a tumour suppressor. Recently, biochemical and functional evidence has exposed EPLIN as a negative regulator of EMT and invasiveness in prostate cancer cells. A down regulation of EPLIN was seen

to significantly disrupt epithelial structures, initiate actin cytoskeleton remodelling via the EPLIN link between actin filaments and β-catenin, affect explicit gene expression profiles and trigger a pro-EMT program (Zhang et al. 2011).

3 The Use of ECIS Analysis in the Study of EMT in Relation to Cancer

3.1 The ECIS System

Giaever and Keese' (1984) original ECIS system consisted of a large (~2 cm^2) and four small (~3×10^{-4} cm^2) electrodes bathed in tissue culture medium. An electric field was applied which produced a voltage drop at the margin between the medium and the small electrodes of a few mV at a current density of a few mA/cm2. Initial experiments involved the addition of fibroblasts, at varying cell densities, to the electrodes to which a small externally applied oscillating electric field was applied (AC 4,000 Hz). It was seen that the population of cells that attached and spread on the electrode had a noticeable effect on the measured impedance causing it to fluctuate with time. Thus the total impedance of the system was seen to mirror changes in the morphology of the cells and the cell density on the electrode.

Further work on the ECIS system showed that, the attachment and spreading of cells on the surface of the electrode caused up to an eightfold increase in the impedance of the system and that these fluctuations in impedance result from the movement of cells on the electrode (Giaever and Keese 1991).

The detection of cell motility using standard *in vitro* assays is a time consuming process with multiple microscopic observations of cells, usually over a period of days, involving intense user activity to record and analyse the large volumes of data produced. As there is a proven link between the motility of cancer cells in culture and their metastatic behaviour then the ECIS system is ideally suited to investigate changes in cell motility and aid in the understanding of the metastatic process.

The positive value of the ECIS system lies in its flexibility as a range of cell densities, from confluent to low densities, can be measured. Up to 1,000 cells can be monitored on each electrode at one time, but changes in impedance can even be monitored from a single cell. Similarly, the impedance can be sampled several times per second with the total acquisition time being controlled by the user with a range from minutes up to several days.

3.2 ECIS as a Tool in Cancer Studies

Since its invention in 1984, (Giaever and Keese 1984) electric cell-substrate impedance sensing (ECIS) has become accepted as a potent tool in the study of cellular properties and physiological functions of cells. ECIS provides a non-invasive tool

for the analysis of the morphology of living cells as well as providing information, in real-time, concerning cell growth, cell death, cytotoxicity and cell migration/motility (Hong et al. 2011). A number of studies have reported success in utilising the ECIS system to monitor cell attachment and spreading (Wegener et al. 2000; Xiao et al. 2002), in analysing the effects of biochemical compounds on cancer cells (Xiao and Luong 2003; Hug 2003; Atienza et al. 2006; Xi et al. 2008) and to look at cell migration following wounding (Keese et al. 2004; Hong et al. 2011).

It has also been demonstrated that the ECIS system can be used to distinguish cancerous from non-cancerous human ovarian epithelial cells by analysis of the differences in the respective electrical noise produced (Lovelady et al. 2007). The migration of human lung cancer cells (A549 cell line) has been investigated using the ECIS system. The A549 cells were manipulated to knock down expression of placental growth factor (PlGF) and an ECIS-based wounding motility assay was carried out with and without the addition of ROCK inhibitor. Analysis of the ECIS data showed that knock down of PlGF resulted in a marked reduction in migration (Chen et al. 2008). ECIS has proved useful in studying the prostate transglutaminase (TGase-4) which regulates the interaction between prostate cancer and vascular endothelial cells. It was found that over expression of TGase-4 aided the adhesion of prostate cancer cells onto endothelial cells (Jiang et al. 2009). The invasive activities of human prostatic adenocarcinoma cells have also been studied *in vitro* using electric cell-substrate impedance sensing (ECIS) and the results have indicated that an ECIS-based assay using primary human cultures is a valuable and practical technique to establish the metastatic abilities of cells isolated from biopsies (Keese et al. 2002). Similarly, the dynamics of three different human cancer cell lines has been investigated by electrical analysis with frequency fluctuations duplicating the metastatic potential discovered by conventional assays based on the Boyden chamber approach (Tarantola et al. 2010).

3.3 ECIS and EMT

Studies of EMT are often focussed on the changes in morphology of cells which allow them to become motile and usually involve conventional motility, adhesion and wounding assays. For example, looking at motility and invasiveness of PC3 cells, in relation to application of BMP7, Yang et al. (2005) carried out a scratch wounding assay over a period of 6 days with photographs being taken at various time points over 36 h. This method highlighted the part played by BMP7 in this particular cell line but is a time consuming and user intensive method, whereas use of the ECIS system of electrical detection of cell motion in tissue culture would provide an automated method for wounding and attachment of cells with programmed data acquisition in real time over a user defined period. The time and

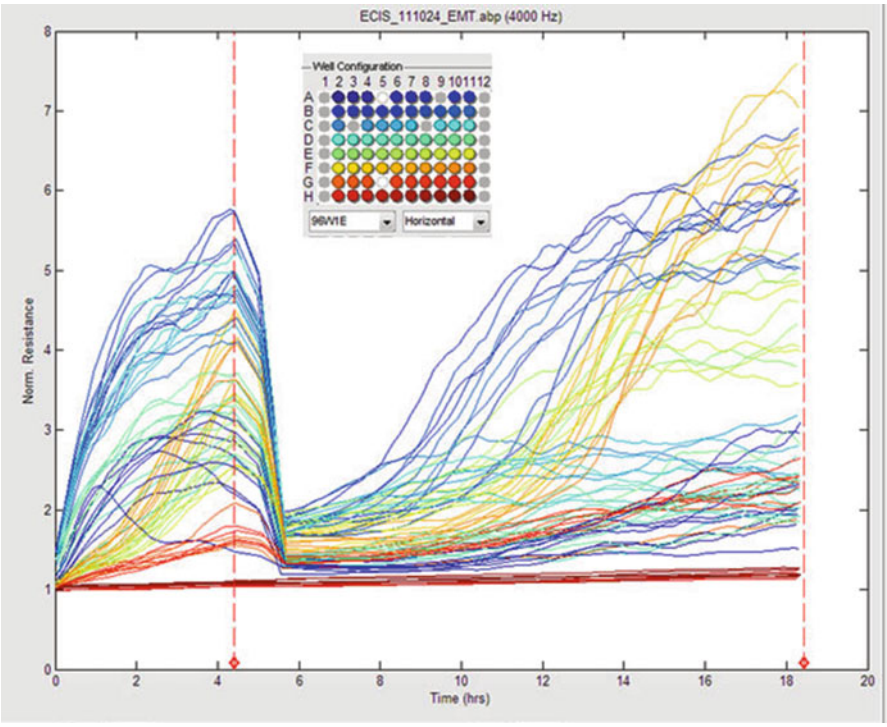

Fig. 1 ECIS time course showing normalised resistance readings for test samples using 96W1E array shown

intensity of the voltage used for electroporation can be user controlled so that cell death does not occur.

In our laboratories, the ECIS 9600 instrument is used to examine the attachment and migration of a number of different cancer cell types. This machine incorporates either an 8 well array, comprised of 10 electrodes per well, or a 96 well array allowing for multiple testing of a large number of samples and provides for easy application of treatments to analyse cellular reactions.

Figure 1 illustrates a typical ECIS plot from a 96 well array, with attachment up to the 4.5 h time point followed by electroporation. The ECIS software plots the impedance of the cells during attachment and as they move to close the wound caused by the electroporation. Individual sets of data can then be identified and analysed to look at the effects of treatment and /or cell manipulation as shown in Figs. 2 and 3.

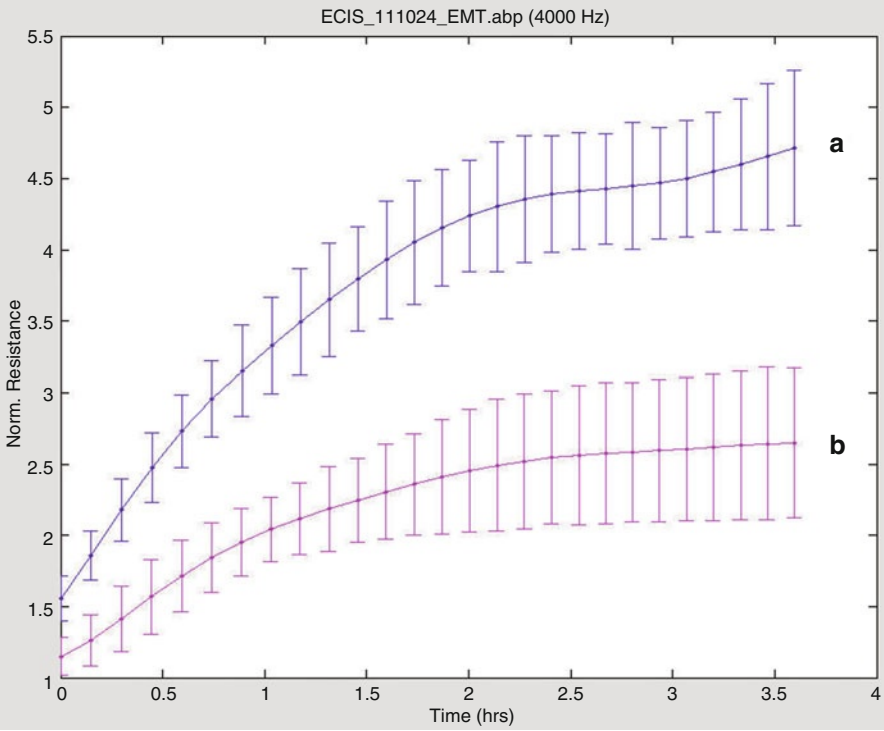

Fig. 2 Normalised resistance of EJ138 bladder cancer cells showing differences in attachment rates; (**a**): EJ138 wild type cells; (**b**): EJ138 genetically manipulated cells

4 Conclusions

As there is a proven link between the motility of cancer cells in culture and their metastatic behaviour then the ECIS system is ideally suited to investigate changes in cell motility and aid in the understanding of the metastatic process. The ease of use, reduction in user interaction time, real-time measurement function and non-invasive nature of the ECIS system provides distinct advantages for studying cancer cell behaviour as well as in testing the efficiency and cytotoxicity of anti-cancer drugs.

Utilising the ECIS system, the abnormal behaviour of cancer cells can be studied in relation to growth factors, proteins etc., in order to assess their effects on cell morphology in relation to epithelial to mesenchymal transition possibly leading to the identification of anti-metastatic properties.

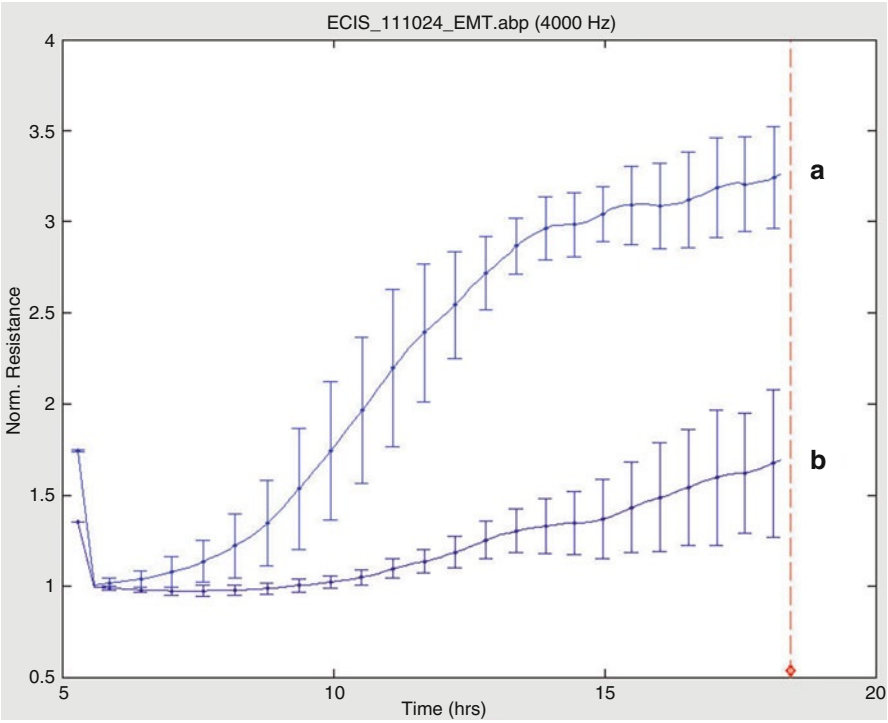

Fig. 3 Normalised resistance of EJ138 bladder cancer cells showing differences in attachment rates after wounding; (**a**): EJ138 wild type cells; (**b**): EJ138 genetically manipulated cells

Acknowledgements The authors wish to thank Cancer Research Wales and the Breast Cancer Hope Foundation for their support.

References

Abe K, Takeichi M (2008) EPLIN mediates linkage of the cadherin– catenin complex to F-actin and stabilizes the circumferential actin belt. Proc Natl Acad Sci 105:13–19

Akhurst RJ, Derynck R (2001) TGF-beta signalling in cancer- a double-edged sword. Trends Cell Biol 11:844–851

Atienza JM, Yu N, Kirstein SL et al (2006) Dynamic and label-free cell-based assays using real-time cell electronic sensing system. Assay Drug Dev Technol 4:597–607

Batlle E, Sancho E, Franci C et al (2000) The transcription factor Snail is a repressor of E-cadherin gene expression in epithelial tumour cells. Nat Cell Biol 2:84–89

Blanco MJ, Moreno-Bueno G, Sarrio D et al (2002) Correlation of Snail expression with histological grade and lymph node status in breast carcinomas. Oncogene 21:3241–3246

Bokobza SM, Ye L, Kynaston H et al (2011) Growth and differentiation factor 9 (GDF-9) induces epithelial-mesenchymal transition in prostate cancer cells. Mol Cell Biochem 349:33–40

Buijs JT, Henriquez NV, van Overveld PGM et al (2007) TGF-β and BMP7 interactions in tumour progression and bone metastasis. Clin Exp Metastasis 24:609–617
Cano A, Perez-Moreno MA, Rodringo I et al (2000) The transcription factor snail controls epithelial-mesenchymal transitions by repressing E-cadherin expression. Nat Cell Biol 2:76–83
Cavallaro U, Christofori G (2004) Cell adhesion and signalling by cadherins and Ig-CAMs in cancer. Nat Rev Cancer 4:118–132
Chen J, Ye L, Zhang L et al (2008) Placenta growth factor, PlGF influences the motility of lung cancer cells, the role of Rho associated kinase, ROCK1. J Cell Biochem 105:313–320
Faassen AE, Schrager JA, Klein DJ et al (1992) A cell surface chondroitin sulfate proteoglycan, immunologically related to CD44, is involved in type I collagen mediated melanoma cell motility and invasion. J Cell Biol 116:521–531
Giaever I, Keese CR (1984) Monitoring fibroblast behaviour in tissue culture with an applied electric field. Proc Natl Acad Sci 81:3761–3764
Giaever I, Keese CR (1991) Micromotion of mammalian cells measured electrically. Proc Natl Acad Sci 88:7896–7900
Gottardi CJ, Wong E, Gumbiner BM (2001) E-cadherin suppresses cellular transformation by inhibiting beta-catenin signalling in an adhesion-independent manner. J Cell Biol 153:1049–1060
Guarino M (2007) Epithelial-mesenchymal transition and tumour invasion. Int J Biochem Cell Biol 39:2153–2160
Hong J, Kandasamy K, Marimuthu M et al (2011) Electric cell-substrate impedance sensing as a non-invasive tool for cancer cell study. Analyst 136:237–245
Huber MA, Kraut N, Beung H (2005) Molecular requirements for epithelial-mesenchymal transition during tumor progression. Curr Opin Cell Biol 17:1–11
Hug TS (2003) Biophysical methods for monitoring cell-substrate interactions in drug discovery. Assay Drug Dev Technol 1:479–488
Islam S, Carey TE, Wolf GT et al (1996) Expression of N-cadherin by human squamous carcinoma cells induces a scattered fibroblastic phenotype with disrupted cell-cell adhesion. J Cell Biol 135:1643–1654
Jiang WG (1996) E-cadherin and its associated protein catenins, cancer invasion and metastasis. Br J Surg 83:437–446
Jiang WG, Mansel RE (2000) E-cadherin complex and its abnormalities in human breast cancer. Surg Oncol 9:151–171
Jiang WG, Martin TA, Lewis-Russell JM et al (2008) Eplin-alpha expression in human breast cancer, the impact on cellular migration and clinical outcome. Mol Cancer 7:71–80
Jiang WG, Ablin RJ, Kynaston HG et al (2009) The prostate transglutaminase (TGase-4, TGaseP) regulates the interaction of prostate cancer and vascular endothelial cells, a potential role for the ROCK pathway. Microvasc Res 77:150–157
Keese CR, Bhawe K, Wegener J et al (2002) Real-0time impedance assay to follow the invasive activities of metastatic cells in culture. Biotechniques 33:842–844
Keese CR, Wegener J, Walker SR et al (2004) Electrical wound-healing assay for cells in vitro. Proc Natl Acad Sci USA 101:1554–1559
Kim K, Lu Z, Hay ED (2002) Direct evidence for a role of beta-catenin/LEF-1 signaling pathway in induction of EMT. Cell Biol Int 26:463–476
Leptin M, Grunewald G (1990) Cell shape changes during gastrulation in Drosophila. Development 110:73–84
Lovelady DC, Richmond TC, Maggi AN et al (2007) Distinguishing cancerous from noncancerous cells through analysis of electrical noise. Phys Rev E Stat Nonlin Soft Matter Phys 76. doi:10.1103/2007/041908
Lynch CC, Vargo-Gogola T, Matrisian LM et al (2010) Cleavage of E-cadherin by matrix metalloproteinase-7 promotes cellular proliferation in nontransformed cell lines via activation of RhoA. J Oncol. doi:10.1155/2010/530745
Martin TA, Goyal A, Watkins G et al (2005) Expression of the transcription factors snail, slug and twist and their clinical significance in human breast cancer. Ann Surg Oncol 12:1–11

Medici D, Hay ED, Olsen BR (2008) Snail and slug promote epithelial-mesenchymal transition through β-catenin-T-cell factor-4-dependent expression of transforming growth factor-β3. Mol Biol Cell 19:4875–4887

Nieman MT, Prudoff RS, Johnson KR et al (1999) N-cadherin promotes motility in human breast cancer cells regardless of their E-cadherin expression. J Cell Biol 147:631–644

Peinado H, Portillo F, Cano A (2004) Transcriptional regulation of cadherins during development and carcinogenesis. Int J Dev Biol 48:365–375

Peinado H, Olmeda D, Cano A (2007) Snail, ZEB and bHLH factors in tumour progression: an alliance against the epithelial phenotype? Nat Rev Cancer 7:415–428

Qiao B, Johnson NW, Gao J (2010) Epithelial-mesenchymal transition in oral squamous cell carcinoma triggered by transforming growth factor- beta1 is Snail family-dependent and correlates with matrix metalloproteinase-2 and −9 expressions. Int J Oncol 37:663–668

Ridley AJ, Paterson HF, Johnston CL et al (1992) The small GTP-binding protein rac regulates growth factor induced membrane ruffling. Cell 70:401–410

Ridley AJ, Schwartz MA, Burridge K et al (2003) Cell migration: integrating signals from front to back. Science 302:1704–1709

Rosivatz E, Becker I, Specht K et al (2002) Differential expression of the epithelial-mesenchymal transition regulations snail, SIP1 and twist in gastric cancer. Am J Pathol 161:1881–1891

Sanders AJ, Martin TA, Ye L et al (2011) EPLIN is a negative regulator of prostate cancer growth and invasion. J Urol 186:295–301

Smith DE, Amo FF, Grindley T (1992) Isolation of Sna, a mouse gene homologous to Drosophila genes snail and escargot: its expression pattern suggests multiple roles during post implantation development. Development 116:1033–1039

Stockinger A, Eger A, Wolf J et al (2001) E-cadherin regulates cell growth by modulating proliferation-dependent beta-catenin transcriptional activity. J Cell Biol 154:1185–1196

Strutz F, Zeisberg M, Ziyedah FN et al (2002) Role of basic fibroblast growth factor-2 in epithelial-mesenchymal transformation. Kidney Int 61:1714–1728

Takeichi M (1991) Cadherin cell adhesion receptors as a morphogenetic regulator. Science 251:1451–1455

Tarantola M, Marel AK, Sunnick E et al (2010) Dynamics of human cancer cell lines monitored by electrical and acoustic fluctuation analysis. Integr Biol 2:139–150

Thierry JP (2002) Epithelial-mesenchymal transitions in tumour progression. Nat Rev Cancer 2:442–454

Thierry JP (2003) Epithelial-mesenchymal transitions in development and pathologies. Curr Opin Cell Biol 15:740–746

Thierry JP, Sleeman JP (2006) Complex networks orchestrate epithelial-mesenchymal transitions. Nat Rev Mol Cell Biol 7:131–142

Wang X, Lu H, Urvalek AM et al (2011) KLF8 promotes human breast cancer cell invasion and metastasis by transcriptional activation of MMP9. Oncogene 30:1901–1911

Wegener J, Keese CR, Giaever I (2000) Electric cell-substrate impedance sensing (ECIS) as a noninvasive means to monitor the kinetics of cell spreading to artificial surfaces. Exp Cell Res 259:158–166

Xi B, Yu N, Wang X et al (2008) The application of cell-based label-free technology in drug discovery. Biotechnol J 3:484–495

Xiao C, Luong JH (2003) On-line monitoring of cell growth and cytotoxicity using electric cell-substrate impedance sensing (ECIS). Biotechnol Prog 19:1000–1005

Xiao C, Lachance B, Sunahara G (2002) An in-depth analysis of electric cell-substrate impedance sensing to study the attachment and spreading of mammalian cells. Anal Chem 74:1333–1339

Xu Z, Jiang Y, Steed H et al (2010) TGFβ and EGF synergistically induce a more invasive phenotype of epithelial ovarian cancer cells. Biochem Biophys Res Commun 22(401):376–381

Yang J, Mani SA, Donaher JL et al (2004) Twist, a master regulator of morphogenesis, plays an essential role in tumor metastasis. Cell 117:927–939

Yang S, Zhong C, Frenkel B et al (2005) Diverse biological effect and Smad signalling of bone morphogenetic protein 7 in prostate tumor cells. Cancer Res 65:5769–5777

Ye L, Lewis-Russell JM, Kynaston H et al (2007) Endogenous bone morphogenetic protein-7 controls the motility of prostate cancer cells through regulation of bone morphogenetic protein antagonists. J Urol 178:1086–1091

Yokoyama K, Katama N, Hayashi E et al (2001) Reverse correlation of E-cadherin and snail expression in oral squamous cell carcinoma cells in vitro. Oral Oncol 37:65–71

Zeisberg M, Hanai J, Sugimoto H et al (2003) BMP-7 counteracts TGF=beta1 induced epithelial-to-mesenchymal transition and reverses chronic renal injury. Nat Med 9:964–968

Zhang S, Wang W, Osunkoya AO et al (2011) EPLIN downregulation promotes epithelial-mesenchymal transition in prostate cancer cells and correlates with clinical lymph node metastasis. Oncogene 30:4941–4952

Zschiesche W, Schonborn I, Behrens J et al (1997) Expression of E-cadherin and catenins in invasive mammary carcinomas. Anticancer Res 17:561–567

Cell Growth and Cell Death Studied by Electric Cell-Substrate Impedance Sensing

Judith Anthea Stolwijk, Stefanie Michaelis, and Joachim Wegener

Abstract Electric Cell-Substrate Impedance Sensing (ECIS) is capable of monitoring proliferation and death of anchorage-dependent mammalian cells *in vitro* continuously without using any kind of label. Instead of counting viable cells at different time points of an experiment to estimate the rate of cell division or cell death by classical means, ECIS reads the coverage of gold-film electrodes deposited on the bottom of the culture dish with non-invasive AC voltages. As dead or dying cells do not form proper cell-substrate interactions, electrode coverage correlates with the number of viable cells in the well at a given time point and therefore mirrors population dynamics. In this chapter we discuss the importance of the AC frequency used for data acquisition, the proper electrode size and the best readout parameter for reliable and reproducible experiments. An overview of the available literature provides an unbiased perspective on the performance of the device in real-life experiments. Several interesting experimental details will be addressed like the superior sensitivity of ECIS recordings to detect the onset of apoptosis as well as its ability to detect correlated cytokinesis in synchronized cell populations. The discussion about pros and cons of ECIS as a non-invasive means for cell proliferation monitoring is accompanied by rather short introductions of established label-based assays, competing label-free technologies and their individual experimental performance.

Keywords Electric Cell-Substrate Impedance Sensing • Quartz Crystal Microbalance • Cell Proliferation • Apoptosis • Necrosis • Electroporation • Electrochemotherapy • Bleomycin

J.A. Stolwijk • S. Michaelis • J. Wegener (✉)
Institut fuer Analytische Chemie, Chemo- & Biosensorik, Universitaet Regensburg, Universitaetsstr. 31, Regensburg 93053, Germany
e-mail: Joachim.Wegener@ur.de

W.G. Jiang (ed.), *Electric Cell-Substrate Impedance Sensing and Cancer Metastasis*, Cancer Metastasis - Biology and Treatment 17, DOI 10.1007/978-94-007-4927-6_6,

Abbreviations

ECIS	Electric Cell-Substrate Impedance Sensing
ECM	Extracellular Matrix
QCM	Quartz Crystal Microbalance
CBB	Coomassie Brilliant Blue
PS	Phosphatidyl-Serine
OWLS	Optical Waveguide Lightmode Spectroscopy
SPR	Surface Plasmon Resonance
CAM	Calcein Acetoxymethylester (AM)
ETHD	Ethidium Homodimer
CHX	Cycloheximide
HC	Hydrocortisone

1 Cell Division and Cell Death: The Left and Right Parenthesis of Life

Cell proliferation, which is the increase in cell number by cell division, and cell death, can be considered as being the left and right parenthesis of life as these two most fundamental processes of cell biology define the beginning and the end of the smallest unit of life. For a multi-cellular organism cell proliferation and cell death are equally important as these two processes ensure a well-controlled and strictly-regulated balance between production of new cells and removal of old or dysfunctional ones. If either one of the two key processes looses its physiological functionality the organism as a whole will face serious problems and suffer from neoplasia, possibly cancer.

Cell *proliferation* is controlled by the cell cycle (Fig. 1), a periodic sequence of events subdivided into two major phases: *interphase* and *M-phase* (Fig. 1 inner circle). During *interphase*, which is subdivided in G_1-, S- and G_2-phase, cells replicate their

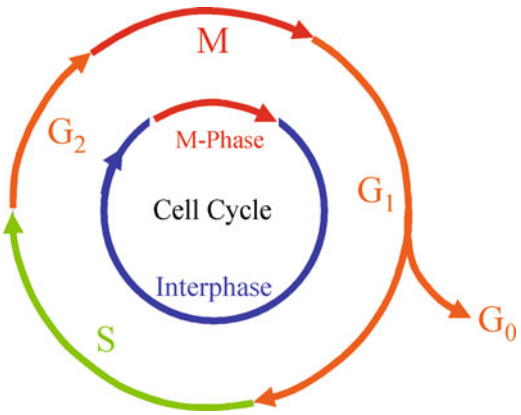

Fig. 1 Schematic of the cell cycle that controls cell proliferation

genome, they grow in size and produce enough organelles and other cell constituents so that in subsequent *M-phase* two complete daughter cells with roughly equal shares of all these building blocks are born. Often *M(itosis)-phase* is used synonymously with the term *mitosis*. However, *M-phase* describes the process of cell division which consists of *mitosis*, i.e. the separation of the duplicated chromosomes in two identical subsets, and *cytokinesis*, which is the division of the cell body into two daughter cells. Due to the semi-conservative DNA replication the two daughter cells are genetically identical to each other and to the ancestor cell. *M(itosis)-phase* is flanked by the two *G(ap)-phases* G_1 and G_2 during which the cell takes up nutrients and grows – except for DNA replication which is restricted to *S-phase*.

G_1 and G_2 are, however, not only phases of cell growth, they are also very important for cell cycle regulation as they contain several checkpoints at which the cell decides to proceed through the cell cycle or to halt. When mammalian cells sense a lack of growth factors or whenever space becomes limited, they may enter from G_1- into G_0-phase, which is also called a *quiescent* phase. Here, the cells do not grow anymore and they do not make any preparation for cell division. Exiting the cell cycle and entering G_0-phase because of limitations in space in the confined space of a tissue or in a dense culture is called *contact inhibition of cell proliferation*. Even though cells are not proliferative in G_0 they are certainly vital and metabolically active. Entering G_0 is a one way ticket for some cell types of the human body; others rest there until new growth factors or new spaces stimulate them to re-enter the cell cycle in G_1-phase and undergo mitosis and cell division. G_0 is also a phase for terminal differentiation into a highly specialized phenotype like, for instance, a neuronal phenotype. Most cell types will not re-enter the cell cycle once they have undergone terminal differentiation like the above mentioned neurons (Freshney 2010).

Mammalian cells cannot run through the cell cycle for an infinite number of times and replicate continuously. At least *in vitro* it was found that a typical mammalian cell can perform about 60 rounds of cell division before it becomes *senescent* or *post-mitotic*, meaning that it can't divide anymore. The limit of approximately 60 cell divisions was first described by Hayflick and co-workers (Hayflick 1965) so that it is nowadays often called the *Hayflick limit*. The reasons for this cellular aging are intensively studied and it seems likely that the finite life span is the result of a genetic program in combination with environmental factors. It is believed that nature's rational behind cell senescence is the fact that mutations accumulate in the DNA along a cell's lifetime. When the number of mutation passes a critical threshold, chances for malignant transformation increase. Thus, senescence might be a natural measure of precaution to avoid cell transformation and the development of cancer (Saab 2011). *In vitro* senescence can be overcome by *immortalization* which is provided by a set of (random) mutations that overrule the genetically programmed senescence (Freshney 2010).

Whereas cell division is the beginning of a new cell's lifespan, *apoptosis* or *necrosis* mark its end. Apoptosis and necrosis are two different pathways for animal cells to die. Whereas *apoptosis* is a strictly regulated, metabolic, genetically encoded and evolutionary selected active cell 'suicide' that mediates the safe and controlled deletion of unwanted cells, *necrosis* is more a passive, catabolic, 'accidental' and pathological cell death (Wyllie et al. 1980). *Necrosis* is not believed to ever occur in

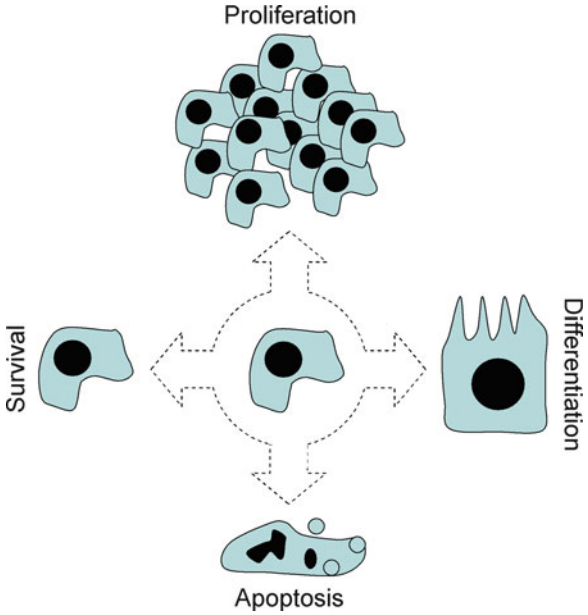

Fig. 2 Crossroads of cell fate. Dependent on internal and external factors an individual cell can proliferate, differentiate, rest or undergo apoptosis

a living organism under strictly physiological conditions but it does occur when cells are severely poisoned or compromised by other external factors. In contrast, *apoptosis* – also called *programmed cell death* – is as important for the normal development of multi-cellular organisms as cell division and differentiation and it is regarded as the indispensable counterpart to *mitosis*. For example, 10^{11} cells die by apoptosis in a human body per day to ensure tissue homeostasis, so that within a typical year a person loses as many cells by apoptosis as corresponds to its total body weight (Wu et al. 2001). Disturbances in a cell's ability to undergo apoptosis may lead to severe pathologies, most notably the progression and growth of solid tumors (Thompson 1995). The precise regulation and importance of programmed cell death is impressively documented by the normal development of the nematode *Caenorhabditis elegans* during which exactly 131 cells die in a strictly regulated genetic program (Hengartner and Horvitz 1994).

According to the fundamental processes described above each cell of the human body will be stimulated by a myriad of extrinsic and intrinsic factors to follow one out of four possible physiological pathways (Fig. 2). Dependent on the availability of growth factors and space, on cellular age and proliferative capacity and dependent on the presence of death signals, the cell (1) can follow the cell cycle and proliferate; (2) it can enter G_0-phase and differentiate into a highly specialized phenotype to take over tissue-specific functions or (3) it can simply rest quiescent in G_0-phase. As the last option (4) the cell can undergo apoptosis in response to internal or external death signals for the benefit of the entire organism. The factors that determine the direction at the *crossroads of cell fate* (Fig. 2) are enormously complex and not fully understood in all details.

Ever since the culture of animal cells has been established in the beginning of the twentieth century by pioneers like Harrison (1907) and Carrel (1912), cell division and cell death, the vertical axis in Fig. 2, were studied intensively throughout the following decades. This was at least partly driven by the motivation to understand the initiation and progression of cancer as one of the major causes of death in the northern hemisphere. The endeavors were further boosted and supported by the first successful *in vitro* culture of human cells (HeLa) in 1953 (Scherer et al. 1953). Remarkably, HeLa cells are even today one of the most widely used cell lines in cancer research and related fields. Even though cancer research is nowadays dominated by molecular approaches, measuring the integral rates of cell proliferation and cell death are still important and indispensable laboratory assays as the net growth of a cell population is ultimately connected to *the* hallmark of cancer, neoplasia. Besides several well-established cell proliferation assays that are based on staining and counting the number of cells in a given population at a certain time along the experiment, non-invasive and label-free approaches have gathered increasing importance as they provide a continuous monitoring of the population dynamics and quantitative readout parameters. Among these *Electric Cell-Substrate Impedance Sensing* (ECIS), which was first described in 1984 by Giaever and Keese (1984), is developed the farthest with respect to information content, throughput and time resolution. This statement also applies with some restrictions to the ECIS-based successor techniques described in more recent years. Before ECIS-based monitoring of cell proliferation and cell death is discussed in detail, a short but not comprehensive summary will be given about the available alternative assays.

2 Quantifying Cell Growth and Death Means Counting Viable Cells

2.1 Established Label-Based Assays to Quantify Population Dynamics

Experimental assays to quantify cell proliferation and cell death rely on determining the number of viable cells in a given sample as a function of time, either directly by numerical counting or indirectly with the help of colorimetric assays.

Direct counting of cells requires removal of adherent cells from their growth surface by proteolytic digestion of anchoring proteins, dispersing them to the single cell level and then counting them in suspension. Counting cells can be done manually using a hemocytometer or automatically whenever a Coulter counter or a flow cytometer is available. Very often direct counting techniques are combined with some pre-staining of the cell population in order to discriminate live from dead cells. Pre-staining is usually done with a membrane-impermeable dye that cannot enter the cytoplasm by diffusion. Only if the integrity of the cell membrane is compromised – as in most dead cells – the dye can enter the cell and stain the cell interior.

This so-called *dye-exclusion assay* is a very simple way to count the living cells in a cell population and to identify the dead ones (cp. Table 2). A very popular dye in this respect is Trypan Blue. In flow cytometer based cell counting the identification of dead cells is commonly achieved using fluorescent probes like Propidium Iodide or Ethidium Homodimer. Again, both molecules can only get into cells when the membrane has become permeable. If membrane integrity is compromised the dyes get access to the nucleus, intercalate into the DNA and mark dead cells with a bright nuclear fluorescence, which can be easily detected. The change in the number of viable cells as a function of time indicates the rate of cell proliferation or cell death under the experimental conditions applied. It is noteworthy that in the context of cell proliferation and cell death assays flow cytometry can provide a much more detailed analysis about a cell population under study (Diermeier-Daucher and Brockhoff 2010). It is, for instance, possible to determine the fraction of all cells that are in a certain phase of the cell cycle at a given time point. These more specific assays of course rely on more specific (fluorescent) labels or procedures that are capable of reporting on the property of interest.

Besides the above mentioned direct assays indirect colorimetric assays have found widespread application as they bypass the problem of numerical cell counting and proteolytic removal of the cells from their growth substrate. Instead, cell numbers are conveniently determined by photometry after the cell population has been stained for an intracellular indicator molecule that is proportional to cell number. Several variants of these assays are known that will not be reviewed here comprehensively. The Coomassie Brilliant Blue (CBB) assay will be described as an example: the adherently growing cell population is stained by a dye like CBB that is known to stain all cellular protein fairly unspecific. After an appropriate incubation time the dye solution is removed and the cell population is washed extensively. The protein-bound dye, however, is not washed off. After all unbound dye molecules have been removed the stained cells are treated with an ‘extracting solution’ that is capable of dissolving the bound dye from the cellular protein. Thus, the extracting solution contains a concentration of dye molecules that is proportional to the total cell protein and is therefore proportional to the number of cells in the sample under study. Assays based on protein-binding dyes are, however, insensitive to a live/dead discrimination. Other approaches make use of a dye precursor like, for instance, MTT that is capable of diffusing across the plasma membrane. Inside a living cell with active electron transport chain, the dye precursor is reduced to a strongly colored dye with the help of cellular redox-enzymes. The reduced from of the dye can be conveniently quantified by photometry and it should be approximately proportional to the number of vital cells at the time of dye addition (cp. Tables 1 and 2).

Even though these indirect colorimetric assays do not require cell removal from the growth surface and cell dispersion, they are all endpoint assays as the cell population has to be sacrificed by the addition of the experimental reagents. Time-resolved readings are only possible with a sufficiently high number of samples that are analyzed individually at different time points of the experiment. Therefore, a given cell population cannot be monitored continuously and details of the population dynamics are not available due to the very rude time resolution of these assays

Table 1 Label-based assays to quantify cell proliferation

Indicator	Reagent(s)	Mechanism	Detection
INCREASE IN BIOMASS			
Total protein	Coomassie brilliant blue G Sulforhodamine B Naphthol blue-black Crystal violet	Dyes bind to cellular proteins, the amount of bound dye is proportional to the biomass of cells	Absorbance of cell extract or fixed cell layer
Total DNA	DAPI Hoechst 33258 Hoechst 33342	Dyes bind to DNA, the amount of bound dye is proportional to the DNA content of cells	Fluorescence of cell homogenate or fixed cell layer
PROLIFERATION ACTIVITY			
DNA synthesis	^{3}H-Tymidine ^{125}I-Deoxyuridine	Incorporation of (radio)-labeled nucleotide analog during DNA replication in dividing cells	Scintillation
	BrdU (5-bromo-2′-deoxyuridine)		Anti-BrdU antibody, ELISA, Microscopy
	EdU (5-ethynyl-2′deoxyuridine)		Click reaction with fluorescent dyes
Protein synthesis	^{3}H-Leucine, ^{35}S-Methionine	Incorporation of radio-labeled amino acid in proliferating cells	Scintillation
Markers for cell proliferation	Antibodies to Ki-67, PCNA, cyclins and others	Immunological detection of characteristic proteins in proliferating cells	Immunocytochemistry, ELISA
METABOLIC ACTIVITY			
Reducing coenzymes (NADH, NADPH; FADH, FMNH)	Tetrazolium salts MTT; XTT; MTS; WST-1;INT;	Reduction of tetrazolium salts in presence of reducing coenzymes forms colored water-soluble or insoluble formazan dyes	Absorbance of solubilized formazan
	Resazurin	The blue, non-fluorescent resazurin is reduced by living cells to give the pink fluorescent dye resorufin	Absorbance of educt or fluorescence of product in the extracellular medium
Enzyme activity e.g. cellular esterase activity	e.g. Calcein AM, Fluorescein Diacetate	Intracellular hydrolysis of fluorogenic probe-precursor by cellular esterases	Fluorescence of stained cells
ATP level	Luciferase, Luciferin	ATP-dependent conversion of Luciferin to luminescent Oxyluciferin	Luminescence in cell hydrolysate
pH gradients (ATP level)	Neutral Red	Neutral Red accumulates in lysosomes due to ATP-driven pH gradients in living cells	Absorbance of cell extract

Table 2 Label-based assays to distinguish live and dead cells

Indicator	Reagent(s)	Mechanism	Detection
MEMBRANE INTEGRITY			
Dye exclusion assays	Naphthalene Black Trypan Blue	Cytoplasm of dead cells with permeable membranes is stained by the dye which is not membrane-permeable	Bright field microscopy of blue-black stained dead cells
	Propidium Iodide Ethidium Homodimer-1	Dead cells with permeable membranes are stained by the membrane-impermeable dye. If cell membranes are damaged, dye stains nucleic acids by intercalation in double-stranded DNA	Red fluorescence from nuclei of dead cells
Enzyme leakage assay e.g. Lactate Dehydrogenase (LDH)	Lactate, NAD+, Diaphorase, Resazurin	Cytosolic housekeeping enzyme LDH is released from cells with damaged membranes and catalyzes oxidation of lactate to pyruvate in extracellular buffer producing NADH; NADH then reduces resazurin to fluorescent resorufin catalyzed by diaphorase	Fluorescence or absorbance in extracellular medium
METABOLIC ACTIVITY			
Reducing coenzymes (NADH, NADPH; FADH, FMNH)	Tetrazolium salts MTT (is) MTS (s)	Reduction of yellow water-soluble tetrazolium salts by reducing coenzymes to colored water-insoluble (is) or water-soluble (s) formazan dyes	Absorbance of solubilized formazan
	Resazurin (e.g. AlamarBlue©, PrestoBlue©)	Reduction of non-fluorescent membrane-permeable resazurin (blue) by reducing coenzymes to membrane-permeable red-fluorescent resorufin	Fluorescence or absorbance in extracellular medium
Enzyme activity (e.g. intracellular esterase activity)	Fluorescein Diacetate Calcein AM	Intracelllular hydrolysis of membrane-permeable precursor (fluoresceine diacetate, calcein AM) by cellular esterases to membrane-impermeable fluorophore (fluorescein, calcein) which is trapped in the cell	Green cytoplasmic fluorescence of stained viable cells
ATP level	Luciferase, Luciferin	ATP-dependent conversion of Luciferin to luminescent Oxyluciferin	Luminescence in cell hydrolysate
pH gradients (ATP level)	Neutral Red	Neutral Red accumulates in lysosomes due to ATP-driven pH gradients in living cells	Absorbance of solubilized stain

in contrast to non-invasive approaches. Moreover, most of these assays do have a significant uncertainty, which is due to the fact that they rely on the activity of enzymes or the availability of metabolites (e.g. NADH, $FADH_2$) which are not necessarily proportional to the number of cells in all experimental situations. On the other hand the above mentioned colorimetric assays are easy to pursue, they do not rely on high-end and expensive equipment and the reagents are fairly affordable. Table 1 summarizes label-based assays that are frequently used for cell proliferation studies.

2.2 Detailed Analysis of Cell Death: Apoptosis or Necrosis

The rate of cell death is most obviously determined by quantifying the number of viable cells in a given cell population as a function of time. Table 2 summarized the most widely used label-based assays to distinguish live cells from dead ones in a given population.

From cell counting assays – directly or indirectly – it remains, however, unclear whether a cells died by *necrosis* or *apoptosis* (Tsujimoto 2012). In order to distinguish between these two forms of cell death more specific experimental assays have to be performed as the number of viable cells decreases in either case. As the two mechanisms of cell death are different with respect to morphological and molecular events, these differences can be used as a basis for their discrimination. *Necrotic* cells, that die because the cell environment becomes unfavorable (heat, pH, salt), start to swell and their cell membrane eventually ruptures leading to cell lysis. Permeabilization of the plasma membrane allows intracellular components to diffuse into the extracellular space. Within intact organisms the latter leads to an inflammatory response as intracellular constituents are present in the extracellular environment and are recognized by immune surveillance. In contrast, *apoptosis* is a genetically encoded, strictly regulated cell suicide during which the cells digest themselves. The cell bodies shrink, the membrane shows characteristic blebs but remains intact, the nucleus and other intracellular components are degraded and packed into vesicles. In an intact organism these vesicles can be safely removed without intracellular components getting into the extracellular space. Thus, among other markers *necrotic* and *apoptotic* cells can be distinguished by their ultra-structural morphology (swelling vs. shrinking), the different integrity of their plasma membranes, the appearance of their nuclei and the activation of apoptosis-specific proteases, the so-called *caspases* that pursue cell self-degradation. Accordingly, several assays have been established to screen a given cell population for the degree of apoptosis. Some of these assays are integral in nature, i.e. the assays measure the activity of the intracellular *caspases* or the degree of *DNA fragmentation* integrated over the entire cell population. Others were developed to label individual apoptotic cells in a cell population, so that the number of 'positive' cells can be quantified by microscopy or flow cytometry. One of the most widespread assays of this kind is the so-called *Annexin-5 assay* which is based on the specific binding of fluorescence-labeled

Annexin-5 to the plasma membrane of apoptotic cells (van Engeland et al. 1998). This membrane binding occurs as apoptotic cells flip phosphatidylserine (PS) from the inner leaflet of the plasma membrane, where it is exclusively localized in healthy cells, to the extracellular outer leaflet of the membrane. After this very early indicator of apoptosis, PS becomes 'visible' from the extracellular side and Annexin-5 can bind to PS and label this particular cell. Taken together, several assays exist to discriminate between apoptotic and necrotic cell death that are based on the individual molecular and morphological hallmarks of either pathway. All these assays are label-based, invasive and only provide endpoint information.

2.3 Non-Invasive Assays to Monitor Cell Proliferation and Cell Death

Besides ECIS which is discussed in all details below there are a few more non-invasive and label-free assays known that can be used to follow a cell population with respect to cell growth and cell death. In this chapter, we will summarize the alternative techniques briefly and rather cursorily. Label-free techniques other than ECIS or any of the impedance-based successor techniques can be roughly subdivided into two classes: (i) piezoelectric approaches and (ii) optical approaches based on evanescent fields.

Among the piezoelectric approaches to study growth and death of adherent cells the quartz crystal microbalance (QCM) technique has been used the most and we confine the discussion here to QCM. The technique is based on a piezoelectric quartz disk sandwiched between two gold film electrodes on either surface. The surface electrodes are used to excite the crystal to perform shear oscillations parallel to its surfaces. Based on this type of mechanical oscillation the term *thickness shear mode* resonator is used synonymously. When the oscillator operates under resonant conditions a standing acoustic wave travels through the crystal and is reflected at either side. The mechanical amplitude is maximal at the crystal faces with a node in the center of the disk. The characteristic parameters of the resonant oscillation are extremely sensitive to adsorption or desorption processes at the resonator's surface and the observed changes of resonance frequency and energy dissipation provide insights into the mechanical properties of the adsorbed material. With some limiting assumptions the recorded shifts of the resonance frequency are directly proportional to the amount of mass deposited on the surface with sensitivity down to the submicrogram level. The interested reader is referred to this reference (Steinem and Janshoff 2007) for a comprehensive overview. Initially the technique has been used to study molecular recognition events – e.g. antigen-antibody binding, ligand-receptor binding – at the solid-liquid interface before its potential to study cell-substrate interactions has been recognized. It was found that the shift of the resonance frequency is directly proportional to the fractional coverage of the quartz crystal with cells (Gryte et al. 1993; Wegener et al. 1999) which sets the basis for application in proliferation monitoring. In recent years the QCM technique has been used to study

the time course of cell adhesion and spreading (Andersson et al. 2003; Li et al. 2005a; Marxer et al. 2003), cell proliferation (Li et al. 2005b; Zhou et al. 2000) and cytotoxicity (Braunhut et al. 2005; Hug 2003). Moreover, it has been recognized that the technique provides information about the cytomechanics of the cells adhered to the crystal surface (Heitmann et al. 2007). At first glance it seems that an oscillating culture substrate cannot guarantee non-invasive readings of cell behavior. However, the amplitude of the mechanical oscillation is below one nanometer and the substrate oscillates at a MHz frequency which makes it very unlikely that the cells are capable of sensing this input of the measurement. Moreover, it has been experimentally proven that it takes amplitudes in the order of several tens of nanometers to trigger a cell response to the oscillating growth surface (Heitmann and Wegener 2007).

Among the available optical techniques we will focus on a short description of those that are integral and non-imaging in nature. Of course there are quite a few microscopic approaches known that can be used to document cell proliferation and cell death. However, these are limited to rather small fields of view, require sophisticated image analysis to extract cell proliferation rates from the raw data and they commonly have only a moderate throughput with limited time resolution when parallel experiments are performed. In the group of non-imaging optical techniques those that rely on evanescent electric fields are farthest developed to study adhesion, spreading, growth and death of anchorage-dependent cells. They differ with respect to the technical approach how the evanescent field is generated and how deep the evanescent wave penetrates into the sample but share the common principle: a beam of – most often – visible light is directed to the surface of a glass substrate that is covered with a material of lower refractive index at an angle beyond the critical angle of total reflection. Under these conditions the incident light will experience total internal reflection. Even though the light is totally reflected, a small fraction of the energy is transmitted through the boundary in form of an evanescent wave. This electromagnetic wave has a penetration depth into the sample on the other side of the glass substrate that is in the same order of magnitude as the wavelength of the incident light. When the material in direct contact to the device's surface changes composition or its refractive index, this interferes with the intensity or phase of the reflected light for a given angle of incidence. As these parameters can be recorded very sensitively, the refractive index of the material in contact to the glass surface can be followed with a time resolution in the order of seconds. When anchorage-dependent cells adhere and spread to the surface of such a glass substrate, the presence of the cell body changes the refractive index accordingly such that adhesion, spreading and proliferation of the cells can be monitored (Horvath et al. 2008; Ramsden et al. 1994). Hug et al. (2001) demonstrated that the readout in *optical waveguide lightmode spectroscopy* (OWLS) reports on the contact area between cell and surface and, therefore, provides a non-invasive, label-free approach to monitor cell spreading kinetics. In more long-term measurements (46 h) the signals reported correctly on the cell density on the sensor surface (Hug et al. 2002a, b) which is a prerequisite to use the device for proliferation monitoring. Moreover, it was demonstrated that the technology is capable of detecting the impact of chemicals and toxins on the rate of cell growth and cell-substrate adhesion (Hug et al. 2002a).

The second important approach based on evanescent fields is *surface plasmon resonance* (SPR) spectroscopy. SPR is *the* well-established key technology when adsorption, desorption or molecular interactions are studied at the solid–liquid interface. But only in the last decade it has been discovered that it can also be used to study the interactions of anchorage-dependent cells with the surface used for SPR-based sensing (Robelek 2009; Peterson et al. 2010; Giebel et al. 1999). The difference between SPR and OWLS is the nature of the growth surface. In SPR the glass surface is coated with a thin film of gold. When resonant conditions are met the fraction of the incident light that is transmitted through the interface excites density fluctuations of the conduction band electrons in the metal. The surface density fluctuations are called *surface plasmons*. The resonance conditions are sensitive to the refractive index of the material in contact to the surface – as described above for OWLS. Accordingly, adhesion of anchorage-dependent cells can be recorded non-invasively and with a time resolution in the order of seconds if needed. It has been shown in a recent report that the number of cells on the surface of an SPR-chip is proportional to SPR-readings (Yanase et al. 2007). Moreover, it was shown that the technique is sensitive enough to detect the cell response to molecules like thrombin or lipopolysaccharides (Chabot et al. 2009). Even though cell proliferation monitoring has not been explicitly reported to the best of our knowledge, SPR-based sensors do in principle meet all technical requirements. The data is recorded label-free and non-invasively. With current instrumentation the experimental throughput is, however, lacking behind.

It is important to note that both, piezoelectric sensors and those based on evanescent fields, only monitor those parts of the cellular body that are in direct contact to the sensor surface. The penetration depth of the mechanical shear wave in QCM-based sensors is in the sub-μm regime similar to the penetration depth of the evanescent field. ECIS in contrast integrates over the entire cell body and is also sensitive to changes in cell morphology at those sides of the cell body that are most distant to the growth surface like, for instance, the apical plasma membrane. It is a matter of proper frequency selection to confine the information of ECIS recordings to certain parts of the cellular body like cell-cell contacts, cell-matrix contacts or the plasma membrane. The next chapter will address this issue in more detail before ECIS-based proliferation and cell death assays are discussed.

3 Counting Adherent Cells Using ECIS – Preliminary Remarks

ECIS can be used as a label-free, non-invasive and highly automated alternative to the above described cell counting techniques. With ECIS the cell number is not counted directly but the change in surface coverage of the electrode can be recorded as a function of time. The biggest advantage of the ECIS approach compared to the above mentioned colorimetric and microscopic assays is the inherent quantitative nature of the ECIS raw data and the unprecedented time resolution in combination

with the high degree of parallelization. Right now 96 samples can be routinely monitored in parallel with a time resolution that is in the order of minutes and, thus, by far more than needed to monitor population dynamics.

Before the available literature data is summarized, this chapter will provide a few preliminary remarks and theoretical considerations about the technology and the appropriate readout parameters for this particular application. When performed in the spectroscopic mode (MFT = **M**ultiple **F**requencies followed with **T**ime) ECIS experiments offer a wealth of information as the complex impedance of the cell population under study is recorded over a wide range of frequencies typically ranging between 10 Hz and 100 kHz. At each of the preset discrete frequencies the complex impedance is recorded and then broken down into the impedance magnitude ($|Z|$), the real component of the impedance called resistance (*RES*) and the imaginary component called reactance (*REAC*). Ever since the ECIS technology has been first described, the reactance is not used directly as a measured parameter. Instead, an equivalent capacitance (*CAP*) is calculated from the measured reactance:

$$\mathrm{CAP} = 1/(2\cdot\pi\cdot \mathrm{f}\cdot \mathrm{REAC}) \tag{1}$$

In Eq. (1) f denotes the frequency of the AC signal. The rationale behind this formalism is that reactance contributions can in principle only be caused by either capacitive (capacitors) or inductive components (coils) within the system under test. It is well-known that cellular plasma membranes behave like capacitors but there is no structural entity in biological systems providing inductive properties. Thus, all reactance contributions of the sample are capacitive in nature and are therefore expressed as an equivalent capacitance of the system. The advantage of using capacitance instead of reactance is that capacitance is easier to interpret and easier to correlate with cellular properties or electrode coverage.

Accordingly, three pieces of information are available at each time point of the experiment for any of the AC frequencies. As the monitoring frequency determines the current pathway (through the cells or around the cells) readings at different frequencies give very different information. Therefore, it is important to discuss the question which frequency and which of the above mentioned quantities $|Z|$, *RES* or *CAP* might be best suited to follow cell proliferation or cell death. Looking over the existing ECIS literature most of the data has been recorded at an AC frequency of 4 kHz as this frequency has been found to be most sensitive for the most commonly used cell lines using the typical electrode sizes of 5×10^{-4} cm^2 (8W1E) or 5×10^{-3} cm^2 (8W10E). Moreover, at this frequency the complex impedance can be measured very accurately without significant contributions form the cables or other electronic sources. However, it has been recognized over the last decade that measurements at 400 Hz and 40 kHz – one decade below or one decade above the traditional center frequency – can be very useful for certain applications (Wegener et al. 2000). So the discussion below is limited to these three frequencies – 400 Hz, 4 kHz and 40 kHz – as the most interesting aspects are covered by these.

In general ECIS measurements are sensitive to (i) coverage of the electrode and (ii) morphological changes of the cells that adhere to the electrode surface. In cell proliferation experiments cell shape changes are not of primary interest, whereas

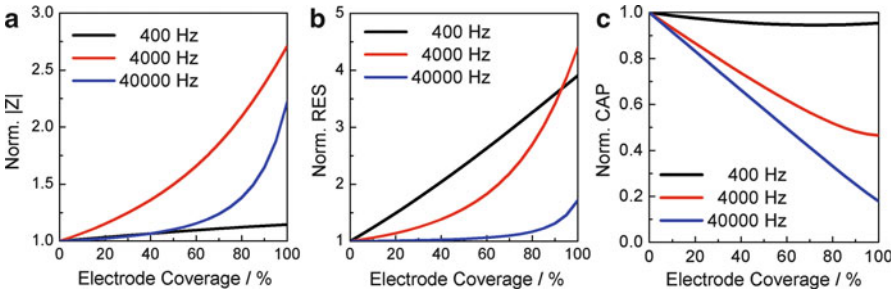

Fig. 3 (**a**) Normalized impedance magnitude |*Z*|, (**b**) normalized resistance *RES* and (**c**) normalized capacitance *CAP* at three distinct frequencies as a function of electrode surface coverage with cells. The curves have been calculated based on the ECIS model (from Giaever and Keese 1991, with the assumptions detailed in the text)

proliferation is indeed mirrored in the change of electrode coverage as a function of time. Accordingly, the monitoring frequency and the electrical quantity that is used for data analysis should be tailored to this focus of interest. To illustrate the different sensitivities of ECIS readings at different AC frequencies and the inherent suitability of the different ECIS parameters to monitor cell proliferation, the change in |*Z*|, *RES* and *CAP* has been calculated as a function of fractional electrode coverage for the three frequencies 400 Hz, 4 kHz and 40 kHz. For this calculation some assumptions were necessary but neither of them was critical for the outcome. The assumptions were as follows: (i) Calculations were performed for electrodes of the type 8W10E or 8W10E+ which are electrically identical. (ii) In areas where the electrode was covered with cells, we assumed the cell layer to have an average α value of 10 $\Omega^{0.5}$·cm, an average R_b value of 2 Ω·cm² and an average membrane capacitance C_m of 2 μF/cm². α, R_b and C_m are the cell-specific parameters of the so-called ECIS model that theoretically predicts the complex impedance of cell-covered electrodes (Giaever and Keese 1991). (iii) In those areas of the electrode that were not covered with cells, we replaced the cell bodies in the calculation by culture medium. Figure 3 shows (A) impedance magnitude |*Z*|, (B) resistance *RES* and (C) capacitance *CAP* for the three frequencies 400 Hz (black), 4 kHz (red) and 40 kHz (blue) as a function of electrode coverage. The values for |*Z*|, *RES* and *CAP* have been normalized to the value of the cell-free electrode (0 % coverage).

Figure 3a shows that the normalized impedance at 400 Hz is rather insensitive to electrode coverage. At 4 kHz the sensitivity is significantly improved, however, the normalized |*Z*| shows a non-linear dependence of electrode coverage. At the highest frequency of 40 kHz the non-linearity of the curve is even more pronounced. Thus, cell proliferation and gradual coverage of the electrode can be monitored with the help of normalized impedance readings, but it is not easy to extract proliferation rates or doubling times as this would require a rather complicated calibration. The same is true for the resistance (Fig. 3b). Using the lowest and the intermediate frequency gradual coverage of the electrode can be monitored with sufficient sensitivity but the resistance is also not linearly dependent on the degree of electrode

coverage. Please note: the resistance at an AC frequency of 400 Hz looks almost linearly dependent on coverage but this situation changes as soon as the α value of the ECIS model is increased – or in other words, the correlation is no longer linear for cells with closer adhesion to the electrode. Figure 3c provides the dependence of the normalized capacitance on electrode coverage for the three frequencies under consideration. Whereas the normalized capacitance at 400 Hz is basically insensitive, readings at 4 and 40 kHz get increasingly sensitive to gradual electrode coverage. Moreover, readings at the highest frequency show a strictly linear correlation with coverage of the growth substrate. This linear correlation holds true even if (i) the parameters that were assumed in the calculation for cells residing on the electrode or (ii) the electrode surface area were changed in any meaningful way. In other words, high frequency capacitance readings truly mirror the coverage of the electrodes for almost any cell type and the signal is directly proportional to the fractional area occupied by the cells. Thus, this data can be used to calculate proliferation rates and doubling times without any preceding calibration.

As a conclusion of this paragraph: impedance magnitude $|Z|$ and resistance *RES* can be used to monitor the growth of cells on the ECIS electrodes with time as long as the results are only compared for one particular cell line under rather constant experimental conditions. It is important to note that the observed changes in $|Z|$ and *RES* are dependent on the electrical characteristics of the cells under study. Moreover, the relationship between impedance or resistance change with electrode coverage is only linear for fractions of the entire scale such that proliferation rates and doubling times cannot be calculated without a cumbersome calibration. Nevertheless, time-resolved impedance and resistance readings are well-suited to monitor changes in the proliferative capacity of a given cell type as long as no deeper analysis of the data is needed. High frequency capacitance readings are devoid of these complications – they show the highest sensitivity and a strictly linear correlation with electrode coverage that is insensitive to changes of the electrical properties of the cells on the surface (as long as they are considered within realistic limits).

4 Monitoring Cell Proliferation Using ECIS

The *non-invasive nature* of ECIS recordings is the technological basis that this approach can be used so favorably for time-resolved, long-term assays like it is necessary for studying cell proliferation. The automatic data acquisition does not even require lab personnel to be present for days while the experiment is running. The only limitation in terms of observation time is that the cells need to receive fresh medium every 2–3 days. In contrast, microscopic documentation of cell proliferation or any of the above mentioned colorimetric endpoint assays requires the researcher to be present, do microscopic documentation or take colorimetric readings of the population after it has been sacrificed by staining at a time point of interest. An important experimental issue in proliferation experiments is the size of the electrode relative to the total growth area or, in other words, the fraction of the growth

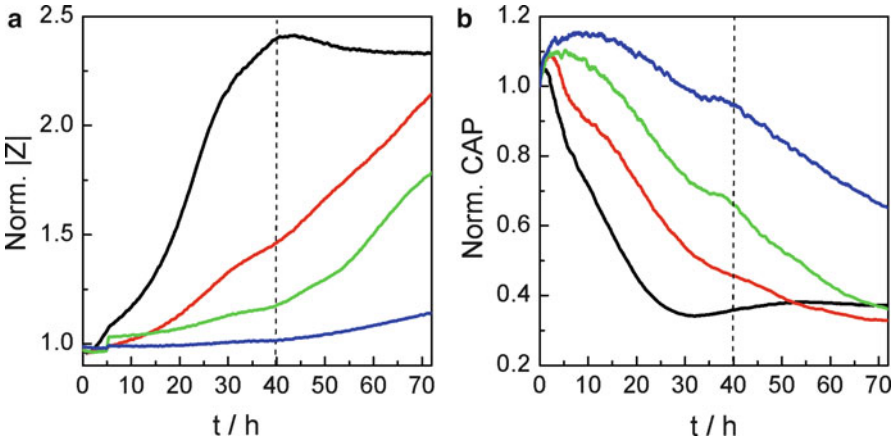

Fig. 4 (**a**) Time course of the normalized impedance during adhesion and subsequent proliferation of suspended NRK cells that were seeded in four different inocula. (**b**) Time course of the normalized capacitance for the same experiment as shown in (**a**). The monitoring frequency was set to 16 kHz. The cell densities were as follows: *black*: 3.4×10^5 cm^{-2}; *red*: 1.1×10^5 cm^{-2}; *green*: 0.45×10^5 cm^{-2}; *blue*: 0.08×10^5 cm^{-2}

area covered with electrodes. Whereas the commercial 8W1E electrodes provide the highest sensitivity down to the single cell level, they only cover less than 0.1 % of the total surface area of the well. If the surface density of the cells after sedimentation is not entirely homogeneous or very low, the well-to-well reproducibility may be impaired as in each well data recording is restricted to a small fraction of the available surface area and there is no averaging of several measuring fields. Thus, for proliferation experiments it is important to use electrode arrangements that provide a sufficient coverage of the entire well so that the recorded signals represent average values that are typical for the situation in the entire well. Commercial electrode arrays well-suited for proliferation experiments provide typical electrode coverage of the well surface of more than 40 %. Under these conditions well-to-well reproducibility is improved significantly and satisfactory. However, as an unavoidable trade-off the sensitivity of this kind of electrode is smaller compared to a single small electrode as in 8W1E.

Figure 4 shows the result of a typical proliferation experiment using Normal Rat Kidney (NRK) cells that were seeded in different seeding densities in wells with electrode coverage of 40 %. Figure 4a shows the time course of the normalized impedance at a sampling frequency of 16 kHz whereas Fig. 4b shows the time course of the normalized capacitance of the same experiment at the same frequency. Cells were seeded in four different concentrations. The black line corresponds to a rather high inoculum with sufficient cells to cover 50 % of the growth surface after adhesion. The red curve corresponds to a seeding density providing app. 20 % coverage, the green line corresponds to app. 5 % coverage and the blue line represents a post-adhesion coverage of 2.5 %. Both, impedance and capacitance readings mirror the different seeding densities by their very distinct time courses which are caused

by gradual coverage of the initially cell-free electrodes due to cell proliferation. Experiments like this are used heavily to study the impact of a given drug or toxin on cell growth and cell cycle (Xiao and Luong 2003). Any decrease in proliferative capacity would slow down the change in impedance or capacitance. The change in slope can be analyzed in quantitative terms, for instance, to establish dose-response studies.

The following observations are noteworthy: (a) The monitoring frequency was set to 16 kHz in this experiment because the total surface area of the electrodes used here was much larger compared to the simulations shown in Fig. 3. The frequency-dependent impedance and capacitance are shifted towards lower frequencies with increasing surface area of the electrodes. Thus, all frequency recommendations are dependent on the type of electrodes that are being used. Readings at 16 kHz for this electrode size behave approximately like the 'high frequency case' (40 kHz) as it was described above. (b) According to the simulations shown in Fig. 3 the *sensitivity* of impedance readings *increases* with increasing coverage. For a low electrode coverage below 40 % the high frequency impedance hardly changes but the slope of the curve in Fig. 3 steeply increases when the coverage is beyond 80 %. Capacitance on the other hand is linearly dependent on electrode coverage and, thus, equally sensitive from a cell-free electrode to a fully covered one. The dashed line in Fig. 4 has been introduced to give experimental support for this theoretical conclusion. After an experimental time of 40 h the impedance of the red, green and blue case shows a much smaller change relative to the cell-free electrode compared to the corresponding change in capacitance for exactly the same electrodes. The measured impedance for the lowest inoculum (Fig. 4a, blue) only starts to increase slowly whereas the capacitance has already changed by more than 50 % of the total shift (Fig. 4b, blue). These experimental observations support the usefulness of the simulations presented in Fig. 3. (c) Careful inspection of the capacitance curves for the blue, green and red case reveals some correlations between them. The slope of all three curves changes temporarily at an experimental time of approximately 40 h. This change in slope is very likely due to simultaneous cytokinesis of a fraction of the cells on the electrode. During cytokinesis the cell body rounds up and divides into two daughter cells. Cell rounding and detachment leads to a transient increase in capacitance before the two daughter cells spread out upon the surface. To some degree the same phenomenon can be observed in the time courses of the impedance. Simultaneous cell division is commonly only observed in synchronized cell populations. In this particular case (Fig. 4) the population has not been synchronized by any of the established protocols. However, the ancestor cells that were used to prepare the cell suspension for this experiment had been grown to confluence and were cultured 2 days beyond. Due to contact inhibition at least a fraction of the cells was arrested in the G_0-phase of the cell cycle and, thus, synchronized when they were collected by trypsin detachment.

This data interpretation is supported by literature data. Wang and coworkers have performed a similar experiment as the one shown in Fig. 4 except that they used HeLa cells that were synchronized by a double thymidine block along the time of the experiment (Wang et al. 2010). Consequently, a larger fraction of the cells underwent mitosis and cytokinesis simultaneously and caused a much more pronounced

signature in the impedance time course measured at a sampling frequency of 60 kHz. Reoccurring dips in the impedance time course indicate subsequent rounds through the cell cycle. From the periodicity of the impedance signals the authors could determine the doubling time to 21.7 h. Moreover, they could show by accompanying FACS analysis that the depth of the individual impedance dips throughout mitosis is a quantitative measure for the level of synchrony of the cell population.

In the same context Xiao et al. performed an ECIS-microscopy correlation study (Xiao and Luong 2003). They seeded V79 fibroblasts upon ECIS electrodes and determined the number of cells that were actually residing on the electrode after sedimentation. Afterwards, the cells were allowed to grow for 25 or 41 h, respectively, before the number of cells on the electrode was determined again from phase contrast micrographs. From the time dependent increase of the cell number they derived an empirical power law describing the number of cells as a function of time. By calculating the resistance contribution of a single V79 fibroblast the growth curve (based on cell numbers) was transformed into a relationship predicting the resistance increase at 4 kHz as a function of time and initial seeding density. This type of 'response function' was then used to analyze the impact of toxicants on cell growth quantitatively. The experimental response function $R(4\ kHz) = f(N_0, t)$ provided by the authors (Xiao and Luong 2003) is in good agreement with the simulations shown in Fig. 3.

Similarly, Chen et al. (2012) studied the application of mathematical growth models to describe and analyze the change in resistance at an AC frequency of 4 kHz as a function of initially seeded cell numbers in order to derive population doubling times from the recorded data. With such a quantitative analysis it might be possible to sense subtle changes in population dynamics when the cells are exposed to a compound of interest that interferes with cell proliferation.

The available literature data on ECIS-based proliferation experiments as summarized above strongly underlines that the non-invasive nature of the measurement together with the unique time resolution and the rather unlimited observation time provide all options to perform an in-depth analysis of population dynamics.

5 Watching Mammalian Cells Dying: Necrosis and Apoptosis

As described in paragraph 2.2 there are two different mechanisms of cell death: *necrosis* and *apoptosis*. Whereas *apoptosis* is a strictly regulated, genetically encoded and evolutionary selected active cell 'suicide' that mediates the safe and controlled deletion of unwanted cells, *necrosis* is more a passive, 'accidental' and pathological cell death (Wyllie et al. 1980). In most recent reports *apoptosis* is also more and more considered when cell death induced by toxic chemicals in moderate concentrations is discussed (Robertson and Orrenius 2000; Zaucke et al. 1998). Apoptosis and necrosis are characterized by very distinct morphological signatures that are specific enough that they can be used as a criterion to identify the particular mechanism of cell death by ultrastructural techniques. *Apoptotic cells* shrink without

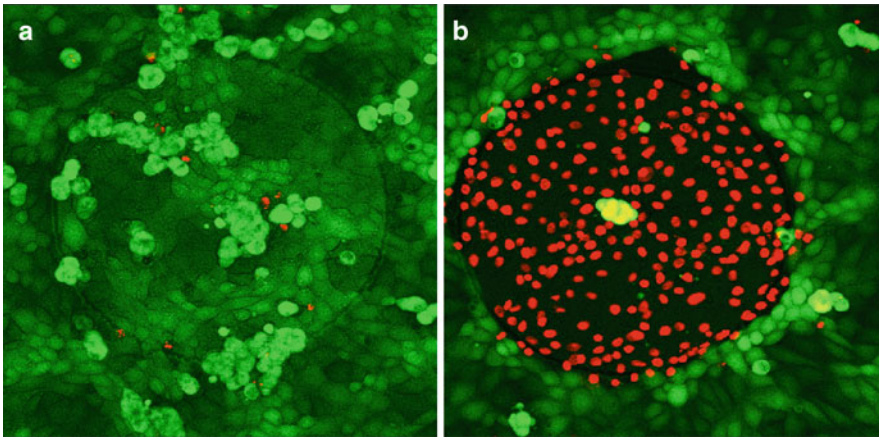

Fig. 5 Fluorescence micrographs of NRK cell layers grown to confluence on ECIS 8W1E electrodes after staining with CAM/ETHD. The cell population in (**a**) was kept under control conditions whereas the population in (**b**) was exposed to a sinusoidal voltage pulse of 5 V, at 40 kHz for 30 s. The pulse was used to kill the cells on the electrode surface

loosing the integrity of their plasma membrane. Along the time course of *apoptosis* these cells loose contacts to their neighbors, form cytoplasmic vacuoles, show nuclear and plasma membrane blebbing, a characteristic chromatin condensation and DNA fragmentation (Gobe and Harmon 2001; McConkey 1998). In contrast, *necrotic cells* swell and their plasma membrane eventually ruptures so that cytoplasmic molecules escape into the extracellular space.

5.1 The Fingerprint of Cell Death in ECIS Recordings

As ECIS is particularly sensitive to changes in cell shape and membrane integrity, it seems obvious that impedance readings should be well-suited to monitor both processes with time and reveal the dynamics of cell death. When apoptosis or necrosis affect the entire cell population the electrical current will no longer be blocked or impeded by the dielectric cell bodies – either because of cell rounding or membrane permeabilization. The measured impedance should eventually reach the values of a cell-free electrode no matter which frequency is recorded. This fingerprint of cell death can be demonstrated rather drastically by electrical wounding of the cells on the electrode as an unambiguous example for fast and irresistible *necrosis*. When confluent cells grown on ECIS electrodes are exposed to an invasive electric potential difference of several volts for some tens of seconds, irreversible dielectric breakdown of the plasma membrane is induced providing an irreversible membrane permeabilization and subsequent cell lysis. The cells die due to the high voltage within several minutes. Figure 5 shows fluorescence micrographs of NRK cells

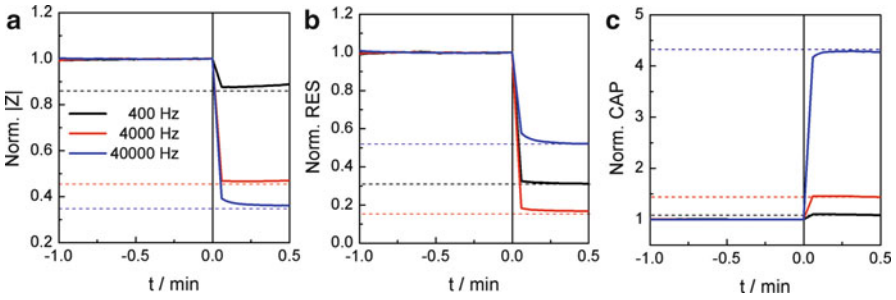

Fig. 6 (**a**) Time course of the normalized impedance (Norm. $|Z|$), (**b**) the normalized resistance (Norm. *RES*) and (**c**) the normalized capacitance (Norm. *CAP*) when confluent NRK cells are exposed to an invasive electric voltage of 5 V amplitude, 40 kHz frequency and 30 s pulse duration at t = 0 min. Pulse conditions are the same that were applied before recording of the fluorescence micrograph shown in Fig. 5b. Data was recorded using an 8W1E electrode array. *Dashed lines* indicate the values of a cell-free electrode

grown to confluence on 8W1E ECIS electrodes after they were stained with the Ethidium Homodimer (ETHD)/Calcein AM (CAM) live-dead stain. The cell population in Fig. 5a has not been exposed to an invasive electric field whereas the population shown in Fig. 5b was exposed to a voltage pulse of 5 V for 30 s. CAM, a membrane-permeable, non-fluorescent precursor of Calcein, is converted to fluorescent but membrane-impermeable Calcein in the cytoplasm of living cells by unspecific esterases. Afterwards the fluorophore cannot diffuse out anymore and enriches inside the cytoplasm. Thus, *living cells* show a strong *green fluorescent* cytoplasm. In contrast, ETHD is a membrane-impermeable, essentially non-fluorescent dye. When the cell membrane of the cells under study is compromised, the dye diffuses into the cells, gets access to the nucleoplasm, integrates into the DNA and shows a bright red fluorescence. Accordingly, the nuclei of *dead cells* show a strong *red fluorescence*. Taken together, CAM/ETHD staining provides a clear distinction of live and dead cells when these are studied under a fluorescence microscope.

The microscopic images in Fig. 5 clearly demonstrate that the untreated control cells in (a) are vital and only a very small number of red stained nuclei is visible. In contrast, all cells in figure (b) that are hovering on the electrode surface show a strong red nuclear fluorescence indicating loss of membrane integrity and cell lysis. All cells that were exposed to the electric field are dead but the cell debris is still residing on the electrode surface. Due to the electrical permeabilization of the membrane there is, however, no measurable restriction to current flow anymore as summarized in Fig. 6. All ECIS parameters recorded at the three frequencies 400 Hz, 4 kHz and 40 kHz report unanimously on a complete breakdown of the dielectric properties of the plasma membrane either immediately after pulse application or within a few minutes. All values approach the corresponding readings of a cell-free electrode which are indicated by dashed lines. The cell debris on the electrode surface does apparently not provide a significant contribution to the overall signal.

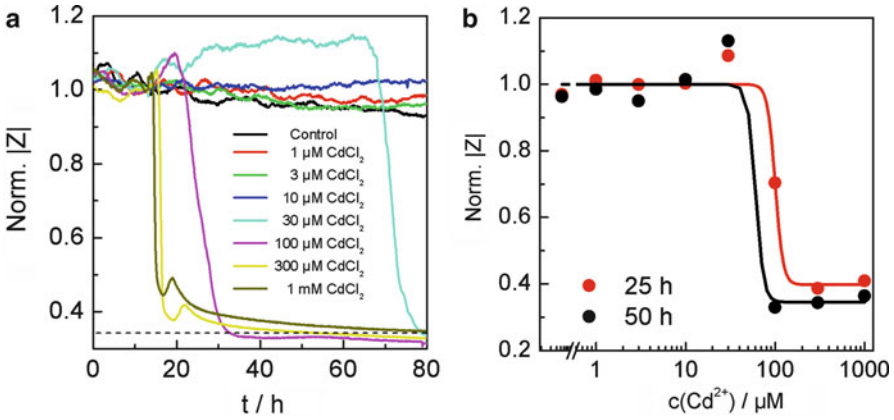

Fig. 7 (**a**) Time course of the normalized impedance |Z| at a sampling frequency of 40 kHz when confluent NRK cell layers were exposed to increasing concentrations of $CdCl_2$ as indicated in the legend. $CdCl_2$ was added after app. 12 h of baseline recording. Impedance readings were normalized to the last data point before $CdCl_2$ addition. (**b**) Dose–response analysis of the raw data shown in figure (**a**). The normalized impedance was extracted for each concentration either after 25 or 50 h of experimental time. The EC_{50} value was determined to 100 µM (*red*) or 60 µM (*black*)

The time course data shown in Fig. 6 also provides an estimate for the sensitivity of ECIS recordings for cell death monitoring at different frequencies. When impedance or capacitance is used as monitoring parameter, sensitivity is highest in the kilohertz regime whereas resistance recordings provide best sensitivity in the intermediate frequency range. This conclusion is, however, only valid for the electrode size and the specific cell type used here as other cell lines have individual electrical parameters. The electrical wounding experiment shows that cell death is clearly revealed by readings of |*Z*|, *RES* or *CAP*. Cell rounding – as expected along the time course of apoptosis – results in similar frequency-dependent changes of the individual parameters as observed for membrane permeabilization.

After discussing the impedimetric profile of *electrical* cell killing as a drastic illustration how the ECIS parameters change when the cells die, we will now focus on chemically induced cell death. One example of particular importance is heavy metal nephrotoxicity. In order to study the impact of cadmium (Cd) on kidney cells *in vitro*, Normal Rat Kidney (NRK) cells were grown to confluence on ECIS 8W1E electrodes. After the cell monolayer was completely established within several days prior to the heavy metal exposure, the experiment was started by recording baseline data for 12 h. Then, the confluent NRK cells were challenged with increasing concentrations of cadmium chloride ($CdCl_2$) dissolved in regular cell culture medium. Figure 7a shows the time course of the normalized impedance |*Z*| at a sampling frequency of 40 kHz for different populations of NRK cells in contact to increasing concentrations of $CdCl_2$.

The data indicates that the highest concentrations of 1 mM or 300 µM $CdCl_2$ induce an immediate cytotoxicity which brings down the measured impedance to the values of a cell-free electrode (dashed line). The impedance decrease triggered

by 100 μM of $CdCl_2$ is somewhat slower and only starts after a lag phase of several hours. It requires an incubation time of more than 60 h before 30 μM of $CdCl_2$ affect NRK cells. All lower concentrations do not show any measurable effect on the cells within the time of observation. For all cell layers that show a toxic response the overall impedance drops to the values of a cell-free electrode indicating complete cell death. When readings of the normalized impedance after an incubation time of 25 h are used to establish a dose–response relationship (Fig. 7b, red), an EC_{50} value of approximately 100 μM $CdCl_2$ is returned. After 50 h of incubation the corresponding EC_{50} value is reduced to 60 μM (Fig. 7b, black). The time-resolved nature of the data allows extracting EC_{50} values at any time point of the experiment and, thus, provides this important toxicological parameter as a function of exposure time. Similar information is only available from endpoint assays when a huge number of samples are studied in parallel.

The nephrotoxicity of cadmium has been studied extensively throughout the literature and it has often been associated with apoptosis. Lee et al. found – also with the help of ECIS-based toxicity monitoring – that the mode of action in tubular kidney cells is ceramide-mediated apoptosis (Lee et al. 2011). It is, however, not always possible to identify the mechanism of death unequivocally as the two pathways may get activated in parallel and overlap. Sometimes high doses of a given compound cause a rather fast necrotic response whereas smaller doses lead to a delayed onset of apoptosis. Therefore, the question arose how sensitive ECIS can detect the onset of apoptosis in comparison to the well-established and highly specific molecular assays.

5.2 ECIS is More Sensitive to Apoptosis than Biochemical Assays

Since (i) apoptotic cells within a confluent monolayer tend to disassemble their cell contacts to their nearest neighbors and (ii) ECIS is exceptionally sensitive for changes in cell-cell contacts, we anticipated that a combination of ECIS with cells that express tight intercellular junctions will provide a very sensitive assay to monitor the onset of apoptosis (Arndt et al. 2004). Endothelial cells derived from brain capillaries were selected as an appropriate cell type for an ECIS-based apoptosis assay. These cells line the wall of the cerebral micro-vessels *in vivo* and form the so-called *blood–brain barrier*, a cell-based diffusion barrier between the circulating blood and the central nervous system (CNS). The restriction of metabolite diffusion ensures a constant chemical environment in the CNS (Bradbury 1993). The functionality of the blood–brain barrier is based on the expression of tight cell-cell contacts that occlude the diffusion pathway along the intercellular cleft between two adjacent endothelial cells. Since the tightness of this endothelial barrier (Hoheisel et al. 1998), which is accessible from ECIS readings, is extraordinary sensitive for changes in cell shape we used monolayers of these particular cells as a test system to compare ECIS monitoring with molecular assays for apoptosis.

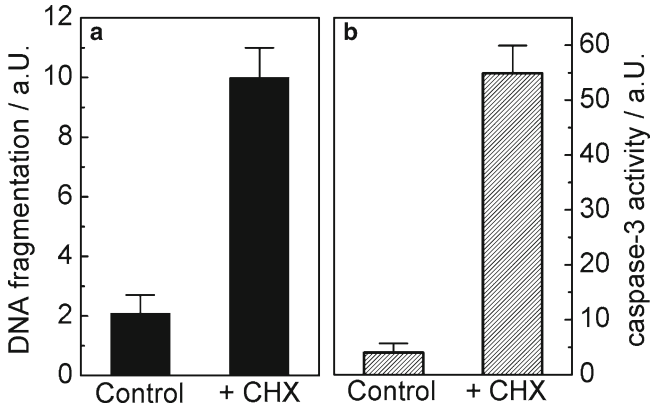

Fig. 8 (**a**) DNA fragmentation and (**b**) caspase-3 activity determined for microvessel endothelial cells that had been exposed to 25 μM cycloheximide (CHX) for 16 h. Control cells were only exposed to an identical dose of DMSO (0.1 %) that was used as a solvent for cycloheximide (Arndt et al. 2004)

To trigger apoptosis in the capillary endothelial cells in a well-defined way we have selected cycloheximide (CHX) as an easy to control chemical inductor. Figure 8 demonstrates that CHX induces a fivefold increase of DNA fragmentation (a) and an even stronger increase of caspase-3 activity (b) in CHX-treated endothelial cells compared to control cells exposed to DMSO as a vehicle control only. Caspase-3 is probably the most relevant and efficient *effector caspase* and it is therefore called the *death caspase*. Both, DNA fragmentation as well as caspase-3 activation are two hallmarks along the apoptosis pathway and the results shown in Fig. 8 consistently prove the release of programmed cell death under conditions applied here.

To monitor the onset of apoptosis in brain capillary endothelial cells upon exposure to CHX by ECIS, we first determined the monitoring frequency that provides maximum sensitivity. Here, it was not the primary objective to read electrode coverage accurately, but to detect cell shape changes associated with apoptosis as early as possible. The most sensitive monitoring frequency for such an application can be extracted from frequency scans of the cell-covered and the cell-free electrode *before* the cells are challenged with a compound of interest. Figure 9a shows the magnitude of impedance $|Z|$ as a function of frequency for an electrode of 0.03 cm² either covered with a confluent layer of brain capillary endothelial cells (red) or just immersed in cell culture medium (black). Obviously the contribution of the cell layer to the total impedance of the system is maximal in the center region of the spectrum between 10 and 10^5 Hz. When the impedance of the cell-covered electrode is divided by the impedance of the cell-free electrode at the same frequency along the entire frequency range, the calculation returns something like an empirical sensitivity spectrum (Fig. 9b). This way of presenting frequency-resolved impedance data of a cell-covered electrode relative to the impedance values of the same electrode without cells is referred to as the *normalized impedance* in the ECIS literature.

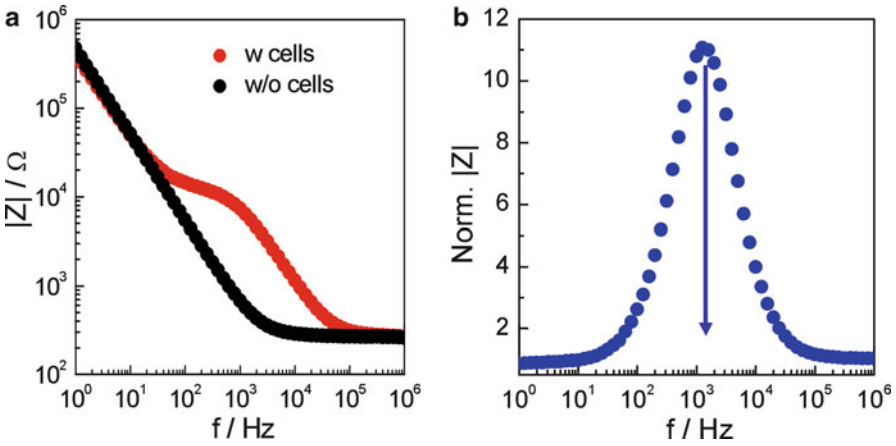

Fig. 9 (**a**) Frequency-dependent impedance magnitude |*Z*| of an ECIS electrode of 0.03 cm² surface area covered with a confluent monolayer of brain capillary endothelial cells (*red*) or just immersed in cell culture medium (*black*). (**b**) Normalized impedance of the data shown in (**a**). The normalized impedance equals the impedance of the cell-covered electrode divided by the impedance of the cell-free electrode at the same frequency. The maximum of the curve indicates the frequency of highest sensitivity for morphological changes in the cell layer under study

The higher the value of the *normalized impedance* at a given frequency, the higher is the contribution of the cell layer to the overall impedance of the entire system. As the impedance of the cell-covered electrode approaches the values of the cell-free electrode at the low and high frequency end of the spectrum, where the total impedance is dominated either by the electrode or the bulk electrolyte, the normalized impedance is a maximum function. The maximum indicates the frequency providing the best sensitivity for subtle changes in cell morphology. For capillary endothelial cells grown on ECIS electrodes with a surface area of 0.03 cm² the curve of the normalized impedance peaks at 1 kHz, so that ECIS readings for the comparative sensitivity study were performed at this particular frequency. Please note that this frequency selection is no contradiction to the statements made in the preceding paragraphs about the use of high frequency readings to monitor electrode coverage. It is only a different viewpoint that focuses on maximum sensitivity and not on interpretation of the recorded impedance data in terms of electrode coverage.

Morphological changes in confluent layers of brain capillary endothelial cells were then followed with time during exposure to 25 μM cycloheximide or the corresponding vehicle control at a monitoring frequency of 1 kHz. Figure 10a summarizes the time courses of the impedance magnitude for cells under control conditions (black), cells exposed to 25 μM CHX (red) or cells exposed to 25 μM CHX together with 550 nM hydrocortisone (HC, blue). HC is known to exert an anti-apoptotic influence. When cerebral capillary endothelial cells are exposed to 25 μM CHX (red) the impedance drops monotonically and approaches values of a cell-free electrode within 6 h after CHX addition. To get a quantitative measure for the dynamics of apoptosis-induced changes we determined the time necessary for half-maximum reduction of

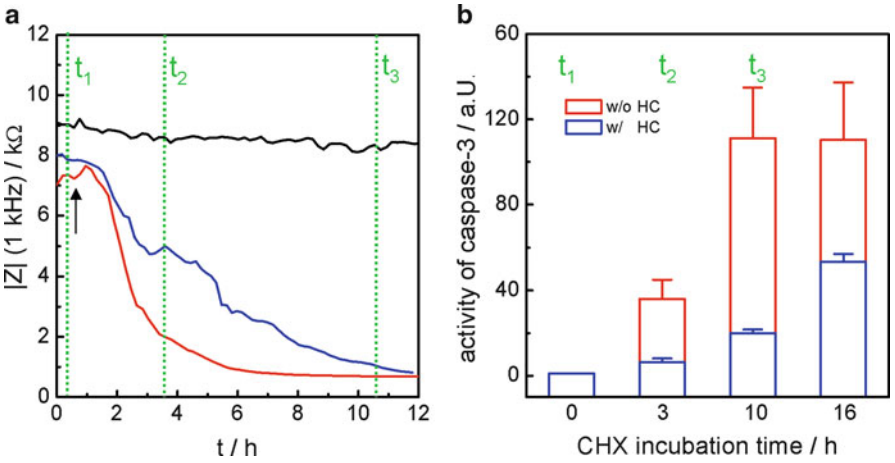

Fig. 10 (**a**) Time course of the impedance magnitude at a sampling frequency of 1 kHz when confluent micro-vessel endothelial cells were exposed to 25 μM cycloheximide (*red* and *blue*). The cells were incubated in serum-free medium either with (*blue*) or without (*red*) 550 nM hydrocortisone. In the control experiment (no hydrocortisone present) the cells were exposed to a corresponding dose of DMSO (*black*) that served as solvent for CHX. The corresponding control in presence of hydrocortisone (data not shown) behaved identically. Addition of CHX or DMSO is indicated by the *arrow*. (**b**) Time-dependent caspase-3 activity for micro-vessel endothelial cells upon exposure to 25 μM cycloheximide. *Red* columns represent enzyme activity in serum-free medium, whereas *blue* columns represent caspase-3 activity in serum-free medium supplemented with 550 nM hydrocortisone. The times (t_1, t_2, t_3) when samples were taken and analyzed for caspase-3 activity are indicated in figure (**a**) by *dashed green lines* (Arndt et al. 2004)

the impedance at 1 kHz (t_{Z50}). Analysis of 19 time courses similar to the one shown in Fig. 10a returned a mean value for t_{Z50} of (1.2 ± 0.1) h. Control conditions (black) did not produce any significant changes in the electrochemical impedance.

Figure 10b illustrates the activity of caspase-3 before and several hours after exposing the cells to 25 μM CHX (red columns). For easy comparison the time markers t_1 (prior to CHX addition), t_2 (3 h after CHX addition) and t_3 (10 h after CHX addition) at which caspase activity has been recorded are included in Fig. 10a in green letters. Comparing ECIS- and caspase-data indicates that even very small and clearly sub-maximum levels of caspase-3 activity go hand in hand with rather drastic changes in impedance. After 3 h of CHX exposure caspase-3 activity amounts to less than 30 % of its final value while the impedance of the cell layer at 1 kHz has already decreased for more than 75 % of the total change indicating the improved sensitivity of the impedance assay. After 10 h of CHX exposure the caspase-3 activity has reached its maximum levels whereas the impedance changes are final after 6 h. Accordingly, the time for half-maximum activation of caspase-3 ($t_{Caspase50}$) was determined to (3.3 ± 0.1) h by fitting a sigmoidal curve (Boltzmann-type) to the recorded data.

When brain capillary endothelial cells are co-incubated with 550 nM of the glucocorticoid hydrocortisone (HC) the impedance decrease is significantly slower as illustrated by the blue curve in Fig. 10a. The time necessary for half-maximum

impedance reduction t_{Z50} was determined to (3.0 ± 0.3) h and is, thus, significantly higher compared to the same experiment without HC in the incubation medium. This retardation of apoptosis by HC is also expressed in the time course of caspase-3 activation (Fig. 10b, blue columns). Even after 16 h of CHX-exposure caspase-3 does not reach the same activity compared to the situation without the anti-apoptotic HC in the incubation buffer. The time necessary for half-maximum activation of caspase-3 amounts to $t_{Caspase50}$ as (16 ± 6) h when HC is present in the incubation buffer. Taken together, this comparison indicates that ECIS correctly reports on the time course of apoptosis and it is capable of monitoring the anti-apoptotic activity of compounds like hydrocortisone. Moreover, changes in cell morphology as reported by ECIS are obviously a very sensitive and early indicator for the onset of apoptosis since the cell shape responds drastically even to small increases in caspase-3 levels (Arndt et al. 2004).

These results were independently confirmed in principle by a most recent study from Xie et al. (2012). Here, the authors wanted to study the nephrotoxicity of classical anti-cancer drugs like, for instance, *cis*-platinum *in vitro*. They used a renal tubular cell line as sensors that were grown to confluence on ECIS electrodes and exposed to the compounds of interest. Five hours after seeding of the initially suspended cells upon the ECIS electrodes the anti-cancer drug was added in increasing concentrations to the culture medium and the impedance was continuously followed (at an unknown frequency) for 48 h. Taking the results of *cis*-platinum as an example, the impedance of the different cell-covered electrodes decreased with time in a dose-dependent manner. Labeling the cells with Annexin-V/propidium iodide (PI) was performed at discrete time points along the experiment in parallel and revealed a close correlation between the number of apoptotic cells and the measured decrease in impedance (Xie et al. 2012). The change in electrical impedance was found to be more sensitive for the apoptotic changes than Annexin-V labeling, even though the latter is known as an early marker of apoptosis. Late stage apoptosis was determined by double staining with Annexin-V/propidium iodide (PI). PI is – similar to Ethidium Homodimer – a DNA intercalating drug that labels the nuclei of cells after the integrity of their plasma membrane has been compromised. Membrane permeabilization only occurs in very late stages of apoptosis. A clear and quantitative differentiation between early and late stage apoptosis was performed by flow cytometry analysis after Annexin-V/PI double labeling. Interestingly, flow cytometry analysis produced a significant underestimation of late apoptotic cells which was caused by the experimental necessity to remove the cells from their culture substrate prior to analysis (Xie et al. 2012). This observation highlights another advantage of ECIS recordings: readings are taken without handling of or interference with the sample. The study by Xie et al. compared the *cis*-platinum induced impedance decrease with respect to its time and dose-profile as recorded by the metabolic MTT assay. The correlation was found to be excellent in both categories with correlation coefficients better than 0.96. The authors, however, also state that MTT assays can never be performed with a similar time resolution compared to ECIS recordings and that some of the dynamic features of the cell response will escape a MTT detection (Xie et al. 2012). Similar to our own study described in the preceding paragraph the authors also looked into

the impact of anti-apoptotic substances that might be used in clinical therapy to reduce unwanted side effects of chemotherapeutics. The results clearly showed that ECIS-based impedance readings are capable of revealing the anti-apoptotic activity of test compounds as well as their capacity to reduce apoptosis.

In a most recent report the same group demonstrated the integration of ECIS electrodes in a PDMS-based microfluidic device (Xu et al. 2012). A gradient generator allowed premixing of a given drug with culture medium in several well-defined dilutions before the liquid is directed into cavities which hold the cell-covered ECIS electrodes. Air-bubble valves were used to control the flow of liquid without any mechanical interference with the ECIS-chip that could disturb the measurement. The combination of ECIS with microfluidic approaches may pave the way to high throughput screening campaigns for new drugs in cancer therapy or to screen for side effects in any tissue.

Several other authors have used ECIS as a label-free monitoring approach to perform time-resolved studies of cytotoxicity – mediated either by apoptosis or necrosis (Hong et al. 2011). As toxicity screening is addressed in another chapter of this book, we will only discuss those studies here that provide a new perspective or a new experimental approach to cell death studies.

For instance, an entirely new approach of ECIS-based apoptosis monitoring has been described most recently (Stolwijk et al. 2011) in the context of cancer therapy and the constant endeavors to develop screening devices for new chemotherapeutics. One clinical therapy approach for superficial (skin) tumors is electrochemotherapy which relies on systemic administration of chemotherapeutics like bleomycin that are only poorly membrane-permeable. To introduce the drug selectively into the tumor cells but not in healthy body cells, a local electroporation is applied at the site of the tumor. Electroporation is defined as reversible membrane permeabilization by short electric pulses. Electropores will form in the membranes of those cells close to the electrodes such that extracellular compounds can diffuse into the cytoplasm. Bleomycin – one of the most potent compounds in electrochemotherapy – is known to induce double strand breaks of the DNA and, thus, apoptosis once it gets into the cells (Mir et al. 1996; Povirk et al. 1977; Pron et al. 1999). Due to the locally confined electroporation-assisted delivery of bleomycin into the target cells, systemic side effects are minimized.

Since there is a strong interest in the development of simplified, miniaturized multi-well assay devices to screen candidate compounds for their potential use in electrochemotherapy (Choi et al. 2009; Neumann et al. 2000), ECIS-based cell monitoring in combination with *in situ* electroporation (ISE) of the cells residing on the electrode surface might become a powerful screening approach for this purpose. It has been shown previously that the membranes of adherent cells grown on ECIS electrodes can be reversibly permeabilized by short voltage pulses of several volts amplitude (Gosh et al. 1993; Wegener et al. 2002). If the duration of the voltage pulse is in the order of several hundred milliseconds and the voltage amplitude is tailored to the cell line under study, the membrane reseals again after the electrical field has been switched off. Molecules like bleomycin are then trapped inside the cells. When the electroporation conditions are properly selected, more than 80 % of

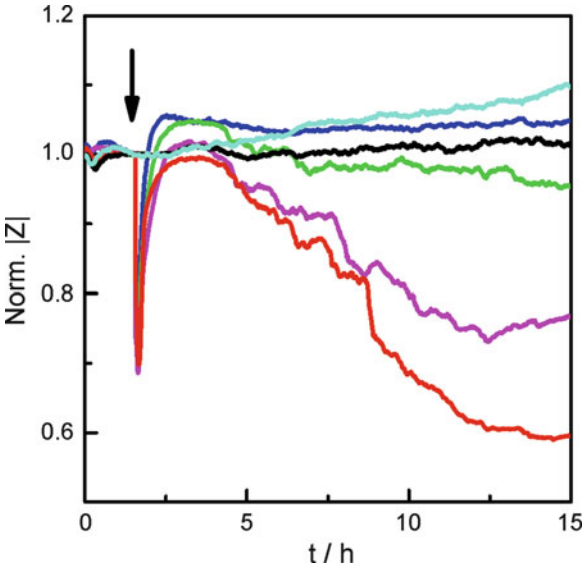

Fig. 11 Time course of the normalized impedance upon electroporation (*arrow*) of confluent NRK cells with different concentrations of bleomycin: 0 μM (*blue*), 3 μM (*green*), 30 μM (*magenta*), 100 μM (*red*). Control cells were incubated with 100 μM bleomycin but were not electroporated (*black*) or they remained entirely untreated (*cyan*). The surface area of the electrode is 5×10^{-4} cm² (8W1E)

the cells on the electrode are loaded with extracellular probe molecules and probes as big as 2×10^6 g/mol have been successfully introduced (Stolwijk et al. 2011).

Figure 11 summarizes the time courses of the normalized impedance $|Z|$ at a monitoring frequency of 4 kHz when confluent Normal Rat Kidney (NRK) cells become electroporated in the presence of increasing concentrations of bleomycin in a serum-free incubation buffer. When 100 μM bleomycin are present (no electroporation) in the medium of a confluent layer of NRK cells (Fig. 11, black), there is essentially no cellular response, as the compound cannot enter the cytoplasm. Thus, the time course of the normalized impedance in the presence of 100 μM bleomycin (black) closely parallels the bleomycin-free control population (Fig. 11, cyan). Cell layers electroporated in control solution without bleomycin (Fig. 11, blue) regain initial impedance values within 1 h which is a typical recovery time for ECIS-based *in situ* electroporation. Electroporations in the presence of increasing concentrations of bleomycin (green → 3 μM; magenta → 30 μM; red → 100 μM) induced a drastic decrease of the normalized impedance with time dependent on the bleomycin dose. For the highest concentration, the response approaches values of a cell-free electrode with no sign of recovery. For the lowest concentration of 3 μM the impedance decreases very slowly with time to 90 % of the pre-pulse value. Obviously, bleomycin-induced apoptosis is mirrored in the recorded impedance data providing time-resolved information on bleomycin action.

Xiao et al. (2002) studied the time dependent toxicity of cadmium chloride, benzalkonium chloride and sodium arsenate on V79 fibroblasts. In this study the cells were seeded upon the electrode at time zero with the potential toxicant in the seeding medium in different concentrations. Please note, that the chemical has been added to the cell suspension during attachment and spreading instead of a fully-established, confluent cell monolayer. The resistance increase relative to the cell-free electrode at an arbitrarily selected endpoint of 16 h was used as a quantitative indicator for the

toxicity of the compound under study. A dose–response function could be established and the concentration for half-maximum toxicity was determined in good agreement with more established biochemical assays. In a follow-up study the same cells were challenged with increasing concentrations of mercury chloride and 1,3,5-trinitrobenzene (TNB) (Xiao and Luong 2003). Studying the impact of chemical or biological stimuli during cell adhesion and spreading has become increasingly popular. Most often the mechanism of cell death is not analyzed in detail. It is, however, noteworthy that this assay is in some respect different than the cadmium toxicity assay described in Fig. 7 which starts with a fully established, confluent, polarized and stationary cell monolayer. Exposing cells to some compound of interest during attachment and spreading catches the cells most likely in a more vulnerable situation and may result in an enhanced sensitivity of the cells for harsh conditions. It seems, for instance, very likely that multi-drug resistance transporters are not or not fully active in rounded cells that just start to spread out and polarize. Moreover, it is difficult to exclude a simple interference with the cell adhesion machinery compared to a complete metabolic cell death.

In contrast to this approach Yeon and Park (2005) used confluent and established monolayers of HepG2 cells, a human hepatocyte cell line, in order to study their sensitivity to drugs like tamoxifen and menadione, two compounds that are used in combination with others in some special forms of cancer therapy.

A more detailed study from the ECIS viewpoint was provided by Opp et al. (2009) who analyzed the response of human umbilical vein endothelial cells (HUVECs) to cytochalasin D, a fungal toxin known to inhibit the polymerization of g-actin. As the rate of actin depolymerization is unaffected, the drug leads to a net reduction of filamentous actin. Besides dose–response studies established from readings of the total impedance, the authors emphasized the analytical capabilities provided by impedance readings at multiple frequencies. When the impedance is measured over a set of frequencies the data can be analyzed by the so-called ECIS model as it was briefly described above (Giaever and Keese 1991). This model breaks down the impedance contribution of the cell layer into three cell-related parameters that describe the morphological changes within the cells: R_b denotes the resistance of the cell-cell junctions, α describes the impedance contributions from cell-matrix adhesion and C_m quantifies the membrane capacitance. Analyzing time-resolved impedance measurements at various frequencies with the help of this model provides the time courses of the three cell-related parameters R_b, α and C_m. When HUVECs were exposed to 0.1 μM cytochalasin D this analysis revealed that breakdown of the actin cytoskeleton weakens endothelial barrier function and decreases R_b whereas the membrane capacitance increases. The change in R_b is in line with the response of other barrier-forming cell types to cytochalasin D but the change in membrane capacitance requires further clarification. These studies by Opp et al. highlight that ECIS-based cellular assays not only provide the gross biological response in quantitative terms but also more specific information about the mechanism of action when the experiment is performed accordingly.

In a similar approach Qiu et al. (2009) studied the impact of TNF-α on cardiomyocytes by impedance analysis of cell-covered ECIS electrodes and subsequent equivalent circuit modeling of the raw data. From frequency-resolved

impedance data they extracted the distance *h* between basal plasma membrane and electrode surface and followed its changes during the time of exposure. The distance between membrane and electrode is an integral part of the parameter α of the ECIS model as described above. The rationale of this approach is that apoptotic cells will shrink, round up and eventually detach, so that an increase of the distance *h* was expected. The authors found that short-term exposure decreases the distance *h* indicating a strengthening of cell-matrix contacts whereas long-term exposure increases the cell-substrate separation distance as expected for cells that round up while they are undergoing apoptosis. Apoptosis was independently verified for the TNF-α treatment by established biochemical assays.

6 Conclusion

This chapter has demonstrated that ECIS and its successor techniques provide enormous sensitivity and rather new, unprecedented perspectives on cell proliferation and cell death as long as certain experimental boundary conditions are fulfilled. With this closer and more detailed view on the growth of a given cell population in combination with the available experimental throughput, ECIS may become a powerful tool to analyze the impact of toxins or drugs on population dynamics. As the effective well-size of ECIS electrode arrays can be minimized to several mm² with an experimental volume of only 25 µl, it seems realistic to anticipate that ECIS and related techniques might be used in the future to study an individual patient's biopsy material and become the basis for individualized therapeutic approaches. In the field of cell death monitoring ECIS has proven to be equally or even more sensitive in detecting the onset of apoptosis than the established biochemical assays. As the morphological signature of *apoptosis* and *necrosis* are clearly distinct and distinguishable, it seems to be only a matter of smart electrode design, tailored selection of experimental parameters and an in-depth data mining to pave the way for a label-free, impedance-based identification of either of the two types of cell death from ECIS profiles. The established merits of the technology, currently performed technical improvements and exciting concepts for future developments renders ECIS one of the most promising technology platforms for cell-based assays with great potential for *in vitro* cancer research.

Acknowledgements The authors would like to thank the *Allianz Industrie Forschung* (AiF-ZIM) for their generous financial support.

References

Andersson A, Glasmastar K, Sutherland D, Lidberg U, Kasemo B (2003) Cell adhesion on supported lipid bilayers. J Biomed Mater Res A 64A(4):622–629

Arndt S, Seebach J, Psathaki K, Galla HJ, Wegener J (2004) Bioelectrical impedance assay to monitor changes in cell shape during apoptosis. Biosens Bioelectron 19(6):583–594

Bradbury MW (1993) The blood–brain barrier. Exp Physiol 78(4):453–472
Braunhut SJ, McIntosh D, Vorotnikova E, Zhou T, Marx KA (2005) Detection of apoptosis and drug resistance of human breast cancer cells to taxane treatments using quartz crystal microbalance biosensor technology. Assay Drug Dev Technol 3(1):77–88
Carrel A (1912) On the permanent life of tissues outside of the organism. J Exp Med 15(5):516–528
Chabot V, Cuerrier CM, Escher E, Aimez V, Grandbois M, Charette PG (2009) Biosensing based on surface plasmon resonance and living cells. Biosens Bioelectron 24(9):1667–1673
Chen SW, Yang JM, Yang JH, Yang SJ, Wang JS (2012) A computational modeling and analysis in cell biological dynamics using electric cell-substrate impedance sensing (ECIS). Biosens Bioelectron 33:196–203
Choi YS, Kim HB, Kwon GS, Park JK (2009) On-chip testing device for electrochemotherapeutic effects on human breast cells. Biomed Microdevices 11(1):151–159
Diermeier-Daucher S, Brockhoff G (2010) Dynamic proliferation assessment in flow cytometry. Curr Protoc Cell Biol 8:1–23
Freshney IR (2010) The culture of animal cells: a manual of basic technique. Wiley, Hoboken
Giaever I, Keese CR (1984) Monitoring fibroblast behavior in tissue culture with an applied electric field. Proc Natl Acad Sci U S A 81(12):3761–3764
Giaever I, Keese CR (1991) Micromotion of mammalian cells measured electrically. Proc Natl Acad Sci U S A 88(17):7896–7900
Giebel KF, Bechinger C, Herminghaus S, Riedel M, Leiderer P, Weiland U, Bastmeyer M (1999) Imaging of cell/substrate contacts of living cells with surface plasmon resonance microscopy. Biophys J 76(1):509–516
Gobe G, Harmon B (2001) Apoptosis: morphological criteria and other assays. In: Nature encyclopedia of life sciences. Wiley, London
Gosh PM, Keese CR, Giaever I (1993) Monitoring electropermeabilization in the plasma membrane of adherent mammalian cells. Biophys J 64:1602–1609
Gryte DM, Ward MD, Hu WS (1993) Real-time measurement of anchorage-dependent cell-adhesion using a quartz crystal microbalance. Biotechnol Prog 9(1):105–108
Harrison RG (1907) Observations on the living developing nerve fiber. Proc Soc Exp Biol Med 4:140–143
Hayflick L (1965) The limited in vitro lifetime of human diploid cell strains. Exp Cell Res 37:614–636
Heitmann V, Wegener J (2007) Monitoring cell adhesion by piezoresonators: impact of increasing oscillation amplitudes. Anal Chem 79(9):3392–3400
Heitmann V, Reiss B, Wegener J (2007) The quartz crystal microbalance in cell biology: basics and applications. In: Steinem C, Janshoff A (eds) Piezoelectric sensors. Springer, Berlin
Hengartner MO, Horvitz HR (1994) Programmed cell death in Caenorhabditis elegans. Curr Opin Genet Dev 4:581
Hoheisel D, Nitz T, Franke H, Wegener J, Hakvoort A, Tilling T, Galla HJ (1998) Hydrocortisone reinforces the blood–brain properties in a serum free cell culture system. Biochem Biophys Res Commun 247(2):312–315
Hong J, Kandasamy K, Marimuthu M, Choi CS, Kim S (2011) Electrical cell-substrate impedance sensing as a non-invasive tool for cancer cell study. Analyst 136(2):237–245
Horvath R, Cottier K, Pedersen HC, Ramsden JJ (2008) Multidepth screening of living cells using optical waveguides. Biosens Bioelectron 24(4):805–810
Hug TS (2003) Biophysical methods for monitoring cell-substrate interactions in drug discovery. Assay Drug Dev Technol 1(3):1–10
Hug TS, Prenosil JE, Morbidelli M (2001) Optical waveguide lightmode spectroscopy as a new method to study adhesion of anchorage-dependent cells as an indicator of metabolic state. Biosens Bioelectron 16(9–12):865–874
Hug TS, Prenosil JE, Maier P, Morbidelli M (2002a) On-line monitoring of adhesion and proliferation of cultured hepatoma cells using optical waveguide lightmode spectroscopy (OWLS). Biotechnol Prog 18(6):1408–1413
Hug TS, Prenosil JE, Maier P, Morbidelli M (2002b) Optical waveguide lightmode spectroscopy (OWLS) to monitor cell proliferation quantitatively. Biotechnol Bioeng 80(2):213–221

Lee WK, Torchalski B, Kohistani N, Thevenod F (2011) ABCB1 protects kidney proximal tubule cells against cadmium-induced apoptosis: roles of cadmium and ceramide transport. Toxicol Sci 121(2):343–356

Li J, Thielemann C, Reuning U, Johannsmann D (2005a) Monitoring of integrin-mediated adhesion of human ovarian cancer cells to model protein surfaces by quartz crystal resonators: evaluation in the impedance analysis mode. Biosens Bioelectron 20(7):1333–1340

Li M, Cui T, Mills DK, Lvov YM, MJ M (2005b) Comparison of selective attachment and growth of smooth muscle cells on gelatin- and fibronectin-coated micropatterns. J Nanosci Nanotechnol 5(11):1809–1815

Marxer CM, Coen MC, Greber T, Greber UF, Schlapbach L (2003) Cell spreading on quartz crystal microbalance elicits positive frequency shifts indicative of viscosity changes. Anal Bioanal Chem 377(3):578–586

McConkey DJ (1998) Biochemical determinants of apoptosis and necrosis. Toxicol Lett 99(3):157–168

Mir LM, Tounekti O, Orlowski S (1996) Bleomycin: revival of an old drug. Gen Pharmacol 27(5):745–748

Neumann E, Tonsing K, Siemens P (2000) Perspectives for microelectrode arrays for biosensing and membrane electroporation. Bioelectrochemistry 51(2):125–132

Opp D, Wafula B, Lim J, Huang E, Lo JC, Lo CM (2009) Use of electric cell-substrate impedance sensing to assess in vitro cytotoxicity. Biosens Bioelectron 24(8):2625–2629

Peterson AW, Halter M, Tona A, Bhadriraju K, Plant AL (2010) Using surface plasmon resonance imaging to probe dynamic interactions between cells and extracellular matrix. Cytometry A 77A(9):895–903

Povirk LF, Wubker W, Kohnlein W, Hutchinson F (1977) DNA double-strand breaks and alkali-labile bonds produced by bleomycin. Nucleic Acids Res 4(10):3573–3580

Pron G, Mahrour N, Orlowski S, Tounekti O, Poddevin B, Belehradek J Jr, Mir LM (1999) Internalisation of the bleomycin molecules responsible for bleomycin toxicity: a receptor-mediated endocytosis mechanism. Biochem Pharmacol 57(1):45–56

Qiu Y, Liao R, Zhang X (2009) Intervention of cardiomyocyte death based on real-time monitoring of cell adhesion through impedance sensing. Biosens Bioelectron 25(1):147–153

Ramsden JJ, Li SY, Prenosil JE, Heinzle E (1994) Kinetics of adhesion and spreading of animal cells. Biotechnol Bioeng 43(10):939–945

Robelek R (2009) Surface plasmon resonance sensors in cell biology: basics & application. Bioanal Rev 1(1):57–72

Robertson JD, Orrenius S (2000) Molecular mechanisms of apoptosis induced by cytotoxic chemicals. Crit Rev Toxicol 30(5):609–627

Saab R (2011) Senescence and pre-malignancy: how do tumors progress? Semin Cancer Biol 21(6):385–391

Scherer WF, Syverton JT, Gey GO (1953) Studies on the propagation in vitro of poliomyelitis viruses. IV. Viral multiplication in a stable strain of human malignant epithelial cells (strain HeLa) derived from an epidermoid carcinoma of the cervix. J Exp Med 97(5):695–710

Steinem C, Janshoff A (2007) Piezoelectric sensors, vol 5, Chemical sensors and biosensors. Springer, Berlin

Stolwijk JA, Hartmann C, Balani P, Albermann S, Keese CR, Giaever I, Wegener J (2011) Impedance analysis of adherent cells after in situ electroporation: non-invasive monitoring during intracellular manipulations. Biosens Bioelectron 26(12):4720–4727

Thompson CB (1995) Apoptosis in the pathogenesis and treatment of disease. Science 267(5203):1456–1462

Tsujimoto Y (2012) Multiple ways to die: non-apoptotic forms of cell death. Acta Oncol 51:293–300

van Engeland M, Nieland LJ, Ramaekers FC, Schutte B, Reutelingsperger CP (1998) Annexin V-affinity assay: a review on an apoptosis detection system based on phosphatidylserine exposure. Cytometry 31(1):1–9

Wang L, Wang L, Yin H, Xing W, Yu Z, Guo M, Cheng J (2010) Real-time, label-free monitoring of the cell cycle with a cellular impedance sensing chip. Biosens Bioelectron 25(5):990–995

Wegener J, Janshoff A, Galla HJ (1999) Cell adhesion monitoring using a quartz crystal microbalance: comparative analysis of different mammalian cell lines. Eur Biophys J 28(1):26–37

Wegener J, Keese CR, Giaever I (2000) Electric cell-substrate impedance sensing (ECIS) as a noninvasive means to monitor the kinetics of cell spreading to artificial surfaces. Exp Cell Res 259(1):158–166

Wegener J, Keese C, Giaever I (2002) Recovery of adherent cells after in situ electroporation monitored electrically. Biotechniques 33:348–357

Wu M, Ding H-F, Fisher DE (2001) Apoptosis: molecular mechanisms. In: Encyclopedia of life sciences. Wiley, New York, pp 1–8

Wyllie AH, Kerr JF, Currie AR (1980) Cell death: the significance of apoptosis. Int Rev Cytol 68:251–306

Xiao C, Luong JH (2003) On-line monitoring of cell growth and cytotoxicity using electric cell-substrate impedance sensing (ECIS). Biotechnol Prog 19(3):1000–1005

Xiao C, Lachance B, Sunahara G, Luong JH (2002) Assessment of cytotoxicity using electric cell-substrate impedance sensing: concentration and time response function approach. Anal Chem 74(22):5748–5753

Xie F, Xu Y, Wang L, Mitchelson K, Xing W, Cheng J (2012) Use of cellular electrical impedance sensing to assess in vitro cytotoxicity of anticancer drugs in a human kidney cell nephrotoxicity model. Analyst 137:1343–1350

Xu Y, Lv Y, Wang L, Xing W, Cheng J (2012) A microfluidic device with passive air-bubble valves for real-time measurement of dose-dependent drug cytotoxicity through impedance sensing. Biosens Bioelectron 32(1):300–304

Yanase Y, Suzuki H, Tsutsui T, Hiragun T, Kameyoshi Y, Hide M (2007) The SPR signal in living cells reflects changes other than the area of adhesion and the formation of cell constructions. Biosens Bioelectron 22(6):1081–1086

Yeon JH, Park JK (2005) Cytotoxicity test based on electrochemical impedance measurement of HepG2 cultured in microfabricated cell chip. Anal Biochem 341(2):308–315

Zaucke F, Zöltzer H, Krug HF (1998) Dose-dependent induction of apoptosis or necrosis in human cells by organotin compounds. Fresenius J Anal Chem 361:386–392

Zhou T, Marx KA, Warren M, Schulze H, Braunhut SJ (2000) The quartz crystal microbalance as a continuous monitoring tool for the study of endothelial cell surface attachment and growth. Biotechnol Prog 16(2):268–277

Tight Junctions in Cancer Metastasis and Their Investigation Using ECIS (Electric Cell-Substrate Impedance Sensing)

Tracey A. Martin and Wen G. Jiang

Abstract Tight Junctions (TJ) control the paracellular diffusion of ions and certain molecules and it has become evident that the TJ has a vital role in maintaining cell to cell integrity. Loss of cohesion of the TJ structure can lead to invasion and ultimately to the metastasis of cancer cells. Modulation of expression of TJ molecules results in key changes in TJ barrier function leading to the progression of cancer and progression of metastasis. This chapter will discuss how ECIS (Electric Cell-substrate Impedance Sensing) can contribute to the investigation of these changes.

Abbreviations

TJ	Tight Junctions
ECIS	Electric Cell-substrate Impedance Sensing
EMT	epithelial mesenchymal transition
TER	Transepithelial or transendothelial resistance
PCP	Paracellular Permeability
FGF-2	lymphangiogenic factors fibroblast growth factor-2
HGF	hepatocyte growth factor
VEGF-A	vascular endothelial growth factor-A
VEGF-C	vascular endothelial growth factor-C
ROCK	Rho kinase
PKC	protein kinase C
2ME	microtubuledisruptor2-methoxyestradiol

T.A. Martin (✉) • W.G. Jiang
Metastasis & Angiogenesis Research Group, Cardiff School of Medicine, Cardiff University, Heath Park, Cardiff CF14 4XN, UK
e-mail: Martinta1@cf.ac.uk

W.G. Jiang (ed.), *Electric Cell-Substrate Impedance Sensing and Cancer Metastasis*, Cancer Metastasis - Biology and Treatment 17, DOI 10.1007/978-94-007-4927-6_7,

ERM	ezrin radixin, and moesin
MEK	mitogen-activated protein kinase
ppMLC	phosphorylated myosin light chain
PAMR	perijunctional actomyosin ring
BBB	The blood–brain barrier
OxPAPC	oxidized 1-palmitoyl-2-arachidonyl-sn-glycero-3-phosphocholine
CPE	*Clostridium perfringens* enterotoxin
HIVE	human immunodeficiency virus-1 encephalitis

1 Introduction

The Tight Junction (TJ) creates an intercellular barrier and intramembrane diffusion fence due to its organisation at the region where the plasma membrane of adjacent cells forms a series of contacts that appear to completely occlude the extracellular space (Wong 1997) (Fig. 1a). TJs govern the permeability of epithelial and endothelial cells and are the most topical structures of these cell types (Jiang et al. 1998, 1999; Tsukita and Furuse 1999). Interaction and penetration of the vascular endothelium by dissociated cancer cells is a key step in the formation of cancer metastases. TJ in endothelial cells function as a barrier through which molecules and inflammatory cells can pass. In epithelial cells the TJ functions in an adhesive manner and can prevent cell dissociation (Hollande et al. 2001). TJ are therefore the first barrier that cancer cells must overcome in order to metastasize, with TJ of vascular endothelium in vivo functioning as a barrier between blood and tissues against metastatic cancer cells (Martin et al. 2002) (Fig. 1b). Changes in tumour and endothelial cells are necessary for the successful growth and spread of cancer cells. An changes in cancer cells by up-regulation or down-regulation of relevant TJ proteins results in loss of cell-cell association, cell contact inhibition, leading to uncontrolled growth, loss of adhesion to and degradation of the basemen membrane. To facilitate the passage of the cancer cells through this barrier these must be a concurrent loss of cell-cell association in the endothelium and modulation of the TJ proteins involved.

Following the early work of Martinez-Paloma (1970) and others (Inoue et al. 1984; Mullin and O'Brien 1986), experimental evidence has emerged to place TJ in the frontline as the structure that cancer cells must overcome in order to metastasize (Hoevel et al. 2002; Ren et al. 1990; Satoh et al. 1996). A considerable body of work now exists on TJ and their role in a number of diseases. TJ protein expression and function can be modulated by growth factors, cytokines, regulatory mechanisms or promoter methylation and regulatory mechanisms may be via epithelial-mesenchymal-transition (EMT), as the process of acquisition of an invasive phenotype by tumours of epithelial origin can be regarded as a pathological version EMT (Ikenouchi et al. 2003; Martin et al. 2005). The TJ can therefore rapidly change their permeability and functional properties in response to stimuli and can be regulated in response to physiological and tissue-specific requirements (Wong 1997).

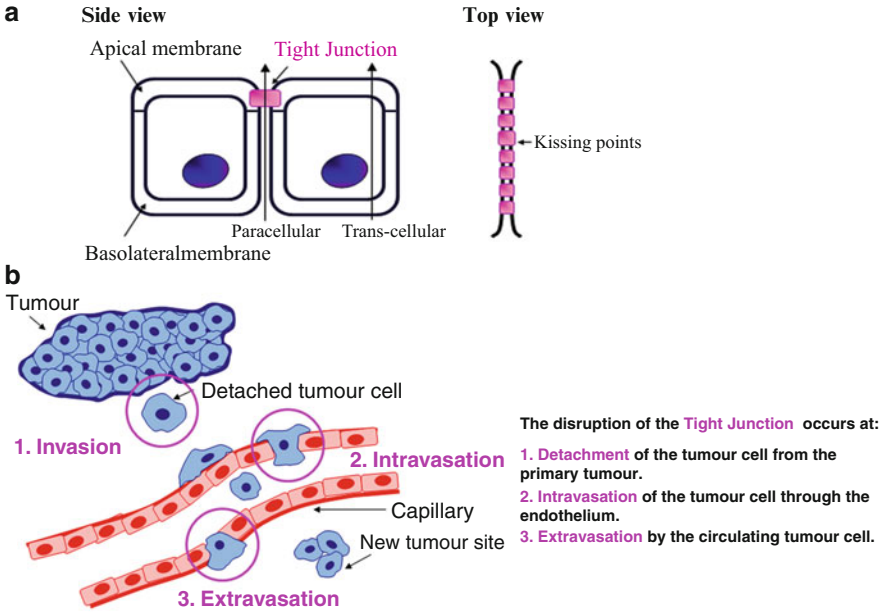

Fig. 1 (**a**) View of TJ location between epithelial and endothelial cells, showing apical and basolateral membranes. (**b**) Involvement of TJ in cancer metastasis

It is evident that changes in the function and regulation of TJ in cancer is not just a consequence of cancer progression but is essential to its development and persistence, eventually enabling metastasis and secondary disease. Discovering how TJ are involved in metastasis is vital to the effort in understanding and possibly treating this terrible disease. This chapter will discuss the progress that has been made in understanding how role of TJ in the invasion and metastasis of cancer via changes barrier function usually due to modulations of TJ protein expression and alterations in the structure of the TJ itself.

2 Experimental Measurements of Tight Junction Function

There are a number of universally used methods for analyzing the function of TJ in epithelial and endothelial cells that are easily carried out but are labour intensive and time consuming. Generally, functional assays involve the use of permeable transwell inserts or Ussing chambers that allow the passage of tracer molecules (such as varying sizes of labelled Dextran) across the cell layer and the measurement of electric currents that allow the measurement of resistance across cell monolayers. Such methods have their own inherent problems, not least user error.

Transepithelial or transendothelial resistance (TER) and Paracellular Permeability (PCP) both use carbonate filter inserts with a pore size approximately 0.4 μm (for 24 well plates) (Greiner Bio-One Ltd., Stonehouse, Glos, UK), FITC-conjugated Dextran (20 and 40 kDa) (Molecular Probe Inc., Eugene, OR), an EVOM Voltohmmeter (EVOL, World Precision Instruments, Aston, Herts, UK) with a STX-2 chopstick electrodes (WPI, Sarasota, Florida, USA) (Inoue et al. 1984). Cells are seeded into the 0.4 μm pore size insert (upper chamber) and allowed to reach full confluence. Inserts without cells, inserts with cells in medium and inserts with modified or treated can be tested by measuring resistance across the cell monolayer. Electrodes are placed at the upper and lower chambers and resistance measured with the voltohmmeter. At least three readings should be obtained for each time point. Paracellular permeability (PCP) can be determined using fluorescently labeled molecules such as dextran FITC-Dextran, with the cells prepared and treated as in the TER study, but with the addition of labelled Dextran to the upper chamber. At each time point, medium is removed from the lower chamber and retained. The relative fluorescence from these collections can then read on a multichannel fluorescence reader to show how much labeled molecule has passed through the cell monolayer and into the bottom chamber. Increased fluorescence indicates increase permeability.

Problems with TER and PCP results are caused by: fluctuations in temperature, pertubation of cultures by transit and changes of buffer/medium, differing levels of medium and the possible introduction of infection/contamination. Moreover, it is difficult to measure a large number of cultures simultaneously and there will always be a time lag during time courses with large numbers of replicates.

It should be noted that neither TER nor PCP reflect only properties of the paracellular pathway but are a composite of the paracellular and the transcellular routes. In most low-resistance epithelia, the electrical resistance of the paracellular route is much lower than the transcellular resistance. Since the two pathways are arranged in parallel, $1/\mathrm{TER} = (1/\mathrm{Rtranscellular}) + (1/\mathrm{Rparacellular})$, the measured TER essentially reflects paracellular resistance (Matter and Balda 2003). Moreover, paracellular resistance is the sum of the junctional resistance and the resistance along the paracellular space (Matter and Balda 2003).

3 ECIS in Tight Junction Function Measurement

Since the advent of ECIS technology, measurement of barrier function of cell layers in tissue culture via ECIS has proven to be a significant and rapidly growing use of this technology. The utilization of ECIS to monitor barrier function was first demonstrated in 1992 using bovine pulmonary endothelial cells (Tiruppathi et al. 1992). Following this early publication, ECIS measured barrier function has become an attractive alternative to previous TER and PCP methodology. In addition to its convenience in gathering TER data with a minimum of labour, measurements do not require the addition of labelled molecules or tracers. The relatively low values of TER for some monolayers make precise determinations possible, in contrast to the more traditional methods.

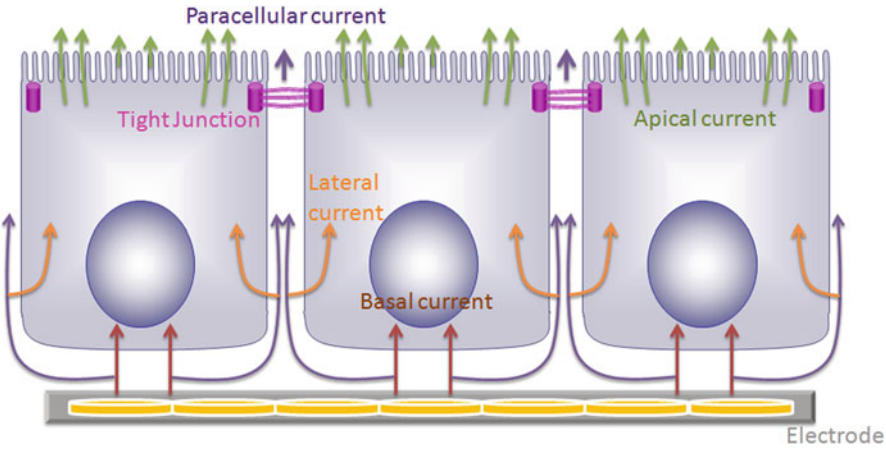

Fig. 2 Pathway of electrical current through a cell monolayer from the electrode during ECIS experimentation

As already stated, TER using inserts/chambers does not measure the true barrier function (the resistance of the paracellular pathway between the cells) but rather a combination of the constricted paths beneath the cells and the transcellular pathway (Fig. 2). This is due to complications arising from the constricted current flow in the space between the basal cell membrane and the cell support (Lo et al. 1999). For molecules to travel from the lower chamber to the space above the cell layer, they must also travel in the constricted space beneath the cells to reach the intercellular junctions. The ECIS method is unique in being able to distinguish between the two pathways, as they both affect the measured resistance and capacitance monitored by ECIS in different ways. Using The ECIS™ Model the true barrier function due to changes in intercellular junctions can be calculated (Giaever and Keese 1993). Briefly, in the model, the resistance and capacitance of the cell free electrode is measured at several different frequencies. Cells are treated as disc shapes that hover a small distance above the electrode, have an insulating membrane and filled with a conducting electrolyte. It is then assumed that the resistance and capacitance of the gold electrode (substratum) remains unchanged, however, changes in these parameters occur due to the cells altering the flow or current. Some of the current will flow through the constricted space beneath the cells (between the cells and the electrode), whereas some of the current will flow though the spaces between the cells, which is termed barrier resistance. Additionally, current also passes through the cells themselves (Fig. 2). Consequently, the model fits data using three parameters; barrier resistance or Rb which is of most interest to those investigating TJ function (Fig. 3), the measurement of the constraint on current beneath the cells, or alpha, which related information on size and height above the electrode and the capacitance of the plasma membrane of the cells, or Cm can be determined by measuring at different frequencies.

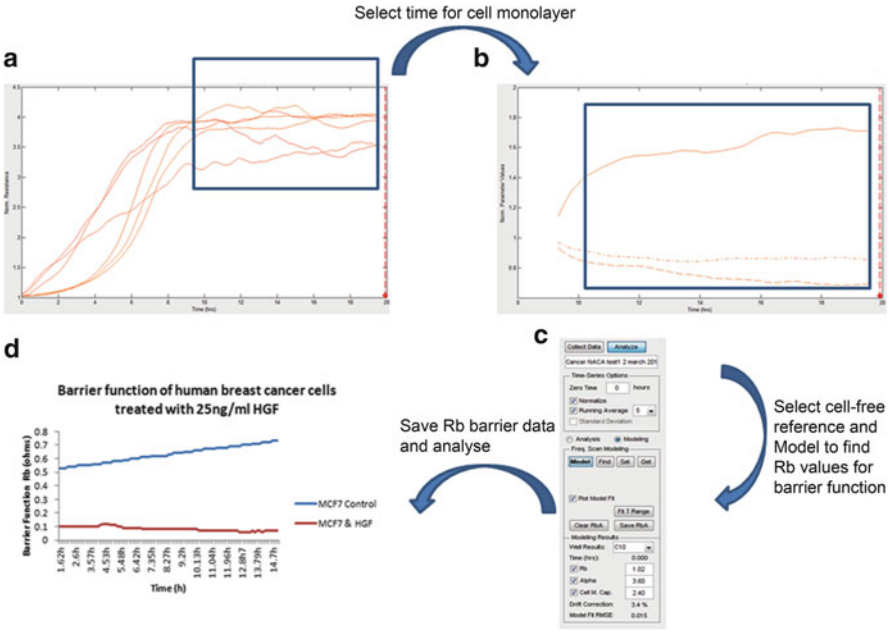

Fig. 3 Schematic summarizing the use of ECIS technology in analyzing TJ function

As stated above, modeling is required to calculate barrier function for TJ investigation and can measure both true barrier function as the resistance of the paracellular pathway and being able measure and the transcellular pathway. How this has been achieved in practice is now discussed.

4 Practical TJ Function Analysis Using ECIS

At least half of the patients already present clinically detectable metastatic disease at the time of diagnosis of cancer. A higher number of patients will also have micrometastases that would be beyond conventional detection techniques. Metastasis is therefore the single event that results in the death of most patients with cancer. During the three processes key to successful metastasis, the TJ is the first structure impeding the path to successful metastasis of the cancer cell: TJ exist between the cancer cells themselves, the cells of the stroma and the cells of the endothelium. For the tumour cell to proceed effectively, the TJ structure must be disturbed and dismantled to enable penetration of the cancer cell. ECIS analysis can therefore be used to investigate changes between cells of the cancer, cells of the stroma and cells of the endothelium. We will now discuss studies that have used ECIS technology to analysis TJ function in endothelia, cancer cells and TJ.

4.1 ECIS and Endothelial Cell TJ Function

Larrieu-Lahargue et al. (2010) used ECIS graphs to illustrate their work on Netrin-4, a laminin-related secreted protein is an axon guidance cue recently shown essential outside of the nervous system, regulating mammary and lung morphogenesis as well as blood vascular development. They showed that Netrin-4, at physiologic doses, induces proliferation, migration, adhesion, tube formation and survival of human lymphatic endothelial cells in vitro comparable to well-characterized lymphangiogenic factors fibroblast growth factor-2 (FGF-2), hepatocyte growth factor (HGF), vascular endothelial growth factor-A (VEGF-A), and vascular endothelial growth factor-C (VEGF-C). *In vivo*, Netrin-4 induced growth of lymphatic and blood vessels in the skin of transgenic mice and in breast tumours. Its overexpression in human and mouse mammary carcinoma cancer cells led to enhanced metastasis. Moreover, Netrin-4 stimulated *in vitro* and *in vivo* lymphatic permeability by activating small GTPases and Src family kinases/FAK, and down-regulating tight junction proteins. Such data provide evidence that Netrin-4 is a lymphangiogenic factor contributing to tumour dissemination and represents a potential target to inhibit metastasis formation (Larrieu-Lahargue et al. 2010).

Apoptosis is a strictly regulated and genetically encoded cell 'suicide' that may be triggered by cytokines, depletion of growth factors or certain chemicals (Arndt et al. 2004). It is morphologically characterized by severe alterations in cell shape like cell shrinkage and disintegration of cell–cell contacts. Arndt et al. used ECIS to monitor the apoptosis-induced changes in cell shape in an integral and quantitative fashion with a time resolution in the order of minutes. Apoptosis was induced by cycloheximide (CHX) and verified by biochemical and cytological assays. The time course of cell shape changes was followed with unprecedented time resolution by impedance readings at 1 kHz and correlated with biochemical parameters. From impedance readings along a broad frequency range of 1–106 Hz the authors could assign the observed impedance changes to alterations on the subcellular level. They observed that disassembly of barrier-forming tight junctions precedes changes in cell–substrate contacts and correlates strongly with the time course of protease activation (Arndt et al. 2004). This paper contains a well explained methodology for ECIS technology and how to analyse barrier function.

Activation of p39 and Rho kinase (ROCK) via microtubuledisruptor2-methoxyestradiol (2ME) induces hyperpermeability of the endothelial monolayers (Bogatcheva et al. 2011). Using the protein kinase C (PKC) inhibitors Ro-31–7549 and Ro-32–0432, it has been shown in vitro and in vivo that 2ME-induced barrier dysfunction is also PKC-dependent. Moreover, microtubuledisruptor2-methoxyestradiol (2ME) induces via mechanisms that include the activation of p38 and ROCK and rearrangement of the actin cytoskeleton. Bogatcheva et al. (2011) showed that the application of 2ME leads to a dramatic increase in the level of ERM phosphorylation are implicated in the regulation of endothelial Permeability. Overexpressing phosphorylation deficient ERM mutants, exhibit less attenuation of 2ME-induced barrier disruption in response to the PKC inhibitor Ro-31–7549 as assessed using

ECIS (Bogatcheva et al. 2011). These results suggest a critical role of PKC activation in response to microtubule disrupting agents, and implicate the phosphorylation of ERM in the barrier dysfunction induced by 2ME.

The blood–brain barrier (BBB) is composed of a number of cell types in addition to the cerebral microvascular endothelium. Hartmann et al. (2007) investigated the impact of endogenous extracellular matrices on the barrier function of BBB microvascular endothelial cells cultured in vitro. Using ECIS technology, the authors observed that endogenously isolated ECM from both, astrocytes and pericytes, improved the tightness of cerebral endothelial cells significantly compared to ECM that was derived from the endothelial cells themselves as a control. Moreover, when cerebral endothelial cells were grown on extracellular matrices produced by non-brain endothelial cells (aorta), the electrical resistances were markedly reduced (Hartmann et al. 2007). Such observations indicate that glia-derived ECM – as an essential part of the BBB – is required to ensure proper barrier formation of cerebral endothelial cells.

Generation of phospholipid oxidation products in atherosclerosis, sepsis and lung pathologies affects endothelial barrier function which has significant consequences on disease outcome in general (Starosta et al. 2012). At low concentrations, OxPAPC (oxidized 1-palmitoyl-2-arachidonyl-sn-glycero-3-phosphocholine) increases endothelial cell barrier function but decreases it at higher concentrations. The authors determined the mechanisms responsible for the pulmonary endothelial cell barrier dysfunction induced by high OxPAPC concentrations. Low OxPAPC concentrations enhanced barrier function. In contrast, higher OxPAPC concentrations rapidly increased permeability, which was accompanied by increased total cell protein tyrosine phosphorylation, phosphorylation at Tyr-418 and activation of Src kinase, and phosphorylation of adherens junction protein VE-cadherin at Tyr-731 and Tyr-658, which was not observed in EC stimulated with low OxPAPC doses. Early tyrosine phosphorylation of VE-cadherin was linked to dissociation of VE-cadherin – p120-catenin/β-catenin complexes and VE-cadherin internalization, while low OxPAPC doses promoted VE-cadherin – p120-catenin/β-catenin complex formation. High, but not low OxPAPC doses increased ROS production and protein oxidation. Inhibition of Src by PP2 and ROS production by NAC inhibited disassembly of VE-cadherin – p120-catenin complexes and attenuated high OxPAPC-induced barrier disruption (Starosta et al. 2012). These results show differential effects of OxPAPC doses on VE-cadherin – p120-catenin complex assembly and barrier function. These data suggest that rapid tyrosine phosphorylation of VE-cadherin and other potential targets mediated by Src and ROS-dependent mechanisms plays a key role in dissociation of AJ complexes and barrier dysfunction induced by high OxPAPC doses (Starosta et al. 2012).

4.2 ECIS and Cancer Cell TJ Function

The review by Hong et al. (2010), provides an excellent explanation of the use of ECIS in cancer cell studies in general. Examples where ECIS has been used to

demonstrate changes in cancer cell TJ function include the work of Winkler et al. (2010). *Clostridium perfringens* enterotoxin (CPE) binds to the extracellular loop 2 of a subset of claudins, such as claudin-3. The authors analysed the molecular mechanism of the CPE-claudin interaction. Incubation of Caco-2 cells with recombinant CPE-(116–319) reduced junctional resistance and transepithelial electrical resistance, and increased the permeation coefficient of fluorescein.

Previous research suggests DNA methylation is a mechanism for claudin-4 over expression in cancer and that C-CPE acts as an absorption-enhancing agent in claudin-4–expressing cells. Litkouhi et al. (2007) sought to correlate claudin-4 over expression in epithelial ovarian cancer with clinical outcomes and TJ barrier function. They found that Claudin-4 overexpression in epithelial ovarian cancer does not correlate with survival or other clinical endpoints and is associated with hypomethylation. Claudin-4 overexpression correlated with Rb and C-CPE treatment of epithelial ovarian cancer cells significantly decreased Rb in a dose- and claudin-4–dependent noncytotoxic manner and concluded that C-CPE treatment of epithelial ovarian cancer cells leads to altered TJ function and that further work could lead to possible drug delivery strategies.

4.3 ECIS and TJ Function in General

Since the conception of ECIS technology it has been envisages that it would be excellent for investigating TJ function and response to factors that control TJ function. This is best described by the original paper of Lo et al. (1995). Transepithelial impedance of Madin-Darby canine kidney cell layers was measured by ECIS and used to analyze impedance changes on removal of Ca2+ from confluent Madin-Darby canine kidney cell layers. The authors showed that reduction of Ca2+ concentration causes junction resistance between cells to drop and the distance between the basal cell surface and substratum to increase.

The follow up study (Lo et al. 1999) explained that whilst TER measurement has often been used to study the paracellular transport properties of epithelia grown on permeable filters, especially the barrier function of TJ. However, the TER value includes another source, the resistance caused by cell–substrate contact that may give rise to a high TER value if cell–substrate separation is small. Lo et al. (1999) used ECIS to measure both paracellular resistance and the average cell–substrate distance of MDCK (II), HEp-2, and WI-38 VA13 cells. Comparing ECIS data with those from TER measurements of cell layers cultured on polycarbonate filters, they obtained the approximate extra resistance resulting from cell–substrate contact for each cell type. The value of cell–substrate resistance was also estimated by two theoretical calculations that bracket the true values. The results demonstrated that cell–substrate contact substantially influences the TER data measured using polycarbonate filters and that the extra resistance due to cell–substrate spaces depends on both cell type and filter property.

Previously, it has been shown that an elevated content of fibrinogen increased formation of filamentous actin and enhanced endothelial layer permeability

(Patibandla et al. 2009). The authors then tested the hypothesis that fibrinogen binding to endothelial cells alters expression of actin-associated endothelial TJ proteins. Confluent rat cardiac microvascular endothelial cells were treated with fibrinogen and/or, mitogen-activated protein kinase (MEK) kinase inhibitors, anti-ICAM-1 antibody or BQ788 (endothelin type B receptor blocker), endothelin-1, endothelin-1 with BQ788, or medium alone for 24 h. Fibrinogen induced a dose-dependent decrease in junction integrity (ECIS). Western blot analysis and RT-PCR data showed that the higher dose of fibrinogen decreased the contents of TJ proteins such as occludin, ZO-1, and ZO-2. Fibrinogen -induced decreases in contents of the TJ proteins were blocked by the inhibitors, or anti-ICAM-1 antibody. While BQ788 inhibited endothelin-1-induced decrease in resistance, it did not affect fibrinogen -induced decrease in TER. This suggests that fibrinogen increases endothelial cell layer permeability via the MEK kinase signaling pathway by affecting occludin, ZO-1, and ZO-2 (Patibandla et al. 2009).

Ramachandran and Srinivas (2010) investigated the role of actin cytoskeleton in the disassembly and reformation of adherens junctions and TJ in bovine corneal endothelial monolayers. Extracellular Ca2+ depletion leads to activation of RhoA, increase in phosphorylated myosin light chain ppMLC, decrease in TER (assessed using ECIS), contraction of the perijunctional actomyosin ring (PAMR), and redistribution of zonula occludens-1 (ZO-1) and cadherins. These effects were reversed on Ca2+ add-back. Pretreatment with Y-27632 and blebbistatin (as inhibitors of actomyosin contraction) reduced the rate of decline in TER, opposed the contraction of the PAMR, and blocked the redistribution of ZO-1 and cadherins. Both drugs reduced the recovery in TER and opposed the normal redistribution of ZO-1 and cadherins on Ca2+ replenishment. Cytochalasin D, which led to dissolution of the PAMR, also reduced the recovery of TER on Ca2+ replenishment. The authors concluded that the (Ca2+ depletion)-induced disassembly of adherens junctions accelerates the breakdown of TJs through a concomitant increase in the actomyosin contraction of the PAMR, and that the contractile tone of the PAMR is essential for assembly of the apical junctional complex (Ramachandran and Srinivas 2010).

In BBB studies, TJ are critical to the proper maintenance of the BBB integrity. Posttranslational modifications of essential endothelial TJ proteins, occludin and claudin-5, contribute and possibly disrupt BBB integrity. Yamamoto et al. (2008) built on previous work showing that ROCK activation mediates occludin and claudin-5 phosphorylation resulting in diminished barrier tightness and enhanced monocyte migration across BBB in the setting of human immunodeficiency virus-1 encephalitis (HIVE). They then examined phosphorylation of cytoplasmic domains of recombinant claudin-5 and occludin by ROCK and found that ROCK predominately phosphorylated two sites on occluding (T382 and S507) and one site on claudin-5 (T207). Specific anti-phosphopeptide antibodies were developed for these sites, allowing the detection of phosphorylated occludin at T382 and S507, and claudin-5 at T207 from full-length recombinant occludin and claudin-5 transiently expressed in COS-7 cells and mouse brain microvascular endothelial cells. These phosphospecific anti bodies demonstrated enhanced staining of brain endothelial cells in the mouse model for HIVE and human HIVE brains featuring mononuclear cell infiltration

across disrupted BBB. These results demonstrated the direct phosphorylation of occludin and claudin-5 by ROCK at specific sites, which was increased in encephalitic brain (Yamamoto et al. 2008).

5 Summary

We can see from the work carried out that ECIS technology can provide a valuable resource for analysis of changes in TJ function in cancer cells and thus can contribute to investigations of cancer metastasis. Although the actual number of published articles using ECIS directly in cancer TJ analysis is low, it can be hoped that its usage will become more widespread.

Acknowledgement We acknowledge the support of Cancer Research Wales

References

Arndt S, Seebach J, Psathaki K, Galla HJ, Wegener J (2004) Bioelectrical impedance assay to monitor changes in cell shape during apoptosis. Biosens Bioelectron 19(6):583–594

Bogatcheva NV, Zemskova M, Gorshkov B, Kim K, Daglis G, Poirier C, Verin D (2011) Ezrin, Radixin, and Moesin Are Phosphorylated in Response to 2-Methoxyestradiol and Modulate Endothelial Hyperpermeability. Am J Respir Cell Mol Biol 45:1185–1194

Giaever I, Keese CR (1993) Micromotion of mammalian cells measured electrically. Proc Natl Acad Sci U S A 88(17):7896–7900. Erratum in: Proc Natl Acad Sci U S A 1993 90(4):1634

Hartmann C, Zozulya A, Wegener J, Galla HJ (2007) The impact of glia-derived extracellular matrices on the barrier function of cerebral endothelial cells: an in vitro study. Exp Cell Res 313(7):1318–1325

Hoevel T, Macek R, Mundigl O, Swisshelm K, Kubbies M (2002) Expression and targeting of the tight junction protein CLDN1 in CLDN1-negative human breast tumor cells. J Cell Physiol 191(1):60–68. doi:10.1002/jcp. 10076 [pii]10.1002/jcp.10076

Hollande F, Blanc EM, Bali JP, Whitehead RH, Pelegrin AG, Baldwin S, Choquet A (2001) HGF regulates tight junctions in new nontumorigenic gastric epithelial cell line. Am J Physiol Gastrointest Liver Physiol 280(5):G910–G921

Hong J, Kandasamy K, Marimuthu M, Choi CS, Kim S (2010) Electrical cell-substrate impedance sensing as a non-invasive tool for cancer cell study. Analyst 136(2):237–245

Ikenouchi J, Matsuda M, Furuse M, Tsukita S (2003) Regulation of tight junctions during the epithelium-mesenchyme transition: direct repression of the gene expression of claudins/occludin by Snail. J Cell Sci 116(Pt 10):1959–1967. doi:10.1242/jcs.00389jcs.00389 [pii]

Inoue T, Shimono M, Yamamura T, Saito I, Watanabe O, Kawahara H (1984) Acinic cell carcinoma arising in the glossopalatine glands: a report of two cases with electron microscopic observations. Oral Surg Oral Med Oral Pathol 57(4):398–407

Jiang WG, Bryce RP, Horrobin DF, Mansel RE (1998) Regulation of tight junction permeability and occludin expression by polyunsaturated fatty acids. Biochem Biophys Res Commun 244(2):414–420. doi:S0006-291X(98)98288-2 [pii] 10.1006/bbrc.1998.8288

Jiang WG, Martin TA, Matsumoto K, Nakamura T, Mansel RE (1999) Hepatocyte growth factor/scatter factor decreases the expression of occludin and transendothelial resistance (TER) and increases paracellular permeability in human vascular endothelial cells. J Cell Physiol

181(2):319–329. doi:10.1002/(SICI)1097-4652(199911)181:2<319::AID-JCP14>3.0.CO;2-S [pii], 10.1002/(SICI)1097-4652(199911)181:2<319::AID-JCP14>3.0.CO;2-S

Larrieu-Lahargue F, Welm AL, Thomas KR, Li DY (2010) Netrin-4 induces lymphangiogenesis in vivo. Blood 115(26):5418–5426

Litkouhi B, Kwong J, Lo CM, Smedley JG 3rd, McClane BA, Aponte M, Gao Z, Sarno JL, Hinners J, Welch WR, Berkowitz RS, Mok SC, Garner EI (2007) Claudin-4 overexpression in epithelial ovarian cancer is associated with hypomethylation and is a potential target for modulation of tight junction barrier function using a C-terminal fragment of Clostridium perfringens enterotoxin. Neoplasia 9(4):304–314

Lo CM, Keese CR, Giaever I (1995) Impedance analysis of MDCK cells measured by electric cell-substrate impedance sensing. Biophys J 69(6):2800–2807

Lo CM, Keese CR, Giaever I (1999) Cell-substrate contact: another factor may influence transepithelial electrical resistance of cell layers cultured on permeable filters. Exp Cell Res 250(2):576–580

Martin TA, Mansel RE, Jiang WJ (2002) Antagonistic effect of NK4 on HGF/SF induced changes in the transendothelial resistance (TER) and paracellular permeability of human vascular endothelial cells. J Cell Physiol 192(3):268–275. doi:10.1002/jcp. 10133

Martin TA, Goyal A, Watkins G, Jiang WG (2005) Expression of the transcription factors snail, slug, and twist and their clinical significance in human breast cancer. Ann Surg Oncol 12(6):488–496. doi:10.1245/ASO.2005.04.010

Martinez-Paloma A (1970) Ultrastructural modifications of intercellular junctions in some epithelial tumors. Lab Invest 22(6):9

Matter K, Balda M (2003) Functional analysis of tight junctions. Methods 30:228–234. doi:10.1016/S10466-2023(3)00029-X

Mullin HM, O'Brien TG (1986) Effects of tumor promoters on LLC-PK1 renal epithelial tight junctions and transepithelial fluxes. Am J Physiol 251(4 Pt 1):C597–C602

Patibandla PK, Tyagi N, Dean WL, Tyagi SC, Roberts AM, Lominadze D (2009) Fibrinogen induces alterations of endothelial cell tight junction proteins. J Cell Physiol 221(1):195–203

Ramachandran C, Srinivas SP (2010) Formation and disassembly of adherens and tight junctions in the corneal endothelium: regulation by actomyosin contraction. Invest Ophthalmol Vis Sci 51(4):2139–2148

Ren J, Hamada J, Takeichi N, Fujikawa S, Kobayashi H (1990) Ultrastructural differences in junctional intercellular communication between highly and weakly metastatic clones derived from rat mammary carcinoma. Cancer Res 50(2):358–362

Satoh H, Zhong Y, Isomura H, Saitoh M, Enomoto K, Sawada N, Mori M (1996) Localization of 7H6 tight junction-associated antigen along the cell border of vascular endothelial cells correlates with paracellular barrier function against ions, large molecules, and cancer cells. Exp Cell Res 222(2):269–274. doi:S0014-4827(96)90034-8 [pii] 10.1006/excr.1996.0034

Starosta V, Wu T, Zimman A, Pham D, Tian X, Oskolkova O, Bochkov V, Berliner JA, Birukova AA, Birukov KG (2012) Differential regulation of endothelial cell permeability by high and low doses of OxPAPC. Am J Respir Cell Mol Biol 46:331–341

Tiruppathi C, Malik AB, Del Vecchio PJ, Keese CR, Giaever I (1992) Electrical method for detection of endothelial cell shape change in real time. Proc Natl Acad Sci USA 89:7919–7923

Tsukita S, Furuse M (1999) Occludin and claudins in tight-junction strands: leading or supporting players? Trends Cell Biol 9(7):268–273. doi:S0962-8924(99)01578-0 [pii]

Winkler L, Gehring C, Wenzel A, Müller SL, Piehl C, Krause G, Blasig IE, Piontek J (2010) Molecular determinants of the interaction between Clostridium perfringens enterotoxin fragments and claudin-3. J Biol Chem 284(28):18863–18872

Wong V (1997) Phosphorylation of occludin correlates with occludin localization and function at the tight junction. Am J Physiol 273(6 Pt 1):C1859–C1867

Yamamoto M, Ramirez SH, Sato S, Kiyota T, Cerny RL, Kaibuchi K, Persidsky Y, Ikezu T (2008) Phosphorylation of claudin-5 and occludin by rho kinase in brain endothelial cells. Am J Pathol 172(2):521–533

Epithelial Wound Healing and the Effects of Cytokines Investigated by ECIS

Electric Cell-Substrate Impedance Sensing in Epithelial Research

Katalin Szaszi, Matthew Vandermeer, and Yasaman Amoozadeh

Abstract Epithelial layers are prone to injury that disrupts the continuity of the tissue. They are also equipped with powerful injury repair capabilities. Epithelial wound healing is a vital process that has relevance to many important diseases. We are now starting to understand the underlying mechanisms, however there are a large number of outstanding questions. The Electrical Cell-substrate Impedance Sensing (ECIS) wound healing assay offers a highly reproducible, real-time method that can provide information not only about the restoration of the continuity of the layers but also about regeneration of function. This assay has already provided some interesting insights into how epithelial monolayers repair themselves and in the coming years will certainly prove to be an invaluable tool in research on wound healing. This chapter reviews the use of ECIS wound healing assays in epithelial research. An overview of epithelial wound healing processes and mechanisms involved, and the effects of inflammatory cytokines on wound healing is also given. Classical in vitro methods used by researchers to study wound healing are summarized and compared with the ECIS method. Research using ECIS to explore epithelial wound healing is presented. In the final sections the use of the ECIS wound healing assay is demonstrated through experiments with tubular epithelial cell lines and practical aspects, special considerations and some caveats are also discussed.

K. Szaszi (✉) • M. Vandermeer • Y. Amoozadeh
Keenan Research Center in the Li Ka Shing Knowledge Institute, St. Michael's Hospital, Toronto, ON M5B 1T8, Canada

Department of Surgery, University of Toronto, Toronto, ON, Canada
e-mail: szaszik@smh.ca

W.G. Jiang (ed.), *Electric Cell-Substrate Impedance Sensing and Cancer Metastasis*, Cancer Metastasis - Biology and Treatment 17, DOI 10.1007/978-94-007-4927-6_8,

List of Abbreviations

ADAM	A disintegrin and metalloprotease
AJ	adherens junctions
AMD	age-related macular degeneration
APC	adenomatous polyposis coli
aPKC	atypical Protein Kinase C
C	capacitance
CFTR	cystic fibrosis transmembrane conductance regulator
ECM	extracellular matrix
EGF	Epidermal Growth Factor
EGFR	Epidermal Growth Factor Receptor
EMT	epithelial-mesenchymal transition
EPLIN	Epithelial protein lost in neoplasm
ERK	Extracellular Signal Regulated Kinase
FAK	Focal Adhesion Kinase
FGF	Fibroblast growth factor
GAP	GTPases Activating Proteins
GDI	GDP dissociation inhibitor
GEF	GDP/GTP exchange factor
HGF	Hepatocyte Growth Factor
IL	Interleukin
IECs	Intestinal epithelial cells
MCP-1	Macrophage Chemoattractant Protein-1
MDCK	Madin-Darby Canine Kidney
MMP	Matrix metalloprotease
NHBE	normal human bronchial epithelial
NFκB	Nuclear Factor Kappa Beta
NRK	Normal Rat kidney
PAK	p21 activated kinase
PDGF	platelet-derived growth factor
R	resistance
Scrib	scribble
siRNA	short interfering RNA
RPE	retinal pigment epithelium
ROK	Rho kinase
TER	transepithelial resistance
TGFβ1	Transforming Growth Factor β1
TGF-α	Transforming Growth Factor
TJ	tight junctions
TNF-α	Tumor Necrosis Factor-α

1 Introduction

Epithelial layers are prone to cell injury that disrupts the continuity of the tissue. Thus epithelia are equipped with powerful injury repair and wound healing capabilities. Research from many laboratories from all over the world had substantially improved our understanding of the process of epithelial wound healing. As in any field however, a better understanding also brings about novel questions and opens up new areas of research. This chapter will discuss a new tool that has recently been added to our research arsenal to investigate epithelia. The Electric Cell-substrate Impedance Sensing (ECIS) wound healing assay offers a highly reproducible, real time and automated way of monitoring wound healing. In addition to providing an overview of the application of the ECIS method in epithelial wound healing studies, the chapter will offer a general introduction to the process of epithelial wound healing. Accordingly, the first sections will provide an overview of epithelial functions, and discuss the types, characteristics and mechanisms of epithelial wound healing. Next, the effects of inflammatory cytokines on wound healing will be briefly reviewed. As the literature in these fields is overwhelming, the reader will be directed to appropriate reviews, where further references to individual research papers can be found. Section 5 contains an overview of the classical in vitro methods used by researchers to study wound healing, while Sect. 6 is dedicated to the ECIS wound healing assay itself. In this part an overview of studies that used ECIS to explore epithelial wound healing will be presented. Further, the use of the ECIS wound healing assay will be demonstrated through experiments with tubular epithelial cell lines. Practical aspects, special considerations and some caveats will also be discussed.

2 Characteristics of Epithelial Monolayers

2.1 Epithelial Cells Generate Polarized Monolayers

Vital organs are lined with highly organized epithelial tissues which create a barrier between the inside of the body and the external environment. Most epithelial tissues consist of a single layer of cells, an epithelial monolayer. Such monolayers are found in the mucosa of various internal organs (e.g. the respiratory, the uritogenital and the digestive tracts), and the ducts of exocrine glands (e.g. the pancreas, the prostate and the mammary glands). The skin is also lined with epithelial cells, but these are arranged in multiple layers, with the top layer consisting of flat scale-like cells (squamous epithelium). Cells within the epithelial monolayers show a high degree of apico-basal polarization. Thus, each cell has an apical (facing the lumen) and basolateral (facing the tissue of the organ) side, with unique protein composition and function. The cells are connected to each other through four distinct intercellular junctional complexes: the tight junctions (TJ), adherens junctions (AJ), desmosomes

and gap junctions, that can be distinguished based on the proteins found in them and their functional properties. The cadherin-based AJs regulate tissue formation and organization by generating Ca^{2+}-dependent adhesions between adjacent cells (Rudini and Dejana 2008). The TJs have at least two roles. First, they seal off the intercellular space and form a paracellular pathway that allows only some selective transport (gate function). Second, the TJs also separate the apical and basolateral membrane compartments (fence function) (Hartsock and Nelson 2008). The gap junctions are made up from connexins that are permeable for ions, and generate a direct connection between the cytoplasms of adjacent cells (Sohl and Willecke 2004). Desmosomes provide resistance against mechanical forces and enhance stable cell-cell adhesions (Delva et al. 2009). TJs, AJs and desmosomes consist of specific transmembrane proteins that interact through their cytosolic tails with a multitude of proteins. These cytosolic protein complexes serve as signalling nodes. The junctions also bind to the cytoskeleton: the TJs and AJs interact with actomyosin structures, while the desmosomes are anchored to the intermediate filaments.

Importantly, epithelial layers serve not only as protective barriers, but also mediate limited and controlled exchange of water, ions and various substances. Transport through an epithelial layer occurs either through transcellular or through paracellular pathways. Transcellular transport is achieved by the coordinated action of apical and basolateral transport proteins. The differential localization of these transporters on the apical and basolateral sides is a prerequisite for unidirectional transport (Nelson 2003). Limited passive paracellular transport of water and ions also occurs through the TJs, where proteins of the claudin family form size- and charge-selective channels (Tsukita and Furuse 2000). Taken together, the overall permeability of an epithelial layer is determined by the combined action of all transcellular and paracellular pathways. As the expression of specific transcellular transport proteins and claudins in different tissues varies, the permeability of epithelial layers also differs significantly from one organ to another.

2.2 Need for Effective Injury Repair in Epithelial Layers

A number of factors render epithelial layers prone to injury and create a need for potent repair mechanisms that can reduce the consequences of cell loss. First, since epithelial cells are located at the interface between the external and internal environments, they are continuously exposed to harmful chemicals, toxins, infectious agents, mechanical stress, and other potentially injury-causing effects. Second, the high energy demand of the transport processes makes these cells sensitive to the reduction in oxygen supply or the presence of toxins. Third, turnover of cells in some epithelial tissues (e.g. the intestine and the cornea) is rapid with continuous loss and replacement of cells. The high turnover means not only that cells are frequently lost from the layer, but also renders the epithelium more prone to injury. Physiological or pathological cell loss disrupts the continuum of the tissue. Importantly, reestablishment of tissue integrity has to be achieved through a process that ensures minimal

disruption of other, uninjured areas. In response to injury, epithelial monolayers rapidly initiate a well orchestrated series of events that results in efficient cell replacement and restoration of barrier and transporting functions. The mechanism of this wound healing process will be discussed in the next section.

3 Epithelial Wound Healing

3.1 Types of Epithelial Wound Healing and General Characteristics

Injury to an epithelial monolayer induces a highly coordinated series of events that culminates in the restoration of tissue integrity. In vivo this complex process involves responses not only of the epithelial cells in the intact areas adjacent to the injury, but also of cells in the surrounding tissues. Tissue damage is a potent initiator of inflammation, because injured cells release both inflammatory cytokines and chemoattractants for white blood cells. The recruited inflammatory cells in turn contribute to the removal of cell debris. They also release more inflammatory cytokines, which exert a positive feedback on inflammation and enhance wound healing (see Sect. 4). Despite its beneficial effects on wound healing, however, inflammation is not a prerequisite for successful monolayer repair. Epithelial cells are able to efficiently repair injuries and regenerate the continuity of the tissue without any other contributing cells and without the effects of inflammatory cytokines.

The response of epithelial cells to injury starts immediately. Two major types of epithelial repair mechanisms can be distinguished (Garcia-Fernandez et al. 2009; Jacinto et al. 2001). The first one involves lamellipodial crawling of the intact cells to cover the denuded area. During this process the epithelial cells move as a single unit, dragged forward by the cells adjacent to the injury. This type of migration is referred to as sheet migration (Khalil and Friedl 2010; Rorth 2009) and it seems to be the dominant process during repair of a relatively large area.

The second mechanism of wound repair is referred to as the purse-string closure (Baur et al. 1984). It is very effective in closing small, circular wounds. In response to injury of the neighbouring cells, the apical actomyosin rings in cells adjacent to the wound constrict (Bement et al. 1993; Danjo and Gipson 1998). Since the actomyosin ring is attached to the cell-cell contacts, these structures create a contractile belt throughout many cells. The contraction of these structures gradually brings cells closer together, and closes the gap between them; similar to when a purse is closed using a string. This fascinating wound healing mechanism was first described in embryos, but there is now evidence that it also occurs in adult epithelial tissues for example in the cornea and the gut (Garcia-Fernandez et al. 2009; Martin and Parkhurst 2004; Russo et al. 2005).

Although sheet migration and purse-string closure involve distinct mechanisms, there are likely significant overlaps, and both mechanisms have their role during

in situ wound repair. Since during the ECIS wound healing assay the predominant process is sheet migration, here we will focus only on this mechanism. Readers interested in the purse-string closure are referred to some excellent reviews (Fenteany et al. 2000; Garcia-Fernandez et al. 2009; Redd et al. 2004).

3.2 Epithelial (Sheet) Migration During Wound Healing

When cells are lost from an epithelial layer, the first response of intact neighbouring cells is to spread and migrate into the denuded area to cover it. Below a certain wound size, cell migration alone is sufficient to close the gap without contribution of cell proliferation (Jacinto et al. 2001). Wound healing assays, including the ECIS assay that study closure of small wounds (i.e. injury repair that is over within a few hours) reflect the efficiency of cell migration. In the past years the molecular events and machinery of cell migration has become better understood. On the other hand, the majority of our knowledge regarding the processes of cell migration is derived from studies of individual cells. While this knowledge proved to be mostly applicable to the epithelial layers, especially to cells at the leading edge, collective migration clearly shows unique characteristics too. A large boost to research into epithelial migration associated with wound healing came with the recognition that it resembles the processes of developmental epithelial migration (Jacinto et al. 2001). Pathways identified in the developmental settings turned out to be relevant for wound healing and cell migration in adult epithelia (Wood et al. 2002).

During wound healing associated with epithelial sheet migration cells move as a multicellular unit (Friedl and Wolf 2010; Khalil and Friedl 2010; Poujade et al. 2007; Rorth 2009). The cells adjacent to the injury exhibit characteristic morphological changes, extend membrane protrusion and start migrating into the denuded area. However, they retain their contacts with cells behind them, and thus the whole sheet is dragged forward. Interestingly, as described in Sect. 3.2.2. during these processes all cells exhibit active migration and cells further away from the wound are not or not only passively dragged forward.

3.2.1 Migration at the Leading Front

The general process of directional cell migration is remarkably similar in all cell types with some cell specific variations (Rikitake and Takai 2011). Importantly, although the migration in an epithelial sheet has unique characteristics, the events at the front and the mechanisms involved are similar to those described for single cell migration. In general, cell migration is a complex, cyclical, multistep process (Horwitz and Webb 2003; Petrie et al. 2009). As described below in more details, the first step in directional migration is the appearance of a migratory stimulus, which in the case of wound healing is provided by the injury of cells and the appearance of newly exposed extracellular matrix proteins. This stimulus initiates a series of

events leading to cytoskeletal remodelling and significant morphological changes. The next sections describe some important aspects of directional migration, including development of new cell-substrate interactions, front-rear polarization, extension of membrane protrusions at the front and enhanced tension that propels the cell forward relative to its substratum. Fine spatio-temporal control of molecules involved is key for efficient directional migration. After the overview of the sequence of events that are cyclically repeated during migration, a more detailed description of some of the important molecular pathways regulating these events will follow in Sect. 3.3.

Initiation of Migration: Directional Sensing and Functional Polarization

In a wounded monolayer both soluble and insoluble factors can serve as directional migration cues. The injured epithelium (and during later stages of the wound healing infiltrating inflammatory cells) releases migration enhancing soluble factors, such as growth factors and cytokines (Beers and Morrisey 2011; Crosby and Waters 2010; Iizuka and Konno 2011; Sturm and Dignass 2008). A concentration gradient of these factors with highest concentrations around the injured area is an important directional cue. The newly exposed extracellular matrix (ECM) proteins in the injured area are the most crucial non-soluble migration signals (Wickstrom and Fassler 2011). The ECM proteins form new interactions with their cellular receptors, the integrins, leading to their clustering and activation. Since this happens only at the leading edge adjacent to the wound, integrin activation can provide directional signals for migration.

The disassembly of intercellular junctions at the injury site is also thought to promote migration. However, in contrast to integrin activation, our understanding of how loss of cell-cell contacts affects migration is limited. The presence of cell-cell contacts exerts a strong inhibitory effect on migration (Contact inhibition of locomotion, CIL) that is lost when contacts are disassembled. Contact inhibition was first described by Abercrombie and coworkers (Abercrombie and Heaysman 1954). This complex and not entirely understood mechanism is activated when cells, such as epithelia or fibroblasts encounter each other during migration or growth. The formation of epithelial intercellular junctions, most importantly the AJs contributes to contact inhibition (Mayor and Carmona-Fontaine), and therefore loss of junctions allows for enhanced motility. Importantly, the junctions are disassembled only in the leading cells, and this effect probably also represents a directional cue. The junction-related molecular pathways involved in migration will be described in Sect. 3.3.3.

Development of Front-Rear Polarity

Junction disassembly also leads to loss of apico-basal polarity. Motile cells instead develop front-rear polarization (Etienne-Manneville 2008). In fact, the polarization

is key for maintaining directionality of the migration and it is due to remodelling of the actin cytoskeleton and the microtubules. Localized activation of integrins and Rho family small GTPases are essential for the development of rear-front polarity (see Sects. 3.3.1 and 3.3.2). Activation of the small GTPases alters actin dynamics, leading to enhanced actin polymerization at the leading edge that is necessary for the formation of membrane protrusions. Another important factor in polarization of the cells is the rearrangement of the microtubular system and the asymmetric vesicular transport, which results in the delivery of specific proteins to the leading edge. The resulting protein compartmentalization further enhances the front-rear asymmetry necessary for directional migration.

Extension of Membrane Processes and Forward Movement

The localized activation of two small molecular weight GTPases, Rac and cdc42, in the front induces local actin polymerization, which in turn drives the development of membrane protrusions. Lamellipodia are large membrane ruffles, the formation of which requires Rac activation, while filopodia, elongated, finger-like membrane structures are developed as a result of cdc42 activation (Rikitake and Takai 2011; Spiering and Hodgson 2011). Newly formed integrin-based adhesion points attach the lamellipodium to the substratum, thereby allowing mechanical force generation (pull) for the forward movement. However, effective movement also requires the release of the rear end of the cell from the substratum and its retraction. Importantly, this latter aspect is different in the case of individual migrating cells and during epithelial sheet movements. Although the cells within the sheet also need to be released from the substratum, they remain connected to the neighbouring cells. The mechanisms involved in the movement of the rear of the cells during sheet migration are probably distinct from those involved in individual cell migration, however the details of this process are still unexplored.

3.2.2 Characteristics of Sheet Migration

Collective migration is characterized by a high degree of coordination between cells. Epithelial sheet migration is distinguishing by the presence and maintenance of intercellular junctions, which can serve as points of force transmission between cells and are also important signalling hubs. Morphological changes, polarization and cytoskeleton remodelling is also coordinated within the layer. The leading edge is a well-defined row of cells adjacent to the wounded area. These cells polarize and form lamellipodia through mechanisms described above. Interestingly however, not only the cells at the front, but the whole group exhibits some degree of front-rear polarization, which is probably due to the retained cadherin-based junctions. The tension developing in the leading cells therefore can be transmitted to cells behind them, promoting polarization and movement of the whole sheet. We do not have a complete understanding of the processes that take place in cells further away from

the leading edge. Farooqui et al. used advanced imaging techniques to investigate the epithelial monolayers of kidney tubular cells during sheet migration in a wounded monolayer. They showed that cells as far as hundreds of microns behind the edge extended lamellipodia towards the substratum beneath cells in front of them, indicative of an active migrating phenotype (Farooqui and Fenteany 2005). The cells nevertheless maintained their cell-cell contacts. Studies exploring the physical forces that arise within wounded monolayers found unexpected fluctuations. Each cell exerts forces on the extracellular matrix as well as on the neighbouring cells, resulting in large variations of the mechanical forces that arise within the sheet (Tambe et al. 2011). Although not all cells seem to pull towards the same directions at all times, the integration of all force vectors still maintains effective forward migration of the sheet towards the injured areas.

How cell-cell contacts are maintained and whether they exhibit dynamic changes during sheet migration is not completely known. In individual migrating cells the tail retraction requires local activation of the small GTPase RhoA that enhances myosin-dependent contractility through its effector Rho kinase (ROK). An interesting recent study by Hidalgo-Carcego and co-workers showed a polarized distribution of actomyosin contractility, with enhanced myosin activation at the leading edge and diminished activity at the cell-cell contacts (Hidalgo-Carcedo et al. 2011). Since enhanced actomyosin contractility is associated with junction disruption, it is likely that reduced local contractility will allow the cells to retain their contacts. Clearly, further studies will be required to explain how the requirement for junction maintenance and motility are coordinated.

Taken together, the process of sheet migration offers huge advantages over individual cell migration during epithelial wound healing. As cell-cell contacts are retained, the barrier function is likely not disrupted and intactness of the sheet is maintained in areas away from the wound. Further, collective migration allows the cells to influence each other, which can ensure appropriate cell distribution and correct shaping of the reformed epithelial tissue. The force exerted as a group can also be larger than that of individual cells, enhancing effective closure of the gap. Thus, collective epithelial cell migration indeed seems to be very adequate for effective regeneration of the highly organized epithelial tissue.

3.3 Molecular Pathways Regulating Migration

The next section will discuss some of the key signalling and effector molecules involved in migration and wound healing. Cytoskeleton remodelling is a main event during migration: actin dynamics drives the development of membrane protrusions, actomyosin contractility is needed for the tension for locomotion and rearrangement of the microtubular system allows asymmetric membrane trafficking. Localized changes in the activity of integrins and small GTPases play crucial role in all steps of the cytoskeleton remodelling. Further, junction-related factors, especially polarity proteins are also key players that orchestrate polarization of the cells. We will also discuss how matrix metalloproteases, a family of proteases affect wound healing.

3.3.1 Integrins

Integrins are a family of heterodimeric transmembrane receptors that bind ECM proteins (Hynes 2002). They mediate cell-substratum adhesion and are indispensable for migration. The cytosolic domains of integrins are connected to the cytoskeleton and a multitude of signalling molecules, with two important consequences. First, the extracellular matrix is coupled to the cytoskeleton through the integrins, and therefore there is a continuum between the extracellular matrix and the cell skeleton. This allows tension to develop that is necessary for pulling the cell forward. Second, important signalling hubs form at the cytosolic side of the matrix-integrin interaction points that affect all aspects of cell functions. Some signalling components found in these complexes include kinases (such as the Focal Adhesion Kinase (FAK), the tyrosine kinase Src and the Extracellular Signal Regulated Kinase (ERK)), as well as small GTPases.

In resting cells, clustered integrins form relatively stable contacts with the matrix, referred to as the focal adhesions. However, at the leading edge the nascent contacts that form between the integrins and ECM proteins are smaller in size and more dynamic. These structures are called focal contacts. Importantly, similar to focal adhesions, focal contacts also act as signal integrators (Gardel et al. 2010), and provide mechanical tension at the leading edge. These two functions are essential for the forward movement of the cell. The newly formed focal contacts can break up and reform relatively easily, which is necessary for leading edge dynamics associated with migration.

3.3.2 Small GTPases

The Rho family constitutes a subgroup of the Ras superfamily of small GTPases. The best studied Rho family members are RhoA, Rac1,2 and cdc42, which are central regulators of migration.

Rho proteins are molecular switches that cycle between active (GTP-bound) and inactive (GDP-bound) forms. Active Rho proteins bind to and activate a large variety of effectors (Guilluy et al. 2011; Parri and Chiarugi 2010; Spiering and Hodgson 2011). The effectors of the small GTPases regulate actin polymerization, F-actin filament organization, actomyosin contractility, cell polarization, microtubule dynamics, membrane trafficking and junction assembly-disassembly (El-Sibai et al. 2008; Nalbant et al. 2009). Two kinases downstream from the small GTPases are especially important for migration: the Rho-regulated ROK and the Rac/cdc42 activated p21 activated kinase (PAK). These two prominent kinases are major regulators of wound healing (Narumiya et al. 2009; Ridley 2011; Zegers 2008).

Rac and cdc42 are active at the leading edge of migrating cells (Rikitake and Takai 2011; Zegers 2008). Rac regulates the de novo actin polymerization and branching processes that push the membrane forward during lamellipodium formation (Firat-Karalar and Welch 2011; Nurnberg et al. 2011). Active cdc42 on the other hand contributes to migration through at least two different effects. First, local cdc42

activation leads to the generation of filopodia. Second, cdc42 is a central regulator of both front-rear and apico-basal polarization. This latter effect of cdc42 involves activation of the Par polarity complex (see below), that contributes to microtubule polarization and stabilization. As for the role of RhoA, initial studies in individual migrating cells showed that it is active at the rear end of migrating cells, where it enhances myosin-based contractility that is necessary for tail retraction. However, this has proven to be a simplistic view, as imaging with sophisticated fluorescent biosensors revealed that RhoA is also active in certain parts of the leading edge (El-Sibai et al. 2008; Nalbant et al. 2009).

Lamellipodium formation is especially important during wound healing not only due to its role in migration. Lamellipodium extension and spreading of cells at the leading edge increase their area and this by itself can cause rapid initial covering of some of the denuded area. Filopodia on the other hand are important for exploring the cell surroundings. Other types of membrane protrusions can also contribute to migration depending on the circumstances. For example, membrane blebbing was shown to play a role during developmental migration and could also be involved in sheet migration (Ridley 2011). Development of all membrane protrusions require finely controlled local actin polymerization. Actin dynamics is regulated by the complex interplay of a large number of regulator proteins, that function as monomer binding, capping, nucleating and severing proteins and also regulate filament branching. Actin regulating proteins with known roles in lamellipodium formation include, among many others, the Arp 2/3 complex, CapZ, cortactin, cofilin, Ena/Vasp proteins and formins (Firat-Karalar and Welch 2011; Nurnberg et al. 2011; Ridley 2011). Most of these proteins are directly or indirectly regulated by small GTPases. Lipid-derived signalling molecules such as phosphatidylinositol 4,5-bisphosphate (PIP_2) and phosphatidylinositol (3,4,5)-triphosphate (PIP_3) also have a role in regulation of small GTPases and actin polymerisation at the leading edge.

Activation of small GTPases during migration exhibits a unique spatio-temporal pattern, which is the basis for cell migration, and the development of cell asymmetry. Small GTPases are regulated by signals from many inputs, including integrins, junction disassembly, and soluble factors such as growth factors and cytokines (Kozasa et al. 2011; Schiller 2006). The activation-inactivation cycle of Rho proteins is controlled by a complex network involving a multitude of regulators (Cote and Vuori 2007; Garcia-Mata and Burridge 2007; Rossman et al. 2005). GDP dissociation inhibitor (GDI) proteins bind to the inactive, GDP-bound Rho proteins, preventing their dissociation from GDP. They also maintain the cytosolic localization of the Rho proteins, preventing them from translocating to the membrane where they exert their effects. The first step of activation therefore involves release of Rho proteins from the GDI. This allows interaction with members of another family of regulators, the GDP/GTP exchange factors (GEFs). As their name implies, GEFs induce the release of GDP from Rho proteins, which is replaced by GTP, that is a more abundant nucleotide in the cytosol. Thus, GEFs catalyze activation of the small GTPases. At the end of the cycle inactivation happens through the hydrolysis of GTP due to the intrinsic GTPase activity of Rho proteins. Their unstimulated

GTPase activity however is very slow, and for fast turnover this activity needs to be enhanced by GTPases Activating Proteins (GAPs). Thus GAPs facilitate inactivation of small GTPases. Rho family specific GEFs and GAPs constitute large families (Garcia-Mata and Burridge 2007; Guilluy et al. 2011). Interestingly, many of these proteins can act on more than one member of the Rho family. Furthermore, each cell expresses a number of these proteins. What is the unique role of GEFs and GAPs, and how are they regulated in a pathway specific manner? This is one of the most exciting questions in the field of Rho proteins to which answers are only now starting to emerge. The local coordination of the activity of GEFs and GAPs is the key to localized activation/deactivation of the Rho proteins during migration (Spiering and Hodgson 2011; Tomar and Schlaepfer 2009). Interestingly, junction related and polarity proteins are emerging as important regulators of local GEF and GAP activity.

3.3.3 Junction-Related Factors and Polarity Proteins

Epithelial cells are unique because they have well developed intercellular junctions, the presence or loss of which is an important signalling event. Adjacent to the wound, as cells lose their neighbours, cadherins, the transmembrane molecules of the AJs become uncoupled from their binding partners on opposing cells. This leads to their endocytosis and degradation and the consequential loss of contact inhibition (Steed et al. 2010). Furthermore, contact disassembly primes cells for the process of epithelial-mesenchymal transition (EMT) (see Sect. 3.4).

Junctional proteins are now known to regulate migration. In most cases the underlying mechanisms are still not known, but some common themes are now emerging. An important aspect is the local regulation of small GTPases activation/deactivation. At least some of the effects of contact disassembly are probably due to alterations in the spatio-temporal regulation of Rho family proteins. Indeed many Rho regulators, including the exchange factors GEF-H1, p114 Rho GEF and Tiam1, have been found to localize at tight and adherent junctions (Citi et al. 2011; Terry et al. 2010). Binding to the junctions not only localizes these proteins, but also controls their activity. Release of these regulators from their junctional binding partners alters their activity and can directly affect Rho proteins (Terry et al. 2010). Indeed, junction disruption using the Ca^{2+} switch method was shown to activate small GTPases (e.g. Samarin et al. 2007; Sebe et al. 2008).

Surprisingly, mounting evidence now suggests that transmembrane proteins of the TJs also affect cell migration. For example, expression of various claudins was found to be altered in cancer cells, which lead to the hypothesis that claudin levels can affect migratory behaviour. Indeed, this seems to be the case, as several studies now verify that experimental down-regulation or overexpression of specific claudins can by itself alter migration (Escudero-Esparza et al. 2011). Claudins might affect migration by altering polarity, cytoskeleton dynamics, small GTPase activity or other junction-related signalling. The underlying mechanisms however remain to be established.

When epithelial cells become migratory, there is a major shift from apico-basally polarized morphology to front-rear polarity. Importantly, the loss of apico-basally polarization and the development of the migratory asymmetric structure has to be coordinated. Studies published in the past years provided an interesting mechanism for such coordination. Proteins that regulate the apico-basal polarity were found to also play crucial roles in migration and the development of front-rear polarity (Dow and Humbert 2007; Etienne-Manneville 2008; Humbert et al. 2006). There are at least three polarity complexes involved in the establishment and maintenance of apico-basal polarity. These are 1, the Par complex that includes the Par proteins and atypical Protein Kinase C (aPKC); 2, The scribble (Scrib) complex that includes scribble, Dlg and Lgl; and 3, the Crumbs complex, including Crumbs (Crb), PALS1 and PATJ (Assemat et al. 2008; Dow and Humbert 2007). These highly conserved protein complexes were first identified in Drosophila, and were subsequently recognized as epithelial polarity regulators in mammalian cells. These proteins are now also emerging as polarity regulators in migrating cells. Although not all details about how the polarity proteins work are clear, it seems that the most important signal for polarization and junction formation is the localized assembly of these complexes. Each complex is known to show a precise localization within the cells at certain areas, and importantly, they are also excluded from other areas. For example, in polarized epithelial cells the Par complex can be found at the apical lateral border, while the Scrib complex is in the lateral membrane. The presence of a polarity complex in certain areas initiates localized signalling events. Localization differences can mark specific spots of the cells for junction formation, cytoskeleton polarization and asymmetric microtubule development, thus establishing cell asymmetry.

Interestingly, both the Par and the Scrib complexes were shown to affect migration (Dow and Humbert 2007; Humbert et al. 2006). For example, the knockdown of Scribble using a short interfering RNA (siRNA) in breast cancer cells inhibited sheet migration and wound healing (Dow et al. 2007). Interestingly however, the role of the scribble complex seems to be context-dependent, as in some cases scribble reduces, rather than promotes migration. Accordingly, depletion of scribble using siRNA in kidney tubular cells enhanced motility (Qin et al. 2005). It is currently not known how the scribble complex is involved in the context-dependent regulation of directional migration. One of the suggested mechanisms involves regulation of E-cadherin (Qin et al. 2005).

The Par complex, that is an effector of cdc42, can affect migration through at least two different ways: by regulating Rac and RhoA and by polarizing the microtubules. In primary rat astrocytes and fibroblasts in response to scratch wounding cdc42 was shown to be activated by integrins at the newly formed leading edge. This resulted in the recruitment and activation of the Par6–aPKC complex (Etienne-Manneville et al. 2005; Petrie et al. 2009). Localized aPKC activation results in microtubule polarization. This effect requires the adenomatous polyposis coli (APC) tumor suppressor protein. Further, aPKC also restricts activity of RhoA, as it recruits the E3 ubiquitin ligase Smurf1 that targets RhoA for degradation. Par3 on the other hand is a regulator of the Rac exchange factor Tiam1 (Wang et al. 2003). Similar to the Scribble complex however, the function of the

Par complex in migration also seems to be context-dependent, with studies showing either enhanced or reduced migration following depletion of Par complex proteins in different cell types (Dow and Humbert 2007; Etienne-Manneville 2008). Finally, a recent study has also implicated the Par3/6 complex in maintaining the cell-cell contacts during collective migration (Hidalgo-Carcedo et al. 2011). Reduced myosin activity at the rear of the cells was found to be necessary for retaining cell-cell junctions. Myosin contractility in individual migrating cells at the rear is regulated by the Rho effector Rho kinase. However, in collectively migrating epithelial cells, Rho kinase was found to be inhibited at the rear by another Rho family protein, RhoE. Interestingly, RhoE was recruited to the rear in a Par3/6-dependent manner. This interesting mechanism can localize reduced ROK and myosin activity specifically to the junctional areas within the migrating sheet without compromising tension development in other areas.

3.3.4 Matrix Metalloproteases and Epithelial Migration

Matrix metalloproteases (MMPs) are a family containing 24 extracellular proteases. MMPs are either secreted or anchored to the cell surface. They act on membrane proteins or extracellular proteins, including ECM proteins (e.g. elastin, gelatin). In fact, many MMPs are known to enhance the turnover and remodelling of the extracellular matrix and many have also been shown to enhance migration.

Most MMPs are not expressed in healthy tissues, but their expression is upregulated during injury repair processes in wounded areas (Chen and Parks 2009). For example, MMP1 is induced in keratinocytes following wounding, and MMP7 expression is markedly increased in injured mucosal epithelium. Inflammatory cytokines have also been shown to increase the expression of MMPs, and this effect is thought to be involved in the stimulatory effects of cytokines on migration. For example, Tumor Necrosis Factor-α (TNF-α), Interleukin (IL)-8 and IL-17A were shown to enhance MMP2 and 9 (Jovanovic et al. 2010; Lehmann et al. 2005; Li et al. 2011).

The role of MMPs in wound healing was verified by both in vivo and in vitro studies. Initially, their effect on cell migration was attributed to their role in cleaving ECM proteins. Indeed, some of the effects of MMPs could involve remodelling of the extracellular matrix that affects integrin activation, alters biophysical forces and removes barriers hindering migration. MMP2 for example was shown to enhance cell migration through the cleavage of laminin-5 (Giannelli et al. 1997). The ECM degrading effect could be especially important for controlling the tumor microenvironment and promoting tumor cell migration and metastasis formation. ECM remodelling however is very likely to be only one mechanism through which MMPs enhance migration. The evidence for further effects comes from observations that some MMPs do not target ECM proteins, but still facilitate migration. Other targets of MMPs might include junctional proteins. Indeed, MMP7 was shown to induce shedding of E-cadherin from the cell surface, and to alter the affinity of integrins for the substratum. Another clue for more complex function is that MMPs are expressed not only in the wound edge. Levels of some members of the family, e.g. MMP3 and

28 are elevated in cells further back from the wound edge. The function of these proteins however is not well understood.

3.4 Epithelial Plasticity During Wound Healing

Plasticity is a genetically defined property of epithelial cells, which helps rapid and effective wound healing. Upon adequate stimuli epithelial cells can undergo a process called Epithelial-Mesenchymal transition (EMT) (Kalluri and Weinberg 2009; Nieto 2011; Revenu and Gilmour 2009), leading to loss of epithelial and acquisition of mesenchymal characteristics. Cells undergoing EMT lose their intercellular junctions and apico-basal polarity and become highly motile and contractile. Cells undergoing EMT also start to produce large amounts of extracellular matrix, which in turn enhances integrin activation. Such processes are happening at the leading edge of the sheet.

EMT has been classified into three types: type 1 is developmental EMT, type 2 takes place during wound healing and may contribute to organ fibrosis, while type 3 is EMT of cancer cells (Kalluri and Weinberg 2009). Type 2 EMT, the process associated with wound healing, is thought to be induced by inflammatory cytokines and growth factors released by injured epithelium and recruited inflammatory cells. EMT-promoting factors include fibroblast growth factor (FGF), platelet-derived growth factor (PDGF) and Transforming Growth Factor β1 (TGFβ1). Exciting new research however revealed that in intact epithelial monolayers TGFβ1 is not able to induce EMT. In fact, the disruption or injury of intercellular contact is a prerequisite for TGFβ1 to induce EMT (Masszi et al. 2004). This powerful mechanism therefore contributes to the inhibition of migration within an uninjured intact epithelial layer.

A full-blown EMT turns non-migratory epithelial cells into highly motile mesenchymal cells, which are no longer part of the epithelial sheet. However, as described above, during wound-induced sheet migration, cells do not completely lose their junctions and their epithelial properties. In fact, junctions are lost only in the front row of cells, in areas facing the wound. This brought about the recognition that EMT is not necessarily an all-or-none phenomenon, but rather a finely tuned process. The cells at the leading edge undergo partial EMT (Revenu and Gilmour 2009), which promotes their motility without major disruption of the integrity of other areas further away from the wound. Importantly, EMT during wound healing is reversible. The reverse process, when mesenchymal cells take up epithelial characteristics is referred to as Mesenchymal-Epithelial Transition (MET).

3.5 Role of Proliferation in Wound Healing

Restoration of the epithelial layer can be completed without cell proliferation exclusively through the process of cell spreading and migration (Garcia-Fernandez et al. 2009).

However, if a larger area is injured, new cells will need to be generated to replace dead cells and to complete the wound closure. Indeed, proliferation within the intact epithelial layer is stimulated within hours after the injury. Many of the growth factors and inflammatory cytokines that promote migration are also potent stimuli for proliferation. Interestingly, however, migration and proliferation are well coordinated events in cells, and are mutually exclusive processes (De Donatis et al. 2010; Zelenka and Arpitha 2008). This might be due to the fact that the two processes both require major, but different type of cytoskeletal remodelling, which cannot happen at the same time. Proliferation is suppressed in cells at the leading edge, but is enhanced in cells located further away from the injury. A concentration gradient of growth factors and cytokines from the wound towards the rows further away might play a role in the coordination of proliferation and migration. Indeed, some growth factors, such as PDGF were shown to have differential effects stimulating either migration, or proliferation, depending on the concentration applied (De Donatis et al. 2008).

3.6 Stop Signals

During successful wound closure, the sheets migrating from opposing sides of the wound reach each other and fuse to re-establish the intact barrier. Once the migrating layers get closer and the size of the wound is reduced, resealing might also involve the purse-string mechanism that was mentioned earlier in Sect. 3.1 (Garcia-Fernandez et al. 2009; Jacinto et al. 2001). All migrating cells extend filopodia to explore their environment. When these processes reach one another, two important things happen: contact inhibition occurs, and the intercellular junctions start to form. Polarity and junction reformation is regulated by the polarity complexes, and by spatio-temporal control of small GTPase activity (Mayor and Carmona-Fontaine 2010). By regenerating contacts, epithelial cells re-establish the integrity of the barrier. As detailed in Sect. 6, the new ECIS wound healing assay revealed that barrier reformation is a slower process than restoration of the continuity of the monolayer.

Contact inhibition, as discussed earlier, is probably the most powerful “stop signal” for both migration and proliferation. Once it is activated, the migration machinery is switched off and disassembled, and the front-rear polarity is replaced by the regenerated apico-basal polarity. The recently described Hippo pathway, a major regulator of organ size, is thought to mediate contact inhibition of growth (Zeng and Hong 2008; Zhao et al. 2008). This highly conserved pathway was named after one of its key signalling components, the protein kinase Hippo (Hpo) (Zhao et al. 2008). The effector of the pathway, the transcriptional coactivator Yap, controls expression of several cell cycle proteins. When junctions form, this pathway seems to be responsible for turning off proliferation (Zeng and Hong 2008; Zhao et al. 2008).

Under pathological conditions cells might fail to stop migration and proliferation as needed. This lack of contact inhibition is characteristic of cancer cells. Dysregulated wound healing is also important in the development of fibrotic diseases. A more

complete elucidation of the stop signals will bring about a better understanding of diseases caused by failure of the appropriate termination of wound healing, migration and proliferation.

4 Effect of Soluble Factors on Epithelial Wound Healing

4.1 Soluble Factors Regulating Epithelial Wound Healing

Epithelial cells around an injured area are exposed to a variety of growth factors and inflammatory mediators derived from the injured cells, and from cells in the local environment (e.g. stroma cells and infiltrating inflammatory cells). The soluble factors that affect migration can be divided into two major groups: growth factors and inflammatory mediators. Growth factors that enhance migration include members of the Epidermal Growth Factor (EGF) family (e.g. EGF itself and Transforming Growth Factor (TGF)-α), FGF, PDGF and Hepatocyte Growth Factor (HGF) (also called Scattering Factor). Levels of these growth factors are elevated in injured epithelium within hours of the injury. The growth factors involved in wound healing will not be discussed in details, but are reviewed in Crosby and Waters (2010), Iizuka and Konno (2011), Sturm and Dignass (2008), Yu et al. (2011). The next sections provide an overview of the effects of inflammatory cytokines on wound healing.

4.2 Effects of Inflammatory Cytokines on Epithelial Migration

Inflammation, although not a requirement for effective wound healing, is a potent stimulator of the process. Accordingly, many inflammatory mediators have been shown to enhance repair and cell migration. Inflammatory mediators produced at the sites of injury include cytokines (e.g. members of the interleukin family, TNF-α, and Macrophage Chemoattractant Protein-1 (MCP-1)), chemokines and other mediators, such as eicosanoids (Beers and Morrisey 2011; Iizuka and Konno 2011; Lu et al. 2001).

Inflammatory cytokines might modulate migration through a number of effects. First, some cytokines induce the productions and release of other factors. For example, TNF-α and some interleukins were shown to release EGF receptor (EGFR) ligands (Itoh et al. 2005; Kakiashvili et al. 2011; Luppi et al. 2007; Yamaoka et al. 2008). Second, cytokines alter gene expression, and might enhance or suppress levels of proteins relevant for migration, such as integrins, focal adhesion proteins, cell-cell contact proteins, proteins of the motility machinery or MMPs. For example, TNF-α and interleukins stimulates the expression of MMPs (Jovanovic et al. 2010; Lehmann et al. 2005; Li et al. 2011). Third, cytokines can activate small GTPases, and alter the organization of the cytoskeleton and the junctions (Koch and Nusrat 2009). Forth, cytokines can enhance EMT.

Although inflammatory cytokines enhance wound healing, and thus have beneficial effects, their migration promoting effects can also contribute to the pathogenesis of diseases. One such example is the connection between inflammation and cancer formation that has been recognized for years, but the underlying causes are not fully understood. Cytokine-induced enhanced migratory phenotype might contribute to the cancer promoting effects of chronic inflammation. A further important area is organ fibrosis and scar formation. In fact, fibrotic processes can be looked upon as dysregulated wound healing. Interestingly, embryonic wound healing, which does not involve inflammation, never results in scar formation or fibrosis (Redd et al. 2004). The inflammation-fibrosis connection is under intense investigation. One of the effects through which cytokines can play a role in fibrosis, is through promoting the process of EMT (Kalluri and Weinberg 2009). Overall, chronic, dysregulated inflammation and locally elevated inflammatory cytokine production is now thought to contribute to the development of fibrosis (Nieto 2011; Redd et al. 2004).

In the next sections we will discuss the role of some important cytokines, namely the interleukin family and TNF-α in stimulating wound healing.

4.2.1 Interleukins

Interleukins comprise a family of more than 40 cytokines. The first interleukins discovered were found to be expressed and secreted by white blood cells. Subsequent research has resulted in an explosion of the interleukin family. Interleukins are now known to be produced by a large variety of cells, including epithelia (Akdis et al. 2011). They are major regulators of the immune response and their levels are elevated during inflammation (Cuneo and Autieri 2009).

Several interleukins have been shown to enhance wound healing and migration of epithelial cells. The response of respiratory and intestinal epithelial cells to ILs is especially well studied due to the disease relevance of their effects. Interleukins play central roles in the pathogenesis of asthma and inflammatory bowel disease. Different members of the interleukin family, including IL-1β, IL-6, IL-8 and interferon-γ can enhance migration of intestinal and respiratory epithelial cells (e.g. Ahdieh et al. 2001; Jiang et al. 2010; White et al. 2008; Wilson et al. 1999 and reviewed in Crosby and Waters 2010; Iizuka and Konno 2011). There are also examples in the literatures of ILs that inhibit migration, including IL-4 and 13 (Ahdieh et al. 2001).

Some of the effects of ILs on cell migration is attributed to alterations in gene transcription, for example through the ERK pathway, or the inflammatory transcription factor Nuclear Factor Kappa Beta (NFκB) pathway. Another fascinating mechanism of action involves activation of the EGFR. Transactivation of the EGFR is now known to mediate effects of many agents acting through non-tyrosine kinase receptors. It involves activating enzymes of the A disintegrin and metalloprotease

(ADAM) family, which release EGF-related growth factors. These can activate receptors of the EGFR family in an autocrine manner. The crosstalk between inflammatory cytokine receptors and the EGF signalling pathway could play a major role in mediating cytokine-induced stimulation of wound healing, and is another example of connections between cancer and inflammation.

4.2.2 Tumor Necrosis Factor-α

This inflammatory cytokine was first described as an inducer of tumor cell death. Indeed, TNF-α is a major mediator of tissue injury. However it is now also recognized that this cytokine can exert differential effects on cells. In fact, in many epithelial cells TNF-α is pro-survival and promotes proliferation (Hilliard et al. 2011; Kakiashvili et al. 2011; Samarin et al. 2007; Yamaoka et al. 2008). Interestingly, TNF-α also enhances migration of mammary (Chen et al. 2004; Montesano et al. 2005), intestinal (Corredor et al. 2003) and bronchial epithelial cells (Wyatt et al. 1997), keratinocytes (Scott et al. 2004) and tumor cells (Rosen et al. 1991). Our own results obtained using the ECIS wound healing assay shows that TNF-α also significantly stimulates migration of tubular epithelial cells (Sect. 6.4).

Multiple mechanisms have been described that might mediate the effects of TNF-α on migration. TNF-α has two receptors that initiate complex signalling processes. In intestinal cells, enhanced migration was shown to be mediated by TNF receptor 2-dependent activation of two kinases, Src and FAK (Corredor et al. 2003). FAK is an integrin regulated kinase, and integrins were found to be important mediators of the effects of TNF-α on migration of keratinocytes (Scott et al. 2004). In some epithelial cells TNF-α might act through the release of other cytokines. For example, in human colonic epithelial cells the migration stimulating effect of TNF-α was found to be dependent on IL-8 release (Wilson et al. 1999). Another way whereby TNF-α can enhance migration is through the increased expression of MMPs. As mentioned earlier, levels of MMP9 were shown to be elevated in keratinocytes and mammary epithelial cells treated with TNF-α (Montesano et al. 2005; Scott et al. 2004). Interestingly, similar to interleukins, in some cells (e.g. mammary, intestinal and tubular epithelial cells) TNF-α can transactivate members of the EGF receptor family (Chen et al. 2004; Hilliard et al. 2011; Kakiashvili et al. 2011). Finally, the pro-inflammatory transcription factor NFκB, that is also implicated in the effects of ILs, was shown to be involved in mediating migration-enhancing effects of TNF-α too. Activation of NFκB acts through the induction of the EMT-related transcription factor Snail, a major inhibitor of expression of numerous epithelial proteins, including junction proteins (Wu and Zhou 2010). This pathway seems to be especially important in promoting cancer cell migration. Taken together, TNF-α has been shown to affect migration through a large number of pathways and molecular mechanisms. Whether these are all active in the same cells, or are activated in a cell-type dependent manner remains to be established.

5 Overview of In Vitro Methods Used to Study Epithelial Wound Healing

In vivo wound healing is a complex process, involving many cell types and soluble and insoluble factors. This complexity called for the use of simpler systems that enable the exploration of cellular mechanisms and molecular pathways. Recognising this need, researchers devised a variety of in vitro methods for quantitative and qualitative evaluation of wound repair in cultured cells. While some of these assays have been developed specifically to explore wound healing and injury repair, others are fundamentally cell migration assays.

The aim of the next sections is to provide an overview and a comparison of methods used in studying wound healing. The discussion will be restricted to in vitro, two-dimensional assays. Before a detailed discussion of the newest of the techniques, the ECIS-based wound healing assay in Sect. 6, three classical approaches will also be introduced (Sect. 5).

5.1 Scratch Wound Assay

Scratch wound assays are among the simplest and most widely utilized methods for studying wound healing (Liang et al. 2007). During the most basic version of this assay, a few rows of cells within a confluent layer are removed by scraping using a fine point such as a sterile needle or pipette tip (Wang et al. 2011). A quick wash to remove debris from the wound prevents any detached cells from reattaching to the denuded area (the "wound"). The result is a linear wound within the confluent cell layer surrounded by some partially injured cells adjacent to the wound and healthy cells both beside the wound and further back. The progression of wound healing and cell migration is observed and quantified using time-lapse microscope imaging (Gough et al. 2011; Liang et al. 2007). The time-lapse images are analyzed using imaging software to obtain quantitative measures of the time required to reepithelialise the denuded area.

While the big advantage of this assay is its simplicity, there are a number of issues that can limit its conclusions. First, the manual scraping used to remove cells leaves a lot of questions regarding wound reproducibility, and creates a high potential for damage to the underlying extracellular matrix (Kam et al. 2008). It is also important to note, that depending on the wound generating methods used, the edges will contain differing amounts and degrees of cellular injury. To counter the low reproducibility of the wound shape and size Hayes et al. (2011) employed an automated scratching system consisting of multi-tipped scratching instruments for wounding many samples simultaneously and more reliably. Some researchers have used silicon tipped drill presses to produce circular wounds in much the same way as scratch wounds (physical removal/disruption of cell within a confluent layer) (Daniel et al. 1999; Kam et al. 2008). This silicon drill method allows for a more

reliable wound shape and size while also controlling the depth of the wound to minimize or eliminate damage to the extracellular matrix (Kam et al. 2008).

The limitations of the scratch wound assay are largely outweighed by the advantage offered by the simplicity and low costs of the assay, and therefore this method is widely used to study cell migration and wound healing. In addition, the imaging used to follow wound healing allows analysis of morphological changes in the cells, cytoskeleton remodelling or the alterations in protein expression both during live imaging or after fixing the samples using immunofluorescence.

5.2 Gap Closure Assay

The gap closure (cell exclusion zone) assay is a popular alternative method for studying wound healing. This method does not, in the literal sense, involve any wounding at all (Poujade et al. 2007). It is therefore notable that during this assay no injured cells are generated in the wound edge. During the gap closure assay the cells are plated on a surface, part of which is physically separated to prevent the growth of the cells. A confluent layer develops on the plate around the physically separated area. The physical barrier can be provided by a rubber stopper (Nizamutdinova et al. 2009), or by a thin polymer stencil with apertures to seed cells (Folch et al. 2000). These barriers can be easily removed after the seeded cells have formed a confluent layer. The assay starts when the barrier is removed to generate a cell free "wound". The sudden appearance of a free surface is ample stimulus to promote growth and migration of epithelial cells (Poujade et al. 2007), that migrate into the cell-free areas from the surrounding monolayer (Nizamutdinova et al. 2009; Poujade et al. 2007). Progression of the wound healing or "gap closure" can be followed using time lapse microscopy similar to the analysis of the scratch wound assay.

When analysing data obtained using the gap closure assay one should always remember that there is no actual injured area or cell damage (Poujade et al. 2007). In contrast to the scratch wounding assay, in the gap closure assay the soluble factors released from injured cells are missing. This however can become an advantage, as the conditions of the assay can be well controlled. Soluble factors to be studied can be added in the required concentrations and combinations. An additional advantage of the gap closure assay is that it overcomes two limitations of the traditional scratch wound assay: it offers consistency and reproducibility of the size and shape of the cell free area, and there is no ECM damage (Hulkower and Herber 2011; Gough et al. 2011). Time lapse microscopy allows real-time observation of migration and cell morphology changes.

Different improved versions of the gap closure assay are now also available commercially. Some companies produce various plates with easily removable barriers. A dissolving gel was also developed to be used as the barrier device, thereby eliminating the need for physical removal of a barrier. This further reduces the risk of damage to cells or the ECM, and also lends a degree of automation to the assay.

5.3 Boyden Chamber Assay

The Boyden chamber, named after its creator (Boyden 1962), is an in vitro method that was initially used for analyzing migration of white blood cells in response to chemotactic effects. It is the prototype of transmembrane migration assays, which has been now adapted for use with many cell types. Although the Boyden Chamber Assay is a migration assay, and not a wound healing assay per se, transmembrane migration assays are valuable tools to explore molecular pathways involved in cell migration and thus wound healing. Further advantage is that this is a relatively simple method that allows the analysis of chemotactic cell migration (Hulkower and Herber 2011).

In this assay the migration takes place through a porous membrane that separates two medium-containing chambers, one on top of the other (Chen 2005). The assay plate consists of a polycarbonate cell culture insert nested inside a culture plate well, with the membrane at the bottom of the insert. The chemotactic reagent of interest is placed into the lower chamber, and cells are introduced into the upper chamber (Goncharova et al. 2006). A suitable incubation time is allowed during which the cells in the top chamber migrate through the membrane towards the bottom chamber (13). Next, the upper medium together with the cells that have not migrated are removed and the membrane is washed (10). Depending on the cell type, the chemoattractant applied, and the incubation time, migrating cells can be found within the membrane, on its side facing the bottom or in the medium of the bottom well. In any case, the cells that migrated through the porous membrane can be stained and counted microscopically (13). Alternatively, the cells can be labelled with fluorescent dyes prior to placing them into the upper well, and the fluorescence of the migrated cells can be quantified on the membrane or in the lower well. While this can largely help with the detection of migrated cells, it is important to verify that the labelling itself does not affect migration.

This assay has been adapted for use with both non-adherent and adherent cell types (Hulkower and Herber 2011), including epithelial cells. For example, Chen (2005) analyzed chemotaxis in Madin-Darby Canine Kidney (MDCK) tubular epithelial cells. Importantly, the assay will show migration using incubation times that are typically shorter than the time of a cell cycle (around 4–6 h). Thus, changes in cell number due to proliferation do not need to be taken into account.

The major difference between the Boyden chamber assay and "proper" wound healing assays is the need for a chemoattractant applied in the lower chamber. On the other hand this can also be an advantage when studying the chemoattractant properties of specific injury-related soluble factors. However, the concentration gradient of the chemoattractant applied to the bottom well is unknown and cannot be controlled. Another limitation is that this is an end point assay, which does not permit real-time analysis, and the results are not quantified until the end of the experiment (Hulkower and Herber 2011). Manual counting of the cells can also be tedious and inaccurate, and quantification can be especially difficult when cells migrate in uneven distributions or are stained unevenly (Hulkower and Herber 2011). This however can be overcome by using prelabelled fluorescent cells.

Microfluidic devices represent a variation of the classical Boyden cell migration assay, which offer real time observation of the migrating cells. These devices have two wells connected by an internal channel. Cells are added to a well on one side of the channel, where they adhere to the bottom. Next, chemotactic agents are added to the opening on the other side of the channel, which induces cell migration that can be observed using a microscope. While in theory these assays are very similar to the Boyden chamber assay, and follow chemoattractant-induced migration, there are several major differences. First, there is no membrane through which cells are migrating. Second, real time observation is possible. Third, the chambers in these plates are very small, and thus they use limited amounts of reagents and few cells. Finally, the linear gradient that develops due to the diffusion of the chemoattractant within the channel shows a better resemblance to the in vivo situation.

6 The ECIS Wound Healing Assay

6.1 Description of the ECIS Wound Healing Assay

The ECIS based wound healing assay is a relatively new, real time method established to study how cells repopulate an area from which cells were eliminated using electroporation (Keese et al. 2004). During the past years the ECIS technique has been established as a valuable tool in studying a variety of cellular processes and phenomena including cell adhesion, spreading, growth, and the generation and regulation of transepithelial or transendothelial resistance (Hong et al. 2011). In addition, the wound healing assay that ECIS offers is an excellent addition to tools used in epithelial cell studies.

ECIS offers an alternative to the traditional methods of studying wound healing, with a number of advantages and solutions to some of the inherent problems that were described in Sect. 5. Furthermore, ECIS offers the only wound healing assay, that provides information not only about the repopulation of the injured area, but can also follow the reestablishment of the barrier function (see below).

The ECIS setup uses arrays of small gold electrodes placed in the bottom of wells on which the cells are grown. The instrument continuously exposes these electrodes to small, biologically inert A/C currents (using currents in the μAmp range). Changes in impedance, a measure of opposing the flow of the current, are measured (Wegener et al. 2000). The equipment uses a range of frequencies of the A/C current to probe the samples. Spreading and growth of cells on the electrode gradually limits the free current flow through the electrode resulting in a drop of capacitance and the rise in impedance (Hug 2003) (Figs. 1, 2 and 3a, b). Measured at high frequencies (typically at 32 kHz), the capacitive portions (C) of the impedance were shown to reflect the coverage of the electrode (cell confluence). In contrast, the resistive portions (R) of the impedance measured at low frequencies (400–4,000 Hz) are indicative of the resistance of the layer, which reflects a combination of transepithelial resistance (TER) and the attachment of cells to the substratum.

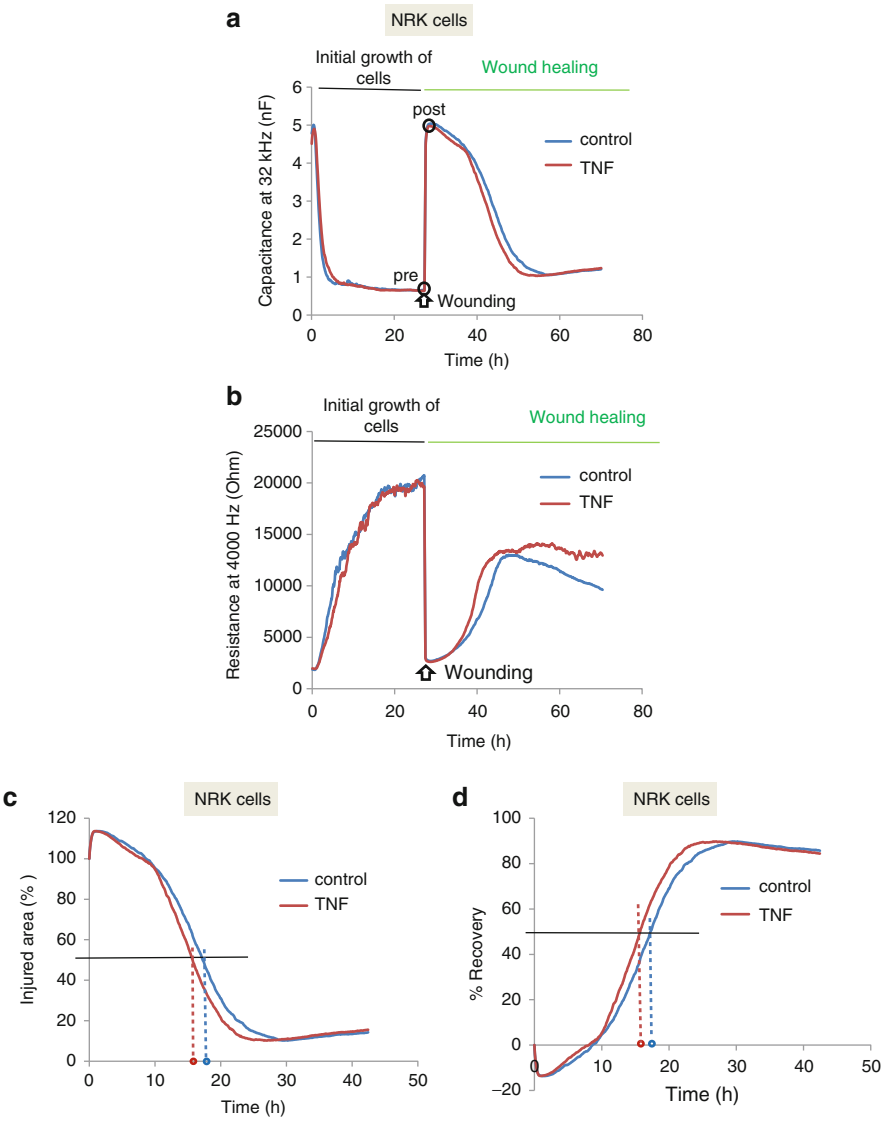
a
NRK cells
Initial growth of cells
Wound healing
Capacitance at 32 kHz (nF)
post
pre
Wounding
control
TNF
Time (h)
b
Initial growth of cells
Wound healing
Resistance at 4000 Hz (Ohm)
Wounding
control
TNF
Time (h)
c
NRK cells
Injured area (%)
control
TNF
Time (h)
d
NRK cells
% Recovery
control
TNF
Time (h)

During the wound healing assay, cells are grown to confluence on the electrode, then are exposed to an elevated current pulse (in the milliamp range). When applied for a few milliseconds, this current causes reversible electroporation of the cells. However, longer exposure (few seconds) of the cells to such currents causes irreversible damage to the membrane that results in cell death (Keese et al. 2004). Importantly, the surrounding cells remain intact, and cells from this intact monolayer can migrate to cover the damaged area.

As ECIS uses the measurement electrode to apply the wounding current, intactness of the electrode after the elevated pulse is applied is key for the reproducibility of the measurement. Keese et al. (2004) discussed this issue and showed that using a high frequency, low amperage A/C current to induce cell death ensures the high reproducibility of the wound. By choosing the right parameters, the wounded area covered the full electrode surface without causing damage to the electrode.

An interesting observation came from examining the wounded area on the electrodes by microscope (Keese et al. 2004). Following the wounding, epithelial cells remained attached to the electrode, even though their morphology was visibly altered (Fig. 4), and the capacitance and resistance values returned to levels typical for the uncovered electrodes. Cell death was verified by staining with vital stain (Keese et al. 2004). The intact layer migrated under the dead cells, displacing them and eventually restoring the monolayer.

The major advantages of the ECIS wound healing assay include its reproducibility, the ease of quantification, the fact that the process can be followed in real

Fig. 1 Wound healing in NRK52E cells. (**a** and **b**). NRK52E cells were plated in culture medium (DMEM supplemented with 10 % Fetal Calf Serum and Penicillin/Streptomycin) on an 8W1E array at 2×10^5 cells/well in 400 µl. The cells were grown to confluence, as indicated by the drop in the Capacitance measured at 32 kHz (**a**), and the rise in the Resistance at 4,000 Hz (**b**) ("Initial growth of cells"). Prior to the generation of the wound the measurement was paused, and the medium was replaced by fresh medium without (*blue curve*) or with 10 ng/ml TNF-α (*red curve*). The measurement was restarted and a wound was generated by electroporation (1 mAmp, 32 kHz, 20 s) (*arrow*). Recovery of Capacitance and Resistance was followed ("wound healing"). The two *black circles* in **a** indicate the last pre-wound C value (pre) and the first post-wound C value (post). The curves show the average of 4 measurements calculated using the ECIS software. (**c**). *Calculation of time needed for 50 % drop in injury size.* The difference in the Capacitance at the last time point before wounding and the first time point after wounding (*black circles* in **a**) was taken as the total injury (100 %), and the Capacitance at each time point was expressed as the % of this value. This is plotted against the time of recovery, where the time at wounding was taken as 0 h. The *black line* indicates 50 % injury size, and the *blue* and *red dashed lines* and *circles* show the times at the 50 % injury size for the control and TNF-α-treated samples, respectively. The 50 % injury size is achieved faster in the TNF-α-treated samples. (**d**). *Calculation of the 50 % recovery time.* The difference in the Capacitance between the last time point before wounding and the first time point after wounding (*black circles* on **a**) was taken as the total recovery (100 %). The highest capacitance value was taken as 0 % recovery, and the recovery % was calculated at each time point. The X axis shows the time of recovery, where the time at wounding was taken as 0 h. The *black line* indicates 50 % wound size, and the *blue* and *red dashed lines* and *circles* show the times at the 50 % wound size for the control and TNF-α-treated samples, respectively. The 50 % recovery is achieved faster in the TNF-α-treated samples

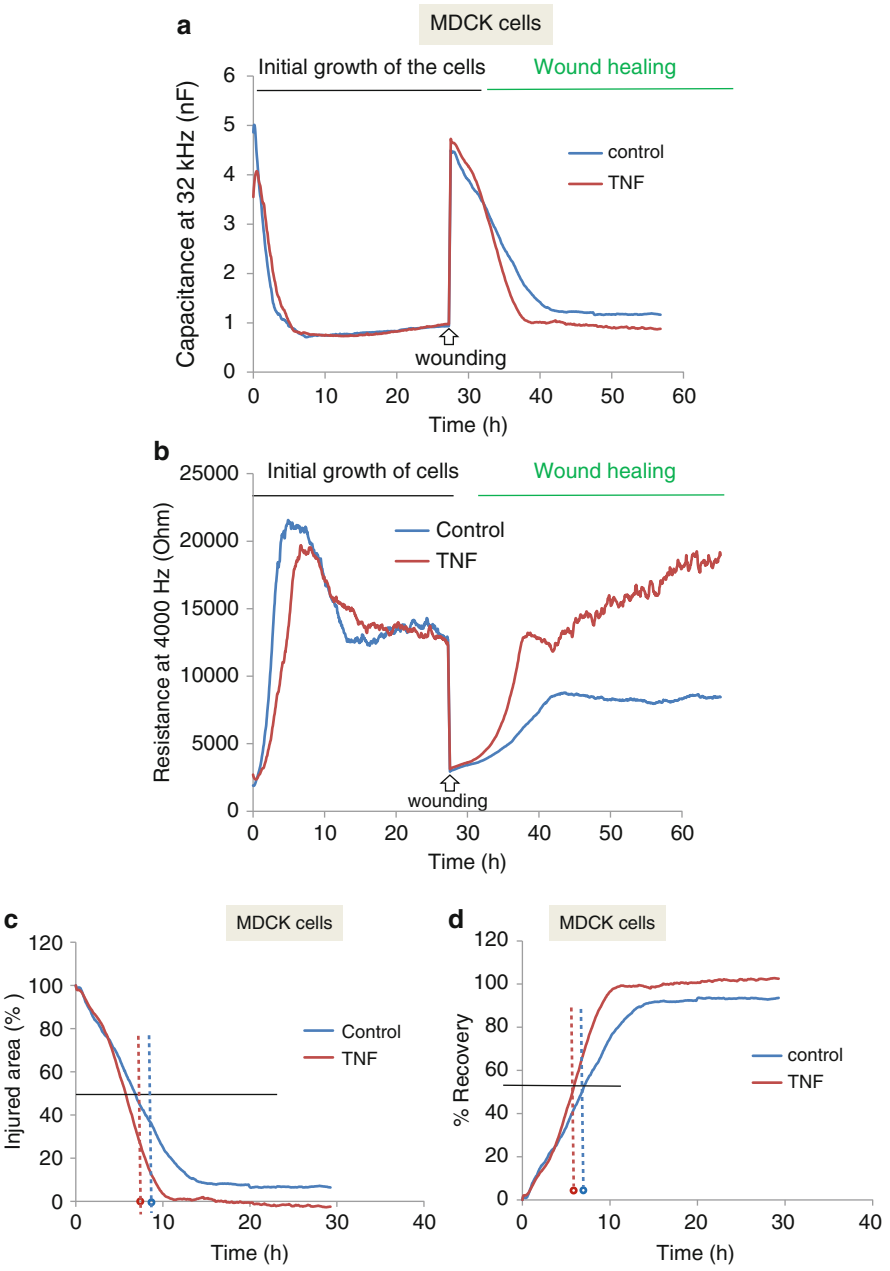

Fig. 2 Wound healing in MDCK cells. (**a** and **b**). MDCK cells were seeded, grown to confluence and wounded as in Fig. 1. Recovery of Capacitance (**a**) and Resistance (**b**) was followed in the absence or presence of 10 ng/ml TNF-α. The data shown are averages of 3 (control) or 4 (TNF-α-treated) wells. (**c**) *and* (**d**). The changes in injury size and the recovery % were calculated from the data in **a** as described in Fig. 1

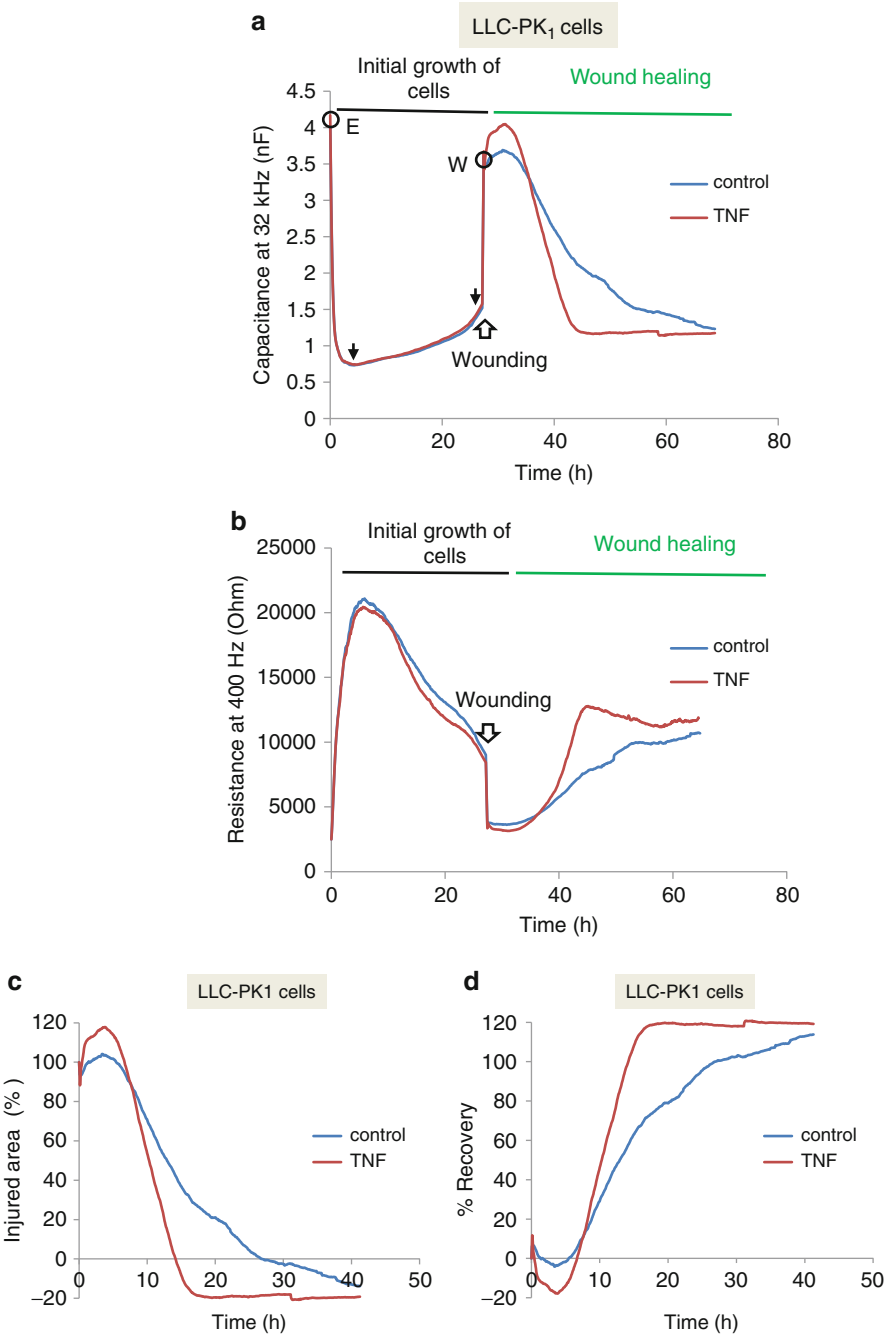

Fig. 3 Wound healing in LLC-PK1 cells. (**a** and **b**). LLC-PK1 cells were seeded, grown to confluence and wounded as in Fig. 1. Recovery of Capacitance (**a**) and Resistance (**b**) was followed in the absence or presence of 10 ng/ml TNF-α. The data shown are averages of 4 wells. In (**a**) the *black arrows* point to a time period when C was rising. The *black circles* indicate the C value of the empty electrode E) and the C value immediately after the wounding (W). (**c**) *and* (**d**). The changes in injury size and the recovery % were calculated from the data in **a** as described in Fig. 1

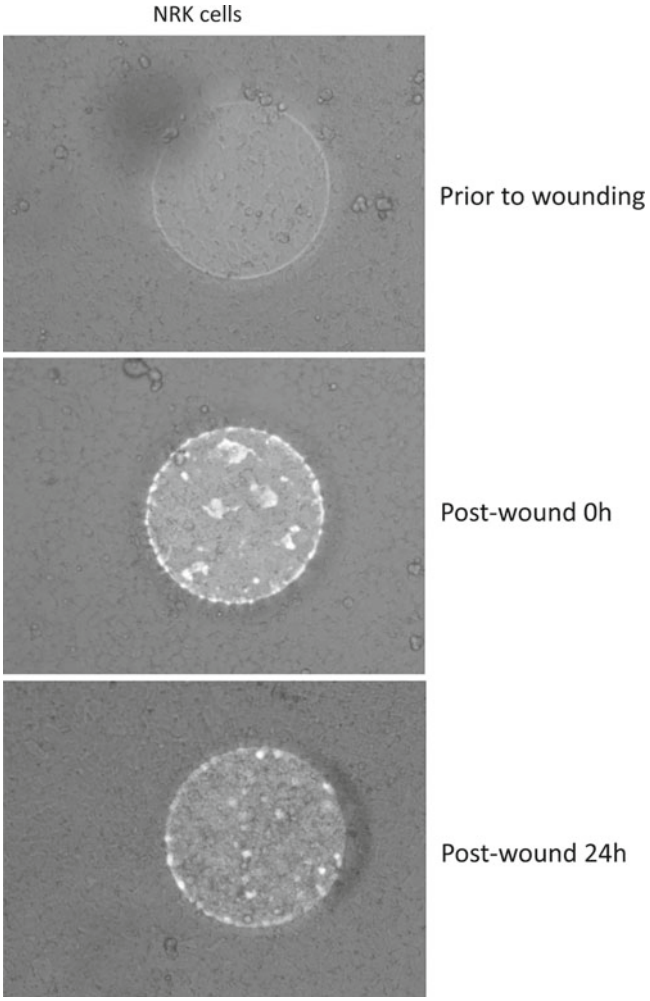

Fig. 4 Pictures showing NRK52E cells on the electrode. NRK cells on the electrode were visualized using a Nikon ECLIPSE TS100 microscope (20× magnification). Pictures were taken after the cells became confluent and prior to wounding (*top picture*), immediately after wounding (*middle picture*) and 24 h after wounding

time and the absence of damage to the ECM by the wounding. High reproducibility results from the well controlled wounding parameters and the given size and shape of the wounded area. When using the same wounding parameters, the system achieves a circular wound covering the full electrode that is the same every time the current is applied. The progression of the wound healing process can be quantitatively followed in real time using the resistance and capacitance changes, which makes quantification easy and automated. In addition, the process of recovery can also be visualized by microscopy (Lee et al. 2006), although this can be complicated

by the fact that the dead cells lift up from the electrode but are not removed. In fact, one of the major considerations regarding the ECIS assay involves this fact. The presence of dead cells that do not attach well to the electrode but have not yet been removed is a clear difference from the situation during the scratch wound assay. While there is no evidence that this hinders wound healing, some investigators include additional washing steps to remove dead cells from the electrode (e.g. Schiller et al. 2011). These issues will be further discussed in Sect. 6.5.

6.2 Overview of the Research on Epithelial Wound Healing Done Using ECIS

As discussed above, the ECIS wound healing assay allows exploration of cell migration during wound healing and the functional restoration of the layer. The method is emerging as a very useful tool to study epithelial and endothelial cell migration and wound healing. Accordingly, the number of published studies employing this assay is rapidly increasing.

The underlying mechanisms of epithelial migration show remarkable similarities irrespective of the organ of origin of the epithelium studied. The molecular information gathered from research using specific cell lines therefore in most cases can be generalized. However, while the general theme is similar, epithelial wound healing is important in many diseases, and unique factors in the case of specific organs and diseases are now starting to emerge. The ECIS method is adding to our knowledge of both the general mechanisms and the unique organ-specific phenomena. In the following paragraphs an overview of how ECIS is applied to address epithelial wound-healing related questions will be given. The studies will be organized according to the organs of origin of the cells studied. A brief overview of the relevance of wound healing for the physiology and pathology of the particular organ will also be provided.

6.2.1 Renal Epithelium

The high energy demand due to the transporting functions makes the tubular epithelium especially susceptible to injury caused by disruption of oxygen supply. In addition, the tubules can also be exposed to a variety of toxic compounds, including drugs and heavy metals. These insults can lead to cell death and injury of the layer. As in the case of other epithelia, repair and restoration of function requires removal of the dead cells and replacement of injured cells. The source of the cells that can replace damaged tubular epithelium has been the topic of numerous studies. While mesenchymal stem cells were shown to improve the recovery of tubular cells after injury (Bussolati et al. 2009), ample evidence also shows that the main source for replacement of injured cells in the tubule are the resident non-injured tubular epithelial cells (Duffield and Bonventre 2005; Guo and Cantley 2011; Humphreys et al.

2011). In fact, injury causes rapid dedifferentiation of the remaining cells (Bonventre 2003), which enhances the recovery of the intact layer.

A number of well established epithelial cell lines are used to study the properties of tubular epithelia. The first description of the ECIS wound healing assay by Keese et al. used the kidney cell lines BS-C-1, Normal Rat kidney (NRK) and MDCK (Keese et al. 2004). They showed that all these cell lines grew well on the gold electrode and readily recovered the intact monolayer following the application of an elevated current pulse. The exact parameters of the wound-healing curves however varied depending on the type of cells studied. NRK cells for example recovered slower than BS-C-1 cells.

As mentioned above, the data obtained using NRK cells also revealed the two steps of wound healing, where migrating cells rapidly repopulate the area of injury, but take a longer time to re-establish the resistance (Keese et al. 2004, also see Figs. 1, 2 and 3). The ECIS wound healing assay is unique in that it is the only one that provides information regarding the functional recovery of the monolayer. The changes in the resistance reflect the process of reestablishment of the junctions and the barrier. Early studies using the ECIS wound healing assay already provided interesting findings about the recovery of the barrier functions. The rebuilding of the intact monolayer proved to be a two-step process (Keese et al. 2004 and Figs. 1, 2 and 3). First, the migrating cells cover the full electrode, and restore the confluence of the layer. This newly formed confluent layer however still exerts low resistance. Restoration of the final high resistance (the barrier) is a slower process, that probably requires further rearrangement (maturation) of the junctions (Keese et al. 2004).

6.2.2 Respiratory Epithelium

The respiratory epithelium is highly exposed to allergens, toxic chemicals and inflammatory agents. Immune and allergic responses often cause damage to the respiratory epithelium, and repeated injury-repair cycles are important features of both acute and chronic lung diseases, such as asthma, chronic obstructive pulmonary disease and pulmonary fibrosis (Beers and Morrisey 2011; Davies 2009). While repair of the respiratory epithelium in vivo is thought to involve progenitor cells (Rock and Hogan 2011), similar to other epithelia, the respiratory epithelium itself also has the capacity for injury repair (Crosby and Waters). The importance of the injury repair mechanism in the pathogenesis of diseases is now well recognised. Thus, epithelial injury and remodelling has emerged as an important contributor to loss of functional respiratory surface and the pathogenesis of diseases.

Heijink et al. (2011) tested and characterized bronchial epithelial cells lines in the ECIS system, including the established and widely used cell lines 16HBE14o-, BEAS-2B, NCI-H292 and A549. They also tested primary bronchial cells. Comparison of these cells revealed interesting differences in their growth on the electrodes as well as the TER they develop. For example, the 16HBE14o- cell line formed a monolayer slower, however reached a higher TER, which correlated well with high expression of junctional adhesion molecules in this cell type. The

16HBE14o- cells line was also found to be superior in the ECIS wound healing assay, and is therefore a good choice for further studies.

The ECIS system allows the assessment of how various chemical agents affect barrier functions and migration. Cigarette smoke extracts for example were shown to impair barrier functions of bronchial epithelial cells. Interestingly this effect was mediated by the EGFR. In addition, the smoke extract also delayed reconstitution of intercellular junctions in the ECIS wound healing assay (Heijink et al. 2010).

The ECIS wound healing assay can be also used to study the specific molecules involved in wound healing, and can contribute to the discovery of new mechanisms. Schiller et al. (2011) investigated wound healing and migration of normal human bronchial epithelial (NHBE) cells and a human airway epithelial cell line of serous gland origin (Calu-3). First, they verified that the wound repair is indeed dependent on an intact cytoskeleton, as the actin polymerization inhibiting drug cytochalasin D blocked closure of the wound. This finding is in line with the notion that major cytoskeleton rearrangement, lamellipodia formation and migration are involved in wound healing. Further, the authors also verified that both NHBE and Calu-3 cells repopulated the denuded area by sheet migration. Next, they studied the role of the cystic fibrosis transmembrane conductance regulator (CFTR) protein on wound repair. Interestingly, when they downregulated the CFTR protein using a short hairpin (sh) RNA, bronchial epithelial cells migrated slower. A similar effect was achieved with an inhibitor of the CFTR anion transport. The inhibitor also reduced lamellipodia formation, suggesting that anion transport through CFTR is necessary for migration and wound repair in respiratory epithelial cells.

6.2.3 Intestinal Epithelium

The epithelium is a key component of the intestinal mucosal barrier. Its cells have a high turnover and the layer is constantly renewing itself. Intestinal epithelial cells (IECs) are also continuously exposed to various harmful substances present in the lumen of the gut, including bacteria, dietary factors, digestive enzymes, toxic agents and drugs. The exposure to these results in regular epithelial injury even under physiological conditions, but this is further enhanced during conditions such as inflammatory bowel disease. Thus, similar to other epithelia, integrity of the intestinal epithelium relies on efficient repair mechanisms to rapidly re-establish function following injury. The first stage of the recovery process involves migration of the epithelial cells to repopulate the denuded area and re-establish the barrier (Lotz et al. 2000). This process, which is independent of proliferation, starts within minutes of injury and has been referred to as epithelial restitution (Iizuka and Konno 2011; Sturm and Dignass 2008). It is followed by the slower processes of proliferation and differentiation. Although the intestinal epithelium, similar to other epithelia, can repair injuries without external factors, in vivo this complex process is under the influence of a large number of regulators including growth factors, inflammatory cytokines, and even dietary factors and probiotic gut bacteria. Normally, these factors are present in combination and modulate the

repair process. Importantly, our understanding of the factors and the underlying signalling pathways that regulate cell replacement and wound healing in the intestine is still incomplete. Charrier et al. (2005) used the ECIS wound healing assay to investigate the role of the ADAM family enzymes in migration and wound healing of colonic epithelial cells. They showed that in Caco2-BBE cells, a colon cell line, overexpression of ADAM-15 causes delayed wound healing. The authors suggest that this effect could be attributed to the inhibition of cell-cell interactions or the modulation of integrin-extracellular matrix interaction. The same group also studied the effects of certain inflammatory molecules on wound healing. They explored how interfering with CD98, a surface glycoprotein involved in integrin-mediated events, affects wound healing of Caco2-BBE cells (Kucharzik et al. 2005). CD98 is upregulated during intestinal inflammation, and might have a role in maintaining the inflammatory reaction. Interestingly, inhibiting CD98 in a normal Caco2-BBE monolayer had no effect on epithelial migration, in line with the fact that normal intestinal epithelium does not express CD98 in abundance. In contrast, when cells were pretreated with dextran sodium sulfate, an agent that induces colon inflammation, the anti-CD98 antibody exerted a significant inhibitory effect on wound healing.

6.2.4 Eye

Studying wound healing in epithelial cells of the eye has significantly contributed to our knowledge of the general processes of epithelial migration. Epithelial layers cover the cornea and lens, the main refractive elements of the visual system. Highly specialized epithelia can also be found is the retina.

The cornea is organized into three layers: epithelial cells, stromal cells and endothelial cells. Similar to all epithelial barriers, the corneal epithelium encounters harmful insults, which can result in loss of barrier function and injury. Proper healing of corneal wounds is required not only for the restoration of the barrier, but also to avoid scar formation. Scars would reduce the clarity of the layer and could interfere with vision. Not surprisingly, the corneal epithelium responds rapidly to injury, and similar to other epithelial layers the barrier is restored by sheet migration of the cells (Lu et al. 2001; Yu et al. 2011; Zelenka and Arpitha 2008).

Similar to the corneal epithelium, the epithelium covering the lens protects the deeper structures, and the intact epithelium is vital for the clarity of vision. Located in the anterior portion of the lens between the lens capsule and the lens fibers, this simple cuboidal epithelium also regulates homeostasis of the organ. In addition, the lens epithelium exhibits a very interesting renewal process, as these cells serve as progenitors for new lens fibers. Cells located at the equator encounter an increasing gradient of proliferative growth factors the source of which is the ciliary and vitreous bodies. These growth factors cause the epithelial cells to divide and migrate away. However, as they migrate, the concentration of growth factors diminishes, and the process of division and migration is replaced by differentiation (Zelenka and Arpitha 2008).

The third important and heavily investigated type of epithelium in the eye is the retinal pigment epithelium (RPE). RPE in adults consists of quiescent and highly differentiated cells. These cells are the topic of intense research, because a number of human degenerative diseases exist, including proliferative vitreoretinopathy, proliferative diabetic retinopathy, and age-related macular degeneration, in which cells of the RPE re-enter the cell cycle, and become proliferative and migratory. The pathologic processes during these diseases perfectly demonstrate how the overstimulation of migration or the inadequate stopping of the process can cause serious damage. Cell reactivation is attributed to exposure to growth factors, cytokines, and neurotransmitters, which normally do not reach the retina, but show elevated levels under pathological conditions.

Primary epithelial cells as well as established cell lines from the eye can be grown on the ECIS gold electrodes, and are used to study regulation of migration, its coordination with proliferation and the effect of potential protective factors. Tsapara et al. showed that in RPE cells TGFβ1-stimulated migration required the RhoA activator exchange factor GEF-H1 (Tsapara et al. 2010). Chan et al. searched for protective agents that could slow down age-related macular degeneration (AMD) by studying migration of Adult Human Retinal Pigment Epithelial (ARPE19) cells (Chan et al. 2009). Using the ECIS wound healing assay they showed that the growth factor PDGF-BB enhanced wound healing in these cells. Lycopene, a potent antioxidant member of the carotenoid family, found in tomatoes and other fruits with red color, was suggested to have immunomodulatory and anticancer activities and to protect against AMD. Chan et al. (2009) showed that in the presence of lycopene the PDGF-induced stimulatory effect was prevented in ARPE19 cells. Further, the authors also showed that lycopene inhibited phosphorylation of the PDGF receptor, and prevented PDGF-induced activation of signalling molecules including phosphattidyl-inositol-3-kinase (PI3K), Akt, ERK and p38. Importantly, lycopene did not have cytotoxic effects in RPE cells. This study therefore raises the possibility that lycopene might have beneficial effects in retina diseases.

6.2.5 Cancer Cell Migration

Inappropriate activation or insufficient deactivation of the migratory machinery is thought to be causing the aggressive phenotype of invasive carcinomas and metastasis formation. This important aspect of epithelial migration has also been studied using ECIS. In fact, a number of established and widely used cell lines that are used in the ECIS wound healing assay and were discussed above, are derived from various carcinomas (e.g. Caco-2, A549).

Epithelial protein lost in neoplasm (EPLIN) is a protein that regulates actin dynamics (Maul et al. 2003). Importantly, this protein is downregulated in a number of human cancers and low levels of EPLIN are associated with poor prognosis (Jiang et al. 2008; Maul and Chang 1999). In normal cells EPLIN is localized along the stress fibers and focal adhesions and in non-transformed cells it inhibits anchorage-independent growth (Song et al. 2002). Using the ECIS migration assay

Jiang et al. (2008) showed that this protein is a powerful regulator of cell migration. Over-expression of EPLIN in MDA-MB231 breast cancer cells significantly reduced motility and rendered the cells less invasive, suggesting that low EPLIN expression might correlate with the metastatic potential of the cells.

Another example where ECIS was used to uncover important mechanisms is the effect of leptin on cancer cell migration. The association between obesity and various malignancies is well established, but the reason for enhanced cancer risk in obese people is not clear. To search for a potential mechanism, Saxena and coworkers studied the effects of leptin, a hormone involved in body weight control, on the behaviour of hepatocellular carcinomas (Saxena et al. 2007). Addition of leptin to HepG2 and Hih7 liver cells not only enhanced proliferation, but also stimulated invasion in a Matrigel assay and increased cell migration in an ECIS wound healing assay. Cells treated with leptin showed a significantly faster recovery from a wounding. This stimulatory effect was blocked by inhibitors of the JAK/STAT signalling pathway and was reduced by ERK and PI3 kinase inhibitors.

6.3 Wound Healing in Kidney Tubular Cells as Measured Using ECIS: Practical Aspects

The ECIS wound healing assay requires the use of specialized electrode arrays (8W1E or 96W1E). The "W1E" series of electrodes consist of a solitary 250 μm diameter gold electrode in each well (8 wells in 8W1E and 96 in 96W1E), which serves both for measurement and for the application of the elevated voltage pulse that generates the wound.

In order to examine cell migration and the wound healing mechanisms in the kidney tubules, we performed wound healing assays using three tubular cell lines. We used NRK52E cells, (Fig. 1), MDCK distal tubule cells (Fig. 2), and LLC-PK_1 porcine proximal tubule cells (Fig. 3). We used the 8W1E arrays containing 8 wells with 1 electrode in each well. Prior to seeding the cells, ECIS gold electrodes require a brief treatment with a 10 mM L-cysteine solution, which promotes electrode stabilization (Wegener et al. 2000). It is also advisable to incubate the wells for a few minutes with the serum-containing medium used for cell growth before the addition of the cells. This will allow serum proteins to coat the electrode, further enhancing cell adhesion. Many cell lines do not require any further preparation of the electrode. However, if necessary, the electrodes can also be coated with a substrate such as fibronectin, gelatin or collagen to promote cell adhesion and spreading. We found that for NRK and MDCK cells a short (10 min) preincubation of the electrode with the serum containing medium is sufficient for good cell attachment and growth and no additional coating is necessary. LLC-PK_1 cells also attach and spread well on the electrode, however once they become confluent, their attachment becomes unstable. Thus, we coated the electrodes with fibronectin prior to plating LLC-PK_1 cells. After preparing the electrodes, we plated identical number of cells in the wells (typically in the range of 2×10^5/wells in 400 μl) and allowed them to grow to confluence.

As shown on Figs. 1, 2 and 3, the growth of the cells causes a drop in the capacitance values as measured at 32 kHz (Figs. 1a, 2a and 3a), and the increase in resistance, as measured at 4,000 Hz (Figs. 1b, 2b and 3b). In the first approx. 3 h cells attach and spread on the electrode (Wegener et al. 2000) and then they grow on the electrodes to generate a confluent layer. Cell confluence (i.e. complete electrode coverage) is reached when the capacitance drops to its minimum (typically around or below 1 nF on the 8W1E electrodes). During the initial growth of the cells, the resistance is also rising, but interestingly, in the case of all tubular cells studied, the maximum resistance is reached several hours after confluence is achieved, as the junctions mature and become tighter after confluence is reached. Another interesting phenomenon can be observed both in MDCK and LLC-PK_1 cells: typically the resistance curve reaches a maximum in about 10–15 h, but after this it decreases before stabilizing at a lower level around 20–24 h after seeding (Figs. 2b and 3b).

Once all wells have reached confluence, and the resistance stabilizes, a baseline is obtained by measuring both the capacitance and resistance for an additional few hours. Next, the wound is generated by exposing the cells on the electrode to an elevated current pulse for several seconds (Keese et al. 2004). In our experiments, a pulse of 1 mAmp at 32 kHz was applied for 20 s. This pulse induces permeabilization of the cell membrane, and the damage kills the cells. The loss of intact cells on the electrode is demonstrated by the immediate elevation in the capacitance values and drop in the resistance (Figs. 1, 2 and 3a, b) (Keese et al. 2004). Settings of the wounding pulse should be chosen so that the C and R parameters return to those of the empty, uncovered electrode following the wounding. Indeed, the capacitance curves verify that for all three cell types used, the wounding resulted in a rise in capacitance close to the values of the empty electrodes (Figs. 1, 2 and 3a, b).

Figure 4 shows microscopic pictures of the NRK cells on the electrodes. The picture taken before the wounding verifies that the cells have formed a homogenous monolayer both on and around the electrode (top picture). Following the wounding, the cells on the electrodes look damaged, the borders between them are no longer visible, consistent with the severe electroporation of the membranes. Although the cells from some areas seem to be lost, in most of the electrode the dead cells are still visible on the electrode (see also Sect. 6.5). Importantly, the layer around the electrode maintains its healthy epithelial morphology, and shows no effects of the wounding current. Full recovery for the NRK cells takes about 28 h. Interestingly, the curves suggest that the recovery process in the experiment presented was not complete even after 40 h (the capacitance remained above and the resistance remained below the original prewound value, Fig. 1a, b) (see Sect. 6.5). In agreement with the C values, the picture taken 24 h after the wounding shows that there are still a few small cell-free areas. These could explain why the C did not return fully to its prewounding values (Figs. 1a and 4). In addition, some cell debris is still visible on the electrodes, but beneath these newly migrating cells have efficiently repopulated the electrode.

The recovery process, indicated by the restoration of capacitance and resistance values, shows cell type-dependent properties. To facilitate comparisons between different cell types and treatments, we used the data obtained from typical wounding

experiments for further analysis. First, we expressed the process of C recovery (i.e. electrode repopulation) as a % of the total over time, starting from 0 % recovery (Figs. 1, 2 and 3c). The full wounding-induced drop in C (i.e. the loss of cells from the surface during wounding) was taken as a 100 % and the time of the wounding was taken as the 0 time point. The % drop in C (i.e. decrease in the injured area) was graphed as a function of the time starting from the wounding. Such representation has the advantage that it is independent of the total values, making comparison between cell types and measurements easier. From such graphs it is easy to determine the time of full recovery, or the time of 50 % recovery. These values can be further combined to provide statistical analyzis. Another way of representing the data is shown on Figs. 1, 2 and 3d. Using data from the graphs sown in Figs. 1. 2 and 3c we expressed the wound healing as % recovery. The total capacitance drop during wounding was also taken as 100 %, but the capacitance value after the wounding was taken as 0 % recovery, and each subsequent point was expressed as the % of the total C change. The data shown on the two graphs are the same, and either of these analysis methods can be chosen for generating comparisons between experiments.

Expression of the data as a % of the full recovery allowed easier comparisons between the data from the three cells. Such comparison revealed that wound healing is fastest in MDCK cells, which required about 8 h to achieve 50 % recovery (Fig. 2c, d). In LLC-PK_1 cells the 50 % recovery time was obtained around 14 h (Fig. 3c, d), while NRK cells required around 19 h to achieve 50 % recovery (Fig. 1c, d).

6.4 Effect of TNF-α on Epithelial Wound Healing as Measured Using ECIS

We wished to investigate the effects of the inflammatory cytokine TNF-α on tubular cells. TNF-α is known to alter barrier properties and enhance migration of some epithelial cells. Its effects on tubular cell migration however have not been studied previously. In our earlier works we had described a signalling pathway underlying TNF-α-induced cytoskeleton remodelling and RhoA activation in tubular cells (Kakiashvili et al. 2009, 2011). We showed that TNF-α acted on RhoA through the EGFR. TNF-α-induced transactivation of the EGFR activated the MAP kinase ERK, that phosphorylated and activated the RhoA exchange factor GEF-H1. GEF-H1 activation induced RhoA activation. We also showed that crosstalk between the TNF and EGF pathways enhanced proliferation of tubular cells. These observations raised the possibility that TNF-α could promote cell migration and wound healing in the tubular cells, which might be mediated by the EGFR. To start exploring this possibility, we used the ECIS wound healing assay. We studied the effects of TNF-α on all three renal tubular cells described above. Prior to wounding fresh medium was added to the cells with or without 10 ng/ml TNF-α. As shown on Figs. 1, 2 and 3, TNF-α enhanced the recovery of capacitance and resistance in all 3 cell lines studied, shifting the half recovery time to the left. The three cell lines however, did not show similar sensitivity to TNF-α, as the stimulation in NRK and MDCK cells

proved to be significantly smaller than in LLC-PK_1 cells. Interestingly, a similar enhanced wound healing was not observed when the cells were treated with IL-1β (not shown).

Thus, using the ECIS wound healing assay, we showed that TNF-α enhances wound healing in several tubular epithelial cells. Such ECIS wound healing assays will allow us to further test the signalling pathways responsible for the effects of TNF-α on wound healing in tubular cells.

6.5 Special Considerations and Troubleshooting

We found the ECIS wound healing assay to be very reproducible in all cell lines we studied. There are, however, some special considerations and troubleshooting that will be discussed in this final section.

1. The maturity of the monolayer prior to wounding is a major determinant of how fast wound healing will proceed. In order to achieve comparable conditions between different experiments the seeding and initial growth should be standardized (e.g. number of cells plated, coating of the electrode, time for growth). Importantly, these conditions might be different for each cell lines used. The wound healing data obtained using LLC-PK_1 cells reveals some challenges regarding the pre-wound growth of the cells (Fig. 3). The pre-wounding C curve shows a steady rise after the minimum value has been reached (see the time period between the two black arrows in Fig. 3a). The reason for this phenomenon is not entirely clear, but could be due to the fact that these cells, when confluent, secrete fluid beneath themselves (dome formation), which can result in a gradual lifting of the monolayer from the electrodes in certain regions. After wound healing however the minimum capacitance reached is closer to the initial minimum, around the first black arrow. As the 100 % recovery time was calculated using the C values immediately before and after wounding, the recovery seems to proceed to a value that exceeds 100 % (Fig 3c, d).
2. Closer inspection of the curves in the experiments shown in Figs. 1, 2 and 3 reveals that in the first hours after wounding (i.e. following the large drop in C caused by the wounding) a further slow decrease occurs in C. This phenomenon is most prominent in the case of LLC-PK_1 cells, but can also be observed in NRK cells. The reason for such an initial drop is not clear. One possibility is that cell death and lifting from the electrode is not immediate in all of the cells, and some damaged cells are still attaching to parts of the electrodes. In the next hours these cells might continue to lift up. This possibility is supported by the fact that on the curves shown, the first post-wound values of C are somewhat below the earliest C values, which represent the empty electrode, especially for the control curve (see Fig. 3a, points indicated by the black circles: E:empty electrode, W: first post-wound value). To troubleshoot this issue, the wounding pulse should be increased in an attempt to promote faster cell death and lifting of cells from the

electrode. Thus, wounding pulses applied for longer times, or higher voltages should be tried. However, this might not solve the problem completely, as the slower lifting from the electrode might be an intrinsic property of certain cells. Another possible way to help the initial lifting of cells is to wash the electrode after wounding. However, vigorous washing may damage the intact cells or cause mechanical stress to them, and therefore this step needs careful standardization.

Although the small drop in C after wounding probably does not pose any serious problem, achieving maximal wounding enhances the reproducibility of the experiments. Further, the issue of cells remaining on the electrode should be considered when the effects of various cytokines and other agents are studied. The interpretation of the data should take into account the possibility that migration-stimulating effects could also arise from enhanced removal of dead cells. If such an effect exists, it should result in a faster initial post-wound C drop in the stimulated cells, and should be possible to test using the C data.

3. Another interesting phenomenon is that resistance does not fully recover to its pre-wounding values in any of the cells studied during the first 35 h of the recovery (Figs. 1, 2 and 3). This might be simply due to a very slow wound healing, where the wound healing process during the investigated time frame is unable to completely restore the function of the layer. Thus, it will be of great interest to study factors that enhance the functional recovery. In this respect it is interesting, that the TNF-α-treated layers show R values that are closer to the pre-wound values (Figs. 1, 2 and 3).
4. The R values reflect not only the resistance of the paracellular pathway, but also the resistance that arises between the cells and their substratum. ECIS however offers a mathematical modelling to distinguish between these components (Giaever and Keese 1991).
5. Migration and wound healing requires the presence of full growth medium, including serum. Without these additions, in most cells wound healing cannot proceed. This fact has to be considered when data are interpreted and compared to assays done in the absence of serum.

7 Concluding Remarks

Epithelial wound healing is a vital process that has relevance to a number of important diseases. In the past years huge progress was achieved in exploring the underlying mechanisms and molecular pathways. Despite this fact, there are still a large number of outstanding questions that need to be answered to achieve full understanding of the processes. The ECIS wound healing assay offers a highly reproducible, real-time method that can provide information not only about the restoration of the continuity of the layers but also about regeneration of function. This assay has already provided some interesting insights into how epithelial monolayers repair themselves and in the coming years will certainly prove to be an invaluable tool in research on wound healing.

Acknowledgments The authors would like to thank Drs Andras Kapus and Caterina Di Ciano-Oliveira for their helpful comments on the manuscript. The experiments presented here were performed using funding from the Kidney Foundation of Canada, the KRESCENT program and CIHR (MOP-97774). K.S is a recipient of an Ontario Early Researcher Award.

References

Abercrombie M, Heaysman JE (1954) Observations on the social behaviour of cells in tissue culture. II. Monolayering of fibroblasts. Exp Cell Res 6:293–306

Ahdieh M, Vandenbos T, Youakim A (2001) Lung epithelial barrier function and wound healing are decreased by IL-4 and IL-13 and enhanced by IFN-gamma. Am J Physiol Cell Physiol 281:C2029–C2038

Akdis M, Burgler S, Crameri R, Eiwegger T, Fujita H, Gomez E, Klunker S, Meyer N, O'Mahony L, Palomares O, Rhyner C, Quaked N, Schaffartzik A, Van De Veen W, Zeller S, Zimmermann M, Akdis CA (2011) Interleukins, from 1 to 37, and interferon-gamma: receptors, functions, and roles in diseases. J Allergy Clin Immunol 127(701–721):e701–e770

Assemat E, Bazellieres E, Pallesi-Pocachard E, Le Bivic A, Massey-Harroche D (2008) Polarity complex proteins. Biochim Biophys Acta 1778:614–630

Baur PS Jr, Parks DH, Hudson JD (1984) Epithelial mediated wound contraction in experimental wounds–the purse-string effect. J Trauma 24:713–720

Beers MF, Morrisey EE (2011) The three R's of lung health and disease: repair, remodeling, and regeneration. J Clin Invest 121:2065–2073

Bement WM, Forscher P, Mooseker MS (1993) A novel cytoskeletal structure involved in purse string wound closure and cell polarity maintenance. J Cell Biol 121:565–578

Bonventre JV (2003) Dedifferentiation and proliferation of surviving epithelial cells in acute renal failure. J Am Soc Nephrol 14(Suppl 1):S55–S61

Boyden S (1962) The chemotactic effect of mixtures of antibody and antigen on polymorphonuclear leucocytes. J Exp Med 115:453–466

Bussolati B, Hauser PV, Carvalhosa R, Camussi G (2009) Contribution of stem cells to kidney repair. Curr Stem Cell Res Ther 4:2–8

Chan CM, Fang JY, Lin HH, Yang CY, Hung CF (2009) Lycopene inhibits PDGF-BB-induced retinal pigment epithelial cell migration by suppression of PI3K/Akt and MAPK pathways. Biochem Biophys Res Commun 388:172–176

Charrier L, Yan Y, Driss A, Laboisse CL, Sitaraman SV, Merlin D (2005) ADAM-15 inhibits wound healing in human intestinal epithelial cell monolayers. Am J Physiol Gastrointest Liver Physiol 288:G346–G353

Chen HC (2005) Boyden chamber assay. Method Mol Biol 294:15–22

Chen P, Parks WC (2009) Role of matrix metalloproteinases in epithelial migration. J Cell Biochem 108:1233–1243

Chen WN, Woodbury RL, Kathmann LE, Opresko LK, Zangar RC, Wiley HS, Thrall BD (2004) Induced autocrine signaling through the epidermal growth factor receptor contributes to the response of mammary epithelial cells to tumor necrosis factor alpha. J Biol Chem 279:18488–18496

Citi S, Spadaro D, Schneider Y, Stutz J, Pulimeno P (2011) Regulation of small GTPases at epithelial cell-cell junctions. Mol Membr Biol 28(7-8):427–444

Corredor J, Yan F, Shen CC, Tong W, John SK, Wilson G, Whitehead R, Polk DB (2003) Tumor necrosis factor regulates intestinal epithelial cell migration by receptor-dependent mechanisms. Am J Physiol Cell Physiol 284:C953–C961

Cote JF, Vuori K (2007) GEF what? Dock180 and related proteins help Rac to polarize cells in new ways. Trends Cell Biol 17:383–393

Crosby LM, Waters CM (2010) Epithelial repair mechanisms in the lung. Am J Physiol Lung Cell Mol Physiol 298:L715–L731
Cuneo AA, Autieri MV (2009) Expression and function of anti-inflammatory interleukins: the other side of the vascular response to injury. Curr Vasc Pharmacol 7:267–276
Daniel TO, Liu H, Morrow JD, Crews BC, Marnett LJ (1999) Thromboxane A2 is a mediator of cyclooxygenase-2-dependent endothelial migration and angiogenesis. Cancer Res 59:4574–4577
Danjo Y, Gipson IK (1998) Actin 'purse string' filaments are anchored by E-cadherin-mediated adherens junctions at the leading edge of the epithelial wound, providing coordinated cell movement. J Cell Sci 111(Pt 22):3323–3332
Davies DE (2009) The role of the epithelium in airway remodeling in asthma. Proc Am Thorac Soc 6:678–682
De Donatis A, Comito G, Buricchi F, Vinci MC, Parenti A, Caselli A, Camici G, Manao G, Ramponi G, Cirri P (2008) Proliferation versus migration in platelet-derived growth factor signaling: the key role of endocytosis. J Biol Chem 283:19948–19956
De Donatis A, Ranaldi F, Cirri P (2010) Reciprocal control of cell proliferation and migration. Cell Commun Signal 8:20
Delva E, Tucker DK, Kowalczyk AP (2009) The desmosome. Cold Spring Harb Perspect Biol 1:a002543
Dow LE, Humbert PO (2007) Polarity regulators and the control of epithelial architecture, cell migration, and tumorigenesis. Int Rev Cytol 262:253–302
Dow LE, Kauffman JS, Caddy J, Zarbalis K, Peterson AS, Jane SM, Russell SM, Humbert PO (2007) The tumour-suppressor Scribble dictates cell polarity during directed epithelial migration: regulation of Rho GTPase recruitment to the leading edge. Oncogene 26:2272–2282
Duffield JS, Bonventre JV (2005) Kidney tubular epithelium is restored without replacement with bone marrow-derived cells during repair after ischemic injury. Kidney Int 68:1956–1961
El-Sibai M, Pertz O, Pang H, Yip SC, Lorenz M, Symons M, Condeelis JS, Hahn KM, Backer JM (2008) RhoA/ROCK-mediated switching between Cdc42- and Rac1-dependent protrusion in MTLn3 carcinoma cells. Exp Cell Res 314:1540–1552
Escudero-Esparza A, Jiang WG, Martin TA (2011) The Claudin family and its role in cancer and metastasis. Front Biosci 16:1069–1083
Etienne-Manneville S (2008) Polarity proteins in migration and invasion. Oncogene 27:6970–6980
Etienne-Manneville S, Manneville JB, Nicholls S, Ferenczi MA, Hall A (2005) Cdc42 and Par6-PKCzeta regulate the spatially localized association of Dlg1 and APC to control cell polarization. J Cell Biol 170:895–901
Farooqui R, Fenteany G (2005) Multiple rows of cells behind an epithelial wound edge extend cryptic lamellipodia to collectively drive cell-sheet movement. J Cell Sci 118:51–63
Fenteany G, Janmey PA, Stossel TP (2000) Signaling pathways and cell mechanics involved in wound closure by epithelial cell sheets. Curr Biol 10:831–838
Firat-Karalar EN, Welch MD (2011) New mechanisms and functions of actin nucleation. Curr Opin Cell Biol 23:4–13
Folch A, Jo BH, Hurtado O, Beebe DJ, Toner M (2000) Microfabricated elastomeric stencils for micropatterning cell cultures. J Biomed Mater Res 52:346–353
Friedl P, Wolf K (2010) Plasticity of cell migration: a multiscale tuning model. J Cell Biol 188:11–19
Garcia-Fernandez B, Campos I, Geiger J, Santos AC, Jacinto A (2009) Epithelial resealing. Int J Dev Biol 53:1549–1556
Garcia-Mata R, Burridge K (2007) Catching a GEF by its tail. Trends Cell Biol 17:36–43
Gardel ML, Schneider IC, Aratyn-Schaus Y, Waterman CM (2010) Mechanical integration of actin and adhesion dynamics in cell migration. Annu Rev Cell Dev Biol 26:315–333
Giaever I, Keese CR (1991) Micromotion of mammalian cells measured electrically. Proc Natl Acad Sci U S A 88:7896–7900

Giannelli G, Falk-Marzillier J, Schiraldi O, Stetler-Stevenson WG, Quaranta V (1997) Induction of cell migration by matrix metalloprotease-2 cleavage of laminin-5. Science 277:225–228

Goncharova EA, Goncharov DA, Krymskaya VP (2006) Assays for in vitro monitoring of human airway smooth muscle (ASM) and human pulmonary arterial vascular smooth muscle (VSM) cell migration. Nat Protoc 1:2933–2939

Gough W, Hulkower KI, Lynch R, McGlynn P, Uhlik M, Yan L, Lee JA (2011) A quantitative, facile, and high-throughput image-based cell migration method is a robust alternative to the scratch assay. J Biomol Screen 16:155–163

Guilluy C, Garcia-Mata R, Burridge K (2011) Rho protein crosstalk: another social network? Trends Cell Biol 21(12):718–726

Guo JK, Cantley LG (2011) Cellular maintenance and repair of the kidney. Annu Rev Physiol 72:357–376

Hartsock A, Nelson WJ (2008) Adherens and tight junctions: structure, function and connections to the actin cytoskeleton. Biochim Biophys Acta 1778:660–669

Hayes NV, Blackburn E, Boyle MM, Russell GA, Frost TM, Morgan BJ, Gullick WJ (2011) Expression of neuregulin 4 splice variants in normal human tissues and prostate cancer and their effects on cell motility. Endocr Relat Cancer 18:39–49

Heijink IH, Brandenburg SM, Postma DS, and van Oosterhout AJ (2010) Cigarette smoke impairs airway epithelial barrier function and cell-cell contact recovery. Eur Respir J 35:894-903

Heijink IH, Brandenburg SM, Noordhoek JA, Postma DS, Slebos DJ, van Oosterhout AJ (2011) Characterisation of cell adhesion in airway epithelial cell types using electric cell-substrate impedance sensing. Eur Respir J 35:894–903

Hidalgo-Carcedo C, Hooper S, Chaudhry SI, Williamson P, Harrington K, Leitinger B, Sahai E (2011) Collective cell migration requires suppression of actomyosin at cell-cell contacts mediated by DDR1 and the cell polarity regulators Par3 and Par6. Nat Cell Biol 13:49–58

Hilliard VC, Frey MR, Dempsey PJ, Peek RM Jr, Polk DB (2011) TNF-{alpha} converting enzyme-mediated ErbB4 transactivation by TNF promotes colonic epithelial cell survival. Am J Physiol Gastrointest Liver Physiol 301:G338–G346

Hong J, Kandasamy K, Marimuthu M, Choi CS, Kim S (2011) Electrical cell-substrate impedance sensing as a non-invasive tool for cancer cell study. Analyst 136:237–245

Horwitz R, Webb D (2003) Cell migration. Curr Biol 13:R756–R759

Hug TS (2003) Biophysical methods for monitoring cell-substrate interactions in drug discovery. Assay Drug Dev Technol 1:479–488

Hulkower KI, Herber RL (2011) Cell migration and invasion assays as tools for drug discovery. Pharmaceutics 3:107–124

Humbert PO, Dow LE, Russell SM (2006) The scribble and par complexes in polarity and migration: friends or foes? Trends Cell Biol 16:622–630

Humphreys BD, Czerniak S, DiRocco DP, Hasnain W, Cheema R, Bonventre JV (2011) Repair of injured proximal tubule does not involve specialized progenitors. Proc Natl Acad Sci U S A 108:9226–9231

Hynes RO (2002) Integrins: bidirectional, allosteric signaling machines. Cell 110:673–687

Iizuka M, Konno S (2011) Wound healing of intestinal epithelial cells. World J Gastroenterol 17:2161–2171

Itoh Y, Joh T, Tanida S, Sasaki M, Kataoka H, Itoh K, Oshima T, Ogasawara N, Togawa S, Wada T, Kubota H, Mori Y, Ohara H, Nomura T, Higashiyama S, Itoh M (2005) IL-8 promotes cell proliferation and migration through metalloproteinase-cleavage proHB-EGF in human colon carcinoma cells. Cytokine 29:275–282

Jacinto A, Martinez-Arias A, Martin P (2001) Mechanisms of epithelial fusion and repair. Nat Cell Biol 3:E117–E123

Jiang WG, Martin TA, Lewis-Russell JM, Douglas-Jones A, Ye L, Mansel RE (2008) Eplin-alpha expression in human breast cancer, the impact on cellular migration and clinical outcome. Mol Cancer 7:71

Jiang GX, Zhong XY, Cui YF, Liu W, Tai S, Wang ZD, Shi YG, Zhao SY, Li CL (2010) IL-6/STAT3/TFF3 signaling regulates human biliary epithelial cell migration and wound healing in vitro. Mol Biol Rep 37:3813–3818

Jovanovic M, Stefanoska I, Radojcic L, Vicovac L (2010) Interleukin-8 (CXCL8) stimulates trophoblast cell migration and invasion by increasing levels of matrix metalloproteinase (MMP)2 and MMP9 and integrins alpha5 and beta1. Reproduction 139:789–798

Kakiashvili E, Speight P, Waheed F, Seth R, Lodyga M, Tanimura S, Kohno M, Rotstein OD, Kapus A, Szaszi K (2009) GEF-H1 mediates tumor necrosis factor-alpha-induced Rho activation and myosin phosphorylation: role in the regulation of tubular paracellular permeability. J Biol Chem 284:11454–11466

Kakiashvili E, Dan Q, Vandermeer M, Zhang Y, Waheed F, Pham M, Szaszi K (2011) The epidermal growth factor receptor mediates tumor necrosis factor-alpha-induced activation of the ERK/GEF-H1/RhoA pathway in tubular epithelium. J Biol Chem 286:9268–9279

Kalluri R, Weinberg RA (2009) The basics of epithelial-mesenchymal transition. J Clin Invest 119:1420–1428

Kam Y, Guess C, Estrada L, Weidow B, Quaranta V (2008) A novel circular invasion assay mimics in vivo invasive behavior of cancer cell lines and distinguishes single-cell motility in vitro. BMC Cancer 8:198

Keese CR, Wegener J, Walker SR, Giaever I (2004) Electrical wound-healing assay for cells in vitro. Proc Natl Acad Sci U S A 101:1554–1559

Khalil AA, Friedl P (2010) Determinants of leader cells in collective cell migration. Integr Biol (Camb) 2:568–574

Koch S, Nusrat A (2009) Dynamic regulation of epithelial cell fate and barrier function by intercellular junctions. Ann N Y Acad Sci 1165:220–227

Kozasa T, Hajicek N, Chow C, Suzuki N (2011) Signaling mechanisms of RhoGTPase regulation by the heterotrimeric G proteins G12 and G13. J Biochem 150:371–383

Kucharzik T, Lugering A, Yan Y, Driss A, Charrier L, Sitaraman S, Merlin D (2005) Activation of epithelial CD98 glycoprotein perpetuates colonic inflammation. Lab Invest 85:932–941

Lee JF, Zeng Q, Ozaki H, Wang L, Hand AR, Hla T, Wang E, Lee MJ (2006) Dual roles of tight junction-associated protein, zonula occludens-1, in sphingosine 1-phosphate-mediated endothelial chemotaxis and barrier integrity. J Biol Chem 281:29190–29200

Lehmann W, Edgar CM, Wang K, Cho TJ, Barnes GL, Kakar S, Graves DT, Rueger JM, Gerstenfeld LC, Einhorn TA (2005) Tumor necrosis factor alpha (TNF-alpha) coordinately regulates the expression of specific matrix metalloproteinases (MMPS) and angiogenic factors during fracture healing. Bone 36:300–310

Li J, Lau GK, Chen L, Dong SS, Lan HY, Huang XR, Li Y, Luk JM, Yuan YF, Guan XY (2011) Interleukin 17A promotes hepatocellular carcinoma metastasis via NF-kB induced matrix metalloproteinases 2 and 9 expression. PLoS One 6:e21816

Liang CC, Park AY, Guan JL (2007) In vitro scratch assay: a convenient and inexpensive method for analysis of cell migration in vitro. Nat Protoc 2:329–333

Lotz MM, Rabinovitz I, Mercurio AM (2000) Intestinal restitution: progression of actin cytoskeleton rearrangements and integrin function in a model of epithelial wound healing. Am J Pathol 156:985–996

Lu L, Reinach PS, Kao WW (2001) Corneal epithelial wound healing. Exp Biol Med (Maywood) 226:653–664

Luppi F, Longo AM, de Boer WI, Rabe KF, Hiemstra PS (2007) Interleukin-8 stimulates cell proliferation in non-small cell lung cancer through epidermal growth factor receptor transactivation. Lung Cancer 56:25–33

Martin P, Parkhurst SM (2004) Parallels between tissue repair and embryo morphogenesis. Development 131:3021–3034

Masszi A, Fan L, Rosivall L, McCulloch CA, Rotstein OD, Mucsi I, Kapus A (2004) Integrity of cell-cell contacts is a critical regulator of TGF-beta 1-induced epithelial-to-myofibroblast transition: role for beta-catenin. Am J Pathol 165:1955–1967

Maul RS, Chang DD (1999) EPLIN, epithelial protein lost in neoplasm. Oncogene 18:7838–7841
Maul RS, Song Y, Amann KJ, Gerbin SC, Pollard TD, Chang DD (2003) EPLIN regulates actin dynamics by cross-linking and stabilizing filaments. J Cell Biol 160:399–407
Mayor R, Carmona-Fontaine C (2010) Keeping in touch with contact inhibition of locomotion. Trends Cell Biol 20:319–328
Montesano R, Soulie P, Eble JA, Carrozzino F (2005) Tumour necrosis factor alpha confers an invasive, transformed phenotype on mammary epithelial cells. J Cell Sci 118:3487–3500
Nalbant P, Chang YC, Birkenfeld J, Chang ZF, Bokoch GM (2009) Guanine nucleotide exchange factor-H1 regulates cell migration via localized activation of RhoA at the leading edge. Mol Biol Cell 20:4070–4082
Narumiya S, Tanji M, Ishizaki T (2009) Rho signaling, ROCK and mDia1, in transformation, metastasis and invasion. Cancer Metastasis Rev 28:65–76
Nelson WJ (2003) Epithelial cell polarity from the outside looking in. News Physiol Sci 18:143–146
Nieto MA (2011) The ins and outs of the epithelial to mesenchymal transition in health and disease. Annu Rev Cell Dev Biol 10(27):347–376
Nizamutdinova IT, Kim YM, Chung JI, Shin SC, Jeong YK, Seo HG, Lee JH, Chang KC, Kim HJ (2009) Anthocyanins from black soybean seed coats stimulate wound healing in fibroblasts and keratinocytes and prevent inflammation in endothelial cells. Food Chem Toxicol 47:2806–2812
Nurnberg A, Kitzing T, Grosse R (2011) Nucleating actin for invasion. Nat Rev Cancer 11:177–187
Parri M, Chiarugi P (2010) Rac and Rho GTPases in cancer cell motility control. Cell Commun Signal 8:23
Petrie RJ, Doyle AD, Yamada KM (2009) Random versus directionally persistent cell migration. Nat Rev Mol Cell Biol 10:538–549
Poujade M, Grasland-Mongrain E, Hertzog A, Jouanneau J, Chavrier P, Ladoux B, Buguin A, Silberzan P (2007) Collective migration of an epithelial monolayer in response to a model wound. Proc Natl Acad Sci U S A 104:15988–15993
Qin Y, Capaldo C, Gumbiner BM, Macara IG (2005) The mammalian Scribble polarity protein regulates epithelial cell adhesion and migration through E-cadherin. J Cell Biol 171:1061–1071
Redd MJ, Cooper L, Wood W, Stramer B, Martin P (2004) Wound healing and inflammation: embryos reveal the way to perfect repair. Philos Trans R Soc Lond B Biol Sci 359:777–784
Revenu C, Gilmour D (2009) EMT 2.0: shaping epithelia through collective migration. Curr Opin Genet Dev 19:338–342
Ridley AJ (2011) Life at the leading edge. Cell 145:1012–1022
Rikitake Y, Takai Y (2011) Directional cell migration regulation by small G proteins, nectin-like molecule-5, and afadin. Int Rev Cell Mol Biol 287:97–143
Rock JR, Hogan BL (2011) Epithelial progenitor cells in lung development, maintenance, repair, and disease. Annu Rev Cell Dev Biol 10(27):493–512
Rorth P (2009) Collective cell migration. Annu Rev Cell Dev Biol 25:407–429
Rosen EM, Goldberg ID, Liu D, Setter E, Donovan MA, Bhargava M, Reiss M, Kacinski BM (1991) Tumor necrosis factor stimulates epithelial tumor cell motility. Cancer Res 51:5315–5321
Rossman KL, Der CJ, Sondek J (2005) GEF means go: turning on RHO GTPases with guanine nucleotide-exchange factors. Nat Rev Mol Cell Biol 6:167–180
Rudini N, Dejana E (2008) Adherens junctions. Curr Biol 18:R1080–R1082
Russo JM, Florian P, Shen L, Graham WV, Tretiakova MS, Gitter AH, Mrsny RJ, Turner JR (2005) Distinct temporal-spatial roles for rho kinase and myosin light chain kinase in epithelial purse-string wound closure. Gastroenterology 128:987–1001
Samarin SN, Ivanov AI, Flatau G, Parkos CA, Nusrat A (2007) Rho/Rho-associated kinase-II signaling mediates disassembly of epithelial apical junctions. Mol Biol Cell 18:3429–3439

Saxena NK, Sharma D, Ding X, Lin S, Marra F, Merlin D, Anania FA (2007) Concomitant activation of the JAK/STAT, PI3K/AKT, and ERK signaling is involved in leptin-mediated promotion of invasion and migration of hepatocellular carcinoma cells. Cancer Res 67:2497–2507

Schiller MR (2006) Coupling receptor tyrosine kinases to Rho GTPases–GEFs what's the link. Cell Signal 18:1834–1843

Schiller KR, Maniak PJ, O'Grady SM (2011) Cystic fibrosis transmembrane conductance regulator is involved in airway epithelial wound repair. Am J Physiol Cell Physiol 299:C912–C921

Scott KA, Arnott CH, Robinson SC, Moore RJ, Thompson RG, Marshall JF, Balkwill FR (2004) TNF-alpha regulates epithelial expression of MMP-9 and integrin alphavbeta6 during tumour promotion. A role for TNF-alpha in keratinocyte migration? Oncogene 23:6954–6966

Sebe A, Masszi A, Zulys M, Yeung T, Speight P, Rotstein OD, Nakano H, Mucsi I, Szaszi K, Kapus A (2008) Rac, PAK and p38 regulate cell contact-dependent nuclear translocation of myocardin-related transcription factor. FEBS Lett 582:291–298

Sohl G, Willecke K (2004) Gap junctions and the connexin protein family. Cardiovasc Res 62:228–232

Song Y, Maul RS, Gerbin CS, Chang DD (2002) Inhibition of anchorage-independent growth of transformed NIH3T3 cells by epithelial protein lost in neoplasm (EPLIN) requires localization of EPLIN to actin cytoskeleton. Mol Biol Cell 13:1408–1416

Spiering D, Hodgson L (2011) Dynamics of the Rho-family small GTPases in actin regulation and motility. Cell Adhes Migr 5:170–180

Steed E, Balda MS, Matter K (2010) Dynamics and functions of tight junctions. Trends Cell Biol 20:142–149

Sturm A, Dignass AU (2008) Epithelial restitution and wound healing in inflammatory bowel disease. World J Gastroenterol 14:348–353

Tambe DT, Hardin CC, Angelini TE, Rajendran K, Park CY, Serra-Picamal X, Zhou EH, Zaman MH, Butler JP, Weitz DA, Fredberg JJ, Trepat X (2011) Collective cell guidance by cooperative intercellular forces. Nat Mater 10:469–475

Terry S, Nie M, Matter K, Balda MS (2010) Rho signaling and tight junction functions. Physiology (Bethesda) 25:16–26

Tomar A, Schlaepfer DD (2009) Focal adhesion kinase: switching between GAPs and GEFs in the regulation of cell motility. Curr Opin Cell Biol 21:676–683

Tsapara A, Luthert P, Greenwood J, Hill CS, Matter K, Balda MS (2010) The RhoA activator GEF-H1/Lfc is a TGF-b target gene and effector that regulates a-smooth muscle actin expression and cell migration. Mol Biol Cell 21:860–870

Tsukita S, Furuse M (2000) The structure and function of claudins, cell adhesion molecules at tight junctions. Ann N Y Acad Sci 915:129–135

Wang HR, Zhang Y, Ozdamar B, Ogunjimi AA, Alexandrova E, Thomsen GH, Wrana JL (2003) Regulation of cell polarity and protrusion formation by targeting RhoA for degradation. Science 302:1775–1779

Wang Y, Tang Z, Xue R, Singh GK, Lv Y, Shi K, Cai K, Deng L, Yang L (2011) TGF-beta1 promoted MMP-2 mediated wound healing of anterior cruciate ligament fibroblasts through NF-kappaB. Connect Tissue Res 52:218–225

Wegener J, Keese CR, Giaever I (2000) Electric cell-substrate impedance sensing (ECIS) as a noninvasive means to monitor the kinetics of cell spreading to artificial surfaces. Exp Cell Res 259:158–166

White SR, Fischer BM, Marroquin BA, Stern R (2008) Interleukin-1beta mediates human airway epithelial cell migration via NF-kappaB. Am J Physiol Lung Cell Mol Physiol 295:L1018–L1027

Wickstrom SA, Fassler R (2011) Regulation of membrane traffic by integrin signaling. Trends Cell Biol 21:266–273

Wilson AJ, Byron K, Gibson PR (1999) Interleukin-8 stimulates the migration of human colonic epithelial cells in vitro. Clin Sci (Lond) 97:385–390

Wood W, Jacinto A, Grose R, Woolner S, Gale J, Wilson C, Martin P (2002) Wound healing recapitulates morphogenesis in Drosophila embryos. Nat Cell Biol 4:907–912

Wu Y, Zhou BP (2010) TNF-alpha/NF-kappaB/Snail pathway in cancer cell migration and invasion. Br J Cancer 102:639–644

Wyatt TA, Ito H, Veys TJ, Spurzem JR (1997) Stimulation of protein kinase C activity by tumor necrosis factor-alpha in bovine bronchial epithelial cells. Am J Physiol 273:L1007–L1012

Yamaoka T, Yan F, Cao H, Hobbs SS, Dise RS, Tong W, Polk DB (2008) Transactivation of EGF receptor and ErbB2 protects intestinal epithelial cells from TNF-induced apoptosis. Proc Natl Acad Sci U S A 105:11772–11777

Yu FS, Yin J, Xu K, Huang J (2011) Growth factors and corneal epithelial wound healing. Brain Res Bull 81:229–235

Zegers M (2008) Roles of P21-activated kinases and associated proteins in epithelial wound healing. Int Rev Cell Mol Biol 267:253–298

Zelenka PS, Arpitha P (2008) Coordinating cell proliferation and migration in the lens and cornea. Semin Cell Dev Biol 19:113–124

Zeng Q, Hong W (2008) The emerging role of the hippo pathway in cell contact inhibition, organ size control, and cancer development in mammals. Cancer Cell 13:188–192

Zhao B, Lei QY, Guan KL (2008) The Hippo-YAP pathway: new connections between regulation of organ size and cancer. Curr Opin Cell Biol 20:638–646

Tumour-Endothelial and Tumour-Mesothelial Interactions Investigated by Impedance Sensing Based Cell Analyses

Wen G. Jiang, Lin Ye, Haiying Ren, Ann Kift-Morgan, Nicholas Topley, and Malcolm D. Mason

Abstract Interaction between tumour cells and endothelial cells is an essential step during the systemic step of cancer metastasis in the body and has been an active area pursued for the past decades. However, methods to investigate tumour-endothelial interactions mostly are tedious and lack of high throughput capability. Similarly, tumour-mesothelial interactions are also important part of the transcoelomic spreading in the body cavities. However, methods to determine tumour-mesothelial interaction face similar challenges to that of tumour-endothelial interactions. This chapter discusses the application of electric cell-substrate impedance sensing (ECIS) in the investigation of tumour-endothelial/mesothelial interactions.

1 Introduction

Metastasis of cancer cells in the body occurs via a few different routes in order to complete the spreading from the primary tumours to the destinations. Systemically, the haematological route and lymphatic route take tumour cells from the primaries

W.G. Jiang (✉) • L. Ye • M.D. Mason
Institutes of Cancer and Genetics, Cardiff University School of Medicine, Cardiff, UK
e-mail: Jiangw@cardiff.ac.uk

H. Ren
Department of Gynaecology and Obstetrics, Beijing Tongren Hospital, Capital Medical University, Beijing, China

A. Kift-Morgan • N. Topley
The TIME Institute, Cardiff University School of Medicine, Cardiff, UK

W.G. Jiang (ed.), *Electric Cell-Substrate Impedance Sensing and Cancer Metastasis*, Cancer Metastasis - Biology and Treatment 17, DOI 10.1007/978-94-007-4927-6_9,

to organs and tissues throughout the body, until they reach suitable locations. Regional and local metastasis occurs via regional lymphatics and lymph nodes, and local tissue invasion. Another special form of metastasis is the transcoelomic spreading of cancers, via which cancer cells spread to the cavities in the body, namely peritoneal, pleural and pericardiac cavities. The transcoelomic route can be the result of systemic spread or regional/local spread of cancer cells which results in the development of metastasis in the cavities.

Different route of spreading have different underlying mechanics. However, systemic and transcoelomic spreading have at least one thing in common, cancer cells have to encounter the lining cell layer on the surface of blood vessel and body cavities. This is frequently described as tumour-endothelial and tumour-mesothelial interaction. Following the interactions, successful tumour cells would invade the vessel wall or the mesothelial lining and settle in tissues to develop metastatic tumours. Investigations into tumour-endothelial/mesothelial interaction have been hot topics in cancer research. A number of methods have been developed to investigate the cell-cell interactions. The present chapter describe the use of impedance sensing as a new approach in determining tumour-endothelial and tumour-mesothelial interactions.

2 Tumour-Endothelial Interactions

Tumour endothelial interactions are critically important during the systemic spread of cancer cells. For example, circulation cancer cells would need to settle over the vascular endothelium bed at a specific and/or non-specific locations in order to adopt process of leaving the circulation, known as extravasation. The past few decades have seen fundamental progress in this area. It is now known that under the flow conditions in the blood vessels, circulation cancer cells and endothelial cells would first use their carbohydrate branches of the surface molecule to interact with each other, an interaction that takes place faster but the strength of interaction is weak. This weak adhesion between tumour and endothelial cells allows the circulating cancer cells to gradually slow down and loosely ‘dock’ to the endothelium. This docking is soon followed by slow but stronger interactions between surface proteins on the two cell populations, which form strong protein-protein interaction, resulting in cell firmly ‘locked’ to the endothelium. Upon locking, tumour cells and endothelial cells will develop mechanisms allowing tumour cells to penetrate the paracellular spaces of the endothelium and underlying basement membrane, in order to settle and regrow in the new secondary site. These knowledge are well documented in the literature and are not the topics of the present chapter. In the following, methods to study tumour-endothelial interaction are reviewed and most importantly, a new method using ECIS to investigate this interaction is discussed.

2.1 Methods to Evaluate Tumour-Endothelial Interactions

Over the past decades, a number of methods have been develop to quantify tumour-endothelial interactions. It is always possible to directly examine the interaction or adhered cancer cells over the endothelial cells. However, without any methods to distinguish the two cell populations, one can not be entirely sure if a cell sitting on the endothelial monolayer a cancer cell or a newly divided endothelial cells. In early days, radioisotopes were used to label cells, mostly cancer cells and following interaction, radioactivities are determined as a way to provide semi-quantified number of cells (Ford 1978; Thornhill et al. 1990). This method is sensitive and largely quantitative. However, the disadvantage is clear: the use of harzadous radioactive materials and tedious. This lead to development of microscope based method, by labelling one cell (mostly cancer cells) with either color dye (such as MTT) or a fluorescent dye, such as Hoescht 33258 and DiI (1,1′-dioctadecyl-3,3,3′,3′-tetramethylindocarbocyanine) (Taka et al. 1986; Oppenheimer-Marks et al. 1990; De Clark et al. 1994; Jiang et al. 1995; Hiscox and Jiang 1997a). Using these labelling dyes, one can either directly quantify the number of adherence cells thus provide absolute cell numbers. One can also extract the dyes or read the plate directly for the colour/fluorescence intensity, to give a indirect account of adherent cells. One example is cellular ELISA with which an ELISA method is used to quantify cancer cell surface markers as a way to semi-quantify the adherent cancer cells (Hiscox and Jiang 1997b). Methods to evaluate tumour-endothelial interaction under flow conditions have also been developed. These methods are quantitative, practical and can be conducted in high throughput. However, an disadvantage is that these methods are mostly end of point tests and are difficult to observe the dynamic changes in real time. Furthermore, it is almost impossible to observe early events when tumour cells meet endothelial cells.

2.2 Evaluation of Tumour-Endothelial Cells by Way of ECIS

We evaluated the tumour-endothelial interaction by using a traditional DiI labelling method and electric cell-substrate sensing (ECIS) (Giaever and Keese 1991; Keese et al. 2004), in order to evaluate the cellular impact of transglutaminase-4 (TGase4) expression (Jiang et al. 2009).

TGase4 belongs to the transglutaminase family of enzymes, which has more than nine members (Ablin and Whyard 1991). These enzymes have relatively broad distribution pattern in the body, with TGase4 being an interesting exception. TGase-4 has a strong pattern of distribution in the prostate gland (Dubbink et al. 1998, 1999; An et al. 1999; Cho et al. 2010). TGase-4 has been shown to be a potential marker for prostate cancer cells and regulates the adhesion, motility and invasion of cancer cells (Davies et al. 2007; Jiang et al. 2009, 2010; Ablin et al. 2011).

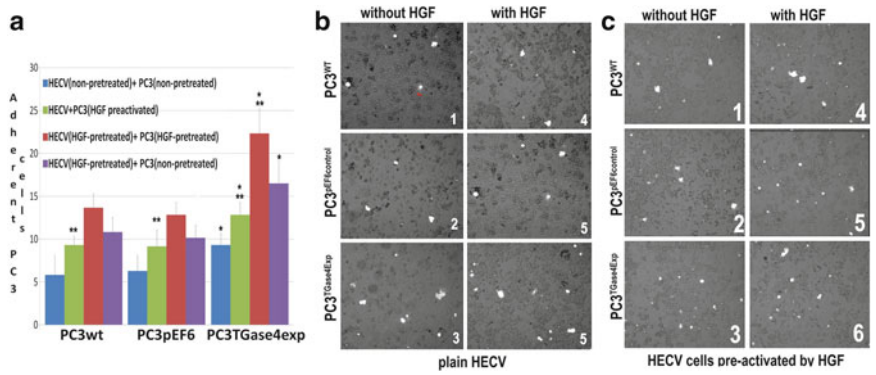

Fig. 1 Validation of TGase-4 expression and quantitative analysis of tumor cell adhesion to human endothelial cells (HECV) (**a**) Number of adherent PC-3 cells to HECV monolayer. Shown are number of cells per high field. * $p<0.01$ vs. the respective PC-3^{wt} and ^{PC4pEF6} cells; ** $p<0.05$ vs. non-activated HECV. (**b**) immunofluorescent image of DiI labelled prostate cancer cell PC-3 (*bright cells*) over quiescent confluent HECV cells (in background). (**c**)DiI labelled prostate cancer cell PC-3 (*bright cells*) over HGF-preactivated HECV cells (in background). HGF concentration used, where indicated, was 40 ng/ml (Adapted from Jiang et al. 2009)

Human endothelial cell line, HECV, was first plated into 96-well and allowed to reach confluence. Prostate cancer cell line, PC-3, control cells and cells transfected with TGase-4 were pre-labelled with DiI and washed. These labelled cells were added to the endothelial monolayer for upto 40 min and then washed to remove the non-adherent cells. Under fluorescence microscope, the adherent PC-3 cells appeared as bright red cells over a monolayer of endothelial cells (Fig. 1b, c). By direct counting, it was shown that TGase-4 over-expressing prostate cancer cells became more adhesive to the endothelial cells (Fig. 1a).

We further created sublines from another prostate cancer cell line, CA-HPV-10 which is positive for TGase-4, by knocking down TGase-4 using anti-TGase4 transgenes. As shown in Fig. 2a, when PC-3 cells and CA-HPV-10 were added to endothelial monolayer, pre-prepared using the 8W1E ECIS array (Applied Biophysics), Expression of TGase-4 was correlated with the adhesiveness of the cells, namely over-expression of TGase-4 in PC-3 cells increased the adhesiveness and knocking down TGase-4 from CA-HPV-10 decreased the adhesiveness (Fig. 2) (Jiang et al. 2009).

In order to assess the very early events after cancer cells immediately meet endothelial cells, we have adopted the fast tracking feature of the ECIS1600R model. We have observed that when TGase-4 over-expressing PC-3 cells were added to endothelial monolayer, there was a marked reduction of resistance followed by sustained rise in resistance (Fig. 3). Interestingly, this rapid change occurs within seconds after the two cells population meet, a feature otherwise difficult to capture (Jiang et al. 2009). We have subsequently found that ROCK, an Rho/Rac signalling intermediate, plays a key role in TGase-4 mediated tumour-cell adhesion (Croft et al. 2004; Li et al. 2006; Jiang et al. 2009).

Collectively, electric cell-substrate impedance sensing is a practical method to tracking tumour-endothelial interaction. It allows real time, long period, label free and

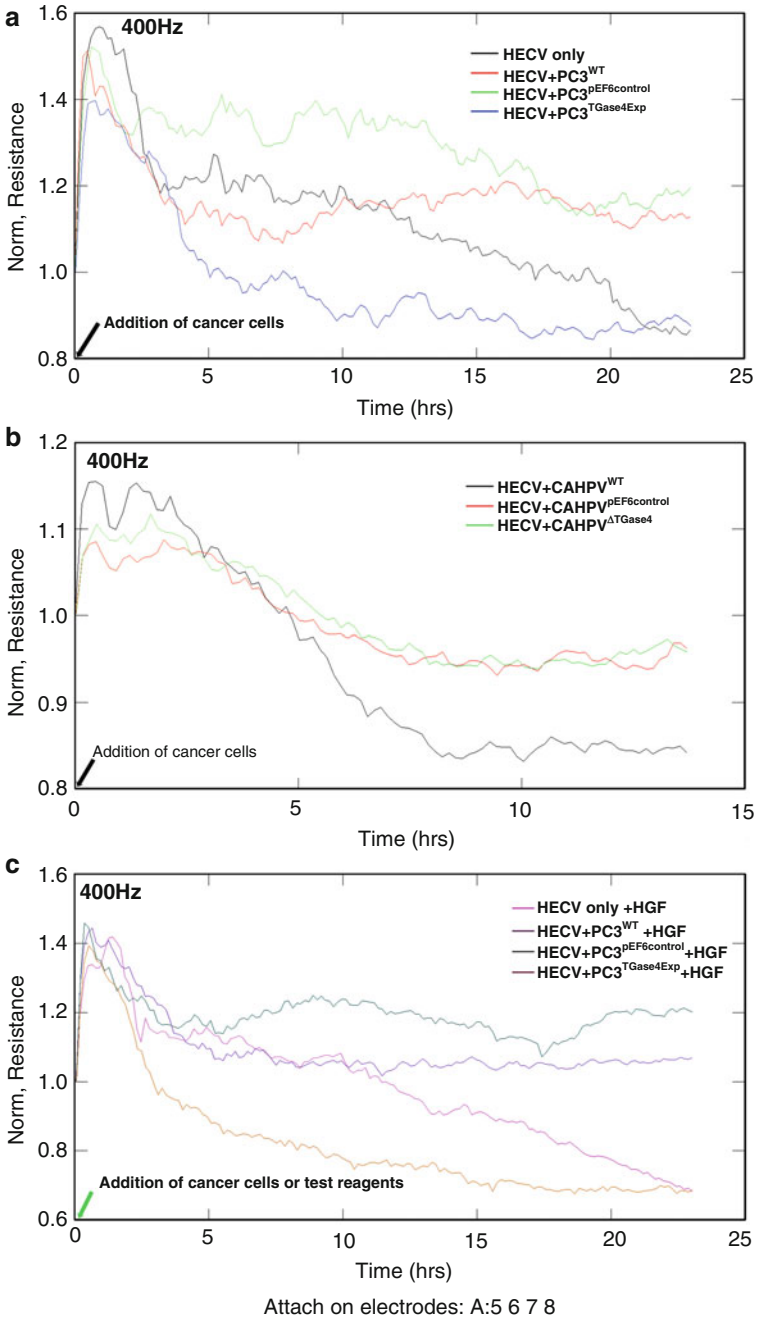

Fig. 2 Interaction between PC-3 and HECV cells affected the barrier function of the endothelial cells. PC-3 cells (**a**) CA-HPV-10 cells (**b**) were added to HECV cells. The electric resistance was immediately recorded after addition on the ECIS1600R. PC-3 over-expressing TGase-4 and CAHPV-10 wild type (naturally expressed TGase-4) resulted in substantial disruption of the barrier function of endothelial cells. (**c**): Effects of HGF pre-activation of PC-3 on the endothelial barrier function. PC-3 cells were pre-treated with HGF (40 ng/ml) for 1 h and then washed. The same number of cells in same volume were added to confluent endothelial cells. HGF pre-activated $PC3^{TGase4}$ cells caused a substantial damage to the barrier function in endothelia cells (Adapted from Jiang et al. 2010)

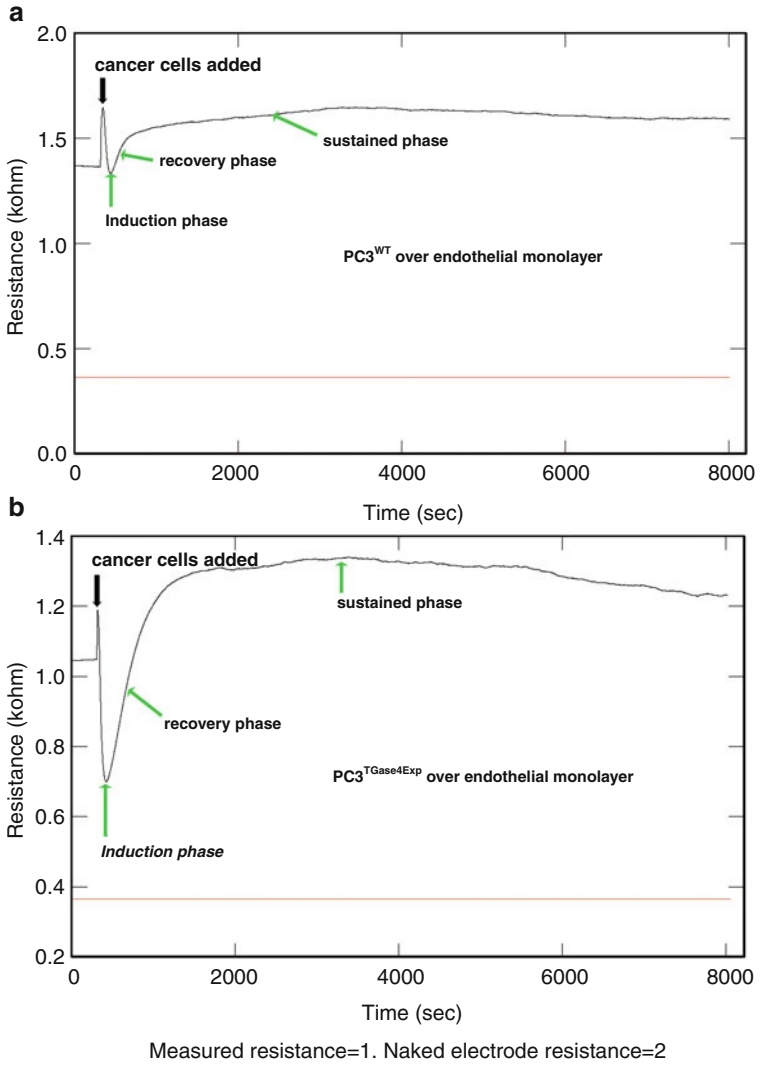

Fig. 3 Detection of early phase changes of the barrier functions of the endothelial cell, during the tumor-endothelial interactions. Using the additive function of ECIS1600R, the changes of electric resistance was recorded in millisecond over a 2 h period. Addition of PC-3^{TGase4} cells (**b**) to the endothelial cell monolayer resulted in a marked change of the barrier function seconds after adhesion, when compared with addition of control PC-3 cells (**a**) (Adapted from Jiang et al. 2009)

automated monitoring of the cell interaction, without extra human phase intervention. Furthermore, the approach allows rapidly tracking cellular events at shorter intervals, otherwise impossible to detect. These features would allow future development in this interesting area in cancer research.

3 Tumour-Mesothelial Interactions and Transcoelomic Metastasis

Spreading and formation of metastatic tumours in the body cavities (mostly in peritoneal and pleural cavities) are a common feature in certain malignant conditions and are broadly referred to as the transcoelomic spread. Transcoelomic spread occurs mostly from tumours adjacent tissues/organs, namely lung for pleural transcoelomic metastasis. Transcoelomic peritoneal metastasis is most coming from pancreatic cancer, colorectal cancer and ovarian cancer, followed by gastric cancer, cervical cancer (Garrison et al. 1986).

3.1 Introduction

The mesothelium is the lining of cavities in the body, mainly the peritoneal cavity, pleural cavity, and pericardiac cavity. The main cell type that forms the mesothelium is mesothelial cell, which is a monolayer of pavement-like cells and carries both mesenchymal and epithelial cell markers. The mesothelium acts as protective and non-adhesive surface and is self renewing. The layer is involved thus in inflammation, tissue repair, fluid and electrolyte transporation and cancer cell adhesion and spreading in the cavities. Malignant transformation of mesothelial cells results in mesothelioma, an aggressive malignant condition that there is little effective treatment.

It has been reported in early days that mesothelial cells may be a privileged site for tumour cells to attach (Cunliffe and Sugarbaker 1989). This was thought to be due to the layer of hyaluronan, a protein released by mesothelial cells and together with other proteins forms a protective surface of the mesothelium. Peritoneal metastasis occurs via one of the two main routes: systemic spreading and local implantation after invasion of local tissues. Tumours away from the cavities are likely to develop transcoelomic metastasis via the systemic route, for example peritoneal metastasis from breast cancer and lung cancer. Perhaps most peritoneal metastases come from tumours originated from organs adjacent to the peritoneal cavity, namely tumours from stomach, colon, pancreas, ovaries, and bladder. Cancer cells from these tumours invade surrounding tissues, breach the peritoneal lining and spread by way of seeding in the peritoneal cavity, although both trans-serosal, inter-serosal and sub-serosal spread can also be seen. It is clear that in most forms of peritoneal spreading, tumour-mesothelial interactions are essential step in establishing a metastatic tumour in the cavity.

An examination of pleural and peritoneal malignant effusions (490 pleural and 359 peritoneal) demonstrated that the most common primary tumour sites of pleural metastases were breast (50.8%) was followed by gynaecologic (21.2%) and lung (19.8%); which of peritoneal metastases were gynaecologic (60.3 %), then followed by gastrointestinal (23.4%) and breast (14.0%) (Antic et al. 2012). When the

tumour cells disseminate through and develop a metastatic lesion in pleural or peritoneal cavity, the cancer cells need to adapt themselves to the environment and interact with the mesothelial cells.

The contact of cancer cells to mesothelial cells is followed consequently by adhesion, invasion and growth of tumour cells at such a new site. The exact role of mesothelial cells in tumour cell adhesion and growth is unclear. Many studies have demonstrated that traumatised mesothelial surfaces are privileged sites for tumour cell adhesion possibly due to binding of tumour cells to the hyaluronan coat of mesothelial cells(Cunliffe and Sugarbaker 1989), upregulation of adhesion molecules on mesothelial cells in response to inflammatory mediators and exposure of underlying ECM. However, hyaluronan in conditioned medium from cultured mesothelial cells prevented tumour cell attachment to mesothelial cells, possibly by binding to CD44 molecules on the tumour cells and preventing their interaction with hyaluronan on the mesothelial cell surface (Jones et al. 1995). On the other hand, factors released from tumour cells or adjacent stroma, which may also provide a favourable environment for the interaction between cancer cells and mesothelial cells. For example, IL-1β or TGF-β1 from cancer cells can act on the mesothelial cells and/or adjacent stroma to promote peritoneal dissemination (Lv et al. 2012; Watanabe et al. 2012). Further investigation into this particular interaction will shed light on the mechanism(s) of cancer cells dissemination in pleural and peritoneal cavities, and may also provide novel therapeutic opportunities.

3.2 Tumour-Mesothelial Interactions Investigation Methods

Method to investigate the interaction between tumour and mesothelial cells remains relatively limited. It can be based on direct observation (Akedo et al. 1986) and/or aided by labelling dyes. Calcein (Fluorexon) is a fluorescent dye that can be transported to the cytoplasm and can be use for measuring cell viability and short term labelling such as cell-cell interaction assays (Alkhamesi et al. 2005). Using calcein to label ovarian cancer cells, Ksiazek et al. 2009 has reported that senescent pritoneal mesothelial cells are able to promote cell adhesion (Catterall et al. 1994; Ksiazek et al. 2009). This method is attractive in that it can use multiple well plates and carry out assays on a plate reader. However and similar to other fluorescent based assay, the method requires labelling of cells and a step to wash the cells. It is also difficult to carry out real-time monitoring during the interactions. Colony forming assay has also been used to investigate the interaction between tumour and mesothelial cells. Casey et al. (2003) reported a method of using permeabilised mesothelial cells with trypan blue staining, in order to visualise the attachment and invasion of ovarian cancer cells. Based on the observations that mesothelial cells do not form colonies, Mitsui et al. (2012) added tumour cells directly to mesothelial and allowed extensive growth period (2 weeks). Formation of colonies, visualised by routine histological method, were thought to be from cancer cells, thus allowing studies to be carried out.

3.3 ECIS in Cytokine-Activated Mesothelial Cells-Tumour Interaction

MDA7/IL-24. To test how exogenous factors may influence tumour-mesothelial interaction and observe the interaction dynamically, we evaluated the effect of MDA-7 in an colon cancer -peritoneal mesothelial interaction setting. MDA-7 (melanoma differentiation associated gene-7), also known as IL-24, was initially identified from cancer cells and found to be up-regulated in melanoma cells (Jiang et al. 1995). The human MDA-7 gene, mapped to 1q32.2-q41, encodes a protein with a predicted size of 23.8 kD. Forced expression of MDA-7 in cancer cells was found to be growth inhibitory (Jiang et al. 1996). The location of the MDA-7 gene is closely linked to the IL-10, IL-19, and IL-20 genes within a 195-kb region -the IL-10 family cytokine cluster. MDA-7/IL-24 functions in cells via its receptor, MDA-7R/IL-24R. The MDA-7 receptor complexes include at least the IL-20alpha and IL-20beta complex and the IL-22R and IL-20beta complex. Limited information is available on the effect of MDA-7 on prostate cancer cells. Studies of adenoviral vector-induced expression of MDA-7 in human prostate cancer cells demonstrated varying degree of inhibition of growth and induction of apoptosis (Lebedeva et al. 2003). The cytokine has shown to be able to affect the adhesion and migration of cancer cells using a ECIS based method (Ablin et al. 2011) (Fig. 4). Collectively, MDA7/IL-24 is a known tumour suppressing cytokine and is currently in clinical trials for its therapeutic value in cancer treatment. There has been no information on its role in the tumour-mesothelial interactions.

Preparation of primary culture human peritoneal mesothelial cells. Greater Omentum from patients undergoing abdominal surgery, with consent, were collected soon after surgery. Primary culture mesothelial cells were obtained based on a procedure previously described (Lang and Topley 1996; Robson et al. 2001; Hurst et al. 2001; Mcloughlin et al. 2003; Colmont et al. 2011). Purified mesothelial cells were used within 8 passages. After washing, mesothelial cells were seeded in the 96W1E arrays at 100,000 per well and allow to reach confluence overnight.

MDA7/IL-24 has an marked impact on mesothelial cells during tumour-endothelial interactions. Primary culture endothelial cells were pretreated with MDA7/IL-24, an known tumour suppressive cytokines, for 24 h, before culture medium replaced. Human colon cancer cells, HRT18, was added to the preactivated mesothelial cell layer at an ratio of 1:4 (HRT18: mesothelial cells). As shown in Fig. 5, addition of HRT18 to control mesothelial cells (non-MDA-7 treated), had a marginal effect on the barrier function of the cell layer and over a 4-h period there is steady change of resistance. However, when the mesothelial cells were preactivated at concentrations greater than 5 ng/ml, addition of HRT18 resulted in a marked increase in the monolayer resistance across all the frequencies tested (Fig. 5a, b, c: 4,000, 16,000 and 64,000 Hz respectively. Figure 5d: the entire frequency spectrum using a 3D model).

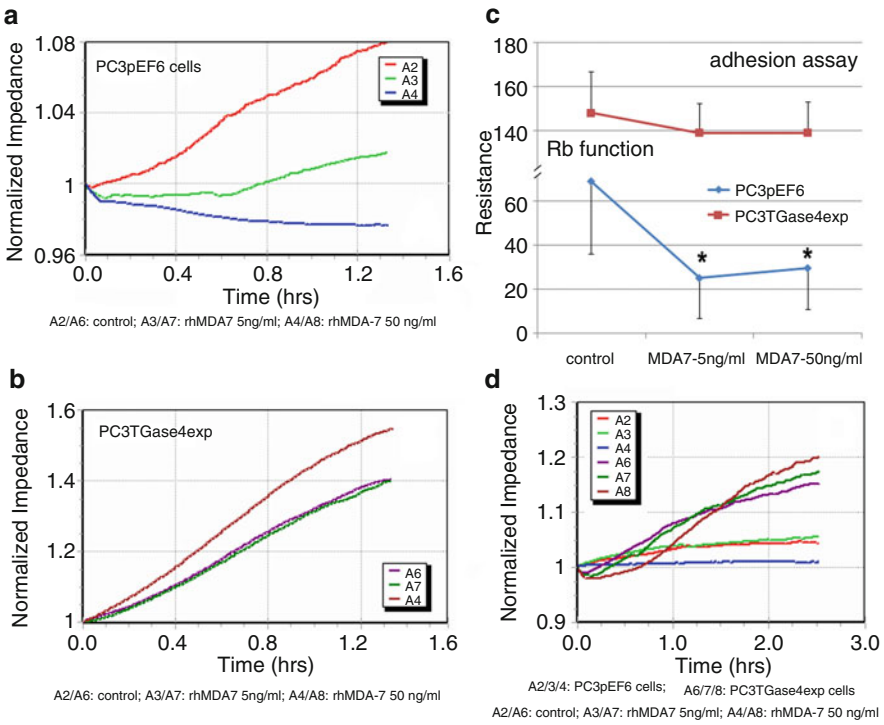

Fig. 4 TGase-4 expression and the cells response to rhMDA-7. (**a**) and (**b**) adhesion assay using ECIS9600 system (**a** – PC-3^{pEF6} control cells; **b** – PC-3^{TGase4exp} cells). (**c**) cell adhesion assay using Rb modelling (ECIS1600R, 4,000 Hz). MDA-7 inhibited cell adhesion in PC-3$^{pEF6\ cells}$ (*top left*), a response lost in PC-3^{TGase4exp} cells. * $p<0.01$ vs. PC-3^{pEF6} cells. (**d**): Inhibition of cell migration by rhMDA-7 was reverted by TGase-4 expression. PC-3^{pEF6} control cells had a slower pace of migration in the presence of rhDMA-7. However, PC-3^{TGase4exp} cells migrated rapidly and had no response to rhMDA-7 (Adapted from Ablin et al. 2011)

These data indicate that after pre-treating the mesothelial cells with the tumour suppressive cytokine MDA7/IL-24, the cell monolayer has a markedly increased resistance, a reflection of intercellular barrier functions at lower frequencies. Although a full evaluation of the impact of this change on the invasion of the mesothelial monolayer by the colon cancer cells, the increased barrier function is a good indication that MDA7/IL-24 may strengthen the mesothelial monolayer and make the monolayer harder for colon cancer cells to adhere and to invade, another reflection of the tumour suppressive role of MDA7/IL-24. A great number of cytokines are known to regulate the interaction between cancer and mesothelial cells including IL-1ß, TNFalpha, VEGF, (Sako et al. 2003; van Grevenstein et al. 2006). MDA7/IL-24 is certainly qualify for being a new mesothelial cell regulatory cytokine.

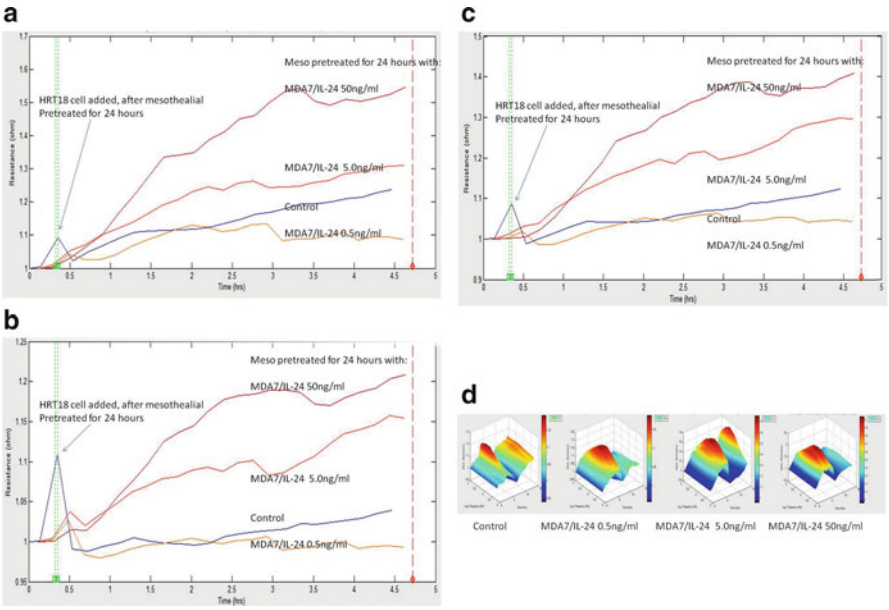

Fig. 5 Detection of interaction between human colorectal cancer cells and peritoneal mesothelial cells. Primary cultured peritoneal mesothelial cells (id 823) were added to 96-well 96W1E ECIS array and pretreated with MDA7/IL-24 for 24 h. Human colon cancer cell line, HRT18 was added after 24 h and the resistance was immediately traced using the Ztheta ECIS instrument. The change of resistance at 4,000 (**a**), 16,000 (**b**) and 64,000 (**c**) Hz are shown in the Fig. 3d modelling after addition of cancer cells were also shown in (**d**). rhMDA7/IL24 was used at 0.5, 5 and 50 ng/ml final concentration

3.4 ECIS in the Interaction Between Mesothelial Cells and Genetically Modified Cancer Cells-ALCAM

Cell surface molecules and tumour-mesothelial interactions. A number of cell surface molecules residing in cancer cells are thought to have a role to play in tumour-mesothelial interactions, including CD133, CD44, ICAM1, VCAM1 (Lessan et al. 1999; van Grevenstein et al. 2006; Mitsui et al. 2012). CD44 is probably the key cell surface protein in cancer cells to interact with hyaluronan present on the mesothelial layer (Tzuman et al. 2010). In addition, integrins on cancer cell surface interact with fibronectin made by mesothelial cells in the interaction (Takatsuki et al. 2004; Ksiazek et al. 2009). Notch3 has been shown to be an important mechanism in the adhesion of ovarian cancer cells to mesothelial cells (Choi et al. 2008). Jagged-1 appears to play an important role in the regulation of this interaction. Another example is the interaction pair of proteins, namely L1 adhesion protein in cancer cells and neuropillin-1 in mesothelial cells (Stoeck et al. 2006). ALCAM is another cell surface molecule that has been indicated to possibly play a role in this interaction (Asahina et al. 2009).

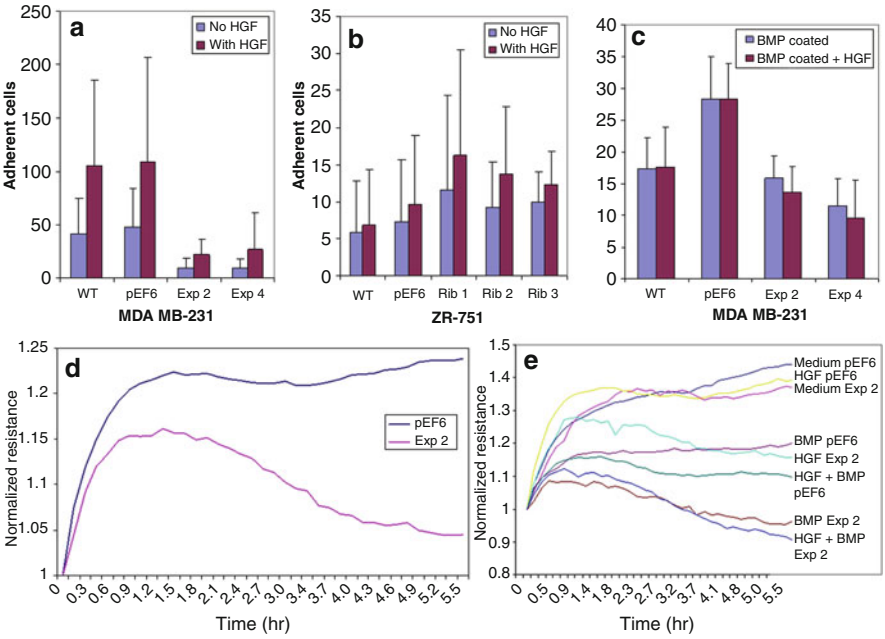

Fig. 6 (**a**) Adherence of the different ZR 751 cell lines in standard and hepatocyte growth factor (HGF). (**b**): Adherence of the different ZR 751 cell lines in standard and hepatocyte growth factor (HGF). (**c**): Adherence of the different MDA 231 cell lines in bone matrix protein (BMP) and a combination of bone matrix protein (BMP) and hepatocyte growth factor (HGF). (**d**): Attachment of MDA MB cell lines pEF6 and Exp 2 to the ECIS central electrode over a 6 h period using an ECIS-9600 model (6 stations). (**e**): Attachment of each of the MDA MB cell lines to the ECIS central electrode over a 6 h period in standard medium, bone matrix protein (BMP), hepatocyte growth factor (HGF) or a combination of BMP and HGF (Adapted from Davies and Jiang 2010)

ALCAM: ALCAM (Activated leukocyte cell adhesion molecule, or CD166) was first identified in activated leukocytes, haemopoietic stem cells and myeloid progenitors (Bowen et al. 1995; Uchida et al. 1997). It is a glycoprotein and is belonging to the immunoglobulin superfamily. When present at the cell surface, ALCAM acts as a cell-cell adhesion protein by both homophilic (ALCAM-ALCAM) and heterophilic (ALCAM-CD6) interactions (van Kempen et al. 2001). In clinical settings, ALCAM has been evaluated for its expression in human solid tumours. Approximately half of the malignant melanoma cases investigated have ALCAM positivity and the expression is seen in the vertical growth phase of melanoma (van Kempen et al. 2001). In prostate cancer, colorectal carcinoma and oesophageal squamous cell carcinoma, ALCAM expression was lost in high grade tumours (Kristiansen et al. 2003; Weichert et al. 2004; King et al. 2004; Verma et al. 2005, Jezierska et al. 2006*)* ALCAM expression level is linked to both the clinical outcome and the presence of bone metastasis (Davies et al. 2008). As show in Fig. 6, when breast cancer cells expressed higher levels of ALCAM, they exhibit slow pace of cell growth and marked reduction in cell migration rate. When ALCAM expressed

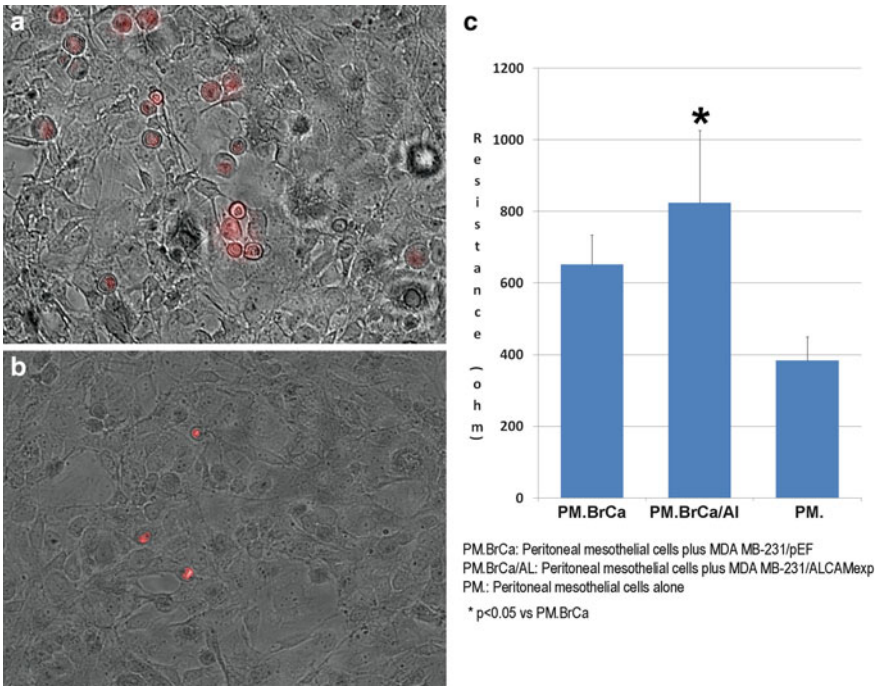

Fig. 7 Interaction between human breast cancer cells, modified for ALCAM expression and primary peritoneal mesothelial cells. (**a**) and (**b**): Direct visualisation of the interaction between control breast cancer cells (**a**) and breast cancer cells over-expressing ALCAM (**b**). Mesothelial cells were added to a 24-well culture plate and allow to reach confluence overnight. DiI (*red cells*) were added to mesothelial cells for 40 min, followed by washing. Photos of the same frame were taken using inverted phase contrast and immunofluorescence microscope and superimposed. Based ground cells are mesothelial cells and red -labelled cells are breast cancer cells. (**c**): Electric resistance during tumour-mesothelial interactions. Primary cultured peritoneal mesothelial cells (id 820) were added to 96-well 96W1E ECIS array for overnight. Breast cancer cell line, MDA MB-231 (control cells or cells transfected with ALCAM expression vector, Exp-2 as in Fig. 5) were added. The resistance was immediately traced using the Ztheta ECIS instrument. Shown are normalised resistance after cell modelling. * vs. MDA MB-231/pEF control cells

is knocked down, the cells have a marked increase in migration rate, particularly in the presence of bone matrix proteins (Davies and Jiang 2010 and Fig. 6). Collectively, it is suggested that ALCAM plays an inhibitory role in tumour-matrix adhesion and migration.

ALCAM expression and tumour-mesothelial interaction. Based on the finding that ALCAM a player in tumour-matrix interaction and possibly in tumour-mesothelial interaction, we created an ECIS-based cell model system to evaluate the role. First, using the same technique employed in Fig. 1, breast cancer cells were first labelled with DiI. After washing, these pre-labelled breast cancer were added to primary culture mesothelial monolayer, followed by washing. As shown in Fig. 7a, b, breast cancer cell, MDA MB-231 control cells which were largely negative for

ALCAM adhered to mesothelial cells (red cells in Fig. 7a). However, MDA MB-231 cells over-expressing ALCAM showed marked reduction in the test (Fig. 7b). Using ECIS based method as shown in Fig. 7c, addition of breast cancer cells to mesothelial cells triggered the mesothelial cells with an increase in resistance, possibly a defence mechanism of the cell. Breast cancer cells carried ACAM triggered a more vigorous response from mesothelial cells with a significantly increased resistance. These observations thus lead to suggestion that ALCAM on cancer cells acts as a protective mechanism when tumour cells meet mesothelial cells, by doing so it hinders the adhesion between the two cell types

4 Summary and Conclusion

Interactions between cancer cells and endothelial/mesothelial cells is a key mechanism during the systemic and transcoelomic spread of cancer cells in the body. Evaluation of the ability of cancer cells to interact with endothelial and mesothelial cells is an important aspect in determining the metastatic potential and aggressiveness of cancer cells. Impedance based method provides a label free, automated and high throughput monitor method in evaluating the interaction. It also allows observation of the dynamic changes during the interaction, without a human interface, thus offering a new approach in the investigation of the aggressiveness of cancer cells.

Acknowledgement The authors wish to thank Cancer Research Wales, Albert Hung Foundation, Breast Cancer Hope Foundation and Robert Benjamin Ablin Cancer Foundation for supporting their work.

References

Ablin RJ, Whyard TC (1991) Identification and biological relevance of spermatozoal transglutaminase. Experientia 47:277–279

Ablin RJ, Kynaston HG, Mason MD, Jiang WG (2011) Prostate transglutaminase (TGase-4) antagonizes the anti-tumour action of MDA-7/IL-24 in prostate cancer. J Transl Med 28(9):49

Akedo H, Shinkai K, Mukai M, Mori Y, Tateishi R, Tanaka K, Yamamoto R, Morishita T (1986) Interaction of rat ascites hepatoma cells with cultured mesothelial cell layers: a model for tumor invasion. Cancer Res 46(5):2416–2422

Alkhamesi NA, Ziprin P, Pfistermuller K, Peck DH, Darzi AW (2005) ICAM-1 mediated peritoneal carcinomatosis, a target for therapeutic intervention. Clin Exp Metastasis 22:449–459

An G, Meka CS, Bright SP, Veltri RW (1999) Human prostate-specific transglutaminase gene: promoter cloning, tissue-specific expression, and down-regulation in metastatic prostate cancer. Urology 54:1105–1111

Antic T, Gong Y (2012) Tumor type and single-cell/mesothelial-like cell pattern of breast carcinoma metastases in pleural and peritoneal effusions. Diagn Cytopathol 40(4):311–315

Asahina K, Tsai SY, Li P, Ishii M, Maxson RE Jr, Sucov HM, Tsukamoto H (2009) Mesenchymal origin of hepatic stellate cells, submesothelial cells, and perivascular mesenchymal cells during mouse liver development. Hepatology 49(3):998–1011

Bowen MA, Patel DD, Li X, Modrell B, Malacko AR, Wang W-C, Marquardt H, Neubauer M, Pesando JM, Francke U, Haynes BF, Aruffo A (1995) Cloning, mapping, and characterization of activated leukocyte-cell adhesion molecule (ALCAM), a CD6 ligand. J Exp Med 181:2213–2220

Casey RC, Koch KA, Oegema TR Jr, Skubitz KM, Pambuccian SE, Grindle SM, Skubitz AP (2003) Establishment of an in vitro assay to measure the invasion of ovarian carcinoma cells through mesothelial cell monolayers. Clin Exp Metastasis 20(4):343–356

Catterall JB, Gardner MJ, Jones LM, Thompson GA, Turner GA (1994) A precise, rapid and sensitive in vitro assay to measure the adhesion of ovarian tumour cells to peritoneal mesothelial cells. Cancer Lett 87(2):199–203

Choi JH, Park JT, Davidson B, Morin PJ, Shih IeM, Wang TL (2008) Jagged-1 and Notch3 juxtacrine loop regulates ovarian tumor growth and adhesion. Cancer Res 68((14):5716–5723

Cho SY, Choi K, Jeon JH, Kim CW et al (2010) Differential alternative splicing of human transglutaminase 4 in benign prostate hyperplasia and prostate cancer. Exp Mol Med 42:310–318

Colmont CS, Raby AC, Dioszeghy V, Lebouder E, Foster TL, Jones SA, Labéta MO, Fielding CA, Topley N (2011) Human peritoneal mesothelial cells respond to bacterial ligands through a specific subset of Toll-like receptors. Nephrol Dial Transplant 26(12):4079–4090, Epub 2011 Jun 1

Croft DR, Sahai E, Mavria G, Li S, Tsai J, Lee WMF, Marshall CJ, Olson MF (2004) Conditional ROCK activation in vivo induces tumor cell dissemination and angiogenesis. Cancer Res 64:8994–9001

Cunliffe WJ, Sugarbaker PH (1989) Gastrointestinal malignancy: rationale for adjuvant therapy using early postoperative Intraperitoneal chemotherapy. Br J Surg 76:1082–1090

Davies S, Jiang WG (2010) ALCAM, activated leukocyte cell adhesion molecule, influences the aggressive nature of breast cancer cells, a potential connection to bone metastasis. Anticancer Res 30(4):1163–1168

Davies G, Ablin RJ, Mason MD, Jiang WG (2007) Expression of the prostate transglutaminase (TGase-4) in prostate cancer cells and its impact on the invasiveness of prostate cancer. J Exp Ther Oncol 6(3):257–264

Davies SR, Dent C, Watkins G, King JA, Mokbel K, Jiang WG (2008) Expression of the cell to cell adhesion molecule, ALCAM, in breast cancer patients and the potential link with skeletal metastasis. Oncol Rep 19:555–561

De Clark LS, Bridt CH, Mertens AM, Moens MM, Stevens WJ (1994) Use of fluorescent dyes in the determination of adherence of human leukocytes to endothelial cells and the effect of fluorochromes on cellular functions. J Immunol Methods 172:115–124

Dubbink HJ, de Waal L, van Haperen R, Verkaik NS, Trapman J, Romijn JC (1998) The human prostate-specific transglutaminase gene (TGM4): genomic organization, tissue-specific expression, and promoter characterization. Genomics 51:434–444

Dubbink HJ, Hoedemaeker RF, van der Kwast TH, Schroder FH, Romijn JC (1999) Human prostate-specific transglutaminase: a new prostatic marker with a unique distribution pattern. Lab Invest 79:141–150

Ford WL (1978) The preparation and labelling of lymphocytes. In: Weir DM (ed) Handbook of experimental immunology, vol 3. Blackwell Scientific, Oxford, p 23.1

Garrison RN, Kaelin LD, Heuser LS et al (1986) Malignant ascites: clinical and experimental observations. Ann Surg 203:644–651

Giaever I, Keese CR (1991) Micromotion of mammalian cells measured electrically. Proc Natl Acad Sci U S A 88:7896–7900

Hiscox SE, Jiang WG (1997a) Quantification of tumour cell-endothelial cell attachment by 1,1′-dioctadecyl-3,3,3′,3′-tetramethylindocarbocyanine (DiI). Cancer Lett 112(2):209–217

Hiscox S, Jiang WG (1997b) Regulation of endothelial CD44 expression and endothelium-tumour cell interactions by hepatocyte growth factor/scatter factor. Biochem Biophys Res Commun 233((1):1–5

Hurst SM, Wilkinson TS, McLoughlin RM, Jones S, Horiuchi S, Yamamoto N, Rose-John S, Fuller GM, Topley N, Jones SA (2001) IL-6 and its soluble receptor orchestrate a temporal

switch in the pattern of leukocyte recruitment seen during acute inflammation. Immunity 14:705–714

Jezierska A, Matysiak W, Motyl T (2006) ALCAM/CD166 protects breast cancer cells against apoptosis and autophagy. Med Sci Monit 12:263–273

Jiang H, Lin JJ, Su ZZ, Goldstein NI, Fisher PB (1995) Subtraction hybridization identifies a novel melanoma differentiation associated gene, mda-7, modulated during human melanoma differentiation, growth and progression. Oncogene 11:2477–2486

Jiang H, Su ZZ, Lin JJ, Goldstein NI, Young CSH, Fisher PB (1996) The melanoma differentiation associated gene mda-7 suppresses cancer cell growth. Proc Nat Acad Sci U S A 93:9160–9165

Jiang WG, Ablin RJ, Kynaston HG, Mason MD (2009) The prostate transglutaminase (TGase-4, TGaseP) regulates the interaction of prostate cancer and vascular endothelial cells, a potential role for the ROCK pathway. Microvasc Res 77(2):150–157

Jiang WG, Ye L, Ablin RJ, Kynaston HG, Mason MD (2010) The prostate transglutaminase, TGase-4, coordinates with the HGFL/MSP-RON system in stimulating the migration of prostate cancer cells. Int J Oncol 37(2):413–418

Jones LM, Gardner MJ et al (1995) Hyaluronic acid secreted by mesothelial cells: a natural barrier to ovarian cancer cell adhesion. Clin Exp Metastasis 13(5):373–380

Keese CR, Wegener J, Walker SR, Giaever I (2004) Electrical wound-healing assay for cells in vitro. Proc Natl Acad Sci U S A 101:1554–1559

King JA, Ofori-Acquah SF, Stevens T, Al-Mehdi AB, Fodstad O, Jiang WG (2004) Activated leukocyte cell adhesion molecule in breast cancer: prognostic indicator. Breast Cancer Res 6:478–487

Kristiansen G, Pilarsky C, Wissmann C, Stephan C, Weissbach L, Loy V, Loening S, Dietel M, Rosenthal A (2003) ALCAM/CD166 is up-regulated in low-grade prostate cancer and progressively lost in high-grade lesions. Prostate 54:34–43

Książek K, Mikula-Pietrasik J, Korybalska K, Dworacki G, Jörres A, Witowski J (2009) Senescent peritoneal mesothelial cells promote ovarian cancer cell adhesion. The role of oxidative stress-induced fibronectin. Am J Pathol 174:1230–1240

Lang MJ, Topley N (1996) Isolation, culture and characterisation of human peritoneal mesothelial cells. In: Doyle A, Griffiths JB, Newell DG (eds) Cell and tissue culture: laboratory procedures. Specialised vertebrate cultures-integumentary systems and muscular tissue. Wiley, Chichester

Lebedeva IV, Sarkar D, Su ZZ, Su Z-Z, Kitada S, Dent P, Stein CA, Reed JC, Fisher PB (2003) Bcl-2 and Bcl-X_L differentially protect human prostate cancer cells from induction of apoptosis by melanoma differentiation associated gene-7, mda-7/IL-24. Oncogene 22:8758–8773

Lessan K, Aguiar DJ, Oegema T, Siebenson L, Skubitz AP (1999) CD44 and beta1 integrin mediate ovarian carcinoma cell adhesion to peritoneal mesothelial cells. Am J Pathol 154(5):1525–1537

Li B, Zhao WD, Tan ZM, Fang WG, Zhu L, Chen YH (2006) Involvement of Rho/ROCK signalling in small cell lung cancer migration through human brain microvascular endothelial cells. FEBS Lett 580:4252–4260

Lv ZD, Wang HB et al (2012) TGF-beta1 induces peritoneal fibrosis by activating the Smad2 pathway in mesothelial cells and promotes peritoneal carcinomatosis. Int J Mol Med 29(3):373–379

McLoughlin RM, Witowski J, Robson RL, Wilkinson TS, Hurst SM, Williams AS, Williams JD, Rose-John S, Jones SA, Topley N (2003) Interplay between IFN-γ and IL-6 signaling governs neutrophil trafficking and apoptosis during acute inflammation. J Clin Invest 112:598–607

Mitsui H, Shibata K, Shiro Suzuki S, Umezu T, Mizuno M, Kajiyama H, Kikkawa F (2012) Functional interaction between peritoneal mesothelial cells and stem cells of ovarian yolk sac tumor (SC-OYST) in peritoneal dissemination. Gynecol Oncol 124:303–310

Oppenheimer-Marks N, Davis LS, Lipsky PE (1990) Human T lymphcyte adhesion to endothelial and transendothelial migration. Alteration of receptor use relates to the activation status of both the T cell and the endothelial cell. J Immunol 145:140

Robson RL, McLoughlin RM, Witowski J, Loetscher P, Wilkinson TS, Jones SA, Topley N (2001) Differential regulation of chemokine production in human peritoneal mesothelial cells: IFN-

gamma controls neutrophil migration across the mesothelium in vitro and in vivo. J Immunol 167(2):1028–1038

Sako A, Kitayama J, Yamaguchi H, Kaisaki S, Suzuki H, Fukatsu K, Fujii S, Nagawa H (2003) Vascular endothelial growth factor synthesis by human omental mesothelial cells is augmented by fibroblast growth factor-2: possible role of mesothelial cell on the development of peritoneal metastasis. J Surg Res 115(1):113–120

Stoeck A, Schlich S, Issa Y, Gschwend V, Wenger T, Herr I, Marmé A, Bourbie S, Altevogt P, Gutwein P (2006) L1 on ovarian carcinoma cells is a binding partner for Neuropilin-1 on mesothelial cells. Cancer Lett 239(2):212–226

Taka H, Shiho O, Kuroshima K, Koyama M, Tsukamoto K (1986) An improved colourimetric assay for interleukin-2. J Immunol 93:156–165

Takatsuki H, Komatsu S, Sano R, Takada Y, Tsuji T (2004) Adhesion of gastric carcinoma cells to peritoneum mediated by alpha3beta1 integrin (VLA-3). Cancer Res 64(17):6065–6070

Thornhill MH, Kyan-Aung U, Haskani DO (1990) T cells and neutrophils exhibit differential adhesion to cytokine-stimulated endothelial cells. Immunology 69:287

Tzuman YC, Sapoznik S, Granot D, Nevo N, Neeman M (2010) Peritoneal adhesion and angiogenesis in ovarian carcinoma are inversely regulated by hyaluronan: the role of gonadotropins. Neoplasia 12(1):51–60

Uchida N, Yang Z, Combs J, Pourquie O, Nguyen M, Ramanathan R, Fu J, Welply A, Chen S, Weddell G, Sharma AK, Leiby KR, Karagogeos D, Hill B, Humeau L, Stallcup WB, Hoffman R, Tsukamoto AS, Gearing DP, Peault B (1997) The characterization, molecular cloning, and expression of a novel hematopoietic cell antigen from CD34_ human bone marrow cells. Blood 89:2706–2716

van Grevenstein WM, Hofland LJ, Jeekel J, van Eijck CH (2006) The expression of adhesion molecules and the influence of inflammatory cytokines on the adhesion of human pancreatic carcinoma cells to mesothelial monolayers. Pancreas 32(4):396–402

van Kempen LC, Nelissen JM, Degen WG, Torensma R, Weidle UH, Bloemers HP, Figdor CG, Swart GW (2001) Molecular basis for the homophilic activated leukocyte cell adhesion molecule (ALCAM)-ALCAM interaction. J Biol Chem 276:25783–25790

Verma A, Shukla NK, Deo SVS, Gupta SD, Ralham R (2005) MEMD/ALCAM: a potential marker for tumor invasion and nodal metastasis in esophageal squamous cell carcinoma. Oncology 68:463–470

Watanabe T, Hashimoto T et al (2012) Production of IL1-beta by ovarian cancer cells induces mesothelial cell beta1-integrin expression facilitating peritoneal dissemination. J Ovarian Res 5(1):7

Weichert W, Knosel T, Bellach J, Dieal M, Kistianse G (2004) ALCAM/CD166 is overexpressed in colorectal carcinoma and correlates with shortened patient survival. J Clin Pathol 57:1160–1164

Application of Electric Cell-Substrate Impedance Sensing in Evaluation of Traditional Medicine on the Cellular Functions of Gastric and Colorectal Cancer Cells

Lin Ye, Ke Ji, Jiafu Ji, Rachel Hargest, and Wen G. Jiang

Abstract Evaluation of the impact of traditional medicine on cancer cells has been challenging, for many reasons including challenges to obtain suitable cell models and reliable and predictive methods. This brief chapter explores the use electric cell-substrate sensing (ECIS) in evaluation of the effect of traditional Chinese medicine *Yanzheng Xiaoji*, commonly used in patients with cancer in China including gastrointestinal malignancies, on the cellular functions of gastric and colonic cancer cells. This study has shown that the extract from the formula had a substantial inhibitory effect on the adhesion and migration of gastric cancer cells (HGC27) and colorectal cancer cells (RKO). These effects were achieved at concentrations without affecting cell growth. It is concluded therefore that ECIS is a useful tool in evaluation of the effect of traditional medicine on cancer cells.

1 Introduction

In December of 2011, a supplementary issue of Nature published correspondence about traditional Asian medicine. This raised interest in looking into the potential of using traditional Asian medicine in the battle against cancer, particularly to study and assess the relevant therapeutic approaches using current scientific research methods.

L. Ye (✉) • K. Ji • R. Hargest • W.G. Jiang
Metastasis and Angiogenesis Research Group, Institute of Cancer and Genetics, Cardiff University School of Medicine, Heath Park, Cardiff CF14 4XN, UK
e-mail: yel@cf.ac.uk

J. Ji
Metastasis and Angiogenesis Research Group, Institute of Cancer and Genetics, Cardiff University School of Medicine, Heath Park, Cardiff CF14 4XN, UK

Key Laboratory of Carcinogenesis & Translational Research (Ministry of Education), Department of Gastrointestinal Oncology, Peking University School of Oncology, Fucheng Road, Haidian District, Beijing, China

W.G. Jiang (ed.), *Electric Cell-Substrate Impedance Sensing and Cancer Metastasis*, Cancer Metastasis - Biology and Treatment 17, DOI 10.1007/978-94-007-4927-6_10,

Traditional Asian medicine includes traditional medicine practised in China, Korea, Japan, and other countries in Asia, which used to seem mystical and pseudoscientific. Although a few successes achieved in the studies of traditional medicine, such as artemisinin for malaria and arsenic trioxide for leukaemia, to date, most of the traditional remedies lack standardisation and scientific evidence to validate their effect, efficiency and applications. As a part of the traditional Asia medicine, Traditional Chinese Medicine (TCM) has been used to prevent and treat various disorders with reports since 2,000 years ago. Acupuncture and herbal remedies have been introduced and practised to some extent in Europe and other area around the world. Recent studies of TCM in cancer have been focused on molecules extracted and purified from anticancer herbs. For example, Icariside II purified from the root of Epimedium koreanum Nakai induces apoptosis of a human acute myeloid leukemia (AML) cell line U937 cells via STAT3 related signalling (Kang et al. 2012). However, the study of effect and mechanisms of TCM in the prevention and treatment of malignancies, particularly anticancer remedies comprising multiple herbs remains poor.

Yangzheng Xiaoji is a traditional Chinese medical formula that has been shown to have anti-cancer actions in patients with various solid tumours. In a recent randomised doubled blinded study of patients with primary liver cancer, patients who received conventional chemotherapy combined with *Yangzheng Xiaoji* (n = 304) showed significantly increased rate of disease remission (complete and partial remissions) compared with patients who received chemotherapy alone (n = 103) (23.3% vs. 14%, respectively, $p < 0.01$) (Zhang et al. 2009). In the study, patients who received combination therapy also had improved quality of life, based on the Karnofsky method. The formula has also been reported to be able to improve atypical hyperplasia in the stomach (Wang et al. 2008).

The mechanisms of the potential anti-cancer action of *Yangzheng Xiaoji* are not clear. It has been shown that patients who received *Yangzheng Xiaoji* and chemotherapy have less bone marrow suppression compared with those who received chemotherapy (Zhang et al. 2009). It has been suggested therefore that one of the mechanisms underlying the clinical observations is that *Yangzheng Xiaoji* may improve the immune function of the body. However, whether the formula has a direct effect on cancer cells is not clear. The current study attempted to examine and study the effect of *Yangzheng Xiaoji* on gastric and colorectal cancer cells using ECIS models with a particular focus on adhesion and migration of the cancer cells.

2 Preparation of Extract from *Yangzheng Xiaoji* for Experimental Use

Medicinal preparation of *Yangzheng Xiaoji* was subject to extraction using DMSO, balanced salt solution and ethanol, on a wheel for 24 hours at 4°C. DMSO preparation was found to be more consistent, reproducible and with better yield compared with the other two methods. DMSO extract was hence used in the subsequent experiments. The extract was standardised by quantifying the optical density of the preparation

using a spectrophotometer at wave length of 490 nm. The 1 in 20 diluted extract which gave 0.5OD was stocked as the master stock and so named as DME25 for the experiments. A test of the DME25 of a dilution up to 1:200 did not show an obvious effect on cell growth in vitro.

3 Effect of DME25 on the Adhesion of Colorectal Cancer Cells

ECIS has multiple applications in examining the cellular functions, such as cell proliferation, adhesion, migration, micromotion and invasion which have been well introduced in other chapters. Current study focuses on assessing the effect of DME25 on adhesion and migration of gastric and colorectal cancer cells. Cell adhesion is an essential function of cancer cells, and plays critical roles in cancer progression and metastasis (Golubovskaya et al. 2009; Mason et al. 2002). We examined the effect of DME25 on adhesive capacities of colorectal cancer cells (RKO) by using ECIS attachment model. RKO is a poorly differentiated colon carcinoma cell line which expresses wild-type p53.

After trypsinisation, RKO cells were harvested which was followed by centrifugation to remove the remaining trypsin. The cells were then resuspended in DMEM medium supplemented with 10% foetal bovine serum (FCS), antibiotics and 15 mM HEPES to reach a density of 40,000 cells per 100 μl. The cells were seeded into a 96-well ECIS array (96E1) which had been pretreated with 10 mM cysteine solution and stabilised to achieve optimal conduction of the electrodes. Medium contained DME25 of different dilutions and control medium were added to each well immediately. Attachment of cells to the electrode was then monitored using ECIS instrument at multiple frequencies over a period up to 4–6 hours.

RKO cells attached to the electrodes rapidly which exhibited a shorter increasing phase of the resistance (Fig. 1). The cells formed a monolayer within one and half hours indicated as the resistance shifted to a stable phase. The attachment of RKO cells were markedly reduced in exposure to DME25 in a concentration dependent manner. A dilution of 1:25,000 of DME25 had exerted an obvious effect on cell adhesion at the first half hour period of cell attachment. In a 3D model, Fig. 2 shows resistances of different frequencies over the period of attachment. A significant impairment of cell adhesion was seen in the cells exposed to DME25 (1:5,000 dilution). Resistances of RKO cells at the end of monitoring period was also analysed in accordance with the measurement at different frequencies, over a range from 1 to 64 kHz, a concentration dependent inhibition on adhesion of RKO cells was demonstrated very well with the resistances measured at frequencies from 1 to 10 kHz. At the highest frequency (64 kHz) no difference was seen in the resistances of RKO cells, as the resistance measured at this frequency is more suitable to assess conductance of cells or monolayer of cells rather than cell-substratum adhesion (Fig. 3). An inhibition of adhesion of RKO cells was clearly shown by treatment with DME25. It suggests that DME25 directly suppress cell-substrate adhesion of colorectal cancer cells which at least partially contributes to its anticancer effect.

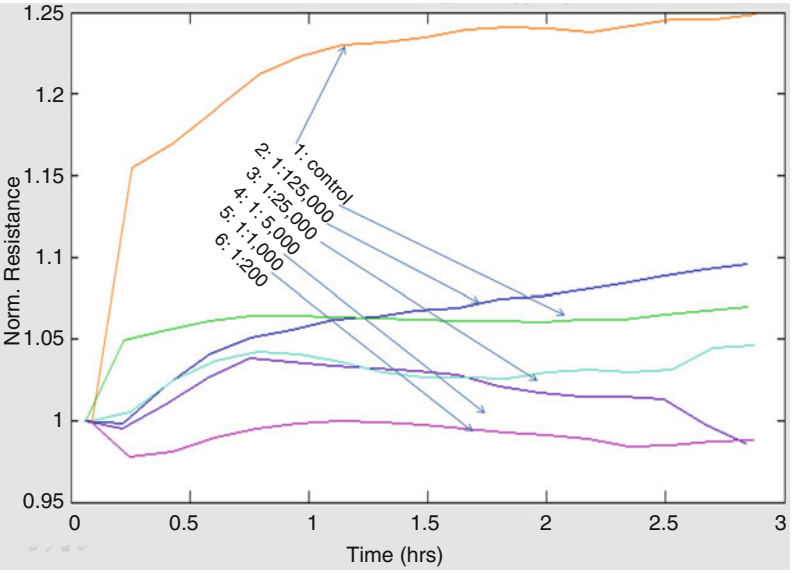

Fig. 1 Influence of DME25 on adhesion of RKO cells. The resistance was measured over a period up to 3 hours after being seeded in a 96-well array (96E1) with/without YLY compound of different dilution. The highest dilution is 1:125,000

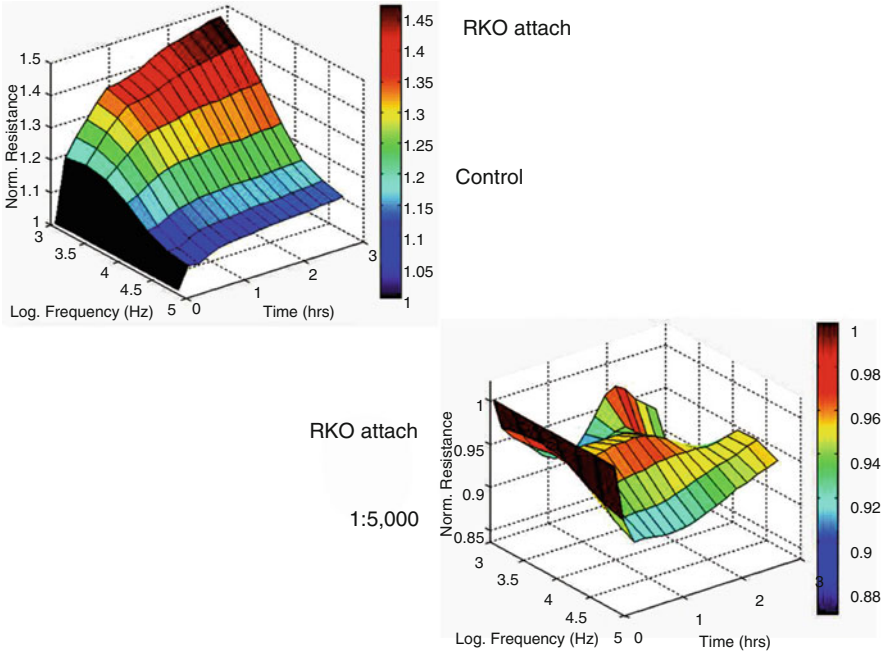

Fig. 2 Influenced of DME25 on attachment of RKO cells using ECIS shown as 3D model. Shown are changes of normalised resistance measured at different frequencies over a period up to 3 hours.

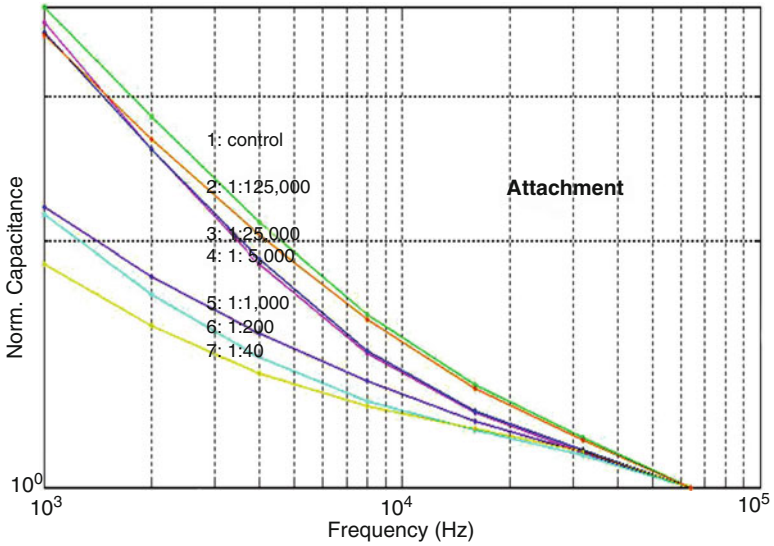

Fig. 3 A different analysis model of ECIS software is used to assess effect on cell adhesion of RKO cells. Normalised capacitance was generated to determine the adhesion RKO cells on the electrode and changes of electric conductance at different frequencies (from 1 to 64 kHz)

4 Effect of DME25 on the Adhesion of Gastric Cancer Cells

Gastric carcinoma is the second most common cancer in Eastern Asia (Jemal et al. 2011). Although *Yangzheng Xiaoji* has been traditionally used to treat malignancies at different stages, to date *Yangzheng Xiaoji* has only been shown as a remedy for management of liver cancer and gastric atypical hyperplasia (Wang et al. 2008). After the test of RKO cells, we examined the effect of DME25 on adhesion of HGC cells to explore its direct effect on functions of gastric cancer cells. HGC-27 is an undifferentiated gastric carcinoma cell line derived from metastatic lymph nodes of a Japanese gastric cancer patient.

Following the aforementioned procedure, HGC-27 cells were collected and seeded on a 96-well ECIS array (96E1), being 35,000 cells in 200 μl of medium with a series dilutions of DME25. The *Yangzheng Xiaoji* extract exerted a concentration dependent effect on the cell attachment which was demonstrated as normalised resistance at a frequency of 4 kHz (Fig. 4). The effect started to be seen in the HGC cells treated with DME25 at a dilution between 1:125,000 and 1:25,000. The most marked inhibition of cell adhesion was seen in HGC-27 exposed to the highest concentration of DME25, of which the dilution was 1:1,000. When we analysed the resistance at a higher frequency of 16 kHz, an even clearer pattern of this inhibition was seen. An obvious inhibition of the gastric cancer cells adhesion was induced by a treatment of DME25 at a dilution above 1:5,000 (Fig. 5).

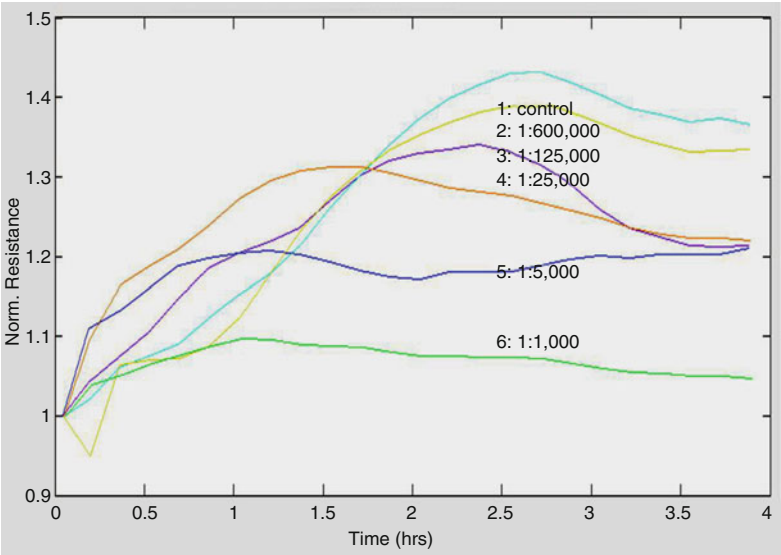

Fig. 4 Effect on adhesion of HGC27 cells by DME25 using ECIS. DME25 extract exhibits a concentration dependent inhibition on adhesion of HGC27 cells. Shown are resistance measured at 4 kHz

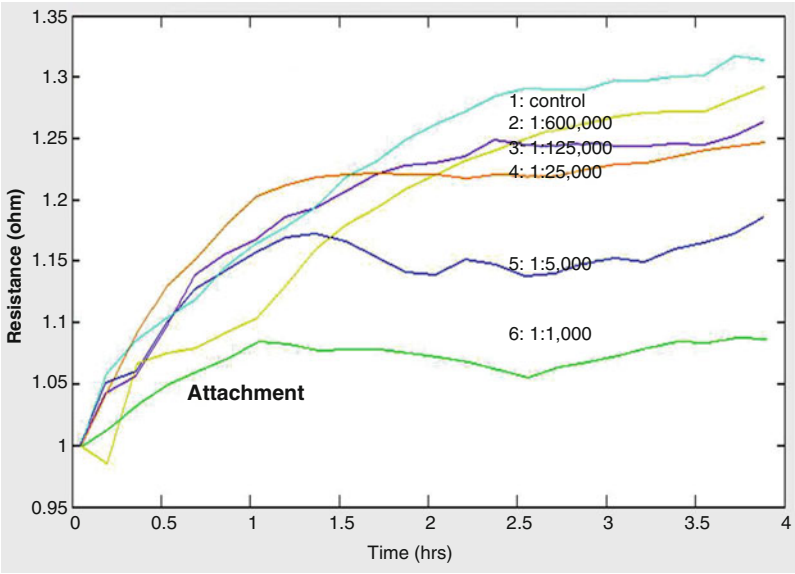

Fig. 5 Effect on adhesion of HGC27 cells by DME25 using ECIS. The extract exhibits a concentration dependent inhibition on adhesion of HGC27 cells. Shown are resistance measured at 16 kHz

5 Effect of DME25 on the Migration of Colorectal Cancer Cells

Together with cell adhesion, migrating capacity of cancer cells plays a critical role in cancer local invasion and distant spread throughout the body. In addition to the investigations of DME25 and adhesion of cancer cells, we further examined its impact on migration of cancer cells by using ECIS model (Giaever and Keese 1991, Keese et al. 2004).

As aforementioned, 30,000–40,000 cells were added to each well of a 96-well ECIS array (96E1) with or without addition of DME25 at different dilutions with 6–8 repeats per group. The array was connected to the ECIS instrument, impedance and resistance were monitored over a period of 2–6 hours allowing the cells form a monolayer before an electric wounding. A high electric pulse of 6,000 μA at 100 kHz was applied to each well for 20 seconds to physically kill the cells attached exactly to the electrodes with minimal effect on the cells surrounding the electrodes or attached at other parts of each well. The resistance was then monitored over a period up to 6–8 hours. An example of the test of colorectal cancer cells (HRT-18) is shown in Fig. 6. HRT-18 is a human rectal adenocarcinoma cell line. Following wounding, surrounding cells migrated onto the empty electrodes showed increasing

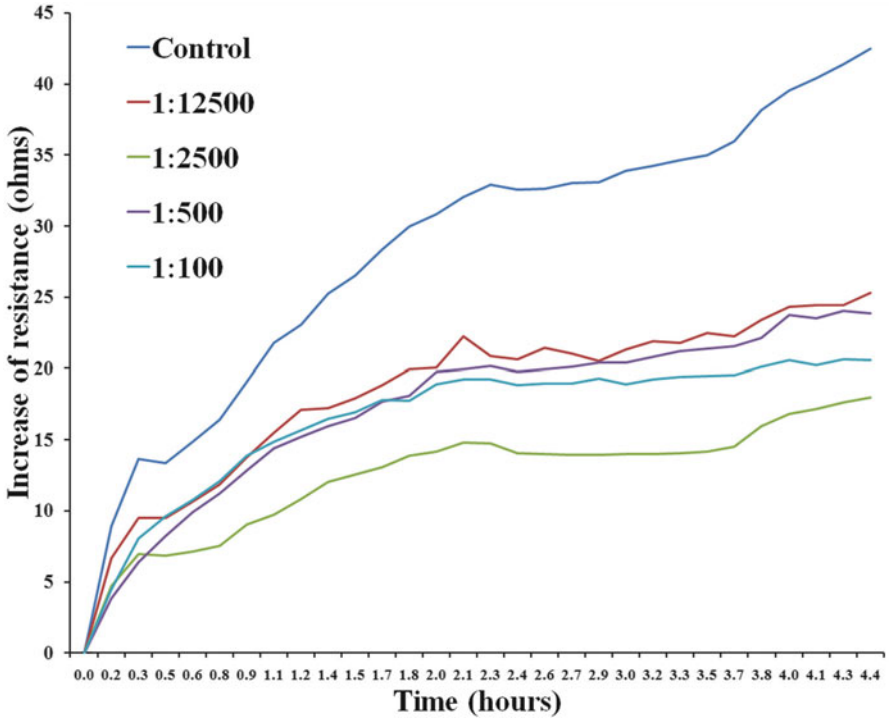

Fig. 6 DME25 affects migration of HRT18 cells using ECIS wounding model

resistances over the monitoring period. Inhibition of migration was seen in HRT-18 cells exposed to DME25 over a concentration of 1:12,500, the resistance was only restored to a level of 50% compared with the control. It indicates that DME25 not only suppresses adhesion of these cancer cells, but is also capable of inhibiting their migration.

6 Discussions and Perspectives

Adhesion and migration, together with invasion are essential capacities of gastric and colorectal cancer cells to progress to a local invasion and distant metastasis. In the current study, we firstly reported the impact on adhesion and migration of gastric and colorectal cancer cells of the *Yangzheng Xiaoji* remedy. Although the relevant underlying mechanisms are yet to investigated, it at least has partially explained its anticancer effect by directly inhibiting adhesion and migration of cancerous cells.

One of the barriers to study traditional Asian medicine is lack of high throughput methods to examine the effect on cancer cells for screening and further evaluation and investigation. In the current study, we provide examples of using ECIS instrument and relevant models to perform such tests. Although the observations and data from ECIS experiments need to be further validated and investigated using different methods, it has at least provided a platform for initial evaluation and selection for further study.

Acknowledgement The authors wish to thank Cancer Research Wales and Albert Hung Foundation for supporting their work.

References

Giaever I, Keese CR (1991) Micromotion of mammalian cells measured electrically. Proc Natl Acad Sci U S A 88:7896–7900

Golubovskaya VM, Kweh FA, Cance WG (2009) Focal adhesion kinase and cancer. Histol Histopathol 24:503–510

Jemal A, Bray F, Center MM, Ferlay J, Ward E, Forman D (2011) Global cancer statistics. CA Cancer J Clin 61:69–90

Kang SH, Jeong SJ, Kim SH, Kim JH, Jung JH, Koh W, Kim DK, Chen CY (2012) Icariside II induces apoptosis in U937 acute myeloid leukemia cells: role of inactivation of STAT3-related signaling. PLoS One 7:e28706

Keese CR, Wegener J, Walker SR, Giaever I (2004) Electrical wound-healing assay for cells in vitro. Proc Natl Acad Sci U S A 101:1554–1559

Mason MD, Davies G, Jiang WG (2002) Cell adhesion molecules and adhesion abnormalities in prostate cancer. Crit Rev Oncol Hematol 41:11–28

Wang QL, Xuo CM, Wu XP, Li YX, Bi XJ (2008) Treatment of atypical gastric dysplasia using *Yangzheng Xiaoji*. Chin J Diffic Compl Case 7:38–39

Zhang SY, Gu CH, Gao XD, Wu YL (2009) A randomly double-blinded and multicentre study of chemotherapy assisted Yangzhengxiaoji capsule on treating primary hepatic carcinoma. Chin J Diffic Compl Case 8:461–464

Electric Cell-Substrate Impedance Sensing as a Screening Tool for Wound Healing Agents

Cheuk Lun Liu, Jacqueline Chor Wing Tam, Andrew J. Sanders, David G. Jiang, Chun Hay Ko, Kwok Pui Fung, Ping Chung Leung, Keith G. Harding, Wen G. Jiang, and Clara Bik San Lau

Abstract As one of the earliest matured techniques for *in vitro* cell migration study in wound healing, traditional scratch assay has been routinely utilized due to its simplicity of setup in cell culture. However, with the emerging needs of acquiring high sensitivity and achieving high-throughput in cell behavior study, researchers in life science started to apply electric cell-substrate impedance sensing (ECIS) technology, with its automated real-time impedance monitoring and standard electrical wounding, in various study fields. Nonetheless, not much information is available regarding the application of ECIS in the screening of wound healing agents. Here we first reviewed the applications of both traditional scratch assay and

C.L. Liu • K.P. Fung
Institute of Chinese Medicine, The Chinese University of Hong Kong, Shatin, New Territories, Hong Kong

State Key Laboratory of Phytochemistry and Plant Resources in West China, The Chinese University of Hong Kong, Shatin, New Territories, Hong Kong

School of Biomedical Sciences, The Chinese University of Hong Kong, Shatin, New Territories, Hong Kong

J.C.W. Tam • C.H. Ko • P.C. Leung • C.B.S. Lau (✉)
Institute of Chinese Medicine, The Chinese University of Hong Kong, Shatin, New Territories, Hong Kong

State Key Laboratory of Phytochemistry and Plant Resources in West China, The Chinese University of Hong Kong, Shatin, New Territories, Hong Kong
e-mail: claralau@cuhk.edu.hk

A.J. Sanders • D.G. Jiang • W.G. Jiang (✉)
Metastasis and Angiogenesis Research Group, Cardiff University School of Medicine, Cardiff, UK
e-mail: Jiangw@cardiff.ac.u

K.G. Harding
Department of Dermatology and Wound Healing, Cardiff University School of Medicine, Cardiff, UK

W.G. Jiang (ed.), *Electric Cell-Substrate Impedance Sensing and Cancer Metastasis*, Cancer Metastasis - Biology and Treatment 17, DOI 10.1007/978-94-007-4927-6_11,

ECIS model in wound healing. We further used a herbal formula NF3 (comprising of individual herbs Astragali Radix and Rehmanniae Radix in the ratio of 2:1) which was previously shown to exhibit profound wound-healing effect in diabetic foot ulcer rat model, as an example for comparison of cell migration studies using both traditional scratch assay and ECIS model. To conclude, with its high sensitivity and efficiency, ECIS demonstrated its reliability as a tool for the screening of wound healing agents.

1 Introduction

Wound healing is a very orderly and orchestrated manner characterized by distinct and overlapping phases: hemostasis, inflammation, angiogenesis, proliferation and remodeling (Diegelmann and Evans 2004). This process involves the coordinated efforts of different cell types includes keratinocytes, fibroblasts, endothelial cells, macrophages and platelets (Barrientos et al. 2008). During the wound healing process, keratinocytes and fibroblasts proliferate in the wound and migrate with the help of the growth factors and take up residence in the wound (Ramzato et al. 2010). Angiogenesis is tightly coupled by angiogenic regulation and endothelial cells migrate to the wound area to form new blood vessels (Lamalice et al. 2007). An inadequate amount of angiogenesis contributes to ulcer formation (Fan et al. 1995). Cell migration plays a pivotal role in overall wound healing process. Assessment of the migrative potential of distinct cell types (i.e. keratinocytes, fibroblasts and endothelial cells) is important for the basic understanding of the molecular mechanisms involved, but also for screening of pharmaceutical compounds that modulates cell migration and thereby might exert beneficial effects in wound healing process.

1.1 In vitro Wound Models

1.1.1 Scratch Wounding Assay

The scratch wounding assay is an easy and economical *in vitro* method that allows researchers to assess a large number of testing compounds on cell motility. Traditionally, *in vitro* migration scratch assay is used by scratching the cell monolayer with pipette tips to produce an open wound mechanically. Removal of cells during wounding initiates signals to adjacent cells and induces their migration to close the wound. The progress of healing is generally estimated using microscope by analyzing the cell migration that leads to wound closure. The images are automatically calculated by software like Tscratch (Gebäck et al. 2009). Migration rate is quantified by comparing the percentage of wound closure area before and after the addition of drug treatment.

One of the major advantages of this scratch assay is that it is a simple, easily available and economical method to study cell migration *in vitro* (Liang et al. 2007).

Besides, a wide range of cells including keratinocytes, fibroblasts, endothelial cells and multipotent stem cells can also be applied to investigate the migratory response, which mimics the actual migration behavior of cells *in vivo*. Another advantage of the scratch assay is that it allows in-depth study of the underlying mechanisms and signaling pathways. It is compatible with microscopical analysis including live cell imaging or immunocytochemistry, allowing for the visualization of intracellular events. For example, tagging of green fluorescent protein for subcellular localization or staining the actin cytoskeleton of myoblasts during migration (Goetsch and Niesler 2011). Besides the simultaneous microscopic assessment of cell morphology and protein distribution, RNA and protein can also be isolated for gene and protein expression studies. In fact, the *in vitro* scratch assay has been combined with other techniques, such as gene transfection, to analyze the effect of exogenous gene towards the migration pattern of individual cell (Smita et al. 2002). Additionally, the migration scratch assay is not only restricted in the study of an individual cell population. It can be modified as a co-culture scratch wound migration assay (CCSWMA) which is composed of an *in vitro* wound healing scratch assay and the use of co-culture system with different cell populations (Oberringer et al. 2007). This advanced approach can serve as a basis for the investigation of the interaction between various cell types together with the cytokines release which is important for the understanding of wound re-epithelialization and neo-angiogenesis.

With the advanced technology development, a high-throughput screening of cell migration scratch assay has been developed in a 384 well plate format (Yarrow et al. 2004). A uniform size wound is generated by a 96 well floating-pin transfer device and the images are automatically captured in the microscopy with the feature of auto-focusing, movement between wells, imaging and image evaluation. One of the major advantages of this high-throughput screening platform is that it provides standard and consistent wound size with inexpensive reagents included in the experimental setup. Besides, this assay provides greater than 10,000 screening to be tested per day. This can allow researchers to screen the cell migration process in a quantitative and information-rich approach.

However, there are a number of limitations of the *in vitro* scratch assay compared to other cell migration methods. For example, human error may be introduced if the worker lacks experience in scratching wounds and performing data analysis. Besides, the migration scratch assay itself is only used to study the defined direction and random movement of cells, but not for detecting the chemotaxis of cell migration as no chemical gradient is established in the scratch experimental setup. Moreover, scratching and removing the cells mechanically to produce a wound may easily damage the cell to cell adhesion that interprets the cellular response and motility. Another point to be considered is that the tightly packed monolayer cells on the culture flask can lead to a wave of expansion, thus filling the wound rather than true cell migration. Furthermore, the cell migratory response generated in the migration scratch assay can be ambiguous as to whether the result is solely due to the cell migration or with the combined effect of cell proliferation (Zantek and Kinch 2001).

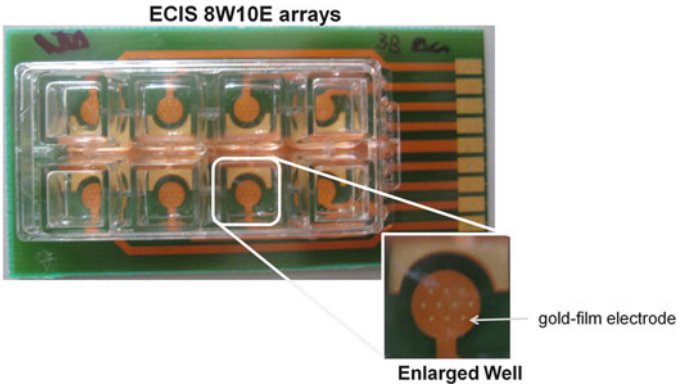

Fig. 1 ECIS array 8W10E. The ECIS arrays (Applied Biophysics Inc., Troy, USA), 8W10E, consisting of eight wells in each array and ten gold-film electrodes lied on each well (Photograph taken by CL Liu)

Despite the above limitations, migration scratch assay is the most common method for the study of cell migration in a laboratory. However, the emerging technology Electric Cell-substrate Impedance Sensing (ECIS) assay has been developed in the biological and biomedical research. ECIS is not only particularly featured in cancer research but also in wound healing study. The precise detection of ECIS on cell attachment and migration allows us to explore and further validate our results of the endothelial cell migration with different drug treatments.

1.1.2 Electric Cell-Substrate Impedance Sensing Assay

Invented by Giaever and Keese in 1980s, the electrical device, electric cell-substrate impedance sensing (ECIS) is one of the most advanced tools to study adherent cell behavior (Giaever and Keese 1984). It is widely applied in different fields, such as in the topic of cancer study (Ablin et al. 2011; Patani et al. 2010; Sharma et al. 2010), wound-healing (Gailit and Clark 1996; Hsu et al. 2010; Jiang et al. 2010; Sanders et al. 2011; Wiesner et al. 2008), toxicology (Kandasamy et al. 2010; Lee et al. 2011; Tarantola et al. 2011), asthma (Heijink et al. 2007, 2010; Ramirez-Icaza et al. 2004), and blood brain barrier (Betzen et al. 2009; Grab et al. 2009; Von Wedel-Parlow et al. 2011). A device called ECIS array is a modified culture dish with multiple wells, of which the bottom lied with small gold surface electrodes (Fig. 1). While the cell culture medium in ECIS serves as the electrolyte, the cells act as insulating agent of the system. Cells were firstly allowed to adhere to the array. With the increase in the adhesion and spreading of the cells on the electrodes, the impedance of the system in the well would increase. The resulted rate of impedance represented the rate in cell adhesion. Upon the formation of cell monolayer in the well, elevated current was introduced to generate a precise and reproducible electrical wound of the cell adhered on the small gold surface electrodes. The surrounding cells would repopulate by migrating inwards onto the electrode as post-wounding;

this would cause an increase in the impedance over time, thus represented the rate of cell migration.

As for the application of ECIS technology in wound healing studies, human skin keratinocyte HaCaT cells were commonly used. Other cell lines, such as human dermal fibroblast and endothelial cells, were also utilized. Under the umbrella of wound healing, researchers applied ECIS in the following themes: (a) cell surface integrins study for the adhesion of human dermal fibroblast (Gailit and Clark 1996); (b) negative pressures wound therapy in chronic wound treatment by applying varied negative pressures to human keratinocytes (Hsu et al. 2010); (c) novel insights of cancer metastasis related biomolecules in wound healing, i.e. WAVEs, the WASP (Wiskott–Aldrich syndrome protein) family of verprolin homologous proteins (Jiang et al. 2010) and activated leukocyte cell adhesion molecule (ALCAM) (Sanders et al. 2011); and (d) potential bioactive wound healing agents screening from a cyanobacteria, Nostoc (Wiesner et al. 2008). The main methodologies employed in these studies were ECIS cell attachment and cell migration. Among these, cell signaling inhibitors (Gailit and Clark 1996; Jiang et al. 2010) were incorporated in ECIS cell attachment or cell migration for in-depth investigation. Besides, gene knockdown of the wound healing related cell line i.e. HaCaT keratinocytes were also combined with the ECIS technology (Jiang et al. 2010; Sanders et al. 2011).

The measurement of ECIS is non-invasive and that only a small electrical current for real-time impedance detection was utilized with no observable effect on cells (Keese et al. 2004). In addition, each wound produced by ECIS machine is highly reproducible and precise. Since the ECIS machine can perform the assays in automated manner, it reduced both the time for optimization of experimental conditions and the risk of biased data processing. As for the traditional scratch wounding assay, optimization of conditions such as the time to check for the cell migration is needed. In addition, the heaps of photographs captured need further processing to reveal the actual wound size even with the most advanced scratch processing softwares. Not only is this photo-processing time consuming, experienced researchers are also required for unbiased photo-editing, otherwise, the results might be of artifacts. The ECIS assay is however designed to be high-throughput and has the function of automated real-time detection of impedance in multiple wells inside the incubator with desired cell culture incubating condition over a long period of time, i.e. can even be over 24 hours.

Although ECIS is one of the most powerful tools to study cell behavior, its use is mainly limited by its high cost. Excluding the high price of the ECIS main stations, the consumables, i.e. the arrays with gold-plated electrodes are expensive. Even though some practices facilitate the re-use of the arrays, it is recommended not to re-use the arrays for many trials since the sensitivity of the assay might be lowered in over-reused cases. Compared with traditional scratch wounding assay, it would be costly if the arrays are frequently consumed for screening purposes. In addition, the ECIS gold-film electrode array is not highly compatible with cell imaging when applying phase-contrast microscopy because of the nature of gold used (Moore et al. 2009). The images are not clear enough even if a thinner layer of gold is used. Hence, it would be difficult to obtain both real-time data of impedance and cell visual image at the same time.

In this chapter, we will review these two migration methods, traditional scratch assay and electric cell-substrate impedance sensing (ECIS), for the *in vitro* study of endothelial cells, keratinocytes and fibroblasts behavior in wound healing mechanism. Based on our previous study, a two-herbs Chinese medicine formula (NF3), comprising of individual herbs Astragali Radix (the root of *Astragalus membranaceus*) and Rehmanniae Radix (the root of *Rehmannia glutinosa*) in the ratio of 2 to 1, was used in the wound healing of diabetic foot ulcer rats and that NF3 was found to act through the promotion of angiogenesis, anti-inflammation and tissue regeneration (Tam et al. 2011). Hence, in the following section, using NF3 as an example, comparison of the study of cell migration using traditional scratch assay and electric cell-substrate impedance sensing (ECIS) model will be performed.

2 Methods and Results

2.1 Scratch Wounding Assay

The migration of human keratinocyte cells (HaCaT) and human umbilical vein endothelial cells (HUVEC) were examined using the wound healing method. HaCaT (German Cancer Institute, Heidelberg, Germany; 2×10^5 cells) and HUVEC (ATCC, USA; 1×10^5 cells) were separately seeded into each well of a 24-well plate and incubated with complete medium at 37 °C and 5 % CO_2. After 24 h of incubation, the cells were starved in medium with 0.5 %v/v FBS for another 24 h. The cells were scrapped horizontally and vertically with a P100 pipette tip and top views of the cross (Fig. 2) were photographed in each well using a camera attached to a microscope at 4× magnification. The medium was replaced with fresh medium in the absence (control group) or presence of NF3 (4.5–37.5 μg/ml for HaCaT and 18.75–300 μg/ml for HUVEC; treatment group). After 24 h of incubation for HaCaT and 16 h of incubation for HUVEC, the second set of images was photographed. To determine the migration of cells, the images were analyzed using Tscratch software. Percentage of the closed area was measured and compared with the value obtained before treatment. An increase of the percentage of closed area indicated cell migration.

Here, we used the cell lines HaCaT and HUVEC as examples to illustrate the wound healing ability of NF3 in the migration scratch assay. As shown in Fig. 3a, 9 μg/ml of NF3 could mildly stimulate HaCaT migration after 24 h, but no statistical significance was achieved; while NF3 (37.5, 75 and 150 μg/ml) could significantly ($p < 0.001$) enhance HUVEC migration after 16 h of incubation by 67, 61 and 50 %, respectively (Fig. 3b). Hence, NF3 could stimulate HUVEC migration in a dose dependent manner in the wound healing scratch assay after 16 h of incubation. From the above finding, we could conclude that administration of NF3 promoted HUVEC migration, mimicking the endothelial cells migration in angiogenesis during *in vivo* wound healing.

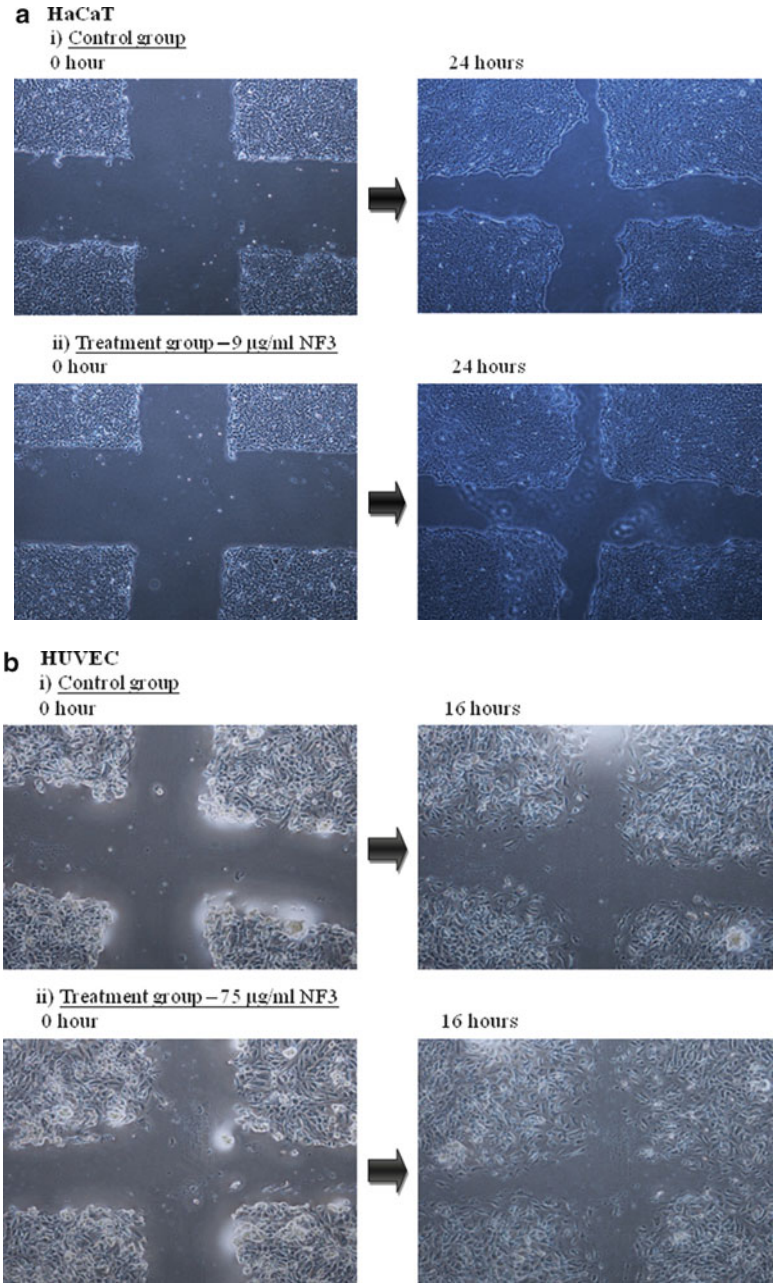

Fig. 2 Scratch images of HaCaT and HUVEC in migration scratch assay. (**a**) Scratch images of HaCaT in (i) control group; (ii) 9 µg/ml NF3 treatment group. (**b**) Scratch images of HUVEC in (i) control group; (ii) 75 µg/ml NF3 treatment group. Cells were scratched horizontally and vertically with P100 pipette tips. Images were captured at 0 h and after 24 h of incubation for HaCaT; and after 16 h of incubation for HUVEC

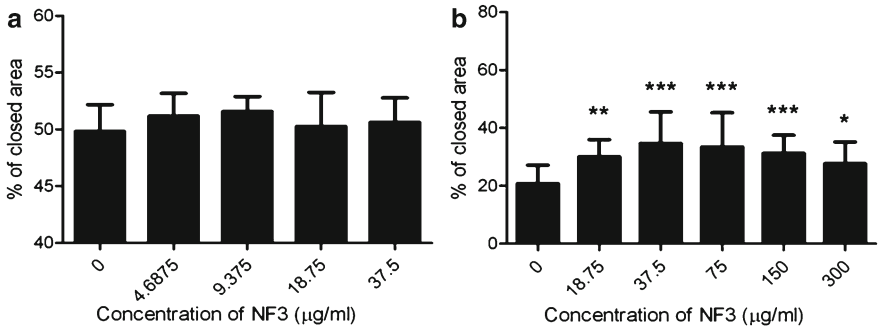

Fig. 3 Effect of NF3 on (a) HaCaT and (b) HUVEC migration in migration scratch assay. Cells were scratched horizontally and vertically with P100 pipette tips. Images were captured at 0 h and various concentrations of NF3 (0–37.5 μg/ml for HaCaT and 0–300 μg/ml for HUVEC) were then added to the wells. Another set of images were photographed after 24 h of incubation for HaCaT and 16 h of incubation for HUVEC. Data are expressed as mean±SD from three to five individual experiments. *$p<0.05$, **$p<0.01$ and ***$p<0.001$ for differences in percentage of closed area from baseline culture without treatment, using one-way ANOVA with Dunnett test

2.2 Electric Cell-Substrate Impedance Sensing (ECIS) Assay

For comparison, the same human keratinocyte cell line (HaCaT) was used in this ECIS assay. The keratinocyte culture was maintained at 37 °C in DMEM-F12 (Sigma, St. Louis, USA), supplemented with 1 % penicillin-streptomycin, and 10 %v/v fetal calf serum (PAA Laboratories Ltd, Somerset, UK).

The ECIS model 9600 (Applied Biophysics Inc., Troy, USA) was employed for studying the effect of NF3 on HaCaT cell migration with reference to previous studies (Keese et al. 2004; Sanders et al. 2011). The ECIS arrays (Applied Biophysics Inc., Troy, USA) used here were 8W10E, consisting of eight wells in each array and ten gold-film electrodes lied on each well (Fig. 1). For stabilization, the ECIS array surface were firstly treated with 10 mM L-cysteine solution for 40 min, and the arrays were then washed with complete medium thrice. For the experimental procedures, in brief, HaCaT cells (300 k cells per well) were plated onto the ECIS 8W10E arrays with simultaneous control group (culture medium only) and NF3 treatment of final concentrations of 1, 10, 100 and 1,000 μg/ml. Cells were allowed to form a confluent monolayer for 4 h; the monolayer was then electrically wounded at 6 V for 30 s. Ten identical wounds were then created in each well. Average impedance from the ten wounds was immediately tracked for up to 4 h post-wounding. The average rate of impedance represented the rate of cell migration. Cell migration was analyzed using ECIS software provided by the manufacturer. Results were presented as the impedance normalized to the impedance tracked at time zero (immediately after wounding).

Here, electric cell-substrate impedance sensing (ECIS) was employed for the advanced study of cell attachment and cell migration activity of NF3. Unlike

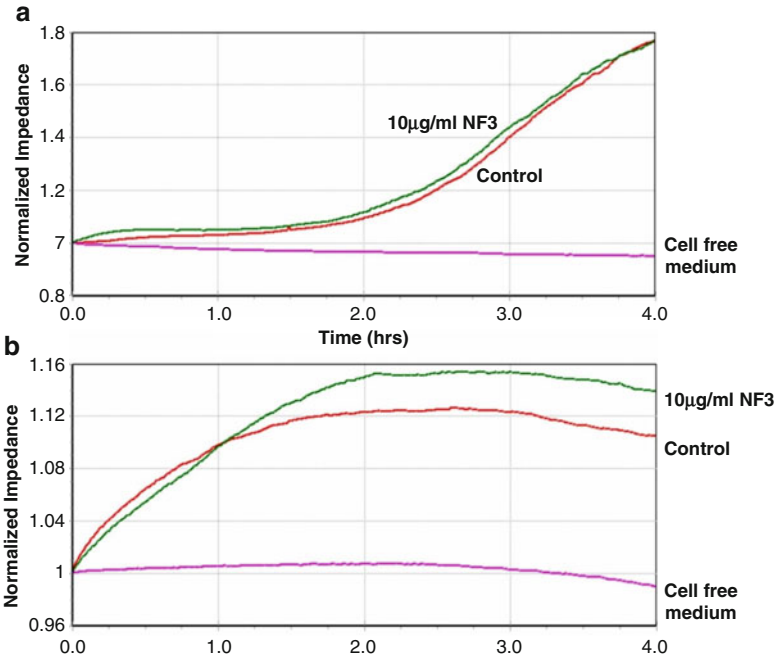

Fig. 4 The effect of NF3 on cell attachment and cell migration using ECIS. The rate of impedance of 10 μg/ml of NF3 sample, medium control, and cell free medium were shown. (**a**) After the simultaneous cell seeding and sample treatment, the NF3-treated HaCaT cells attachment showed a similar trend to that of the medium control (without treatment). (**b**) HaCaT cells were electrically wounded at 6 V for 30 s. The NF3-treated cells migrated at a faster manner from 1-h post-wounding comparing with the medium control

traditional scratch migration assay, an extra function of ECIS is that cell attachment can also be examined. Applying ECIS in cell attachment, 10 μg/ml of NF3-treated HaCaT cells showed a similar trend in cell attachment to the medium control (Fig. 4a). However, regarding the 4-h track of normalized impedance recorded immediately after electrical wounding, HaCaT cells with 10 μg/ml of NF3 treatment exhibited a faster pace of cell migration detected as early as from 1-h post electrical wounding when compared with its medium control (Fig. 4b).

3 Discussion

The migration scratch assay is one of the earliest developed methods in studying cell migration *in vitro* and it is widely used in laboratory due to the simple cell culture setup. In the wound healing research aspect, the basis of the scratch assay involves the artificially removal of cell monolayer to produce a wound following by subsequent cell movement to close the wound. Although this method is not an exact

Table 1 Table showing the comparison between two cell migration assays: scratch vs. ECIS

	Scratch migration assay	ECIS assay
Sensitivity	Low	High (can detect nanometer change of cell behavior (Lo et al. 1993))
Reproducibility	Variation due to scratching procedure	Standard wound generated
Labor	Laborious with skillful technicians; optimization of experimental conditions required	Automated with real-time monitoring; minimal optimization is needed
Sample size per plate	≤24	≤96
Duration of assay	6–24 h (cell types dependent)	2–16 h (cell types dependent)
Data acquisition and analysis	Fixed time image capturing with microscope connected to digital camera; image processing software required	Tailor-made devices and software for detection and processing
Image resolution	High	Poor (due to the gold-film electrodes)
Cost	Low cost with simple experimental cell culture setup	Expensive instrument and consumables
Compatibility with other techniques	Highly compatible with RNA or protein expression analysis and immunohistochemical staining; can be modified into co-culture system	Limited compatibility with RNA expression analysis

replication of cell migration *in vivo*, it mimics the migration of different types of cells in wound healing to certain extent. One of the major advantages of scratch assay is related to its high compatibility with other techniques such as immunohistochemistry or RNA and protein extraction and expression analysis. This allows the researchers to conduct in-depth studies of the underlying signaling pathways and mechanisms. Besides, the scratch assay can be modified into co-culture system for the interaction study of different cell types. In addition, it has been developed in a 384-well plate platform for the high-throughput screening of chemo-attractants or repellants in cell migration. However, some limitations have to be highlighted in migration scratch assay. The scratching procedure produces wound size variation in each well. Besides, the results obtained can sometimes be ambiguous owning to the true cell migratory response or the cell to cell adhesion. Moreover, the sensitivity of this assay is relatively low as it is based on observation with microscopic imaging instead of a real time detection method.

With the demand of acquiring high sensitivity in the study of cell behavior, researchers in life science started to apply ECIS technology in their dynamic fields of study, for example, in cancer research. ECIS technology took over traditional scratch assay in various aspects in which some of the most appealing benefits would be its high sensitivity and the high reproducibility of its electrical wounds as summarized in Table 1.

Since mid-1990s, researchers started to apply ECIS for the advanced study in wound repair. Gailit and Clark (1996), a US research group in Dermatology used ECIS technology to reveal the function of integrins utilized by normal human adult dermal fibroblasts for the adhesion to the components of wound provisional matrix. The group demonstrated that ECIS was sensitive enough to reveal the weak interactions in fibroblast attachment to pure fibrinogen that even the standard adhesion assay cannot be detected. The group also further confirmed the participation of integrins in fibroblast attachment through ECIS, using inhibitory and non-inhibitory peptides, RGD and RGE, respectively. The study aided to understand in-depth as to how the fibroblasts from normal tissues migrate into the wound provisional matrix using their cell surface integrins in the phase of wound healing.

In late 2000s, Wiesner et al. (2008) from Krems, Austria, published a short communication about the screening of potential bioactive wound healing agents from a cyanobacteria, known as Nostoc, using ECIS techniques. They revealed that 6 % of the bioactive agents possessed wound healing functions.

In 2010, Hsu et al. (2010), a research group from Taiwan applied ECIS for the investigation of the effects of negative pressures on epithelial tight junctions and migration in wound healing. Coupling the negative pressure incubator for the generation of various negative pressures with ECIS technology, the optimal negative pressure for the greatest wound healing rate was found to be at 125 mmHg negative pressure by ECIS through screening with a range of negative pressures. These findings were crucial for their subsequent validation of cell migration features using traditional wound healing assay for fluorescent staining of cell junction proteins of which disassembly of cell junction was observed at 125 mmHg negative pressure; hence, the disassembly facilitated epithelial migration for faster wound closure. In August 2010, Jiang et al. published an article concerning a novel link of cancer metastasis related biomolecules, i.e. WAVEs, the WASP (Wiskott–Aldrich syndrome protein) family of verprolin homologous proteins in wound repair study using ECIS (Jiang et al. 2010). The group revealed that knocking down WAVE-3 in human keratinocyte cell line showed remarkable reduction in cell migration using ECIS; while the overexpression of WAVE-2 revealed a distinct increase in cell migration. The study also investigated the signaling pathway of cell migration using signaling inhibitors coupled with ECIS wound healing assay. Besides, it was demonstrated that the effect of WAVE upon cell motility was independent of the PLCg and ERK pathways, however, the downstream needed phosphatidylinositol 3-kinase (PI3K) and RHO-associated coiled-coil-containing protein kinase (ROCK) pathways. The work suggested the crucial roles of WAVE family proteins towards reepithelialization of keratinocytes, and the WAVE proteins could contribute invaluable therapeutic significance in wound repair.

Recently in 2011, Sanders et al. reported the function of activated leukocyte cell adhesion molecule (ALCAM) in wound repair (Sanders et al. 2011). ALCAM expression was shown to increase in non-healing types of chronic venous leg ulcers. With the suppression of ALCAM by gene knockdown, HaCaT cells showed enhanced migration tracked by ECIS. The article gave insights on the effect of cell migration towards chronic wound healing.

However, up till today, not much information is available regarding the application of ECIS in the screening of wound healing agents. Using herbal formula NF3 as an example for studying wound healing agents with ECIS technology, the wound healing mechanisms (cell attachment and cell migration) of NF3 in wound healing associated cell types (i.e. keratinocytes and endothelial cells) were investigated.

Cell migration and cell attachment of keratinocytes are crucial processes in wound repair (Grinnell et al. 1987; Grinnell 1990). In the migration scratch assay, we showed that 9 μg/ml of NF3 treatment could mildly (without significance) enhance HaCaT migration after 24 h of incubation. However, in our study applying ECIS, we demonstrated that even at 10 μg/ml of NF3 treatment could induce an increase in HaCaT migration as early as from 1-h post-electrical-wounding, though not enhancing HaCaT cell attachment. In this example of HaCaT migration, both migration scratch assay and ECIS could demonstrate migratory response of HaCaT with NF3 treatment. However, when comparing the sensitivity of both assays, only a slight increase in HaCaT migration was detected in scratch assay after 24 h incubation; whereas in ECIS, there was obvious cell migration observed in HaCaT as early as 1-h-post-electrical-wounding. Hence, the sensitivity of ECIS is in fact higher than the scratch assay as ECIS can assess cell migration in a more efficient manner with real time detection.

From our results, the increase in HaCaT migration by NF3 can be one of the potential mechanisms of the improved wound healing effect of NF3 as demonstrated in our diabetic rat foot ulcer study. As for endothelial cells, NF3 helped in promoting HUVEC migration; the increased endothelial cell migration could facilitate the process of angiogenesis, leading to the enhanced wound healing effects of NF3. Up till now, regarding the studies of wound healing agents using ECIS, little is known with the use of endothelial cells. Our future work would help to fill this gap by using endothelial cells to study NF3 in ECIS.

In conclusion, with its high sensitivity and efficiency, ECIS demonstrated its reliability as a tool for the screening of wound healing agents.

Acknowledgement This study was supported by the University Grants Committee of the Hong Kong SAR under the Area of Excellence project "Chinese Medicine Research and Further Development" (Ref. No. AoE/B-10/01). We would also like to thank Hop Wai short-term research fellowship for the sponsorship of ECIS training in Cardiff University School of Medicine, Cardiff, United Kingdom.

References

Ablin RJ, Kynaston HG, Mason MD, Jiang WG (2011) Prostate transglutaminase (TGase-4) antagonizes the anti-tumour action of MDA-7/IL-24 in prostate cancer. J Transl Med 9:49

Barrientos S, Stojadinovic O, Golinko MS, Brem H, Tomic-Canic M (2008) Growth factors and cytokines in wound healing. Wound Repair Regen 16:585–601

Betzen C, White R, Zehendner CM, Pietrowski E, Bender B, Luhmann HJ, Kuhlmann CR (2009) Oxidative stress upregulates the NMDA receptor on cerebrovascular endothelium. Free Radic Biol Med 47:1212–1220

Diegelmann RF, Evans MC (2004) Wound healing: an overview of acute, fibrotic and delayed healing. Front Biosci 9:283–289
Fan TPD, Jaggar R, Bicknell R (1995) Controlling the vasculature: angiogenesis, anti-angiogenesis and vascular targeting of gene therapy. Trends Pharmacol Sci 16:57–66
Gailit J, Clark RA (1996) Studies *in vitro* on the role of alpha v and beta 1 integrins in the adhesion of human dermal fibroblasts to provisional matrix proteins fibronectin, vitronectin, and fibrinogen. J Invest Dermatol 106:102–108
Gebäck T, Schulz MMP, Koumoutsakos P, Detmar M (2009) Tscratch: a novel and simple software tool for automated analysis of monolayer wound healing assays. Short Tech Rep 46:265–274
Giaever I, Keese CR (1984) Monitoring fibroblast behavior in tissue culture with an applied electric field. Proc Natl Acad Sci U S A 81:3761–3764
Goetsch KP, Niesler CU (2011) Optimization of the scratch assay for *in vitro* skeletal muscle wound healing analysis. Anal Biochem 411:158–160
Grab DJ, Nyarko E, Nikolskaia OV, Kim YV, Dumler JS (2009) Human brain microvascular endothelial cell traversal by *Borrelia burgdorferi* requires calcium signaling. Clin Microbiol Infect 15:422–426
Grinnell F (1990) The activated keratinocyte: upregulation of cell adhesion and migration during wound healing. J Trauma 30:S144–S149
Grinnell F, Toda K, Takashima A (1987) Activation of keratinocyte fibronectin receptor function during cutaneous wound healing. J Cell Sci 8:199–209
Heijink IH, Kies PM, Kauffman HF, Postma DS, Van Oosterhout AJ, Vellenga E (2007) Down-regulation of E-cadherin in human bronchial epithelial cells leads to epidermal growth factor receptor-dependent Th2 cell-promoting activity. J Immunol 178:7678–7685
Heijink IH, Brandenburg SM, Noordhoek JA, Postma DS, Slebos DJ, van Oosterhout AJ (2010) Characterisation of cell adhesion in airway epithelial cell types using electric cell-substrate impedance sensing. Eur Respir J 35:894–903
Hsu CC, Tsai WC, Chen CP, Lu YM, Wang JS (2010) Effects of negative pressures on epithelial tight junctions and migration in wound healing. Am J Cell Physiol 299:C528–C534
Jiang WG, Ye L, Patel G, Harding KG (2010) Expression of WAVEs, the WASP (Wiskott-Aldrich syndrome protein) family of verprolin homologous proteins in human wound tissues and the biological influence on human keratinocytes. Wound Repair Regen 18:594–604
Kandasamy K, Choi CS, Kim S (2010) An efficient analysis of nanomaterial cytotoxicity based on bioimpedance. Nanotechnology 21:375501–375510
Keese CR, Wegener J, Walker SR, Giaever I (2004) Electrical wound-healing assay for cells *in vitro*. Proc Natl Acad Sci U S A 101:1554–1559
Lamalice L, Boeuf FL, Huot J (2007) Endothelial cell migration during angiogenesis. Circ Res 100:782–794
Lee WK, Torchalski B, Kohistani N, Thévenod F (2011) ABCB1 protects kidney proximal tubule cells against cadmium-induced apoptosis: roles of cadmium and ceramide transport. Toxicol Sci 121:343–356
Liang CC, Park AY, Guan JL (2007) *In vitro* scratch assay: a convenient and inexpensive method for analysis of cell migration *in vitro*. Nat Protoc 2:2
Lo CM, Keese CR, Giaever I (1993) Monitoring motion of confluent cells in tissue culture. Exp Cell Res 204:102–109
Moore E, Rawley O, Wood T, Galvin P (2009) Monitoring of cell growth *in vitro* using biochips packaged with indium tin oxide sensors. Sens Actuator B Chem 139:187–193
Oberringer M, Meins C, Bubel M, Pohlemann T (2007) A new *in vitro* wound model based on the co-culture of human dermal microvascular endothelial cells and human dermal fibroblasts. Biol Cell 99:197–207
Patani N, Douglas-Jones A, Mansel R, Jiang W, Mokbel K (2010) Tumour suppressor function of MDA-7/IL-24 in human breast cancer. Cancer Cell Int 10:29
Ramirez-Icaza G, Mohammed KA, Nasreen N, Van Horn RD, Hardwick JA, Sanders KL, Tian J, Ramirez-Icaza C, Johnson MT, Antony VB (2004) Th2 cytokines IL-4 and IL-13 downregulate paxillin expression in bronchial airway epithelial cells. J Clin Immunol 24:426–434

Ramzato E, Martinotti S, Volante A, Mazzucco L, Burlando B (2010) Platelet lyzate modulates MMP-2 and MMP-9 expression, matrix deposition and cell-to-matrix adhesion in keratinocytes and fibroblasts. Exp Dermatol 20:308–313

Sanders AJ, Jiang DG, Jiang WG, Harding KG, Patel GK (2011) Activated leukocyte cell adhesion molecule impacts on clinical wound healing and inhibits HaCaT migration. Int Wound J 8:500–507

Sharma D, Wang J, Fu PP, Sharma S, Nagalingam A, Mells J, Handy J, Page AJ, Cohen C, Anania FA, Saxena NK (2010) Adiponectin antagonizes the oncogenic actions of leptin in hepatocellular carcinogenesis. Hepatology 52:1713–1722

Smita A, Hiroki U, Zheng CH, Cooper LA, Zhao J, Christopher R, Guan JL (2002) Regulation of focal adhesion kinase by a novel protein inhibitor FIP200. Mol Biol Cell 13:3178–3191

Tam JCW, Lau KM, Liu CL, To MH, Kwok HF, Lai KK, Lau CP, Ko CH, Leung PC, Fung KP, Lau CBS (2011) The *in vivo* and *in vitro* diabetic wound healing effects of a 2-herb formula and its mechanisms of action. J Ethnopharmacol 134:831–838

Tarantola M, Pietuch A, Schneider D, Rother J, Sunnick E, Rosman C, Pierrat S, Sönnichsen C, Wegener J, Janshoff A (2011) Toxicity of gold-nanoparticles: synergistic effects of shape and surface functionalization on micromotility of epithelial cells. Nanotoxicology 5:254–268

Von Wedel-Parlow M, Schrot S, Lemmen J, Treeratanapiboon L, Wegener J, Galla HJ (2011) Neutrophils cross the BBB primarily on transcellular pathways: an *in vitro* study. Brain Res 1367:62–76

Wiesner C, Pflüger M, Kopecky J, Stys D, Entler B, Lucas R, Hundsberger H, Schütt W (2008) Implementation of ECIS technology for the characterization of potential therapeutic drugs that promote wound-healing. GMS Krankenhhyg Interdiszip 3:Doc05

Yarrow JC, Perlman ZE, Westwood NJ, Mitchison TJ (2004) A high-throughput cell migration assay using scratch wound healing, a comparison of image-based readout methods. BMC Biotechnol 4:21

Zantek ND, Kinch MS (2001) Analysis of cell migration. Method Cell Biol 63:549–559

ECIS, Cellular Adhesion and Migration in Keratinocytes

David C. Bosanquet, Keith G. Harding, and Wen G. Jiang

Abstract Evaluation of keratinocyte adhesion and migration using ECIS, as will be shown below, is predominantly used to study the effects of various genes, proteins and molecules on wound healing. Keratinocytes undertake epithelialisation during the process of wound healing, and understanding their function, and their regulating factors, is important in understanding why some wounds fail to heal. This chapter will detail the physiology behind wound healing and epithelialisation, and explore the problem that chronic wounds pose to the clinician today. It will also highlight the importance of both adhesion and migration in cellular movements. Furthermore it will detail the methods by which ECIS has been used to evaluate keratinocyte function, and discuss various methods of interpreting ECIS results. Finally, it will review the current literature on ECIS evaluation of keratinocyte function.

Abbreviations

AC	Alternating Current
ALCAM	Activated Leukocyte Cell Adhesion Molecule
BMP7	Bone Morphogenetic Protein 7
CWIS	Cardiff Wound Impact Schedule
DC	Direct Current
DM	Diabetes Mellitus
DVT	Deep Vein Thrombosis
ECIS	Electrical Cell-Substrate Impedance Sensing

D.C. Bosanquet (✉) • K.G. Harding • W.G. Jiang
Departments of Wound Healing and Surgery, Cardiff University School of Medicine, Heath Park, Cardiff CF14 4XN, UK
e-mail: davebosanquet@hotmail.com

W.G. Jiang (ed.), *Electric Cell-Substrate Impedance Sensing and Cancer Metastasis*, Cancer Metastasis - Biology and Treatment 17, DOI 10.1007/978-94-007-4927-6_12,

ECM	Extra Cellular Matrix
Ehm2	Expressed in high metastatic cells 2
EPLIN	Epithelial Protein Lost In Neoplasm
FAs	Focal Adhesions
HRQoL	Health-related quality of life
HuR	Human antigen R
IL8	Interleukin 8
MDA7	Melanoma Differentiation Associated gene 7
NPFs	Nucleation-Promoting Factors
PAD	Peripheral Arterial Disease
PIP2	Phosphatidylinositol 4,5-bisphosphate
TEM8	Tumour Endothelial Marker 8
WAVE	Wiskott–Aldrich syndrome protein family VErprolin homologs

1 Wound Healing and Chronic Wounds

1.1 Wound Healing

A wound is defined as a breach in the integrity of the skin. Wound healing refers to the process of tissue repair occurring after an injury. It is a complex process, consisting of an intrinsically regulated sequence of cellular and biochemical events. The specific response consists of four distinct but overlapping phases (see Fig. 1), namely:

1. Haemostasis
2. Inflammation
3. Proliferation and
4. Maturation or Remodelling (Schilling 1976)

Each phase requires the orchestration of a large number of different cytokines and cells. For example, erythrocytes, platelets, macrophages and lymphocytes are key players in the ‘early’ stages of wound healing, with fibroblasts, endothelial cells and keratinocytes completing the latter stages. Failure or prolongation of one or more phases results in either healing delay or non-closure of the wound, resulting in a chronic wound.

1.2 Chronic Wounds

The vast majority of cutaneous wounds will heal ‘normally’, with the wound closing within an acceptable period of time. These acute wounds usually occur following a sudden solitary insult, such as a surgical incision or insect bite, and proceed to

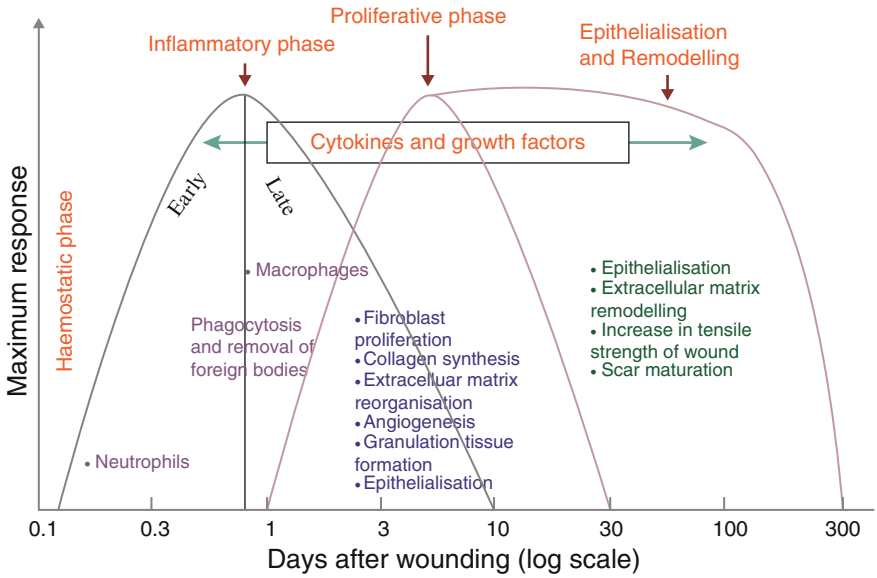

Fig. 1 The phases of wound healing. Epithelialisation occurs towards the end of the wound healing process, and requires healthy, non-infected granulation tissue with an adequate blood supply to occur

close in an orderly manner. In contrast, chronic wounds are commonly caused by an underlying pathological process, which produces either a repeated or prolonged insult to tissues, or greatly interferes with normal wound healing (Wright 2007). What constitutes a non-healing wound is not universally accepted – some authors suggest wounds are chronic if they fail to heal after 6 weeks (Dale et al. 1983; Schultz et al. 2004), whereas others use a 3 month cut-off value. An alternative definition (and one without any specific mention of time) would be "wounds that have failed to return to functional and anatomical integrity in a timely fashion, or wounds that have proceeded through the repair process without a normal functional end result" (Telgenhoff and Shroot 2005). Chronic wounds pose a serious problem to both the patient and the physician – they are a source of much morbidity and even mortality, are costly to treat, and can be difficult to manage (Harding et al. 2002).

1.3 The Cost of Chronic Wounds

Chronic wounds are costly to treat. Costs are incurred with dressings, nurse and doctor time, inpatient admissions and antibiotic usage. Studies published over 10 years ago have estimated the cost of chronic wounds to the NHS to be approximately £1 billion a year (Leaper and Harding 1998), and it is likely that the current

figure is much higher (Posnett and Franks 2008). More recent estimates have suggested wound care accounts for 2–3 % of NHS budget (Drew et al. 2007), which would equate with a yearly cost of £2–3 billion. The annual cost of pressure ulcers alone is estimated to be between £1.8 and £2.6 billion (Posnett and Franks 2008). In the United Kingdom around 24 000 admissions a year are for patients with diabetic foot ulceration, costing the NHS £17 million (Currie et al. 1998). The cost of treating venous leg ulcers has been estimated to be at least £168 to £198 million per year (Posnett and Franks 2008).

These estimates indicate the serious financial drain wounds have on the NHS. However there are other associated costs to the economy as a whole which are harder to evaluate, including missed work opportunities and sick pay.

1.4 The Impact of Chronic Wounds on Patients Daily Life

Chronic wounds are a well documented source of morbidity. Health-related quality of life (HRQoL) scores have been used recently to quantify the day-to-day impact of chronic wounds, allowing physicians to understand in more detail the effect of this disease state on individuals. Studies have shown these questionnaires to be reproducible and reliable, and also responsive to change in the clinical conditions of patients. Wound specific HRQoL questionnaires, such as the Cardiff Wound Impact Schedule (CWIS) (Price and Harding 2004), allow detailed assessment of quality of life issues in patients with lower limb ulcers.

A number of studies have shown a correlation between non-healing of ulcers and reduced quality of life. In a recent multinational study of over 2,000 patients, mostly suffering with venous or arterial leg ulcers, pain is a reported to be a problem ‘most’ or ‘all of the time’ in 36.6 % of patients (Price et al. 2008). When asked to comment on what symptoms bothered patients the most, pain was considered the worst symptom followed by impaired mobility, difficulties in bathing, leakage, odour, and dressing or bandage slippage (Price et al. 2008). In the context of diabetic ulcers non-healing is associated with reduced social functioning (Abdelgadir et al. 2009). The CWIS scoring system (Price and Harding 2004) incorporates questions about social life, physical symptoms, well being and daily living, all of which are affected adversely by the presence of chronic wounds.

1.5 Classifying Chronic Wounds

The vast majority of chronic wounds can be classified into one or more of four categories, namely venous, arterial, diabetic and pressure ulcers (Moreo 2005). Venous, arterial and diabetic ulcers typically affect the legs or feet. Not infrequently wounds may be of ‘mixed’ aetiology (e.g. both venous and arterial).

Venous hypertension, defined as a persistently high pressure within the deep veins, is thought to cause venous leg ulcers. Primary venous hypertension occurs

due to an inherent problem within the superficial or deep venous drainage of the leg, where faulty valves allow backflow of venous blood and an increase in pressure. Secondary venous hypertension occurs after trauma (e.g. surgery) or a deep vein thrombosis (DVT) causes damage to the valves or vein. Patients with venous hypertension may develop a combination of superficial varicosities, venous eczema, lipodermatosclerosis and ulceration. The exact pathophysiology behind venous ulceration is poorly understood, but the elevated venous pressure is thought to 'push' erythrocytes, white blood cells and other factors into the perivascular space, resulting in epithelial cell injury and ulceration (Gohel and Poskitt 2009).

Arterial ulcers develop in people with insufficient arterial supply to the lower leg, typically in patients with peripheral arterial disease (PAD). Blood products and oxygen are required for the timely healing of wounds. In severe PAD, the skin and superficial tissues are inadequately supplied with these essential requirements and any incidental injury will therefore fail to heal. Treatment of these ulcers requires restoration of blood flow, typically via surgical means (Kite and Powell 2007).

Foot ulceration is one of the major complications of diabetes mellitus (DM). It occurs in 15 % of all diabetics, and precedes 84 % of all lower limb amputations (Brem and Tomic-Canic 2007). Ulceration occurs due to a number of factors, which also contribute to non-healing and chronicity: neuropathy, microvascular disease and altered pressure mechanics. Neuropathy occurs frequently in diabetics, resulting in reduced sensation in the extremities. This is accompanied by a loss of protective sensation, which renders the foot at a far greater risk of trauma and thus ulceration (Singh et al. 2005). Microvascular disease, a common occurrence in diabetics, renders the skin and subcutaneous tissue ischaemic, reducing wound healing as described above. Furthermore, diabetes can lead to alteration of the normal foot mechanics, leading to unusual and unhealthy pressure distribution whilst walking. The culmination of this process is known as Charcot's foot, which is associated with ulceration at areas of excessive pressure.

Pressure ulcers occur frequently in people with diseases that reduce or inhibit movement, in bed bound elderly patients, or in patients who are sedated for long periods of time (for example in intensive care). These ulcers typically occur at the sacrum, heels and scapulae although can occur anywhere on the body where there is prolonged pressure. Pressure reduces blood supply to the affected area, rendering the tissues ischaemic and thus prone to ulceration.

2 Epithelialisation and Cellular Migration

2.1 Epithelialisation

Epithelialisation (or re-epithelialisation) is the process by which keratinocytes migrate from the wound edge, proliferate and differentiate to eventually form a complete layer of keratinocytes over a wound (Martin 1997). It could be argued that clinically this represents the most visible and crucial step in wound healing,

as a wound is never regarded as 'healed' until closed by epithelium, regardless of the status of the underlying structures. A number of cellular processes need to occur before a wound is prepared for epithelialisation, most importantly being the formation of adequate Extra Cellular Matrix (ECM), which provides a scaffold for cellular migration, and angiogenesis, to ensure an adequate blood supply for the migrating keratinocytes. These two processes are undertaken by fibroblasts and endothelial cells respectively, in response to a variety of cytokines and other factors (Raja et al. 2007).

Re-epithelialisation occurs as a result of three overlapping functions of keratinocytes: migration, proliferation and differentiation (Raja et al. 2007). However, for migration to commence, marginal basal cells, which are usually firmly adherent to the underlying dermis, need to lose their adhesions to adjacent cells and the underlying matrix. This loss of adhesion occurs as cells retract their intracellular monofilaments and dissolve intercellular desmosomes (which provide physical connection between cells), and hemidesmosomes (which link the epidermis and basement membrane) (Singer and Clark 1999).

Marginal keratinocytes are now free to migrate across the open wound. Migration of cells occurs in a well conserved fashion across a number of cell lines and is discussed in greater detail below. Keratinocytes behind the actively migrating edge undergo proliferation to replenish the keratinocyte population.

In full thickness wounds, keratinocytes can only migrate from the wound edge. In partial thickness wounds keratinocytes also migrate from sweat and sebaceous glands and hair follicles forming islands of epithelial tissue. In sutured wounds, epithelialisation can be short lived, and may be complete within 72 h. Horizontal keratinocyte migration stops when cells meet (termed 'contact inhibition').

2.2 The Role of Cell Migration in Wound Healing

The migration of cells is essential not only for wound healing but also for embryonic development, neuronal development and immune responses. Furthermore, it is this very process which is abnormally overactive in cancer. Tight regulation of this complex process is therefore essential for health. Cells migrate via a process of 'crawling' motility, consisting of four well conserved steps: protrusion of the leading edge, adhesion to the substratum, retraction of the rear, and de-adhesion. This apparently simplistic sequence of events fails to do justice to the complex and well orchestrated process this really is.

In order for this movement to occur, cells need to acquire a polarized morphology for their movement to be directional. Cells generally respond to chemokines (**chemo**tactic cyto**kines**) or other extracellular signals, which provide appropriate signals to begin polarization. At the cell front, termed the 'leading edge', actin assembles both lamellipodia (flat membrane protrusions) and filopodia (fingerlike membrane protrusions that 'sense' the environment into which the cell may move).

It is these lamelliopodia that adhere to the substratum and provide an anchor from which a force can be generated, as well as serving a key role in macropinocytosis and phagocytosis (Small et al. 2002).

Key to both lamellipodial and filopodia production is the assembly and protrusion of actin. Once a leading edge has been created, actin becomes polarised with a forward 'barbed' end and a backward 'pointed' end (both named due to myosin decoration of actin forming an arrow-head type pattern). ATP fuels the disassembly of posterior actin filaments, and the assembly of anterior ones. This process has been referred to as 'treadmilling', and has been shown to occur at much faster rates that predicted should this process only be 'powered' by ATP. As such, other proteins have been shown to interact with actin, and promote this process.

2.3 Actin Movements in Migration

Actin binds myriad proteins with varying roles in terms of its assembly and movement. However, a number of proteins have shown to be 'key players' in actin treadmilling and cellular movements. Pollard and Borisy (2003) provide an excellent summary of the sequence of events and key protein players involved in actin elongation, and thus locomotion.

1. An extracellular stimuli binds to a cell surface receptor (i.e. a chemokine) and produces active Rho-family GTPases (e.g. Rac1 and cdc42) and PIP2 (Phosphatidylinositol 4,5-bisphosphate), which act as intracellular messengers.
2. These activate proteins from the WASP/Scar protein family (acting as promoter proteins to actin assembly), which recruit ARP2/3 complex.
3. The activated ARP2/3 complex (the major actor protein in actin assembly) links to a pre-existing actin filament and begins creation of a new actin 'branch' at a highly characteristic 70° from its actin 'trunk'.
4. After 1 s of extension, the actin filament is capped to halt further progression.
5. ADF/Coffin promotes dissociation of actin filaments from the 'pointed' end, which are 're-energised' by Profilin, increasing the pool of available actin.
6. Steps 3–5 are repeated.

Unsurprisingly, this represents a gross oversimplification of a markedly more complex process. For example, a number of other promoter proteins, termed nucleation-promoting factors (NPFs), have been discovered, and total at least ten, divided into two groups (class 1 and 2 NPFs) (Goley and Welch 2006). Two other 'actor' proteins, commonly referred to as neucleators, have also been discovered alongside ARP2/3 complex (the Formins and Spire (Goley and Welch 2006)). Regardless, actin movements drive the migration of cells, with a number of interacting protein players. In the context of wound healing, it is these proteins which can be studied to determine their role in actin movements, cellular migration and thus epithelialisation.

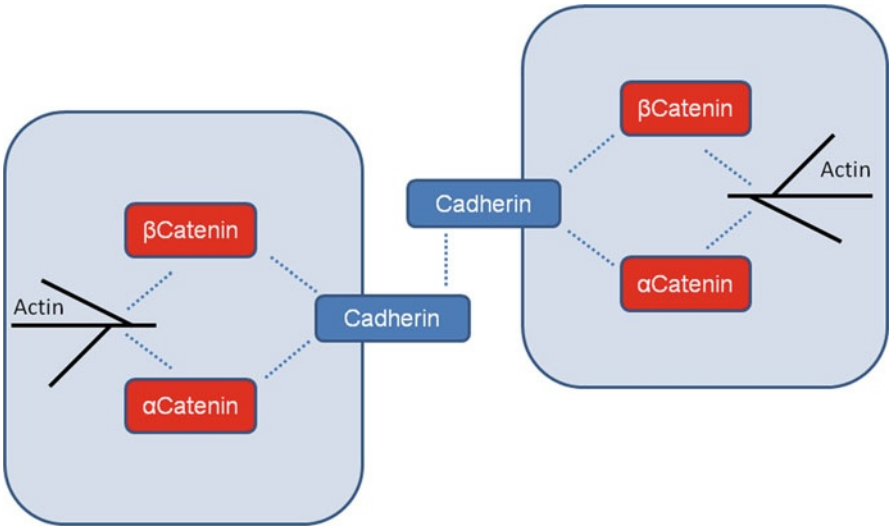

Fig. 2 Simplified diagram of the relationship between Cadherins, Catenins and actin. These proteins provide linkage between the actin cytoskeleton of two adjacent cells. Numerous other proteins are also involved, but are not shown for simplicity

2.4 The Role of Adhesion in Migration

Movements of the actin cytoskeleton can only be converted into forward motion when there exists appropriate adhesion (and dis-adhesion) to the surrounding environment and other cells. As mentioned above, cell-cell and cell-matrix adhesions need to be regulated during migration. These two different types of adhesion are discussed in further detail below.

2.4.1 Cell-Cell Adhesion

Cadherins are the major players in cell-cell adhesion. Cadherins are transmembrane proteins involved in 'homophilic' interactions; extra-cellular bindings occur only between similar cadherins (i.e. E-cadherin binds only E-cadherin, and not, for example, N-cadherin). When cadherins congregate they form desmosomes (also known as adherens junctions). Intracellularly, cadherins bind the actin cytoskeleton via catenins, such as α and βCatenin (Bonifacino 1998; Nelson 2008). Thus, it is possible to show how the actin cytoskeleton of one cell can link directly to another, as shown in Fig. 2. These links need to be dissolved to allow cellular migration to commence.

2.4.2 Cell-ECM Adhesion

With regards to migration, cell-ECM interactions are far more important than cell-cell interactions. Whereas a loss of cell-cell adhesion is required to initiate migration,

there needs to be a continual creation and dissolution of cell-ECM adhesion for a cell to move. Just as cadherins play key roles in cell-cell adhesion, integrins play key roles in cell-ECM adhesion. They are transmembrane proteins (much like cadherins), and consist of an α and β subunit. They attach a variety of ECM proteins, such as laminectin, fibronectin and vitronectin (Grose et al. 2002). When integrins are present in high concentrations, as they are at the tip of lamellopodia, they form FAs (focal adhesions, in much the same way as cadherins form desmosomes). These FAs are in a state of constant flux, especially when cells are moving, and are responsive to the surrounding environment. Integrins act not only as adhesive proteins but also as receptor proteins, and effect not only cell migration, but also apoptosis and cell cycle changes (Le Clainche and Carlier 2008).

The intracellular portion of the FAs ensures it is linked to the actin cytoskeleton. These proteins (in some way synonymous with α and βCatenin) include talin, α-actinin, filamin and vinculin (Le Clainche and Carlier 2008). Again, it is possible to appreciate a continuous protein link from the ECM through to the actin cytoskeleton.

3 ECIS

3.1 Historic Development of ECIS

Historically, cell migration and adhesion have been analysed, using a variety of methods, with a light microscope. The cell migration (wounding) assay is a suitable example of this. Approximately 25 years ago, people began to analyse the adhesion and movements of cells indirectly using electrical fields. Giaver and Keese (1986) describe the changes observed of impedance whilst growing cells on gold electrodes in medium. They passed 1 V through the electrodes and noted the increase in impedance as the cells adhered and spread on the electrode. Due to the insulating properties of their membranes, the cells behave like dielectric particles (i.e. as an electrical insulator that can be polarised by applying an electric field), such that impedance increases with increasing coverage of the electrode until a continuous layer of cells is established. Alternating Current (AC) was used instead of Direct Current (DC) to ensure the electrolytes in the culture media were not deposited upon the electrode, which would have caused the properties of the electrodes to change. As AC is used, impedance is analysed (impedance can be regarded as the AC equivalent of DC resistance). By 1994, Electrical Cell-Substrate Impedance Sensing (ECIS) was performed on a single plate with 6 individual wells, each with their own dedicated electrode (Keese and Giaever 1994). The process has been developed, refined and optimised over the years (Wegener et al. 2000).

Currently, ECIS™ (Applied BioPhysics Inc, USA) equipment is available for 8, 16 and 96 well plates for simultaneous multiple readings. Once seeded with cells, the plates are incubated at optimum conditions for the duration of the experiment. Readings of impedance are measured at a number of different frequencies, and capacitance and resistance are also calculated automatically. ECIS™ software

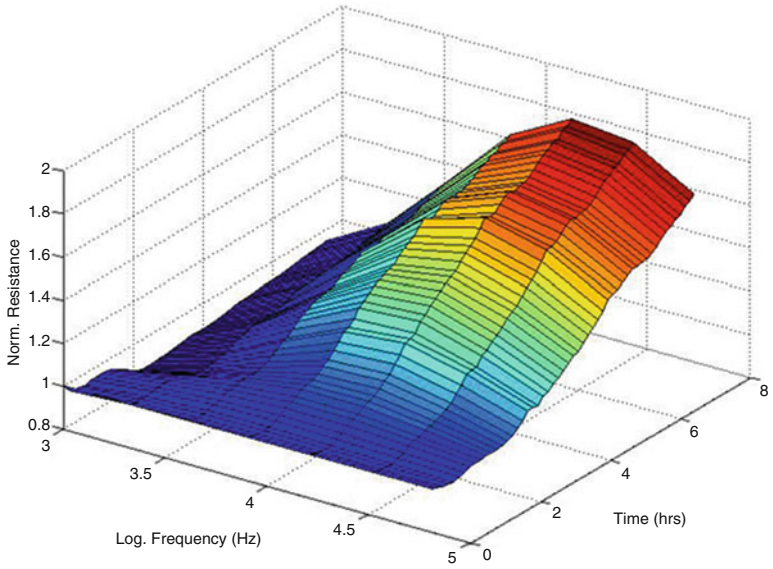

Fig. 3 3D ECIS output displaying a normalised resistance against different frequencies and time for a single run. The greatest resistance changes are seen at 4,000 Hz (corresponding to 'Log. Frequency 4 Hz' on the graph), and it is these readings that are used in our host laboratory for evaluation of results

allows real time observations and analysis of results. Another advance in ECIS™ technology is the ability to wound the cells. Once a confluent monolayer of cells is reached, a stronger current is passed between the two electrodes, wounding the cells, which detach and lower impedance. Cells subsequently migrate over the open electrode, increasing impedance, which can be measured against time. Impedance is measured over a number of different frequencies (1,000–64,000 Hz). The host laboratory typically analyses results at 4,000 Hz. We have found this frequency is most responsive to cellular changes (see Fig. 3).

3.2 Advantages and Disadvantages of ECIS Evaluation

There are a number of advantages of using ECIS over the more traditional wounding assay. ECIS utilised a standardised method to compare multiple cell lines simultaneously (thus avoiding bias using different monolayers at different times with the wounding assay), allows cells to remain in optimum conditions during the experiment, creates a highly reproducible wound which does not affect cells' protein coating, takes measurements automatically and allows data to be quantified and even analysed in real-time. After data has been collected, the data can be further manipulated and analysed using associated ECIS™ software. The drawbacks include the expense of the equipment and the need of a computer to collect data.

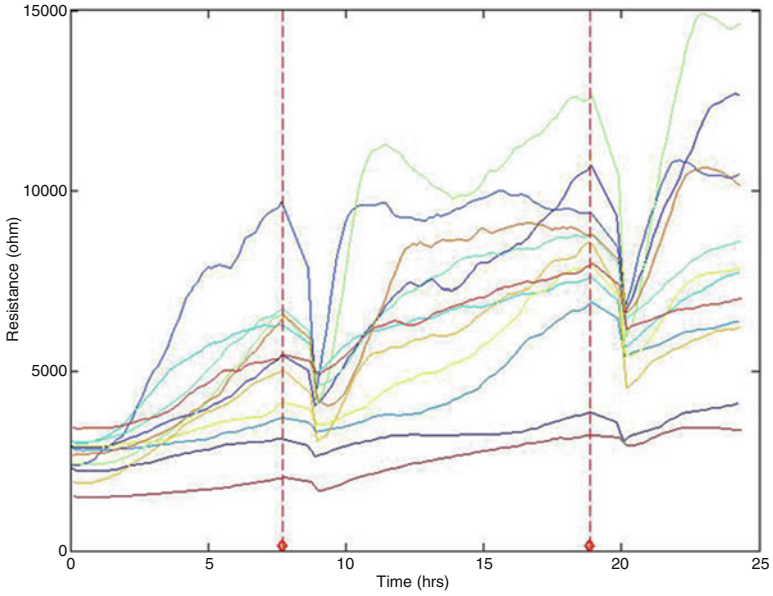

Fig. 4 Data from a typical ECIS reading. Each colour represents a different well. Note that there is an intrinsic resistance within each well, which is between approximately 1,500 and 3,500 Ω here. Note an obvious difference in rate of adhesion between certain lines (difference in slopes in the first 4 h). After wounding (marked by the *red dashed line*), resistance drops markedly as cells die and dis-attach from the electrode. Cellular migration is also markedly different between the cell lines, as assessed by the steepness of the curves after wounding. Note the similarities in individual lines for the response to the first and second wounding

3.3 Interpretation of ECIS Data and Issues Arising from Normalisation

To date, there is no universally accepted method for analysing ECIS data. Typically, data can be represented using images derived from the ECIS software, or manipulated and presented via alternative means (for example, using Excel® etc.).

Figure 4 shows the typical output for ECIS data. Each colour represents an individual well containing either an experimental or control group. Each well has its own intrinsic resistance, hence each tracing will start at a value above 0 (typically 2,000–3,000 Ω). As cells adhere to the electrode, resistance will increase, with the gradient of the slope proportional to the rate of adherence. The horizontal red lines indicate the time of 'wounding' where a large voltage is passed across the electrode (see Fig. 5). Following this, the resistance drops dramatically, reaches its minimum value, and then increases. This corresponds with migration of cells across the electrode. Typically two woundings are undertaken during the period of the experiment, but sometimes people perform either one or three woundings. Occasionally, due either to well leakage, electrode dysfunction or insufficient cell number, the cells

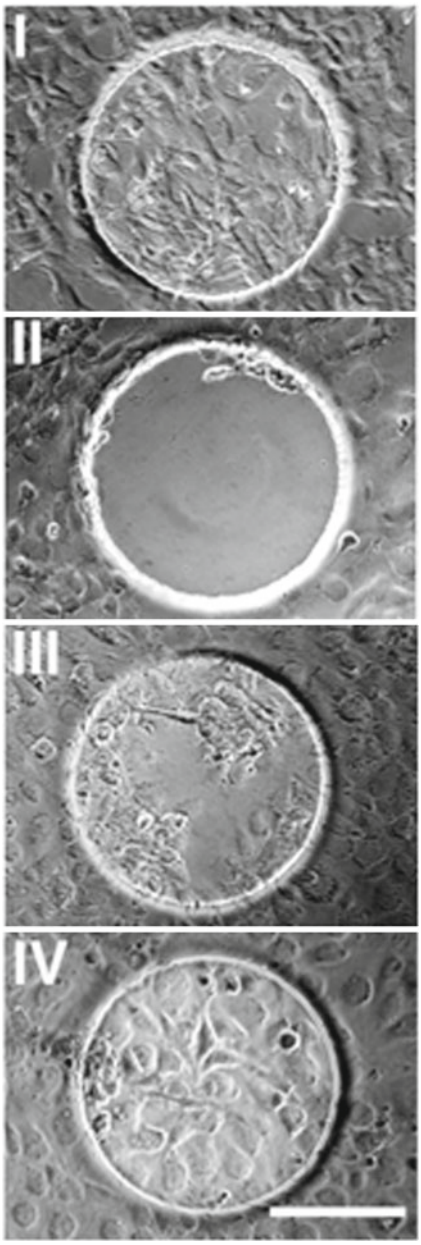

Fig. 5 Images of the ECIS plate prior to wounding (*I*), at the time of wounding (*II*), and following wounding (*III* and *IV*). Note that all cells are removed following wounding, prior to migrating back to cover the electrode

failed to respond to wounding with a typical dip in resistance. Runs can be visually inspected prior to analysis and any such runs excluded from further analysis.

Normalisation of ECIS data is not always required. Occasionally, the intrinsic resistance provided by the hardware is so similar between different wells, there is no need to account for this. If differences between cell lines are obvious, graphical representation may be sufficient.

However, oftentimes data needs to be normalised to account for differences in resistance between wells, and even larger differences encountered between different runs. Two possible methods are presented below, with pros and cons following each. It should be noted that neither of these methods are possible using the ECIS software alone; the data needs to be extracted to a spreadsheet and manipulated therein.

3.4 Normalisation Using Subtraction

The simplest method of normalisation involves nothing more than simple subtraction. To account for the intrinsic resistance within the hardware, the initial resistance reading is selected and subtracting from all subsequent values. Oftentimes, the resistance measured within the system *drops* initially (over the first 30 min) and a slight improvement for this method would be to use the lowest recorded resistance value within the first 30 min of the experiment (the nadir) for normalisation purposes. Thus when normalised, time 'zero' will always be '0' ohms, and no readings will be below zero. Data from wells of identical cell type are pooled and a mean is taken. The advantage of this method is that it is relatively rapid to calculate, and is the authors (DCB) preferred method for normalising adhesion data.

3.5 Normalisation Using Division

The speed of migration is best represented by the steepness of the curve plotted after wounding. For this reason, it could be argued that division for normalisation in this context is preferred. For normalising migration data (after wounding), the nadir (lowest value after wounding) can be selected as time zero. This is important to provide consistency across many woundings. As described above, the intrinsic resistance (as measured in the first 30 min) is *subtracted*. Following this, data can then be normalised to the value at time zero by *dividing* by this number. At time zero, the value obtained will always be '1', and should not drop below this. This method is advantageous as it allows better comparison to be made of the *rate* of change of (true) resistance, and thus migration. This normalisation technique allows migration to be compared using *ratios* (i.e. this cell line migrates *twice* as fast), potentially more useful in this context compared to absolute differences. Also, it removes bias caused by differences in nadir values after wounding.

The importance of division for normalisation can be readily demonstrated below. Assuming this data represents migration (after subtracting for intrinsic resistance) cell line 2 appears to migrate much faster than cell line 1. Yet closer inspection reveals that both cell lines *double* by the completion of their run. The difficulty arises as their starting resistance, and by inference the cells available for migration, is different. Figure 6 shows a simplified hypothetical representation of these runs, showing why they should be considered equivalents. After normalisation, both cell lines would be shown to migrate at an equivalent speed.

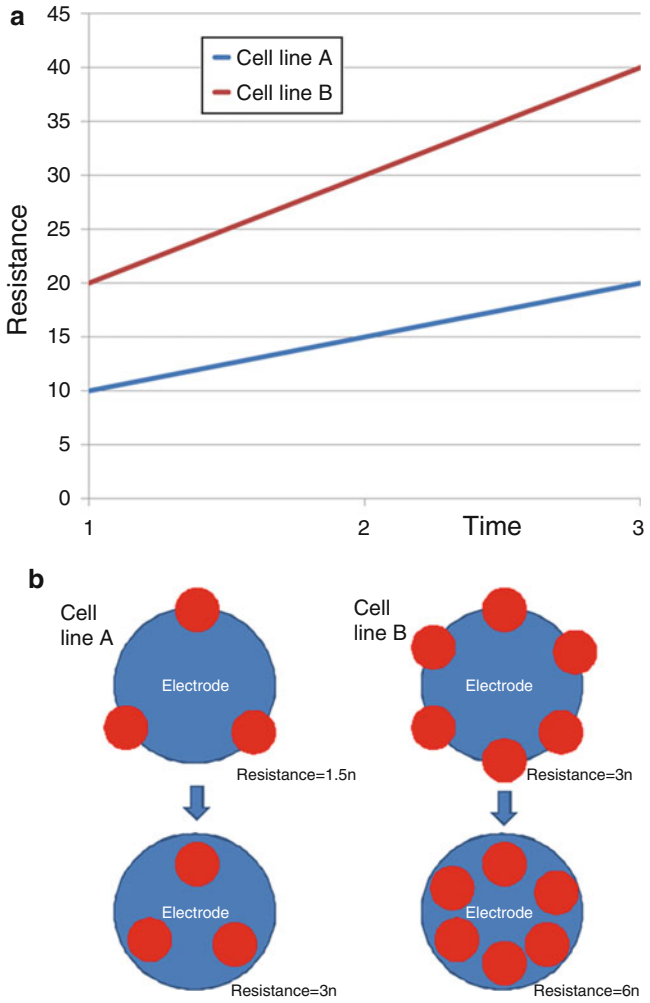

Fig. 6 (**a**) hypothetical ECIS run data, showing two cell line, *A* and *B*, migrating at equal rates, but with differing starting values. (**b**) Diagrammatic representation of changes occurring at the electrode, showing how both cell lines migrate at an equivalent speed

4 Investigation of Epithelialisation Using Knockdown and Overexpression Cell Lines

Suppression or overexpression of proteins to examine subsequent cellular effect is a well documented method of investigating the effect of a protein. *In vitro* ECIS data can be used to examine what effects these proteins have in varying cell lines. In the context of epithelialisation, the human keratinocyte cell line, HaCaT, is most commonly used.

The HaCaT cell line was created in 1988 and is derived from the keratinocytes of a 62 year old male (Boukamp et al. 1988). The following section details the effects, as evaluated by ECIS, of individual proteins on HaCaT migration, and, when data is present, adhesion. These studies help to delineate which proteins are 'key players' in promoting or hindering keratinocyte movements, and thus by inference, epithelialisation. A number of these studies have investigated expression of these proteins in *in vivo* tissue samples, prior to evaluating their role in HaCaT cells. ECIS therefore is very useful to answer the question of *how* it is that different proteins effect epithelialisation. Key results are presented below in prose, and summarised along with other proteins, in Table 1.

It should be noted that all of the following molecules that have been investigated play a known role in cancer (as either a cancer promoter or suppressor). This is due to the fact, as has been mentioned above, that cellular migration is required both for successful epithelialisation, and malignant movements of cancerous cells. Wound healing and cancer share a surprisingly large number of cellular processes, with the only exception being the uncoordinated nature of these processes in the context of cancer (Dvorak 1986; Schafer and Werner 2008).

4.1 Activated Leukocyte Cell Adhesion Molecule (ALCAM) Slows Cellular Migration (Sanders et al. 2011b)

Activated leukocyte cell adhesion molecule (ALCAM, CD166) was cloned and characterised by Bowen et al. in 1995 and mapped to chromosome 3q13.1–q13.2 (Bowen et al. 1995). ALCAM is a transmembrane glycoprotein and is a member of the immunoglobulin superfamily, involved in mediating heterophilic (ALCAM-CD6) and homophilic (ALCAM–ALCAM) cell-cell interactions (Swart 2002) http://onlinelibrary.wiley.com/doi/10.1111/j.1742-481X.2011.00823.x/full-b4.

ALCAM knockdown resulted in increased cellular migration, as assessed using both scratch assay and ECIS. It is therefore assumed that ALCAM slows cellular migration. Tissue data showed expression of ALCAM was significantly higher in chronic non-healed wounds compared to chronic healed wounds. The authors conclude that it is via ALCAMs role in migration through which it has its clinical effect.

4.2 Expressed in High Metastatic Cells (Ehm2) Promotes Wound Healing via Its Positive Effects on Adhesion and Migration (Bosanquet et al. 2011)

Ehm2 was discovered in 1996, cloned in 2000 and shown to be a member of the FERM (four point-1, ezrin, radixin and moesin) family, which are involved in membrane-cytoskeletal interactions (Hashimoto et al. 1996; Shimizu et al. 2000).

Table 1 Summary of effects of various proteins on cancer, migration and adhesion as assessed using ECIS, and thus wound healing

Protein	Role in cancer	Tissue data	Cell line created	Affect on migration	Affect on adhesion	Role in Wound Healing
ALCAM (Activated Leukocyte Cell Adhesion Molecule (Sanders et al. 2011b))	Unclear	Higher in non-healed wounds	Knockdown	Increased	N/A	Suppressor
BMP7 (Bone Morphogenetic Protein 7 (Jiang et al. 2011a))	Promoter	N/A	Over expression	Increased	Increased	Promoter
Ehm2 (Expressed in high metastatic cells 2 (Bosanquet et al. 2011))	Promoter	Higher in healing wounds	Knockdown	Decreased	Decreased	Promoter
EPLIN (Epithelial Protein Lost In Neoplasm (Saravolac et al. 2011))	Suppressor	Higher in non-healed wounds	Over expression	Decreased	Decreased	Suppressor
HuR (Human antigen R (Bosanquet et al. 2012))	Promoter	Marginally higher in healing wounds	Knockdown	None	Reduced	Unclear
IL8 (Interleukin 8 (Jiang et al. 2011b))	N/A	Higher in healing wounds	Over expression	Increased	None	Promoter
MDA7 (Melanoma Differentiation Associated gene 7 (Sanders et al. 2011a))	Promoter	Higher in non-healing wounds	Over expression	Decreased	None	Unclear
TEM8 (Tumour Endothelial Marker 8 (Ye et al. 2011))	Promoter	Higher in healing wounds	Knockdown	Decreased	N/A	Promoter
WAVE1 (Wiskott–Aldrich syndrome protein family VErprolin homologs 1 (Jiang et al. 2010))	Promoter	No difference noted	Knockdown	None	None	Not an effector
WAVE2 (Jiang et al. 2010)	Promoter	Higher in healing wounds	Over expression	Increased	N/A	Promoter
WAVE3 (Jiang et al. 2010)	Promoter	Higher in healing wounds	Knockdown	Decreased	N/A	Promoter

Note the similarity between proteins effects on cancer and wound healing
N/A not applicable (i.e. data absent)

It has been shown to be increased in prostate and breast cancer cell lines, and is generally associated with a poorer prognosis in these cancers (Wang et al. 2006; Yu et al. 2010).

Ehm2 transcript was shown to be greater in acute wounds, compared to chronic wounds. Its effect was examined using an Ehm2 knockdown cell line. Ehm2 knockdown resulted in markedly reduced cellular adhesion and migration. Its effects on migration were analysed using both ECIS and a standard scratch assay.

4.3 EPLIN Enhances Cellular Migration and Adhesion, and Thus Promotes Wound Healing (Saravolac et al. 2011)

Epithelial Protein Lost In Neoplasm (EPLIN) is a cytoskeletal associated protein, which has been implicated as a cancer suppressor. It has been shown to interact with the actin-cadherin-catenin complex, and thus affect migration (Abe and Takeichi 2008).

EPLIN over expression in the HaCaT cell line resulted in a marked decrease in cellular migration, as assessed by both standard scratch assay and ECIS assay. It also reduced cellular adhesion. Tissue data shows its expression is reduced in chronic healed wounds, compared to chronic non-healed wounds.

4.4 Human Antigen R (HuR) Has No Effect on Keratinocyte Migration, and Marginal Effect on Keratinocyte Adhesion (Bosanquet et al. 2012)

HuR is a post-translational modifier of A-and AU- rich mRNAs (Ma et al. 1997; Inoue et al. 2000; Beckel-Mitchener et al. 2002). These inherently unstable mRNAs code for a number of proteins which regulate cell growth and differentiation, signal transduction, transcriptional and translational control, apoptosis, nutrient transport and metabolism. Higher levels are associated with poorer prognosis in a number of cancers (Erkinheimo et al. 2003; Denkert et al. 2004a, b; Mrena et al. 2005; Heinonen et al. 2007).

HuR transcript levels were found to be non-statistically greater in chronic healed wounds, compared to chronic non-healed wounds. However, HuR knockdown had no effect on keratinocyte migration, and only resulted in a marginal reduction in adhesion compared to control. The authors conclude HuR most likely affects wound healing via its effect on cellular growth.

4.5 Wiskott–Aldrich Syndrome Protein Family Verprolin Homologs (WAVEs) Have Differing Effects on Cellular Migration and Wound Healing (Jiang et al. 2010)

WAVEs, proteins sharing common structural design with Wiskott–Aldrich Syndrome proteins (WASP), regulate actin polymerization and influence cellular motility through activation of the ARP2/3 complex. In the context of cancer, WAVEs generally promote cellular migration and thus cancer metastasis (Takenawa and Miki 2001).

The authors examined expression of WAVE1, 2 and 3 in a cohort of acute and chronic wounds, and normal skin. Acute wounds contained significantly greater WAVE2 and 3 transcript, compared to chronic wounds, with no differences noted in WAVE1. They analysed the effect of WAVE2 and 3 on cellular migration using a WAVE2 over expression HaCaT cell line, and a WAVE3 knockdown HaCaT cell line. WAVE2 overexpression resulted in faster cellular migration, and WAVE3 knockdown slowed cellular migration.

5 Conclusion

ECIS has only been used quite recently as a tool for investigating effects of various proteins on epithelialisation. Despite this, there is a relatively substantial body of literature when ECIS has demonstrated interesting and potentially clinically relevant results. This chapter has detailed the problem that chronic wounds pose to clinicians, and the place of epithelialisation within the wound healing process. Furthermore, it has highlighted the most recent and important findings in terms of epithelialisation promoters and inhibitors. ECIS remains a useful tool for assessing adhesion and migration in HaCaT cells and other cell lines involved in wound healing. Large throughput may allow even more rapid identification of key players in the process of cellular movements and thus epithelialisation.

References

Abdelgadir M, Shebeika W, Eltom M et al (2009) Health related quality of life and sense of coherence in Sudanese diabetic subjects with lower limb amputation. Tohoku J Exp Med 217:45–50

Abe K, Takeichi M (2008) EPLIN mediates linkage of the cadherin catenin complex to F-actin and stabilizes the circumferential actin belt. Proc Natl Acad Sci U S A 105:13–19

Beckel-Mitchener AC, Miera A, Keller R et al (2002) Poly(A) tail length-dependent stabilization of GAP-43 mRNA by the RNA-binding protein HuD. J Biol Chem 277:27996–28002

Bonifacino JS (1998) Current protocols in cell biology. Wiley, New York, v. (loose-leaf)

Bosanquet DC, Ye L, Harding KG et al (2011) The role of Ehm2 in wound healing (abstract). Br J Surg 98:6–39

Bosanquet DC, Ye L, Harding KG et al (2012) Role of HuR in keratinocyte migration and wound healing. Mol Med Report 5(2):529–534
Boukamp P, Petrussevska RT, Breitkreutz D et al (1988) Normal keratinization in a spontaneously immortalized aneuploid human keratinocyte cell line. J Cell Biol 106:761–771
Bowen MA, Patel DD, Li X et al (1995) Cloning, mapping, and characterization of activated leukocyte-cell adhesion molecule (ALCAM), a CD6 ligand. J Exp Med 181:2213–2220
Brem H, Tomic-Canic M (2007) Cellular and molecular basis of wound healing in diabetes. J Clin Invest 117:1219–1222
Currie CJ, Morgan CL, Peters JR (1998) The epidemiology and cost of inpatient care for peripheral vascular disease, infection, neuropathy, and ulceration in diabetes. Diabetes Care 21:42–48
Dale JJ, Callam MJ, Ruckley CV et al (1983) Chronic ulcers of the leg: a study of prevalence in a Scottish community. Health Bull (Edinb) 41:310–314
Denkert C, Weichert W, Pest S et al (2004a) Overexpression of the embryonic-lethal abnormal vision-like protein HuR in ovarian carcinoma is a prognostic factor and is associated with increased cyclooxygenase 2 expression. Cancer Res 64:189–195
Denkert C, Weichert W, Winzer KJ et al (2004b) Expression of the ELAV-like protein HuR is associated with higher tumor grade and increased cyclooxygenase-2 expression in human breast carcinoma. Clin Cancer Res 10:5580–5586
Drew P, Posnett J, Rusling L (2007) The cost of wound care for a local population in England. Int Wound J 4:149–155
Dvorak HF (1986) Tumors: wounds that do not heal. Similarities between tumor stroma generation and wound healing. N Engl J Med 315:1650–1659
Erkinheimo TL, Lassus H, Sivula A et al (2003) Cytoplasmic HuR expression correlates with poor outcome and with cyclooxygenase 2 expression in serous ovarian carcinoma. Cancer Res 63:7591–7594
Giaever I, Keese CR (1986) Use of electric-fields to monitor the dynamic aspect of cell behavior in tissue-culture. IEEE Trans Biomed Eng 33:242–247
Gohel MS and Poskitt KR (2009) Venous ulceration. In: ABC of Arterial and Venous Disease. Wiley-Blackwell, Hoboken, p 84
Goley ED, Welch MD (2006) The ARP2/3 complex: an actin nucleator comes of age. Nat Rev Mol Cell Biol 7:713–726
Grose R, Hutter C, Bloch W et al (2002) A crucial role of beta 1 integrins for keratinocyte migration in vitro and during cutaneous wound repair. Development 129:2303–2315
Harding KG, Morris HL, Patel GK (2002) Science, medicine, and the future – healing chronic wounds. Br Med J 324:160–163
Hashimoto Y, Shindo-Okada N, Tani M et al (1996) Identification of genes differentially expressed in association with metastatic potential of K-1735 murine melanoma by messenger RNA differential display. Cancer Res 56:5266–5271
Heinonen M, Fagerholm R, Aaltonen K et al (2007) Prognostic role of HuR in hereditary breast cancer. Clin Cancer Res 13:6959–6963
Inoue M, Muto Y, Sakamoto H et al (2000) NMR studies on functional structures of the AU-rich element-binding domains of Hu antigen C. Nucleic Acids Res 28:1743–1750
Jiang WG, Ye L, Patel G et al (2010) Expression of WAVEs, the WASP (Wiskott-Aldrich syndrome protein) family of verprolin homologous proteins in human wound tissues and the biological influence on human keratinocytes. Wound Repair Regen 18:594–604
Jiang WG, Ye L, Harding KG (2011a) Bone morphogenetic protein (BMP)-7 has a profound impact on the migration of keratinocytes via a SMAD independent pathway (abstract). Wound Rep Regen 19:A69–A96
Jiang WG, Sanders AJ, Harding KG (2011b) Interleukin-8, IL-8, has a direct and profound influence on the migratory capability of human keratinocytes, the potential clinical implications (abstract). Wound Rep Regen 19:A69–A96
Keese CR, Giaever I (1994) A biosensor that monitors cell morphology with electrical fields. IEEE Eng Med Biol 13:402–408

Kite A, Powell J (2007) Arterial ulcers: theories of causation. In: Leg ulcers. A problem-based learning approach. Mosby, Missouri, pp 261–268
Le Clainche C, Carlier MF (2008) Regulation of actin assembly associated with protrusion and adhesion in cell migration. Physiol Rev 88:489–513
Leaper DJ, Harding K (1998) Wounds: biology and management. Oxford University Press, Oxford/New York
Ma WJ, Chung S, Furneaux H (1997) The Elav-like proteins bind to AU-rich elements and to the poly(A) tail of mRNA. Nucleic Acids Res 25:3564–3569
Martin P (1997) Wound healing–aiming for perfect skin regeneration. Science 276:75–81
Moreo K (2005) Understanding and overcoming the challenges of effective case management for patients with chronic wounds. Case Manager 16(62–63):67
Mrena J, Wiksten JP, Thiel A et al (2005) Cyclooxygenase-2 is an independent prognostic factor in gastric cancer and its expression is regulated by the messenger RNA stability factor HuR. Clin Cancer Res 11:7362–7368
Nelson WJ (2008) Regulation of cell-cell adhesion by the cadherin-catenin complex. Biochem Soc Trans 36:149–155
Pollard TD, Borisy GG (2003) Cellular motility driven by assembly and disassembly of actin filaments. Cell 112:453–465
Posnett J, Franks PJ (2008) The burden of chronic wounds in the UK. Nurs Times 104:44–45
Price P, Harding K (2004) Cardiff Wound Impact Schedule: the development of a condition-specific questionnaire to assess health-related quality of life in patients with chronic wounds of the lower limb. Int Wound J 1:10–17
Price PE, Fagervik-Morton H, Mudge EJ et al (2008) Dressing-related pain in patients with chronic wounds: an international patient perspective. Int Wound J 5:159–171
Raja SK, Garcia MS et al (2007) Wound re-epithelialization: modulating keratinocyte migration in wound healing. Front Biosci J Virtual Library 12:2849–2868
Sanders A, Harding KG, Jiang WG (2011a) Suppression of the AKT pathway sensitises keratinocyte's response to interleukin (IL)-7 (abstract). Wound Rep Regen 19:A69–A96
Sanders AJ, Jiang DG, Jiang WG et al (2011b) Activated leukocyte cell adhesion molecule impacts on clinical wound healing and inhibits HaCaT migration. Int Wound J 8:500–507
Saravolac V, Bosanquet DC, Sanders A et al (2011) EPLIN (epithelial protein lost in neoplasm) is a regulator of HaCaT cell migration rates (abstract). Wound Rep Regen 19:A69–A96
Schafer M, Werner S (2008) Cancer as an overhealing wound: an old hypothesis revisited. Nat Rev Mol Cell Bio 9:628–638
Schilling JA (1976) Wound-healing. Surg Clin N Am 56:859–874
Schultz GS, Barillo DJ, Mozingo DW et al (2004) Wound bed preparation and a brief history of TIME. Int Wound J 1:19–32
Shimizu K, Nagamachi Y, Tani M et al (2000) Molecular cloning of a novel NF2/ERM/4.1 superfamily gene, ehm2, that is expressed in high-metastatic K1735 murine melanoma cells. Genomics 65:113–120
Singer AJ, Clark RA (1999) Cutaneous wound healing. N Engl J Med 341:738–746
Singh N, Armstrong DG, Lipsky BA (2005) Preventing foot ulcers in patients with diabetes. JAMA 293:217–228
Small JV, Stradal T, Vignal E et al (2002) The lamellipodium: where motility begins. Trends Cell Biol 12:112–120
Swart GW (2002) Activated leukocyte cell adhesion molecule (CD166/ALCAM): developmental and mechanistic aspects of cell clustering and cell migration. Eur J Cell Biol 81:313–321
Takenawa T, Miki H (2001) WASP and WAVE family proteins: key molecules for rapid rearrangement of cortical actin filaments and cell movement. J Cell Sci 114:1801–1809
Telgenhoff D, Shroot B (2005) Cellular senescence mechanisms in chronic wound healing. Cell Death Differ 12:695–698
Wang J, Cai Y, Penland R et al (2006) Increased expression of the metastasis-associated gene Ehm2 in prostate cancer. Prostate 66:1641–1652

Wegener J, Keese CR, Giaever I (2000) Electric cell-substrate impedance sensing (ECIS) as a noninvasive means to monitor the kinetics of cell spreading to artificial surfaces. Exp Cell Res 259:158–166

Wright K (2007) Acute and chronic wounds: current management concepts. Clin Nurse Spec 21:172–173

Ye L, Ruge F, Patel G et al (2011) TEM8/ATR expression in human wound tissues and its biological impact on keratinocytes (abstract). Wound Rep Regen 19:A69–A96

Yu H, Ye L, Mansel RE et al (2010) Clinical implications of the influence of Ehm2 on the aggressiveness of breast cancer cells through regulation of matrix metalloproteinase-9 expression. Mol Cancer Res 8:1501–1512

Current and Future Applications of ECIS Models to Study Bone Metastasis

Lin Ye, Sivan M. Bokobza, Howard G. Kynaston, and Wen G. Jiang

Abstract Bone metastasis is the most common type of metastasis from the three leading cancers, i.e. prostate, breast and lung cancer. Over the last few decades, intensive studies have been carried out to understand and treat the bone metastasis. To date, the understanding of how certain cancers preferentially metastasise to the bone remains poor, and there is no effective approach to either prevent or treat bone metastases. Electric cell-substrate impedance sensing (ECIS), provides a new and automated experimental method with high throughput to investigate bone metastasis. This chapter is aimed to summarise current experimental models using ECIS to study bone metastasis. These ECIS models include methods to investigate mechanisms of how cancer cells interact with bone cells and tissue to establish bone metastasis; to examine the effect on cancer cells by certain growth factors enriched in bone or by bone extract, and to test certain novel drugs or compounds which may potentially prevent or treat bone metastasis.

Abbreviations

ECIS	electric cell-substrate impedance sensing
NCP	noncollagenous protein
BME	bone matrix proteins extract
BMP	bone morphogenetic protein

L. Ye (✉) • H.G. Kynaston • W.G. Jiang
Metastasis and Angiogenesis Research Group, Institute of Cancer and Genetics,
Cardiff University School of Medicine, Cardiff CF14 4XN, UK
e-mail: yel@cf.ac.uk; sivan.bokobza@googlemail.com; jiangw@cf.ac.uk

S.M. Bokobza
Gray Institute for Radiation Oncology and Biology,
University of Oxford, Oxford OX3 7DQ, UK
e-mail: sivan.bokobaz@oncology.ox.ac.uk

W.G. Jiang (ed.), *Electric Cell-Substrate Impedance Sensing and Cancer Metastasis*,
Cancer Metastasis - Biology and Treatment 17, DOI 10.1007/978-94-007-4927-6_13,

HGF hepatocyte growth factor
ALCAM activated leukocyte cell adhesion molecule
RANK receptor activator of nuclear factor-κB
RANKL RANK ligand
OPG osteoprotegerin

1 Introduction

Cancer is the most common and life threatening disorder in human beings. During lifetime, one in seven of women may develop breast cancer; while it is one in six for men suffering from prostate cancer. The most life threatening aspect of cancer is the dissemination of cancer cells from the primary tumour to a distant organ, leading to development of a secondary tumour (metastasis). Metastasis is the major cause of most morbidities and mortality from cancer. Early detection and improvement in therapeutic approaches have reduced the mortalities from some malignancies. However, the metastases may occur at a very early stage, and stay indolent over a long period. This makes the metastases a great challenge for clinicians and scientists. Intensive efforts have been put in the studies of developing new approaches for early detection and prevention of metastasis. Breast cancer and prostate cancer have the highest frequency of bone involvement, and lung and kidney with less frequency. Bone is the most common metastatic site of prostate cancer, approximately 90 % of patients with advanced prostate cancer (haematogenous metastasis) have skeletal metastasis. Importantly, once tumours metastasize to the bone, they are virtually incurable and result in significant morbidity prior to a patient's death.

The bone is a highly specialized connective tissue, which comprises of four different types of cells and mineralized matrix. Osteoblasts, osteoclasts and bone lining cells are present on bone surfaces, and osteocytes are embedded in the mineralized bone matrix. There are two types of bone tissues: the compact bone which is dense and solid in appearance and the cancellous bone, which is characterized by open space partially filled with an assemblage of needle-like structures. The skeleton consists of approximately 80 % compact bone, largely in peripheral bones, and 20 % cancellous bone, mainly in the axial skeleton. The amount of compact bone varies in different sites according to the need for mechanical support. While cancellous bone accounts for the minority of total skeletal tissue, it is the site of greater bone turnover because its total surface area is much greater than that of compact bone. The principal functions of the skeleton are support, protection, movement, a source of inorganic ions, maintenance of calcium homeostasis, and haematopoiesis in the bone marrow.

Bone metastasis usually leads to severe morbidities which always persist until the death of the patients. This includes; bone pain, hypercalcemia, pathological fracture, spinal cord compression, and consequent paralysis. In bone metastases, along with growth of cancer cells, oesteoblastic and oesteolytic activities are stimulated simultaneously or one occurs in predominance. Osteoblastic lesions are commonly seen in prostate cancer, while osteolytic lesions are present in breast

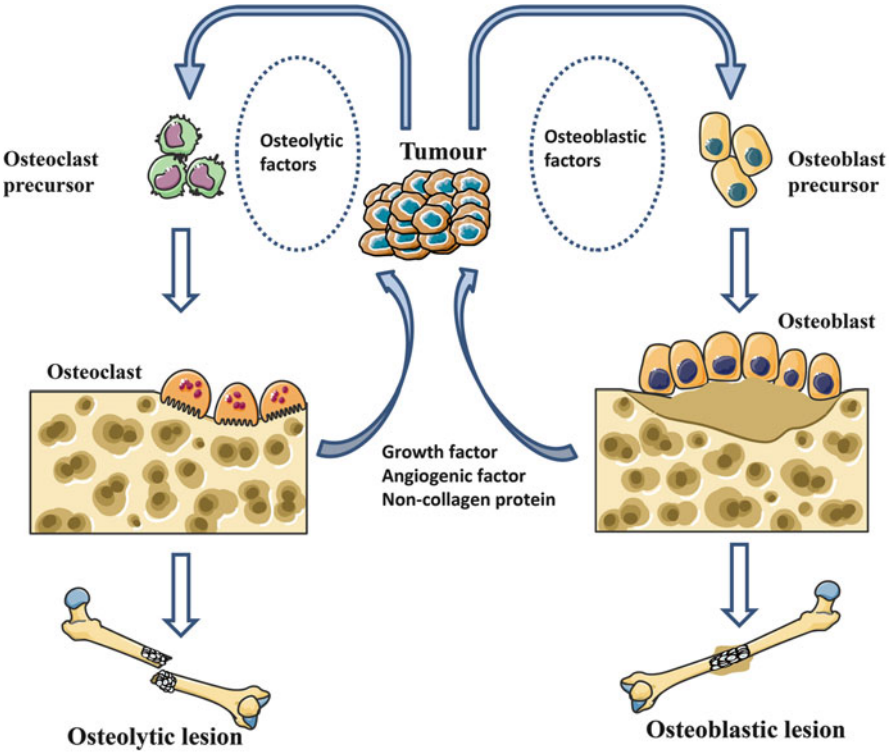

Fig. 1 Vicious circle of bone metastasis. Interactions between metastatic cancer cells and bone microenvironment, which include tumor derived osteoblastic and osteolytic factors, osteoblasts, osteoclasts and bone matrix, contributing to the predominant osteoblastic lesions and osteolytic lesions respectively (Ye et al. 2011)

cancer, lung cancer, and renal cancer. However, certain proportions of bone metastases have demonstrable mixtures of oesteoblastic and oestolytic lesions (Du et al. 2007; Roudier et al. 2008).

Although a century ago Dr. Peget proposed the "seed and soil" hypothesis to describe cancer metastasis, the current knowledge in this critical area remains weak. In bone, interactions amongst cancer cells, bone cells, and bone matrix, constitute a "vicious cycle" in favour of developing a bone metastasis (Reddi et al. 2003; Choueiri et al. 2006; Ye et al. 2007a, b, c). Within the vicious cycle, osteoinductive factors and osteolytic factors derived from cancer cells can act on osteoblasts and osteoclasts or their respective progenitor cells, to stimulate their differentiation and function, leading to corresponding osteoblastic and osteolytic lesions. The reciprocal promotions between osteoblasts and osteoclasts will occur after initial stimulation by tumour-derived factors, which can in turn act to promote colonisation of metastatic cancer cells and their subsequent development. In addition, the bone matrix provides a fertile 'soil' to cancer cells, which is enriched with growth factors and noncollagenous proteins (NCPs). These factors also help cancer cells to survive and proliferate in the bone microenvironment (Fig. 1).

For decades, clinicians and scientists have been working together to seek better approaches in diagnosis, prevention, and treatment of bone metastasis. A variety of different methods and assays have been developed and established in laboratories to investigate bone metastasis, including *in vitro* co-culture models, *ex vivo* and *in vivo* bone metastatic models, from bench in laboratory to bed in ward. Electric cell-substrate impedance sensing (ECIS) is a novel and automated method with high throughput, which can be used to determine cell proliferation, adhesion, cell-cell adhesion and migration, by measuring the impedance of cells attached to an electrode. In this current chapter, we will focus on utilising ECIS technique to study bone metastasis on the bench in a research laboratory. It includes models to examine interaction between tumour cells and bone tissue, and to study the implications of certain cytokines, growth factor and signal pathways in bone metastasis.

2 Effect on Cancer Cells by Bone Extract

The bone matrix comprises of inorganic and organic parts. The inorganic fraction is mainly crystalline mineral salts and calcium, which is present in the form of hydroxyapatite. The organic part of the matrix is mainly Type I collagen. Bone matrix is enriched with various growth factors and cytokines, such as transforming growth factor-β1 (TGF-β1) and bone morphogenetic proteins (BMPs). Bone matrix also contains a number of NCPs, including fibronectin, osteonectin, thrombospondin-2, βig-h3, bone gla protein (BGP, or osteocalcin), matrix gla protein (MGP), Small Integrin-Binding Ligand N-linked Glycoproteins (SIBLINGS) and small bone proteoglycans. The bone matrix plays an important role throughout the whole process of bone metastasis, which is critical for colonisation of cancer cells at early stages of bone metastasis, and the subsequent progression. Investigation of roles played by bone matrix in bone metastasis will provide better understanding of this disorder and also some potential targets for developing novel therapeutic approaches.

At the host laboratory, we have prepared bone matrix proteins extract (BME) following a procedure described recently (Davies and Jiang 2010). Briefly, fresh human bone tissues were obtained immediately after hip replacement, and collected under the ethical committee approval. Bones were crushed at ice cold temperature and subsequently processed using a BioRuptor instrument (Wolf Laboratories, York, UK) in order to extract matrix proteins.

To determine the effect on migration of the cancer cells by the bone matrix, we employed an ECIS wounding assay. 150 μl standard medium alone or supplemented with 10 % BME (v/v) were added to each well of a 96-well array (96W1E). 40,000 MDA-MB-231 cells suspended in 150 μl medium were then seeded into each well. The cells were subject to a wounding using electric pulse of 3,000 μA at 60 kHz for 30 s which was an optimal setting to wound MDA-MB-231 cells acquired from pre-experiment tests on this cell line. For similar wounding effects, different cell lines may be subject to a different setting, which is necessary to be tested in advance. The resistance was monitored over 4–6 h. 3–6 repeats were tested for

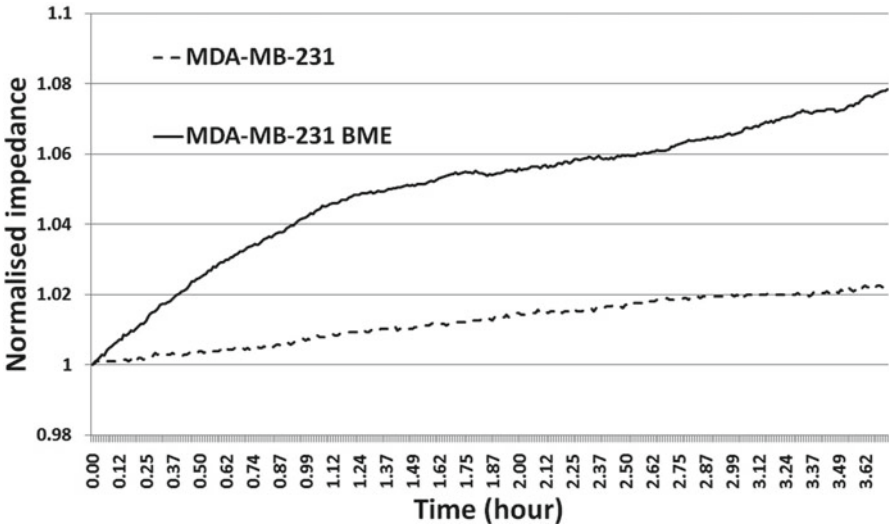

Fig. 2 Effect on migration of breast cancer cells by bone matrix protein extract (BME)

each cell/group. The lowest resistance around 30 min after wounding was used as a starting value. Change in the resistance which represents the migration of cells was normalised against the corresponding starting values of each sample. In Fig. 2, BME treatment led to an increased migration of MDA-MB-231 cells. This has provided a basic model to examine potential candidate molecules/pathways involved in such interactions between bone matrix and cancer cells.

3 Interaction Between Osteoblasts and Cancer Cells

The cellular activities of osteoblasts, osteocytes, and osteoclasts, are essential to the process of bone formation and resorption. Osteoblasts synthesize the collagenous precursors of bone matrix and also regulate its mineralisation. As the process of bone formation progresses, the osteoblasts come to reside in the tiny spaces (lacunae) within the surrounding mineralised matrix, and are then called osteocytes. The cellular processes of osteocytes occupying the minute, canals (canaliculi), permit the circulation of tissue fluids. To meet the requirements of skeletal growth and mechanical function, bone undergoes dynamic remodelling by a coupled process of bone resorption by osteoclasts, and reformation by osteoblasts. Bone lesions are formed when the regulation of bone mass, which is maintained by a balance between bone-forming osteoblasts, and bone-reabsorbing osteoclasts, is perturbed. Several reviews summarsing the understanding of the molecular interactions between osteoblasts and osteoclasts during the processes of bone formation and resorption, have recently been published (Sommerfeldt and Rubin 2001; Roodman 2004;

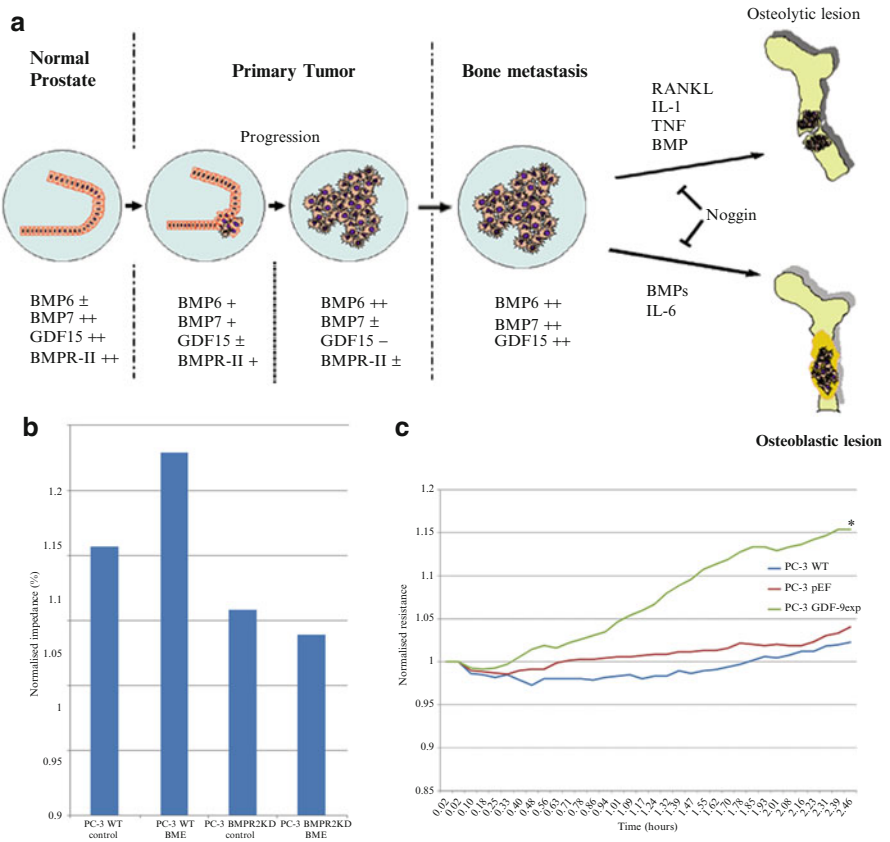

Fig. 3 Implication of BMP in bone metastasis. (**a**): Aberrant expression of BMPs and BMP receptors has been indicated in the disease progression and bone metastasis of prostate cancer. (**b**): Knockdown of BMPRII in PC-3 cells impairs the promotion of cell migration by BME. (**c**). Growth and differentiation factor-9 (GDF-9) promotes migration of PC-3 cells

Raubenheimer and Noffke 2006). Probably, the best understood molecular crosstalk between osteoblasts and osteoclasts is RANK and RANKL (Fig. 1). RANK is a transmembrane receptor expressed on osteoclast precursor cells, while RANKL is expressed by osteoblasts which, upon binding to RANK, leads to osteoclast formation. This process can be interrupted by osteoprotegerin (OPG), a soluble competitive decoy receptor for RANKL, which can be secreted by stromal cells, B lymphocytes, dendritic cells and osteoblasts (Simonet et al. 1997; Hofbauer et al. 2000). This crosstalk also appears to be the mechanism underlying the response of bone to some hormones or local factors, including parathyroid hormone, 1,25-dihydroxyvitamin D_3, oestrogen, IL-11, and prostaglandin E_2 (Sommerfeldt and Rubin 2001; Roodman 2004; Guise et al. 2006; Lee and Lorenzo 2006).

Osteoblasts originate from mesenchymal stem cells which are also the progenitors of chondrocytes, myocytes and adipocytes. Osteoblasts are aligned on the bone

surface, and secrete non-mineralized bone matrix called osteoid, which is primarily comprised of type I collagen and mineralises to become bone. Osteoblasts also regulate the mineralisation during the bone formation by secreting alkaline phosphatase (ALP). Another important function of osteoblasts is the regulation of osteoclast differentiation through various factors including the receptor activator of nuclear factor-κB ligand (RANKL), macrophage colony-stimulating factor (M-CSF), interleukin-1 (IL-1), IL-6, and IL-11 (Ishimi et al. 1990; Girasole et al. 1994; Quinn et al. 1998; Yao et al. 1998; Jimi et al. 1999; Lum et al. 1999). After the bone formation, osteoblasts may have one of these four different fates: 1. to become embedded in the bone matrix as osteocytes; 2. to be transformed into inactive osteoblasts and become bone-lining cells; 3. to undergo apoptosis; or 4. to transdifferentiate into cells that deposit chondroid or chondroid bone (Franz-Odendaal et al. 2006).

Bone lining cells are essentially inactive osteoblasts. They cover all of the available bone surface and function as a barrier for certain ions.

Osteocytes originate from osteoblasts which have migrated into and become trapped and surrounded by bone matrix, which they themselves have produced. The spaces which they occupy are known as lacunae. An osteocyte has numerous cellular protrusions in order to reach out and meet other osteocytes, or other cells on the bone surface, probably for the purpose of communication (Palumbo et al. 1990). The exact role of osteocytes has yet to be fully determined, but it is believed that osteocytes are involved in sensing mechanical stresses in the bone matrix. On the other hand, the mechanical stress is also crucial for maintaining the viability of osteocytes (Takai et al. 2004). It has also recently been reported that osteocytes are constitutive negative regulators of osteoclast activity and may also play an important role in regulating osteoblast' function (Takai et al. 2004; Gu et al. 2005).

Osteoclasts are large multinucleated cells that are originated from the monocyte lineage/macrophages, and are responsible for bone resorption. They secrete bone-reabsorbing enzymes, such as tartrate resistant acid phosphatase from their characteristic ruffled border, and these enzymes digest bone matrix. Osteoclasts are located on bone surfaces in what are called Howship's lacunae. These lacunae, or resorption pits, are left behind after the breakdown of bone and often present as scalloped surfaces. Because the osteoclasts are derived from a monocyte stem-cell lineage, they are equipped with engulfment strategies similar to circulating macrophages. Osteoclasts mature and/or migrate to discrete bone surfaces. Upon arrival, active enzymes are secreted against the mineral substrate. Once the bone matrix is degraded, some factors released as the result of degradation can promote the differentiation and activity of osteoblasts.

In vitro and *in vivo* models, especially using osteoblasts and osteoclasts are critical to investigate the crosstalk between these bone cells and cancer cells. A human fetal osteoblastic cell line, hFOB, was obtained from ATCC (Rockville, MD). The hFOB cell line is cultured in a 1:1 mixture of phenol-free DMEM/Ham's F12 medium containing 10 % fetal bovine serum (FBS), and 1 % gentamicin at the standard conditions (5 % CO_2), and a temperature of 34 °C that allows the expression of the large T antigen. Two million cells were cultured in flasks overnight. The medium is then replaced with fresh medium containing with or without 10 % FBS. The

conditioned medium is then collected after 24 h culture. The medium is subject to a centrifugation for removing cells, and stored at −80 °C until future use. The effect on cell adhesion and migration can be tested using ECIS assays. This is currently being tested in the host laboratory.

4 Impact on Migration of Cancer Cells by BMPs

Knowledge about molecular mechanisms underlying osteoblast and osteolytic lesions has been expanded rapidly over the last few decades. Parathyroid hormone-related protein (PTHrP), interleukin (IL)-11, IL-8, IL-6, and receptor activator of nuclear factor-κB ligand (RANKL) produced by metastatic cancer cells play critical roles in osteolytic bone metastases (Yin et al. 1999; Kakonen et al. 2002; Kudo et al. 2003; Bendre et al. 2005). On the other hand, endothelin-1, BMPs, prostaglandins, and TNFα, have been implicated in the development of osteoblastic lesions (Yin et al. 2005; Yoneda and Hiraga 2005). However, molecular mechanisms underlying the predisposition of the particular malignancies and subsequent colonisation and development of metastatic tumours remain largely unknown.

Bone morphogenetic proteins (BMPs) belong to the transforming growth factor-beta (TGF-β) superfamily. In addition to their ability in facilitating formation of bone and cartilage, BMPs play crucial roles in diverse developmental processes and homeostasis of various tissues and organs including tooth, kidney, prostate, breast, skin, hair, muscle, heart, and neuron, through coordinating cellular differentiation, proliferation and apoptosis.

BMPs have been implicated in various neoplasms, at both primary and secondary tumours, particularly skeletal metastases. Recently studies have also suggested a pivotal role played by BMP signalling and their antagonists in bone metastasis. Aberrant expression of BMPs and BMP signalling molecules has been implicated in a variety of solid tumours and disease specific bone metastasis (Ye et al. 2007a, b, c, 2009a, b). The phenotypic profile of BMPs, BMP receptors, and intracellular signalling molecules can be modified by sexual hormone and growth factors, in order to coordinate biological behaviours of cancer cells during the disease progression. Most BMPs elicit inhibitory effects on proliferation of cancer cells through their receptor signalling. At the primary site, expression of these BMPs is suppressed by hypermethylation or acquired growth independent of sexual hormone, which allows the corresponding cancer cells to grow and progress under reduced influence by the BMPs, such as BMP-2, BMP-4, BMP-7, BMP-9 and BMP-10 (Harris et al. 1994; Horvath et al. 2004; Ye et al. 2007a, b, c, 2008, 2009a, b). Meanwhile expression of some BMPs, including BMP6 and BMP7, are up-regulated and implicated in epithelial-mesenchymal transition (EMT) and enhanced cell invasion and motility, leading to a more aggressive phenotype and subsequent dissemination to secondary sites (Hamdy et al. 1997; Masuda et al. 2003). This adaptable expression profile of BMPs may also occur in bone metastases, such as re-expression of BMP7 by prostate cancer cells assisting colonization of the cancer cells in bone. Involvement of BMP receptor

signalling has also been clearly indicated in the bone metastases, particularly from prostate cancer and breast cancer. BMPs not only directly act on cancer cells to coordinate their abilities during disease progression and bone metastasis; they also indirectly contribute to bone metastasis through regulating tumour related angiogenesis.

Loss of the expression of BMPR-IA, BMPR-IB, and especially BMPR-II, in both prostate cancer tissues and cancer cell lines, has been shown to have an association with the progression of prostate cancer (Ide et al. 1997; Kim et al. 2000, 2004; Ye et al. 2008). The inhibitory effect of BMPs on tumour growth, mediated through BMPR-II, has been illustrated in an *in vivo* murine tumour model using a BMPR-II knock-out prostate cancer cell line (PC3M) (Kim et al. 2004). An elevated level of BMP-6 is associated with higher grade primary tumours and advanced prostate cancer with metastasis (Bentley et al. 1992; Barnes et al. 1995; Hamdy et al. 1997; Tamada et al. 2001). BMP-6 may contribute to the progression of prostate cancer independent of androgen stimulation (Barnes et al. 1995; Tamada et al. 2001). In contrast to BMP-6, BMP-2, -4, -7 and BMP-9 are expressed predominantly in normal prostate tissues. These molecules tend to exhibit a pattern of reduced expression or are absent during the development and progression of prostate cancer at the primary site (Harris et al. 1994; Thomas et al. 2001; Horvath et al. 2004; Masuda et al. 2004; Ye et al. 2008), and may be re-expressed in bone metastases (Fig. 3a).

Reduced expression of BMPs, including BMP-2, -4, -6, -7, and GDF9a, has been revealed in a cohort of breast cancer samples using both quantitative real time PCR and immunohistochemical methods. The decreased expression of BMP-2, BMP-7, GDF9a, and BMP-15, was associated with poor prognosis of the patients (Hanavadi et al. 2007; Davies et al. 2008). A similar reduction of these BMPs has been demonstrated in other studies (Clement et al. 1999; Reinholz et al. 2002). Decreased BMP-7 expression in primary tumours was associated with bone metastasis (Buijs et al. 2007). In contrast to these findings, elevated expression of BMPs, such as BMP-2, BMP-4, BMP-5 and BMP-7, has been demonstrated in other studies (Bobinac et al. 2005; Raida et al. 2005; Alarmo et al. 2006, 2007; Davies et al. 2008). Although the expression of specific BMPs, such as BMP-2, 4, 6 and 7 in breast cancer remains controversial, the abnormalities in their expression have been indicated as a role in the development and progression of breast cancer.

In addition to the aberrant expression of BMPs in certain malignancies, increased expression of BMP receptors and activation of BMP signalling has also been implicated in breast cancer, and the corresponding bone metastasis from the tumour. For example, BMPR-IB was up-regulated in oestrogen receptor-positive carcinomas and was associated with high tumour grade, high tumour proliferation, cytogenetic instability, and a poor prognosis (Helms et al. 2005). Activation of the Smad pathway of BMPs (Smad1/5/8) and TGF-β (Smad2) was revealed in the nuclei of breast cancer cells at both primary tumours and bone metastasis, an observation supported by studies using *in vivo* tumour models (Katsuno et al. 2008).

Together with osteoblastic factors, osteolytic factors, and other elements in the bone microenvironment, BMPs and their receptors signalling form a vicious cycle during the development of bone metastasis. To elucidate the mechanisms underlying their implications in bone metastasis, we have employed ECIS models to examine

the influence on functions of cancer cells by certain BMPs. For example, we determined the cell motility after over-expression of GDF-9 in PC-3 cells using the ECIS wounding assay. The migration was in increased in the GDF-9 over-expressing PC-3 cells, compared with the wild type and empty vector control cells (Fig. 3c). We also utilised the BME to examine responses of cancer cells following manipulation of certain elements of BMPs and their signalling. One of our previously established PC-3 sublines of BMPRII knockdown, was incubated with BME, and then the effect on their migration was determined using the ECIS assay (Fig. 3b). Reduced response to BME was seen in the promoted migration by knockdown of BMPRII.

5 Testing of Novel Drugs for Bone Metastasis

ECIS models also provide high throughput and automated methods to test and validate new drugs and compounds, *in vitro*. In the host laboratory, we have tested some new compounds targeting hepatocyte growth factor (HGF) signalling. HGF is a cytokine that has a diverse but potential role in cancers including breast cancer. HGF, whose action is mediated by its specific receptor, cMET, stimulates the aggressiveness of cancer cells by increasing the invasiveness and cellular migration. HGF is also a potent angiogenic factor. Small inhibitors to the HGF receptor are currently being investigated in clinical trials of various cancers. In solid tumours which have the potency of developing bone metastases, HGF and particularly cMET, have been found to be over-expressed in tumour cells that had metastasised to the bone.

A present study is aimed to examine the effect of a small inhibitor of cMET (PF02341066) on *in vitro* growth and motility of breast cancer cells under common culture condition and a culture condition which uses bone matrix extract (BME) to mimic the bone environment. Additionally, involvement of an adhesion molecule; activated leukocyte cell adhesion molecule (ALCAM), in HGF regulated cell migration, has also been investigated.

ALCAM also known as melanoma metastasis clone D (MEMD) or CD166, was first identified on activated leukocytes and in haemopoitic stem cells and myeloid progenitors. ALCAM mediated cell adhesion is mediated by both homophilic (ALCAM-ALCAM) and heterophilic (ALCAM-CD6) interactions between cells, with the heterophilic interactions being approximately 100 times stronger than the homophilic interactions. The influence of ALCAM on cell adhesion has inspired a number of studies to evaluate its expression in human tumours including melanoma, prostate cancer, breast cancer, colorectal carcinoma, bladder cancer and oesophageal squamous cell carcinoma. ALCAM expression has been shown to have clinical implications. In malignant melanoma, approximately half of the cases investigated were found to have ALCAM positivity and the expression is seen in the vertical growth phase of melanoma.

A panel of breast cancer cell lines (MDA-MB-231 and ZR-751) were used. Cell growth was determined using a colourimetric method, while cell adhesion and migration, were investigated using an ECIS model. Bone matrix proteins were

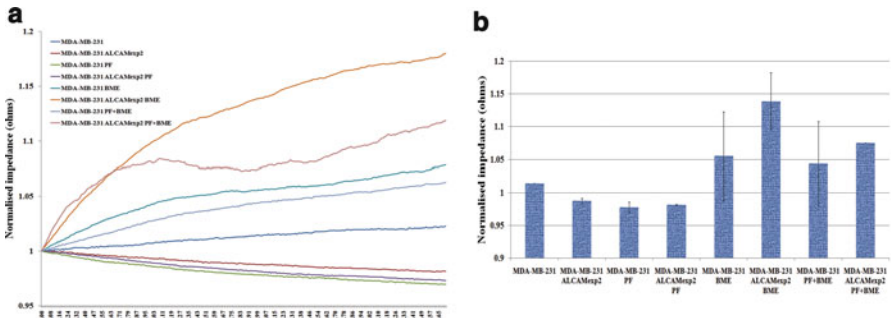

Fig. 4 Effect on migration by BME and cMET inhibitor. (**a**): Both MDA-MB-231 ALCAM overexpression and control cells moved faster in exposure to BME compared with the respective cells under normal culture condition. This effect was partially inhibited by PF02341066, particularly the ALCAM overexpression cells. (**b**): *Bar graph* shows average impedance of each group at 2 h after electrical wounding (n = 6). *Error bars* represent standard deviation

prepared from fresh bones. A small inhibitor to human cMET, PF02341066 was used in the present study in all of the cell models.

The breast cancer cells migrated rapidly in the presence of the bone marrow environment, in comparison with the controls. This was also inhibited by the cMET inhibitor. The study further showed that cells over-expressing a molecule linked to bone metastasis, namely ALCAM (Davies and Jiang 2010), responded more vigorously to the cMET inhibitor in the matrix adhesion and cellular migration models (Fig. 4).

Figure 4, shows the effect on migration by BME and the cMET inhibitor, 2 h after electrical wounding. Both the MDA-MB-231 ALCAM overexpressing and control cells, moved faster in exposure to BME compared with the respective cells under normal culture conditions. This effect was partially inhibited by PF02341066, particularly the ALCAM overexpressing cells.

6 Perspectives

ECIS models for determining cell adhesion, migration, and proliferation, are automated assays to directly examine these functions of cancer cells. These models can also be used to examine the interaction (crosstalk) between cancer cells and the bone environment, i.e. bone matrix, bone cells, vascular endothelial cells, growth factors and cytokines enriched in bone sites. These provide useful methods to understand how cancer cells response to bone, colonise at bone, and eventually establish a bone metastasis. Certainly, there are problems using these ECIS models. For example, the resistance and impedance acquired using ECIS can reflect the cell-cell junctions/adhesion and cell-substratum adhesion. These junctions and adhesions are often dynamically changed/disturbed when cells are subject to certain circumstances or stimuli. The growth factors and cytokines involved in metastasis

of cancer cells often play pivotal roles in regulating these functions of cancer cells. There are certain variations that can be seen in the impedance/resistance upon action of these factors. Experimental conditions need to therefore be pre-tested and optimised for each experiment. Mathematical models to calculate the change of resistance/impedance for reflecting cell migration, adhesion, and growth, require further improvement. These elements need to be considered for such an improvement.

Angiogenesis is an important event during the development and progression of both primary and secondary tumours. It has been suggested that BMPs promote angiogenesis indirectly through up-regulation of the expression of VEGF in both cancer cells and osteoblasts. Noggin, a BMP antagonist, produces the same effect as anti-VEGF antibody: it diminishes the pro-osteoblastic activity of osteoblast cells which is induced by conditioned medium from C4-2B cells (Yeh and Lee 1999; Deckers et al. 2002; Dai et al. 2004). Also, the early stage of bone induction by rhBMP-2 can be blocked by the anti-angiogenic agent (TNP-470) (Mori et al. 1998). This evidence indicates that the control of angiogenesis is, to some extent, integrated with the influence which BMPs have over osteoblastic activity. ECIS assays also can be utilised to explore the interactions between cancer cells, bone cells and vascular endothelial cells, thus to shed light on the angiogenic events in bone metastasis.

Acknowledgement The authors wish to thank Cancer Research Wales and Breast Cancer Hope Foundation for supporting their work.

References

Alarmo EL, Rauta J et al (2006) Bone morphogenetic protein 7 is widely overexpressed in primary breast cancer. Genes Chromosom Cancer 45(4):411–419

Alarmo EL, Kuukasjarvi T et al (2007) A comprehensive expression survey of bone morphogenetic proteins in breast cancer highlights the importance of BMP4 and BMP7. Breast Cancer Res Treat 103(2):239–246

Barnes J, Anthony CT et al (1995) Bone morphogenetic protein-6 expression in normal and malignant prostate. World J Urol 13(6):337–343

Bendre MS, Margulies AG et al (2005) Tumor-derived interleukin-8 stimulates osteolysis independent of the receptor activator of nuclear factor-kappaB ligand pathway. Cancer Res 65(23):11001–11009

Bentley H, Hamdy FC et al (1992) Expression of bone morphogenetic proteins in human prostatic adenocarcinoma and benign prostatic hyperplasia. Br J Cancer 66(6):1159–1163

Bobinac D, Maric I et al (2005) Expression of bone morphogenetic proteins in human metastatic prostate and breast cancer. Croat Med J 46(3):389–396

Buijs JT, Henriquez NV et al (2007) Bone morphogenetic protein 7 in the development and treatment of bone metastases from breast cancer. Cancer Res 67(18):8742–8751

Choueiri MB, Tu SM et al (2006) The central role of osteoblasts in the metastasis of prostate cancer. Cancer Metastasis Rev 25(4):601–609

Clement JH, Sanger J et al (1999) Expression of bone morphogenetic protein 6 in normal mammary tissue and breast cancer cell lines and its regulation by epidermal growth factor. Int J Cancer 80(2):250–256

Dai J, Kitagawa Y et al (2004) Vascular endothelial growth factor contributes to the prostate cancer-induced osteoblast differentiation mediated by bone morphogenetic protein. Cancer Res 64(3):994–999

Davies S, Jiang WG (2010) ALCAM, activated leukocyte cell adhesion molecule, influences the aggressive nature of breast cancer cells, a potential connection to bone metastasis. Anticancer Res 30(4):1163–1168

Davies SR, Watkins G et al (2008) Bone morphogenetic proteins 1 to 7 in human breast cancer, expression pattern and clinical/prognostic relevance. J Exp Ther Oncol 7(4):327–338

Deckers MM, van Bezooijen RL et al (2002) Bone morphogenetic proteins stimulate angiogenesis through osteoblast-derived vascular endothelial growth factor A. Endocrinology 143(4):1545–1553

Du Y, Cullum I et al (2007) Fusion of metabolic function and morphology: sequential [18F]fluorodeoxyglucose positron-emission tomography/computed tomography studies yield new insights into the natural history of bone metastases in breast cancer. J Clin Oncol 25(23):3440–3447

Franz-Odendaal TA, Hall BK et al (2006) Buried alive: how osteoblasts become osteocytes. Dev Dyn 235(1):176–190

Girasole G, Passeri G et al (1994) Interleukin-11: a new cytokine critical for osteoclast development. J Clin Invest 93(4):1516–1524

Gu G, Mulari M et al (2005) Death of osteocytes turns off the inhibition of osteoclasts and triggers local bone resorption. Biochem Biophys Res Commun 335(4):1095–1101

Guise TA, Mohammad KS et al (2006) Basic mechanisms responsible for osteolytic and osteoblastic bone metastases. Clin Cancer Res 12(20 Pt 2):6213s–6216s

Hamdy FC, Autzen P et al (1997) Immunolocalization and messenger RNA expression of bone morphogenetic protein-6 in human benign and malignant prostatic tissue. Cancer Res 57(19): 4427–4431

Hanavadi S, Martin TA et al (2007) The role of growth differentiation factor-9 (GDF-9) and its analog, GDF-9b/BMP-15, in human breast cancer. Ann Surg Oncol 14(7):2159–2166

Harris SE, Harris MA et al (1994) Expression of bone morphogenetic protein messenger RNAs by normal rat and human prostate and prostate cancer cells. Prostate 24(4):204–211

Helms MW, Packeisen J et al (2005) First evidence supporting a potential role for the BMP/SMAD pathway in the progression of oestrogen receptor-positive breast cancer. J Pathol 206(3):366–376

Hofbauer LC, Khosla S et al (2000) The roles of osteoprotegerin and osteoprotegerin ligand in the paracrine regulation of bone resorption. J Bone Miner Res 15(1):2–12

Horvath LG, Henshall SM et al (2004) Loss of BMP2, Smad8, and Smad4 expression in prostate cancer progression. Prostate 59(3):234–242

Ide H, Katoh M et al (1997) Cloning of human bone morphogenetic protein type IB receptor (BMPR-IB) and its expression in prostate cancer in comparison with other BMPRs. Oncogene 14(11):1377–1382

Ishimi Y, Miyaura C et al (1990) IL-6 is produced by osteoblasts and induces bone resorption. J Immunol 145(10):3297–3303

Jimi E, Nakamura I et al (1999) Interleukin 1 induces multinucleation and bone-resorbing activity of osteoclasts in the absence of osteoblasts/stromal cells. Exp Cell Res 247(1):84–93

Kakonen SM, Selander KS et al (2002) Transforming growth factor-beta stimulates parathyroid hormone-related protein and osteolytic metastases via Smad and mitogen-activated protein kinase signaling pathways. J Biol Chem 277(27):24571–24578

Katsuno Y, Hanyu A et al (2008) Bone morphogenetic protein signaling enhances invasion and bone metastasis of breast cancer cells through Smad pathway. Oncogene 27(49):6322–6333

Kim IY, Lee DH et al (2000) Expression of bone morphogenetic protein receptors type-IA, -IB and -II correlates with tumor grade in human prostate cancer tissues. Cancer Res 60(11):2840–2844

Kim IY, Lee DH et al (2004) Loss of expression of bone morphogenetic protein receptor type II in human prostate cancer cells. Oncogene 23(46):7651–7659

Kudo O, Sabokbar A et al (2003) Interleukin-6 and interleukin-11 support human osteoclast formation by a RANKL-independent mechanism. Bone 32(1):1–7

Lee SK, Lorenzo J (2006) Cytokines regulating osteoclast formation and function. Curr Opin Rheumatol 18(4):411–418
Lum L, Wong BR et al (1999) Evidence for a role of a tumor necrosis factor-alpha (TNF-alpha)-converting enzyme-like protease in shedding of TRANCE, a TNF family member involved in osteoclastogenesis and dendritic cell survival. J Biol Chem 274(19):13613–13618
Masuda H, Fukabori Y et al (2003) Increased expression of bone morphogenetic protein-7 in bone metastatic prostate cancer. Prostate 54(4):268–274
Masuda H, Fukabori Y et al (2004) Expression of bone morphogenetic protein-7 (BMP-7) in human prostate. Prostate 59(1):101–106
Mori S, Yoshikawa H et al (1998) Antiangiogenic agent (TNP-470) inhibition of ectopic bone formation induced by bone morphogenetic protein-2. Bone 22(2):99–105
Palumbo C, Palazzini S et al (1990) Osteocyte differentiation in the tibia of newborn rabbit: an ultrastructural study of the formation of cytoplasmic processes. Acta Anat (Basel) 137(4):350–358
Quinn JM, Elliott J et al (1998) A combination of osteoclast differentiation factor and macrophage-colony stimulating factor is sufficient for both human and mouse osteoclast formation in vitro. Endocrinology 139(10):4424–4427
Raida M, Clement JH et al (2005) Expression of bone morphogenetic protein 2 in breast cancer cells inhibits hypoxic cell death. Int J Oncol 26(6):1465–1470
Raubenheimer EJ, Noffke CE (2006) Pathogenesis of bone metastasis: a review. J Oral Pathol Med 35(3):129–135
Reddi AH, Roodman D et al (2003) Mechanisms of tumor metastasis to the bone: challenges and opportunities. J Bone Miner Res 18(2):190–194
Reinholz MM, Iturria SJ et al (2002) Differential gene expression of TGF-beta family members and osteopontin in breast tumor tissue: analysis by real-time quantitative PCR. Breast Cancer Res Treat 74(3):255–269
Roodman GD (2004) Mechanisms of bone metastasis. N Engl J Med 350(16):1655–1664
Roudier MP, Morrissey C et al (2008) Histopathological assessment of prostate cancer bone osteoblastic metastases. J Urol 180(3):1154–1160
Simonet WS, Lacey DL et al (1997) Osteoprotegerin: a novel secreted protein involved in the regulation of bone density. Cell 89(2):309–319
Sommerfeldt DW, Rubin CT (2001) Biology of bone and how it orchestrates the form and function of the skeleton. Eur Spine J 10(Suppl 2):S86–S95
Takai E, Mauck RL et al (2004) Osteocyte viability and regulation of osteoblast function in a 3D trabecular bone explant under dynamic hydrostatic pressure. J Bone Miner Res 19(9): 1403–1410
Tamada H, Kitazawa R et al (2001) Epigenetic regulation of human bone morphogenetic protein 6 gene expression in prostate cancer. J Bone Miner Res 16(3):487–496
Thomas R, True LD et al (2001) Placental bone morphogenetic protein (PLAB) gene expression in normal, pre-malignant and malignant human prostate: relation to tumor development and progression. Int J Cancer 93(1):47–52
Yao GQ, Sun B et al (1998) The cell-surface form of colony-stimulating factor-1 is regulated by osteotropic agents and supports formation of multinucleated osteoclast-like cells. J Biol Chem 273(7):4119–4128
Ye L, Kynaston HG et al (2007a) Bone metastasis in prostate cancer: molecular and cellular mechanisms (review). Int J Mol Med 20(1):103–111
Ye L, Lewis-Russell JM et al (2007b) Bone morphogenetic proteins and their receptor signaling in prostate cancer. Histol Histopathol 22(10):1129–1147
Ye L, Lewis-Russell JM et al (2007c) Endogenous bone morphogenetic protein-7 controls the motility of prostate cancer cells through regulation of bone morphogenetic protein antagonists. J Urol 178(3 Pt 1):1086–1091
Ye L, Kynaston H et al (2008) Bone morphogenetic protein-9 induces apoptosis in prostate cancer cells, the role of prostate apoptosis response-4. Mol Cancer Res 6(10):1594–1606
Ye L, Bokobza SM et al (2009a) Bone morphogenetic proteins in development and progression of breast cancer and therapeutic potential (review). Int J Mol Med 24(5):591–597

Ye L, Kynaston H et al (2009b) Bone morphogenetic protein-10 suppresses the growth and aggressiveness of prostate cancer cells through a Smad independent pathway. J Urol 181(6):2749–2759

Ye L, Mason MD et al (2011) Bone morphogenetic protein and bone metastasis, implication and therapeutic potential. Front Biosci 16:865–897

Yeh LC, Lee JC (1999) Osteogenic protein-1 increases gene expression of vascular endothelial growth factor in primary cultures of fetal rat calvaria cells. Mol Cell Endocrinol 153(1–2):113–124

Yin JJ, Selander K et al (1999) TGF-beta signaling blockade inhibits PTHrP secretion by breast cancer cells and bone metastases development. J Clin Invest 103(2):197–206

Yin JJ, Pollock CB et al (2005) Mechanisms of cancer metastasis to the bone. Cell Res 15(1): 57–62

Yoneda T, Hiraga T (2005) Crosstalk between cancer cells and bone microenvironment in bone metastasis. Biochem Biophys Res Commun 328(3):679–687

Index

W.G. Jiang (ed.), *Electric Cell-Substrate Impedance Sensing and Cancer Metastasis*, Cancer Metastasis - Biology and Treatment 17, DOI 10.1007/978-94-007-4927-6,